



TOWN OF CANMORE

Steep Creek Hazard and Risk Assessment: X, Y, and Z Creeks

FINAL
December 21, 2018

BGC Project No.:
1261-025

Prepared by BGC Engineering Inc. for:
Town of Canmore

EXECUTIVE SUMMARY

This report details the findings of a comprehensive debris flow and debris flood hazard and risk assessment on X, Y and Z creeks located to the west of the Town of Canmore, Alberta. The key questions to be answered are: How often do debris flows and debris floods occur on these three creeks, and how large can they be? What is their economic damage and life loss potential?

Several quantitative dating methods were applied to decipher the frequency of debris flows and debris floods on these creeks including air photograph analysis, dendrogeomorphology, radiocarbon dating, channel yield rates, and empirical relationships between fan areas and the creek’s frequency-magnitude relationship. Table E-1 summarizes the findings from the frequency-magnitude analysis. Peak discharge results are estimated at the fan apex and would attenuate downstream.

Table E-1. Steep creek hazard assessment results for X, Y and Z creeks.

Return period	X Creek		Y Creek		Z Creek	
	Sediment volume (m ³)	Peak discharge (m ³ /s)	Sediment volume (m ³)	Peak discharge (m ³ /s)	Sediment volume (m ³)	Peak discharge (m ³ /s)
2013 event	9,600	30	4,200	25	500	1
10 to 30	1,000	20	1,100	5	-	-
30 to 100	7,000	140	3,100	10	900	5
100 to 300	14,000	250	5,100	110	2,400	57
300 to 1000	21,000	350	7,000	140	3,900	86
1000 to 3000	28,000	440	9,000	170	5,400	110

Following the above, it became pertinent to know the runout behaviour and debris-flow impact intensity for the various return periods considered in Table E-1. This was achieved using a two-dimensional debris-flow runout model, called FLO-2D, which was calibrated with debris flows and debris floods that occurred in 2013. Output from the model in terms of maximum flow depth and flow velocity was combined in an impact intensity index, which could then be related to economic damage and life loss potential for individuals and groups.

Using Canmore’s life loss tolerance criteria, BGC estimated that for X Creek, life loss risks are tolerable for individual risk, or within the ALARP zone for group risk. Annualized economic damages are approximately \$13,000. A channel shift (avulsion) towards the development is necessary, before X Creek poses a safety or economic risk. Residual risk could be managed by channel works to reduce avulsion potential and hazard awareness education for residents living in the hazard zone.

Life loss risks on Y Creek are tolerable for individual risk, and within ALARP for group risk. Events larger than the 100-year return period could cause damage to properties including the area that was affected in 2012 and 2013, and shallow flooding may occur in this area during more frequent

events. Average annualized building damage is approximately \$16,000. Risk can be managed by increasing and reinforcing the existing wooden diversion wall, as well as hazard awareness education for residents living in the hazard zone.

Annual individual life loss risk on Z Creek is at the tolerable risk threshold for existing development (1:10,000). Group risk is considered acceptable, and expected annualized economic damages are about \$21,000 per year. The residual risk could be managed by a combination of structural and non-structural measures, including extending the existing system of wooden diversion walls and channels to divert flows away from buildings at risk.

TABLE OF REVISIONS

ISSUE	DATE	REV	REMARKS
DRAFT	Sept 25, 2018	-	Original issue
DRAFT	October 17, 2018	A	Updated with TOC comments
FINAL	December 21, 2018		Updated with Prof. Church and Morgenstern comments

LIMITATIONS

BGC Engineering Inc. (BGC) prepared this document for the account of Town of Canmore. The material in it reflects the judgment of BGC staff in light of the information available to BGC at the time of document preparation. Any use which a third party makes of this document or any reliance on decisions to be based on it is the responsibility of such third parties. BGC accepts no responsibility for damages, if any, suffered by any third party as a result of decisions made or actions based on this document.

As a mutual protection to our client, the public, and ourselves, all documents and drawings are submitted for the confidential information of our client for a specific project. Authorization for any use and/or publication of this document or any data, statements, conclusions or abstracts from or regarding our documents and drawings, through any form of print or electronic media, including without limitation, posting or reproduction of same on any website, is reserved pending BGC's written approval. A record copy of this document is on file at BGC. That copy takes precedence over any other copy or reproduction of this document.

TABLE OF CONTENTS

TABLE OF REVISIONS	iii
LIMITATIONS	iii
TABLE OF CONTENTS	iv
LIST OF TABLES	vii
LIST OF FIGURES	ix
LIST OF APPENDICES	xi
LIST OF DRAWINGS	xi
1. INTRODUCTION	1
1.1. General	1
1.2. Scope of Work	1
1.2.1. Hazard Assessment.....	2
1.2.2. Risk Assessment.....	3
1.2.3. Mitigation Concepts.....	3
1.3. Terminology	3
2. STUDY OVERVIEW	5
2.1. Introduction	5
2.2. What Are Steep Creek Hazards?	5
2.3. Regional Setting	6
2.3.1. Physiography	6
2.3.2. Geology	7
2.3.3. Climate.....	7
2.4. Local Setting – X, Y and Z Creeks	8
2.4.1. Steep Creek Hazards.....	10
2.4.2. Watersheds.....	11
2.4.3. Fan Characteristics	13
2.4.4. Existing Mitigation	14
2.5. Elements at Risk	17
2.6. Summary	18
3. METHODS	20
3.1. Introduction	20
3.2. Hazard Assessment Background	20
3.2.1. Frequency-Magnitude Relationships	20
3.2.2. Return Period Classes	21
3.2.3. Hazard Assessment Workflow.....	22
3.3. Flood and Debris Flood Peak Discharge Assessment	23
3.3.1. Rainfall Analysis.....	23
3.3.2. Peak Discharge Estimation from Cross-Sections	25
3.3.3. Rainfall-Runoff Modelling	26
3.3.4. Impacts of Climate Change	27
3.4. Debris-flow/Debris-flood Assessment – Data Collection and Processing	28
3.4.1. Historical Records	28

3.4.2.	Air Photo Interpretation	29
3.4.3.	Lidar Change Detection.....	29
3.4.4.	Field Investigation	29
3.4.5.	Test Trenching and Radiocarbon Dating	29
3.4.6.	Dendrogeomorphology.....	30
3.4.7.	Delineation of Previous Events.....	32
3.4.8.	Channel Sediment Yield Estimation	33
3.5.	Debris-flow Assessment – Frequency-Magnitude Analysis.....	34
3.5.1.	Interpretation of Desktop and Field Data	34
3.5.2.	Magnitude Cumulative Frequency (MCF) Analysis	35
3.5.3.	Rainfall Sediment Relationship.....	35
3.5.4.	Development of Local Frequency-Magnitude Relationships	39
3.5.5.	Comparison with Regional Sediment Frequency-Magnitude Relationships	40
3.5.6.	Debris Flow Peak Discharge Assessment.....	42
3.5.7.	Error and Uncertainty	43
3.6.	Hydrodynamic Modelling and Hazard Mapping.....	44
3.6.1.	Model Selection – FLO-2D	44
3.6.2.	Two-part Modelling Approach.....	44
3.6.3.	Basic Setup and Input Parameters	45
3.6.4.	Sediment Model Setup and Calibration	46
3.6.5.	Flood Model Setup and Calibration	47
3.6.6.	Hazard Mapping.....	48
3.7.	Risk Assessment Methods	49
3.7.1.	Introduction	49
3.7.2.	Safety Risk.....	49
3.7.3.	Economic Risk	50
3.7.4.	Critical facilities	51
3.7.5.	Lifelines.....	51
3.8.	Conceptual Mitigation Design	51
3.9.	Summary.....	53
4.	X CREEK RESULTS.....	55
4.1.	Previous Events on X Creek.....	55
4.1.1.	Documented Events.....	55
4.1.2.	Assessment of the June 2013 Event	55
4.1.3.	Air Photograph Interpretation	57
4.1.4.	Dendrogeomorphology.....	58
4.1.5.	Radiocarbon Dating	59
4.2.	Frequency Magnitude Relationship	60
4.2.1.	Flood Peak Discharge.....	60
4.2.2.	Debris-flow Sediment Volume and Peak Discharge	60
4.2.3.	Peak Discharge of Debris Flows Compared to Debris Floods	62
4.3.	Numerical Debris-Flow Modelling and Hazard Mapping.....	63
4.4.	Risk Analysis.....	63
4.4.1.	Individual Risk.....	63
4.4.2.	Group Risk.....	64
4.4.3.	Economic Risk	65
4.4.3.1.	Building Damage	65
4.4.3.2.	Business Activity.....	65

4.4.4.	Lifelines.....	66
4.5.	Conceptual Mitigation Design	66
4.6.	Summary.....	68
5.	Y CREEK RESULTS.....	70
5.1.	Previous Events on Y Creek.....	70
5.1.1.	Documented Events.....	70
5.1.2.	Assessment of the June 2013 Event	70
5.1.3.	Air Photograph Interpretation	72
5.1.4.	Dendrogeomorphology.....	72
5.1.5.	Radiocarbon Dating	73
5.2.	Frequency Magnitude Relationship	74
5.2.1.	Flood Peak Discharge.....	74
5.2.2.	Debris-flow Sediment Volume and Peak Discharge	75
5.3.	Numerical Debris-Flow Modelling and Hazard Mapping.....	76
5.4.	Risk Analysis.....	77
5.4.1.	Individual Risk.....	77
5.4.2.	Group Risk.....	77
5.4.3.	Economic Risk	78
5.4.3.1.	Building Damage	78
5.4.3.2.	Business Activity.....	78
5.4.4.	Lifelines.....	79
5.5.	Conceptual Mitigation Design	79
5.6.	Summary.....	82
6.	Z CREEK RESULTS	84
6.1.	Previous Events on Z Creek	84
6.1.1.	Documented Events.....	84
6.1.2.	Assessment of the June 2013 Event	84
6.1.3.	Air Photograph Interpretation	85
6.1.4.	Dendrogeomorphology.....	85
6.1.5.	Radiocarbon Dating	86
6.2.	Frequency Magnitude Relationship	87
6.2.1.	Flood Peak Discharge.....	87
6.2.2.	Debris-flow Sediment Volume and Peak Discharge	87
6.3.	Numerical Debris-Flow Modelling and Hazard Mapping.....	89
6.3.1.	Modelling and Hazard Mapping Results	89
6.3.2.	Interaction with Stones Canyon Creek	89
6.4.	Risk Analysis.....	91
6.4.1.	Individual Risk.....	91
6.4.2.	Group Risk.....	91
6.4.3.	Economic Risk	91
6.4.3.1.	Building Damage	91
6.4.3.2.	Business Activity.....	92
6.4.4.	Lifelines.....	92
6.4.5.	Discussion.....	92
6.5.	Conceptual Mitigation Design	93
6.5.1.	Risk Summary and Design Event.....	93
6.5.2.	Debris-flow Mitigation Concept.....	94

6.6.	Summary	97
7.	CONCLUSIONS	99
7.1.	Limitations	99
7.2.	Conclusions	99
7.2.1.	Hazard Assessment.....	99
7.2.2.	Risk Assessment.....	100
7.2.3.	Risk Reduction.....	100
8.	CLOSURE	101

LIST OF TABLES

Table 1-1.	Terminology used in this report.....	3
Table 2-1.	Summary of lidar data sets used.....	7
Table 2-2.	Watershed characteristics of X, Y and Z Creeks.....	8
Table 2-3.	List of elements at risk considered in the risk assessment.....	17
Table 3-1.	Summary of 24-hour rainfall at the Kananaskis (3053600) climate station using data from 1940 to 2017 with GEV distribution.....	24
Table 3-2.	HEC-HMS model inputs for each creek.....	27
Table 3-3.	Summary of the estimated 24-hour rainfall for a range of return periods at the Kananaskis (3053600) climate station in the period from 2050 to 2100, based on an ensemble of 9 GCMs.....	28
Table 3-4.	Summary of reviewed historical air photographs.....	29
Table 3-5.	Summary of channel yield hikes on X, Y and Z creeks.....	33
Table 3-6.	Frequency and magnitude information that can be inferred from desktop and field hazard assessment methods.....	34
Table 3-7.	Snowmelt factors for the three watersheds.....	40
Table 3-8.	FLO-2D basic input parameters.....	45
Table 3-9.	Components used to model the built environment.....	46
Table 3-10.	Simulated debris-flow and sediment transport scenarios on X, Y and Z Creeks.....	46
Table 3-11.	Rheological parameters used for Bow Valley debris-flow models.....	47
Table 3-12.	Simulated flood scenarios on X, Y and Z Creeks.....	47
Table 3-13.	Definitions and colour coding for debris flow creeks.....	48
Table 4-1.	Comparison of estimated peak discharge values for the June 2013 event on X Creek, using rainfall-runoff modelling and high-water mark cross-sections.....	57
Table 4-2.	Summary of X Creek dendro sample features.....	58
Table 4-3.	Sediment volumes estimated from radiocarbon dates and test pit logging.....	59
Table 4-4.	Estimated peak discharge for X Creek based on historical precipitation at Kananaskis climate station and under possible climate change conditions.....	60

Table 4-5.	Interpreted sediment transport magnitudes for each return period scenario on X Creek.	60
Table 4-6.	Impact intensities at urban development on the X Creek fan.	63
Table 4-7.	Estimated life loss for each scenario on X Creek.	64
Table 4-8.	Summary of estimated building damage at X Creek.	65
Table 4-9.	Summary of business consequence estimates on X Creek.....	66
Table 4-10.	Summary of roads and bridges potentially impacted by debris flow scenarios on X Creek.....	66
Table 4-11.	Comparison of X Creek mitigation options.	67
Table 5-1.	Comparison of estimated peak discharge values for the June 2013 event on Y Creek, using rainfall-runoff modelling and high-water mark cross-sections.	71
Table 5-2.	Summary of Y Creek dendro sample features.	73
Table 5-3.	Sediment volumes estimated from radiocarbon dates and test pit logging.	73
Table 5-4.	Estimated peak discharge for Y Creek based on historical precipitation at Kananaskis Climate Station including climate change effects.	74
Table 5-5.	Interpreted sediment magnitudes for each return period scenario on Y Creek. ..	75
Table 5-6.	Impact intensities at urban development on the Y Creek fan.	76
Table 5-7.	Estimated life loss for each scenario on Y Creek.	78
Table 5-8.	Summary of estimated building damage at Y Creek.	78
Table 5-9.	Summary of business consequence estimates on Y Creek.....	79
Table 5-10.	Summary of roads and bridges potentially impacted by debris flow scenarios of Y Creek.	79
Table 5-11.	Comparison of Y Creek mitigation options.	81
Table 6-1.	Comparison of estimated peak discharge values for the June 2013 event on Z Creek, using rainfall-runoff modelling and high-water mark cross-sections.	84
Table 6-2.	Summary of Z Creek dendro sample features.....	85
Table 6-3.	Sediment volumes estimated from radiocarbon dates and test pit logging.	86
Table 6-4.	Estimated peak discharge for Z Creek based on historical precipitation at Kananaskis Climate Station and under possible climate change conditions.....	87
Table 6-5.	Interpreted debris flow magnitudes for each return period scenario on Z Creek.	87
Table 6-6.	Impact intensities at urban development on the Z Creek fan.....	89
Table 6-7.	Estimated life loss for each scenario on Z Creek.	91
Table 6-8.	Summary of estimated building damage at Z Creek.....	92
Table 6-9.	Summary of business consequence estimates on Z Creek.....	92
Table 6-10.	Summary of roads and bridges impacted by debris flow scenarios of Z Creek.	92

Table 6-11. PDI by scenario, for parcels on Z Creek with PDI > 1:10,000..... 93
Table 6-12. Comparison of Z Creek mitigation options. 96

LIST OF FIGURES

Figure 1-1. Risk management framework (adapted from Canadian Standards Association (CSA) 1997, Australian Geomechanics Society (AGS) 2007, International Organization for Standardization (ISO) 31000:2009 and VanDine, 2012). 2
Figure 2-1. Steep creek flood profile showing peak flow levels for different events. 6
Figure 2-2. Climate normals for 1981 to 2000 period for the Kananaskis climate station. Data were acquired from Environment and Climate Change Canada (ECCC, 2011). 8
Figure 2-3. Watershed area versus fan area for 825 steep creeks in AB and BC (data from Holm, Jakob, Scordo, Strouth, Wang, & Adhikari, 2016 and Lau, 2017). X, Y, and Z Creek data are plotted as large red dots, while Bow Valley creeks are shown in blue..... 9
Figure 2-4. Tendency of creeks to produce floods, debris floods and debris flows, as a function of Melton Ratio and stream length (data from Holm et al., 2016). See.. 10
Figure 2-5. Overview of X, Y and Z Creek watersheds, including the east and west tributaries of X Creek. The Peaks of Grassi subdivision is located on the distal fan. Photo: BGC, June 13, 2018. 11
Figure 2-6. Extensive talus deposits in the upper X Creek east tributary. Photo: BGC, June 13, 2018. 12
Figure 2-7. Aerial view of the upper Y Creek watershed showing three avalanche paths (delineated in white dashed lines) and a rock slide deposit. This channel has significantly more debris storage than Z Creek and can produce larger debris flows. Photo: BGC, June 12, 2018. 13
Figure 2-8. Locations of wooden walls (brown lines) and riprapped channels (blue outlines). Fans are outlined with dashed orange lines..... 15
Figure 2-9. Two wooden walls on the western side of the Z Creek fan. The walls are aligned in a V shape, to funnel water into a riprap-lined ditch (Figure 2-10). BGC photo, June 7, 2018. 16
Figure 2-10. Looking downstream along the western Z Creek riprapped channel. Yellow arrow points to storm drain inlet at the far end. BGC photo, June 7, 2018. 16
Figure 3-1. Conceptual frequency-magnitude curve..... 21
Figure 3-2. Workflow used to develop F-M relationships for X, Y and Z Creeks, for floods and debris floods (blue) and debris flows (purple)..... 22
Figure 3-3. R-generated 24-hour rainfall frequency analysis of the Kananaskis climate station for the period 1940 to 2017 (R, Version 3.5.1)..... 24
Figure 3-4. Impact scars on a spruce tree near Fergusson Creek in southwest BC showing an example of scars that can be dated precisely. The red arrow points at a scar, and the blue arrow points at the center of the tree (from Jakob, 1996). 32

Figure 3-5. Sediment and runoff data from the Swiss and Bow Valley datasets. Datasets compiled by Rickenmann and Koschni (2010) and BGC, respectively. Red text labels indicate outliers in the Swiss dataset (discussed in text) and black lines show the confidence interval.....37

Figure 3-6. Example frequency-magnitude curve for Y Creek, showing the three data sources differentiated. The confidence intervals appear narrow due to the log-log scale.40

Figure 3-7. Regional F-M curve for X Creek, based on a regression fit to three different regional cases, using two different correction factors (six data subsets in total).42

Figure 3-8. Group risk tolerance criteria as defined by GEO (1998) and accepted by Canmore municipal policy (2016).....50

Figure 3-9. Examples mitigation structures: (a) earth-fill retention berm, Glyssibach, Brienz, Switzerland; (b) stone diversion berm, Trachtbach, Brienz, Switzerland; (c) conveyance channel with earthfill berms, Rennebach, Austria; (d) log crib check dams, Gesäuse, Austria; and (e) flexible debris net, Cougar Creek, Canmore, Alberta. Photograph (d) by M. Jakob, other photographs by E. Moase.52

Figure 4-1. Shallow debris deposits from the June 2013 event on the distal areas on the X Creek fan. BGC photograph, June 11, 2018.....56

Figure 4-2. Erosion from the trail avulsion on X Creek. BGC photograph, June 13, 2018.56

Figure 4-3. Deposit delineations from radiocarbon sample dates and test pit locations.....59

Figure 4-4. Interpreted F-M relationship for X Creek (blue), compared with the regional F-M relationship (black).....61

Figure 4-5. F-N curve showing the results of the X Creek risk analysis for groups.....64

Figure 5-1. Water flowing along the eastern Y Creek diversion wall during the June 2013 event, shown looking upstream (left) and east along the wall (right). Photograph provided by the Town of Canmore, dated June 19, 2013 at 10:20 am.71

Figure 5-2. Deposit delineations from radiocarbon sample dates and test pit locations. Note that these delineations are very approximate given the low number of test pits that were possible due to access restrictions.....74

Figure 5-3. Interpreted F-M relationship for Y Creek (purple), compared with the regional F-M relationship (black).75

Figure 5-4. F-N curve showing the results of the Y Creek risk analysis for groups.....77

Figure 5-5. Proposed locations for structural mitigation measures on Y Creek.81

Figure 6-1. Deposit delineations from radiocarbon sample dates and test pit locations.....86

Figure 6-2. Interpreted F-M relationship for Z Creek (green), compared with the regional F-M relationship (black).88

Figure 6-3. Proposed locations for diversion berms or walls on the lower Z Creek fan.....95

Figure 6-4. Z Creek fan apex area, showing possible location of debris flow net and other debris retention measures.96

LIST OF APPENDICES

- APPENDIX A - STEEP CREEK PROCESS TYPES
- APPENDIX B - PEAKS OF GRASSI STORM SEWER SYSTEM
- APPENDIX C - TEST PIT DETAILED LOGS AND PHOTOGRAPH LOGS
- APPENDIX D - RADIOCARBON SAMPLE RESULTS
- APPENDIX E - RISK ASSESSMENT METHODS

LIST OF DRAWINGS

- | | |
|------------|---|
| DRAWING 01 | X, Y and Z Creek Watersheds and Fans |
| DRAWING 02 | X, Y and Z Creek Fans and and Sample Locations |
| DRAWING 03 | Orthophoto of X, Y and Z Creek Fans |
| DRAWING 04 | X, Y and Z Creeks Air Photo Comparison |
| DRAWING 05 | X, Y and Z Creeks Geomorphic Map of Study Area |
| DRAWING 06 | X Creek Debris Flow and Debris Flood Runout and Intensity |
| DRAWING 07 | Y Creek Debris Flow and Debris Flood Runout and Intensity |
| DRAWING 08 | Z Creek Debris Flow and Debris Flood Runout and Intensity |
| DRAWING 09 | Composite Hazard Map |
| DRAWING 10 | Risk to Individuals |

ACRONYMS AND ABBREVIATIONS

Acronyms and abbreviations used in this report:

AEP	Alberta Environment and Parks
AGS	Australian Geomechanics Society
BGC	BGC Engineering Inc.
Canmore	Town of Canmore
CDA	Canadian Dam Association
CN	Curve Number
CSA	Canadian Standards Association
DEM	digital elevation model
Dendro	dendrogeomorphology
ECC	Echo Canyon Creek
ECCC	Environment and Climate Change Canada
FFA	flood frequency analysis
F-M	frequency-magnitude
GCM	global climate model
GEO	Geotechnical Engineering Office
GEV	generalized extreme value
HEC-HMS	Hydrologic Engineering Centre – Hydrologic Modeling System
I _{DF}	intensity (debris flow)
ISO	International Organization for Standardization
lidar	light detection and ranging
MCF	magnitude cumulative frequency
NRCS	National Resource Conservation Service
PCIC	Pacific Climate Impact Consortium
PMP	probable maximum precipitation
QRA	quantitative risk assessment
RCP	representative carbon pathway
RFP	request for proposal
SCS	Soil Conservation Service
TRD	traumatic resin ducts
USACE	United States Army Corps of Engineers



1.0 INTRODUCTION

1. INTRODUCTION

1.1. General

X, Y, and Z creeks are tributaries on the southwest side of the Bow River Valley, southeast of Stones Canyon Creek (Drawings 01, 02 and 03). The creeks are prone to steep creek hazards, and sediment transport events occurred on all three creeks in June 2013. The June 2013 event also caused flooding, debris floods and debris flows elsewhere in the Bow Valley, including on Cougar Creek, Three Sisters Creek and Stoneworks Creek.

In response to the June 2013 events, the Town of Canmore (Canmore) developed a mountain creek hazard mitigation plan, which included detailed assessment of the creeks within Canmore's boundaries. To date, BGC Engineering Inc. (BGC) has completed several of these studies, as follows:

- A hydroclimatic analysis of the 2013 storm (BGC, August 1, 2014)
- A forensic analysis for Pigeon, Stone, Stoneworks, X, Y, Z, Cougar, Three Sisters, Echo Canyon and Stewart creeks (BGC December 2, 2013a-d; December 11, 2013a-b; December 18, 2013; January 3, 2014)
- Detailed hazard assessments for Cougar, Three Sisters, Stone and Stoneworks creeks (BGC March 7, 2014; June 11, 2014; January 20, 2015; May 21, 2015; November 16, 2015)
- Risk assessments for Cougar, Three Sisters, Stone, Stoneworks and Pigeon creeks (BGC June 11, 2014; January 20, 2015; May 21, 2015; October 23, 2015; September 27, 2016; September 30, 2016).

This report is an assessment of the steep creek hazards and risks for X, Y and Z creeks. It is consistent with the previous work completed by BGC for Canmore, and also with a Level 3 assessment as defined by the Draft Guidelines for Steep Creek Risk Assessments in Alberta (BGC, March 31, 2017). The work is based on BGC's proposal dated February 22, 2018 and approved by Canmore on April 5, 2018. Work was completed under the BGC/Canmore Master Service Agreement dated August 28, 2018.

The overall objective of the Level 3 hazard and risk assessment is to estimate the frequency and magnitude of steep creek hazards at X, Y and Z creeks and to identify mitigation options that can reduce risk to a tolerable risk level, if required. Risk, in the context of geohazard management, is a measure of the probability and severity of an adverse effect to health, property or the environment, and is estimated by the product of hazard probability (or likelihood) and consequences. This report focuses on identifying and assessing key risks to people and infrastructure at X, Y and Z creeks that can be used as a basis for cost-effective risk management decision-making.

1.2. Scope of Work

Geohazards considered in this risk assessment include steep creek hazards such as debris flows, debris floods and bedload transport events. Other geohazard types (e.g., earthquakes, snow

avalanches, rock avalanches, subsidence) were not considered. Other landslide types such as translational slides, debris avalanches and rock fall were only considered with respect to providing sediment supply mechanisms to the respective creek channels.

Figure 1-1 describes seven steps of geohazard risk management. The scope of work for this study is structured around Steps 1 through 5 and the initial part of Step 6. The three major work phases include hazard assessment, risk assessment, and mitigation concept development.

Assessment Type		Risk Communication and Consultation Informing stakeholders about the risk management process	Monitoring and Review Ongoing review of risk scenarios and risk management process
Geohazard Assessment	1. Scope Definition a. Recognize the potential hazard b. Define the study area and level of effort c. Define roles of the client, regulator, stakeholders, and Qualified Registered Professional (QRP) d. Identify 'key' consequences to be considered for risk estimation		
Geohazard Risk Identification	2. Geohazard Analysis a. Identify the geohazard process, characterize the geohazard in terms of factors such as mechanism, causal factors, and trigger factors; estimate frequency and magnitude; develop geohazard scenarios; and estimate extent and intensity of geohazard scenarios.		
Geohazard Risk Analysis	3. Elements at Risk Analysis a. Identify elements at risk b. Characterize elements at risk with parameters that can be used to estimate vulnerability to geohazard impact.		
Geohazard Risk Assessment	4. Geohazard Risk Estimation a. Develop geohazard risk scenarios b. Determine geohazard risk parameters c. Estimate geohazard risk		
Geohazard Risk Management	5. Geohazard Risk Evaluation a. Compare the estimated risk against tolerance criteria b. Prioritize risks for risk control and monitoring		
	6. Geohazard Mitigation a. Identify options to reduce risks to levels considered tolerable by the client or governing jurisdiction b. Select option(s) with the greatest risk reduction at least cost c. Estimate residual risk for preferred option(s)		
	7. Action a. Implement chosen risk control options b. Define and document ongoing monitoring and maintenance requirements		

Figure 1-1. Risk management framework (adapted from Canadian Standards Association (CSA) 1997, Australian Geomechanics Society (AGS) 2007, International Organization for Standardization (ISO) 31000:2009 and VanDine, 2012).

The following sections summarize BGC's scope for the three project phases.

1.2.1. Hazard Assessment

- Conduct an integrated steep creek hazard assessment for the X, Y, and Z creeks area. Geohazards to be considered include steep creek geohazards (debris floods and debris flows) and landslide types that are able to feed sediment to the respective creek channels.

- Determine the likely deposition pathways and the effects of events of a given size and/or return period on changing runoff to new pathways.

1.2.2. Risk Assessment

- Develop, demonstrate and provide a comprehensive risk assessment for the study area, including the risk tolerance criteria and rationale adopted for the project.

1.2.3. Mitigation Concepts

- Develop and provide conceptual mitigation options to protect existing residences and infrastructure, including both structural and non-structural approaches.

1.3. Terminology

This assessment uses specific hazard and risk terminology (Table 1-1).

Table 1-1. Terminology used in this report.

Term	Definition
Steep Creek Hazard	Earth-surface process involving water and varying concentrations of sediment.
Debris Flow	Very rapid to extremely rapid surging flow of saturated, non-plastic debris in a steep channel (Hung, Leroueil & Picarelli, 2014). Debris generally consists of a mixture of poorly sorted sediments, organic material and water.
Debris Flood	A very rapid flow of water with a sediment concentration of 3-10% in a steep channel. It can be pictured as a flood that also transports a large volume of sediment that rapidly fills in the channel during an event.
Rock (and debris) Slides	Sliding of a mass of rock (and debris).
Rock Fall	Detachment, fall, rolling, and bouncing of rock fragments.
Hazard	Process with the potential to result in some type of undesirable outcome. Hazards are described in terms of scenarios, which are specific events of a particular frequency and magnitude.
Element at Risk	Anything considered of value in the area potentially affected by hazards.
Consequence	The outcomes for elements at risk, given impact by a geohazard. In this report, consequences considered include potential loss of life, and potential damage to buildings and infrastructure.
Risk	Likelihood of a geohazard scenario occurring and resulting in a particular severity of consequence. In this report, risk is defined in terms of safety or damage level.



2.0 STUDY OVERVIEW

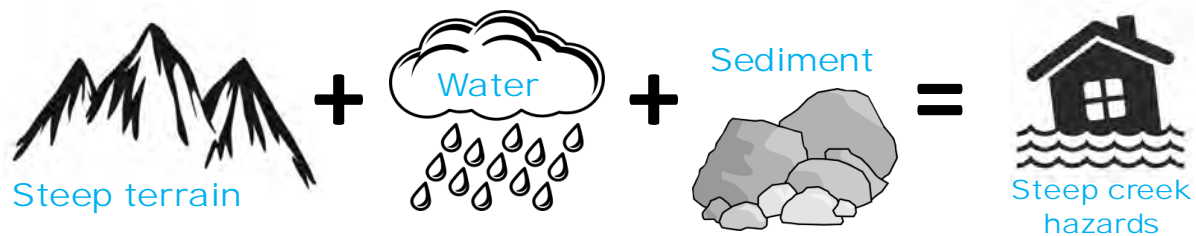
2. STUDY OVERVIEW

2.1. Introduction

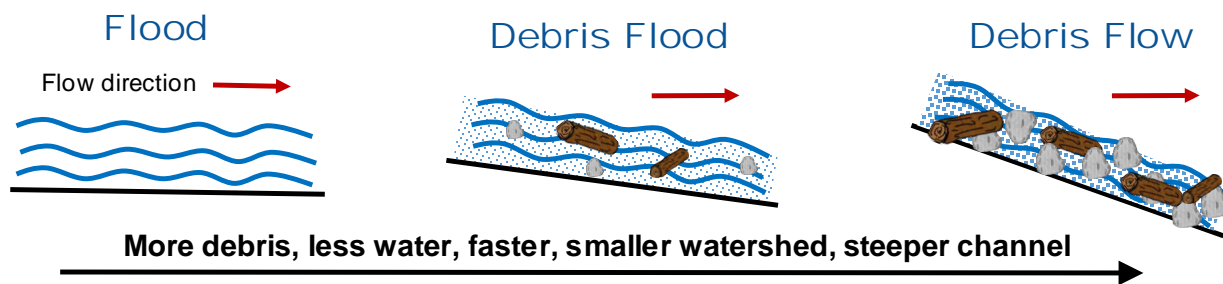
This chapter describes the motivation, necessity and importance of this study, and provides an introduction to steep creek hazards.

2.2. What Are Steep Creek Hazards?

Steep creek or hydrogeomorphic hazards are natural hazards that involve a mixture of water (“hydro”) and debris or sediment (“geo”). These hazards typically occur on creeks and steep rivers with small watersheds (usually less than 100 km²) in mountainous terrain, usually after intense or long rainfall events, sometimes aided by snowmelt and worsened by previous forest fires.



The main types of steep creek hazards are debris floods and debris flows. Debris floods occur when large volumes of water in a creek or river entrain the gravel, cobbles and boulders on the channel bed; this is known as “full bed mobilization”. Debris floods occurred on Cougar Creek, Stoneworks Creek, Three Sisters Creek and several other creeks in the Bow Valley in June 2013. Debris flows involve higher sediment concentrations than debris floods, and may have a consistency similar to wet concrete. Debris flows occurred on X and Y Creeks in June 2013. It’s easiest to think about hydrogeomorphic hazards as occurring in a continuum, as shown below.



In terms of peak discharge, flood, debris flood and debris flow processes can differ widely. A 200-year return period normal flood (with a 0.5% chance of occurrence in any given year) on a given steep creek will typically have a lower discharge than a debris flood with a similar return period on the same creek. If the creek is subject to debris flows, the peak flow may be even higher. Debris floods generated from outbursts of glacial-, beaver-, moraine- or landslide dams can result in sediment concentrations 10 to 30% higher than those of clearwater floods. Debris floods with such high sediment concentrations are better characterized as hyperconcentrated floods. However, “conventional” debris floods are now defined by BGC as floods that mobilize at least

the 80% percentile of all grains and in which the entire surface layer of a gravel bed stream becomes mobile. In those cases, sediment concentrations are believed to be substantially lower (perhaps 3 to 10%) compared to dam outburst floods. As such, it forms a direct continuum with clearwater floods. Higher sediment concentration events (10 to 30%) are considered hyperconcentrated floods (i.e., Pierson, 2005).

Figure 2-1 shows the cross-section of a steep creek, including:

- Peak flow for the 1-year return period (Q_1)
- Peak flow for the 200-year return period normal flood (Q_{200})
- Peak flow for the 200-year debris flood ($Q_{200 \text{ debris flood}}$)
- Peak flow for the 200-year debris flow ($Q_{200 \text{ debris flow}}$).

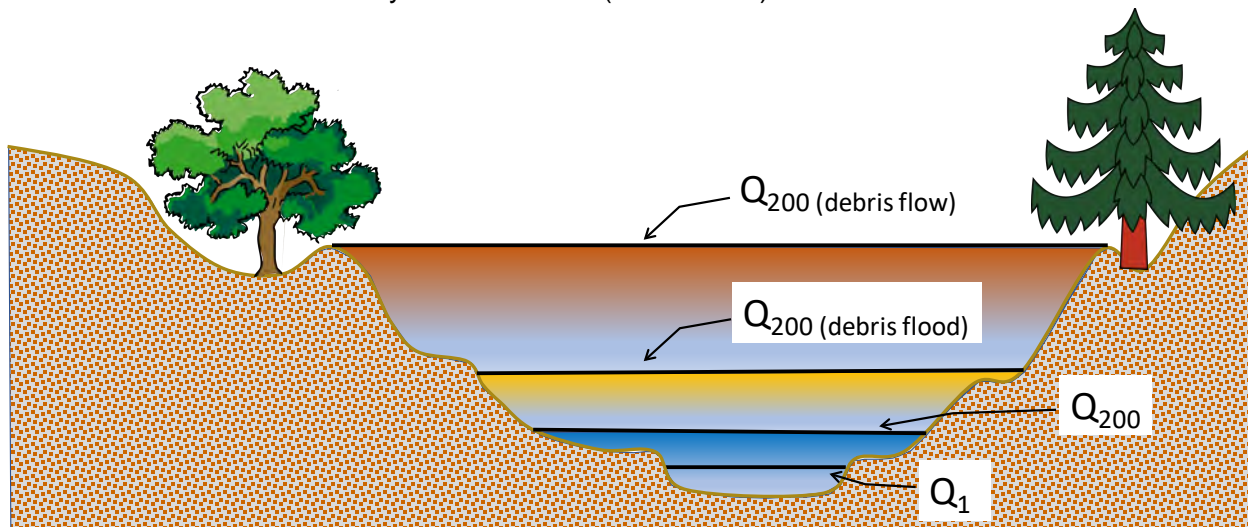


Figure 2-1. Steep creek flood profile showing peak flow levels for different events.

This difference in peak discharge is one of the reasons that process-type identification is very important for steep creeks. If a bridge is designed for a 200-year flood, but subject to a debris flow with a much larger peak discharge, the bridge would likely be damaged or destroyed. Appendix A provides additional technical details about debris flows and debris floods.

2.3. Regional Setting

The following section provides a technical summary of the study area physiography, geology, and climate.

2.3.1. Physiography

X, Y, and Z Creeks are situated on the northeast facing valley wall of the Bow River within the Rocky Mountain Natural Region in southwestern Alberta. This region is characterized by mountainous terrain with steep slopes, pronounced ridges, and valleys carved out by repeated glaciation. Vegetation includes a mix of grasslands and coniferous and deciduous forests in the valleys, and predominantly coniferous trees along valley walls. At higher elevations vegetation is sparse and soil depth is shallow over bedrock (Natural Regions Committee, 2006).

Airborne lidar for the study area was collected in 2009, 2013 and 2015, and provided to BGC by various sources (Table 2-1). Lidar is a remote sensing method that uses non-destructive lasers to measure the location and elevation of the ground surface. In this study, lidar was used for analysis of the watershed and fan characteristics and to contribute to parts of the hazard analysis. Table 2-1 provides a summary of the data set attributes. The data resolution is reported as average points per square metre and is variable across the region depending on the level of vegetation and slope angle. Areas with a greater density of vegetation will have a lower density of points. Steeper slopes will have a lower point density than flat surfaces with similar vegetation cover.

Table 2-1. Summary of lidar data sets used.

Date Flown (year)	Bare Earth Point Density	Source (Lidar Provider)
2009	0.6 pts/m ²	Alberta ESRD (McElhanney)
2013	2.7 pts/m ²	Town of Canmore (Lidar Services International Inc.)
2015	4.8 pts/m ²	Alberta Environment and Parks (Airborne Imaging)

2.3.2. Geology

The Rocky Mountain Region’s topography is characterized by steeply inclined and folded sedimentary bedrock of Devonian to Cretaceous age (approximately 420 to 66 million years old) with very little soil development. Lithologies in the X, Y and Z creek watersheds include dolomite, limestone, siltstone and shale. Slopes mantled by talus and colluvial slopes are common near the mountain tops, which provide sediment sources for debris flows and debris floods. At high elevations periglacial landforms (formed by alpine permafrost) are observed, often on north-facing slopes (Natural Regions Committee, 2006). Along the valley sides, glacial deposits including till, glacial fluvial and morainal deposits prevail and preserve some sediment from the last glacial maximum approximately 10,000 years ago. Low-lying valleys contain fluvial deposits from large rivers, such as the Bow River, and smaller tributaries, such as X, Y, and Z creeks.

2.3.3. Climate

As there are no weather stations in the X, Y and Z creek watersheds, climate normal data were obtained from Environment and Climate Change Canada’s Kananaskis station (1391 m elevation), located approximately 30 km southeast of Canmore (Environment and Climate Change Canada, n.d.). Daily precipitation and temperature data are available from 1939 to 2017. Figure 2-2 shows the average temperature and precipitation for this station from the 1981 to 2000 climate normals. Precipitation peaks in May and June, with mixed rainfall/snowfall in May and heavier rainfall in June. Some variation in precipitation is expected between this weather station and the local weather in the X, Y, and Z creek watersheds, where the mountaintops are more than 1000 m higher than the Kananaskis weather station, which is located in the bottom of the Bow River Valley. Rainstorms with strong convection leading to tall thunderstorm clouds will lead to more rainfall at higher elevation than in the valley bottom, as will orographic influences for larger

frontal systems. As most precipitation gauges are situated in valley bottoms, this may lead to an underestimate of the actual precipitation occurring at high elevation. A new weather station, installed in 2017 in the upper Cougar Creek watershed, is expected to yield precipitation amounts that may be similar to the upper reaches of X, Y and Z creeks.

Details on the rainfall, snowpack and streamflow characteristics of the June 19-21, 2013 storm event that triggered the 2013 debris flows on X and Y creeks and flooding on Z Creek were previously documented by BGC (August 1, 2014) and other sources (Pomeroy et al., 2016; Li et al., 2017; Teufel et al., 2017).

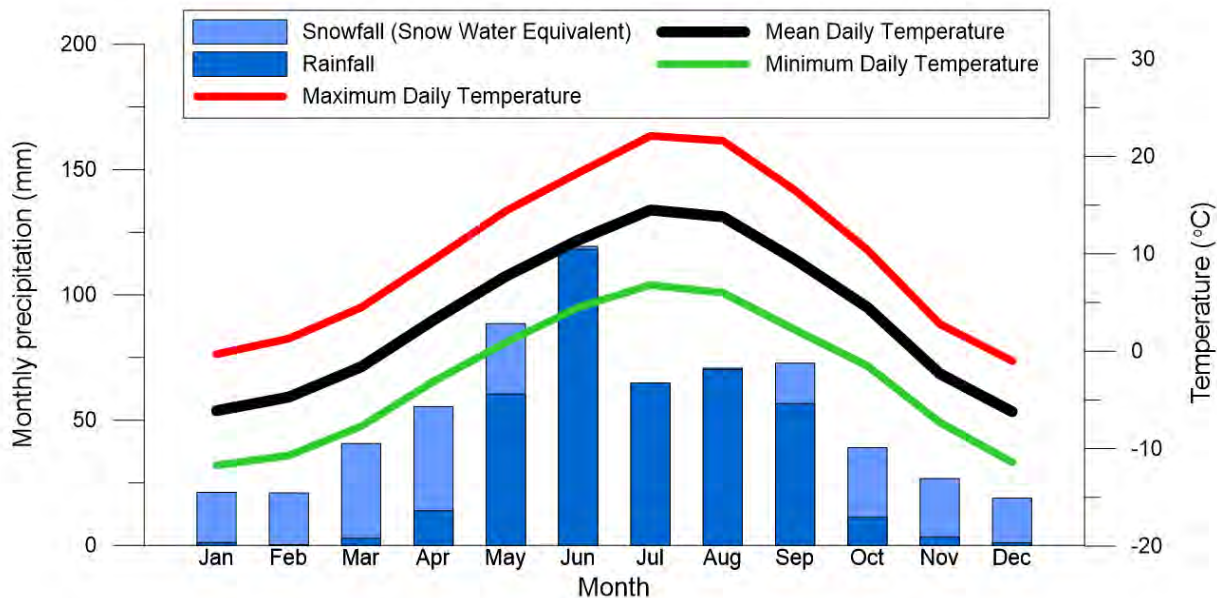


Figure 2-2. Climate normals for 1981 to 2000 period for the Kananaskis climate station. Data were acquired from Environment and Climate Change Canada (ECCC, 2011).

2.4. Local Setting – X, Y and Z Creeks

X, Y, and Z creeks are small creeks on the southwest side of the Bow River valley without direct connectivity to Bow River. Instead they discharge into the stormwater drainage system within the Peaks of Grassi development. Drawing 01 shows the watershed and fan boundaries, and Table 2-2 summarizes geomorphic parameters of the three creeks. Appendix B shows a drawing of the Peaks of Grassi stormwater system provided to BGC by Canmore.

Table 2-2. Watershed characteristics of X, Y and Z Creeks.

Characteristic	X Creek	Y Creek	Z Creek
Watershed area (km ²)	2.62	0.44	0.23
Fan area (km ²)	0.45	0.088	0.063
Maximum watershed elevation (m)	2,706	2,527	2,420
Minimum watershed elevation (m)	1,538	1,513	1,478
Watershed relief (m)	1,168	1,014	942

Characteristic	X Creek	Y Creek	Z Creek
Melton Ratio (km/km) ¹	0.72	1.53	1.96
Average channel gradient of mainstem above fan apex (%)	29	51	47
Average channel gradient on fan (%)	17	21	21
Average fan gradient (%)	21	24	23

These geomorphic parameters indicate that X Creek is a mid-sized watershed and fan, similar in size to Echo Canyon Creek and Stones Canyon Creek, the latter of which has previously been studied by BGC in detail (October 28, 2015). Y and Z creeks have comparatively smaller watersheds, but are steeper than X Creek, with more limited sediment availability. All three fans have similar gradients. Figure 2-3 illustrates the area relationship between the fan and watershed relative to 825 steep creeks in Alberta and British Columbia, with the Bow River Valley steep creeks shown for reference. All three watersheds/fans lie within the scatter of the existing steep creek Bow River Valley dataset, indicating that the fans are not abnormally large or small for their respective watershed size.

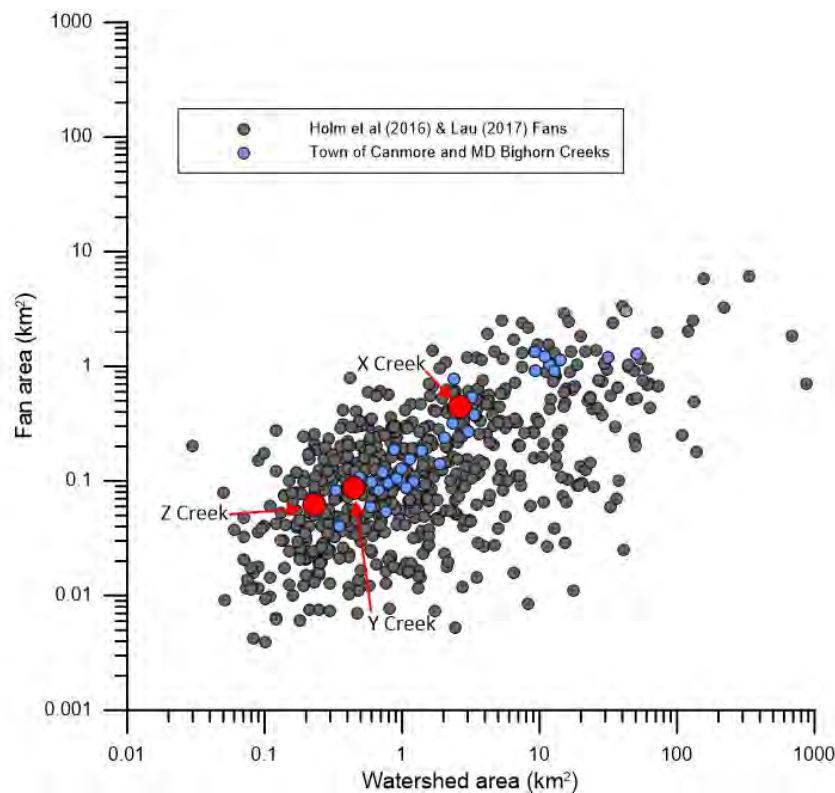


Figure 2-3. Watershed area versus fan area for 825 steep creeks in AB and BC (data from Holm, Jakob, Scordo, Strouth, Wang, & Adhikari, 2016 and Lau, 2017). X, Y, and Z Creek data are plotted as large red dots, while Bow Valley creeks are shown in blue.

¹ Melton ratio is an indicator of the relative susceptibility of a watershed to debris flows, debris floods or floods. See section 2.4.1 below.

2.4.1. Steep Creek Hazards

Figure 2-4 summarizes X, Y and Z creeks with respect to Melton Ratio and watershed length, which indicate the tendency of a creek to produce floods, debris floods or debris flows. Y and Z creeks plot in the data cluster prone to debris flows, while X Creek may experience debris flows and debris floods. X, Y and Z creeks may also be subject to floods and debris floods at lower return periods, or debris flows may transition to watery afterflows in the lower runout zone and after the main debris surge.

During the June 18 to 21, 2013 event, debris flows occurred on the X Creek West tributary and on Y Creek, and a small debris flood or sediment transport event occurred on Z Creek. An initial forensic summary of this event can be found in BGC (December 2, 2013), and further analysis for each creek is presented in the results sections of this report.

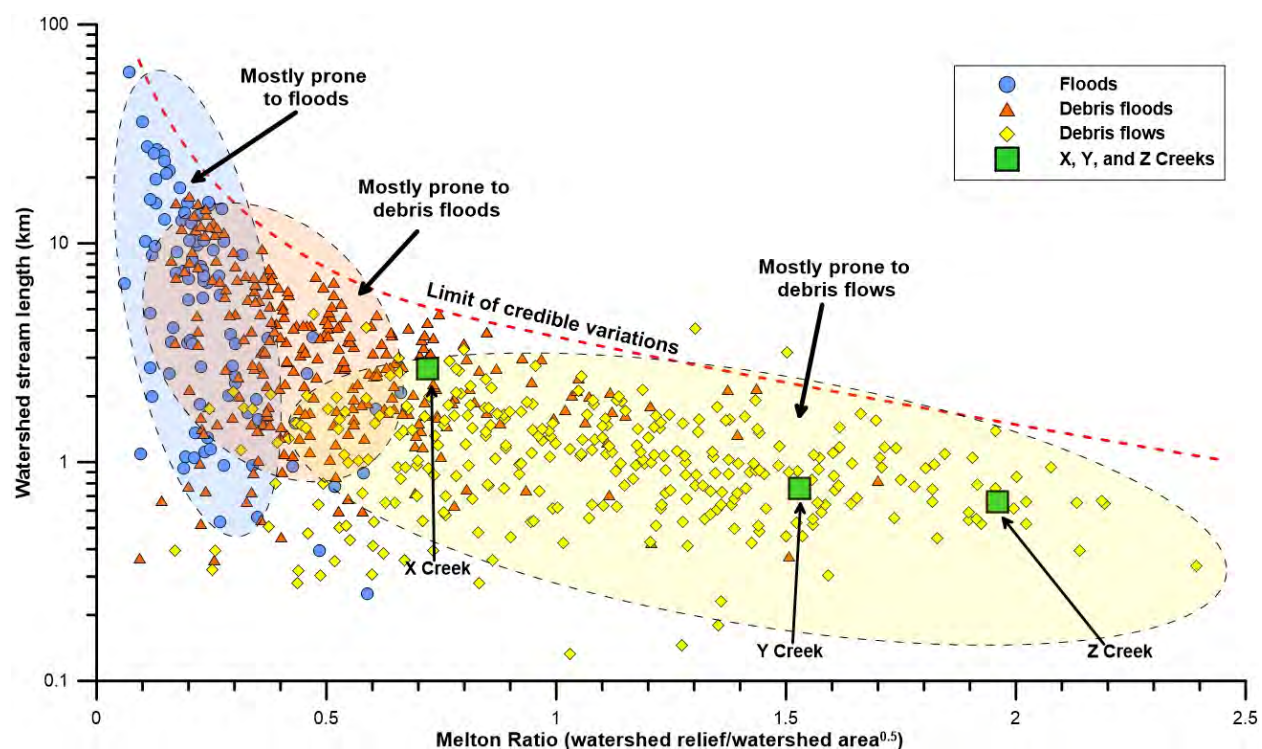


Figure 2-4. Tendency of creeks to produce floods, debris floods and debris flows, as a function of Melton Ratio and stream length (data from Holm et al., 2016). See Table 2-2 for X, Y and Z creeks watershed data.

Because each creek studied is subject to multiple steep creek hazards, BGC assessed potential hazards and risks arising from the full range of possible steep creek hazards: floods; debris floods; and debris flows. In general, the damage caused by floods, debris floods and debris flows depends on the peak discharge of the flow, and the total flow volume, including water and sediment. These quantities were assessed as part of the hazard assessment on X, Y and Z creeks.

2.4.2. Watersheds

The X, Y, and Z creek watersheds are outlined in Drawing 01, which shows a shaded, bare earth² Digital Elevation Model (DEM) of the watersheds, fans and surrounding terrain created from lidar data. The DEM was used to generate the contours shown on Drawings 01, 02, 03 and 05.

The upper watersheds of X, Y, and Z creek watersheds are characterized by steep bedrock controlled cliffs and slopes (Figure 2-5). Small streams follow bedrock fractures and form a dendritic channel network on the steep slopes. All three watersheds are prone to snow avalanches starting from the steep upper watershed slopes. As the watersheds and streams funnel towards their respective fan apex, they have incised through deposits of surficial sediment. Drawing 05 shows a geomorphic map of the study area, including specific landforms and sediment sources in the watersheds.

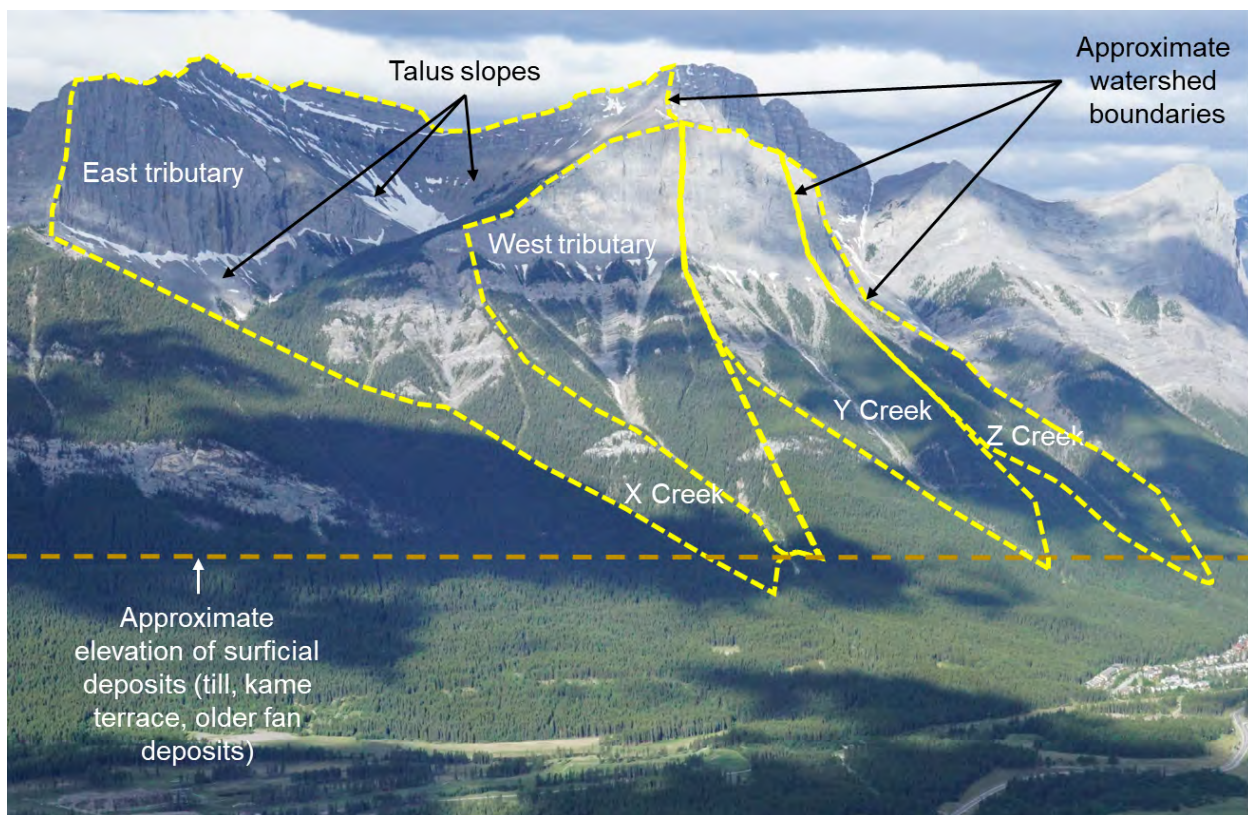


Figure 2-5. Overview of X, Y and Z Creek watersheds, including the east and west tributaries of X Creek. The Peaks of Grassi subdivision is located on the distal fan. Photo: BGC, June 13, 2018.

The X Creek watershed is composed of two sub-watersheds (Figure 2-5); the east tributary is larger (2.1 km²) than the west tributary (0.52 km²) and is characterized by a different geomorphology. The X Creek east tributary is a sediment supply-unlimited watershed, meaning that it has large amounts of sediment available to be transported down to the fan, mostly from

² Vegetation and buildings removed.

entrainment of easily eroded material such as talus and scree below the steep cliffs (Figure 2-6). The X Creek west tributary is a sediment supply-limited watershed, which requires progressive sediment recharge through erosion and weathering processes after a debris flow event, before sufficient materials has accumulated for another debris flow of the same volume to occur (Jakob, 1996). The X Creek west tributary shares similar geomorphological characteristics to the Y and Z creek watersheds and is controlled by steep bedrock slopes with snow avalanches transporting some of the annually accumulated debris in the channel to near the fan apex.

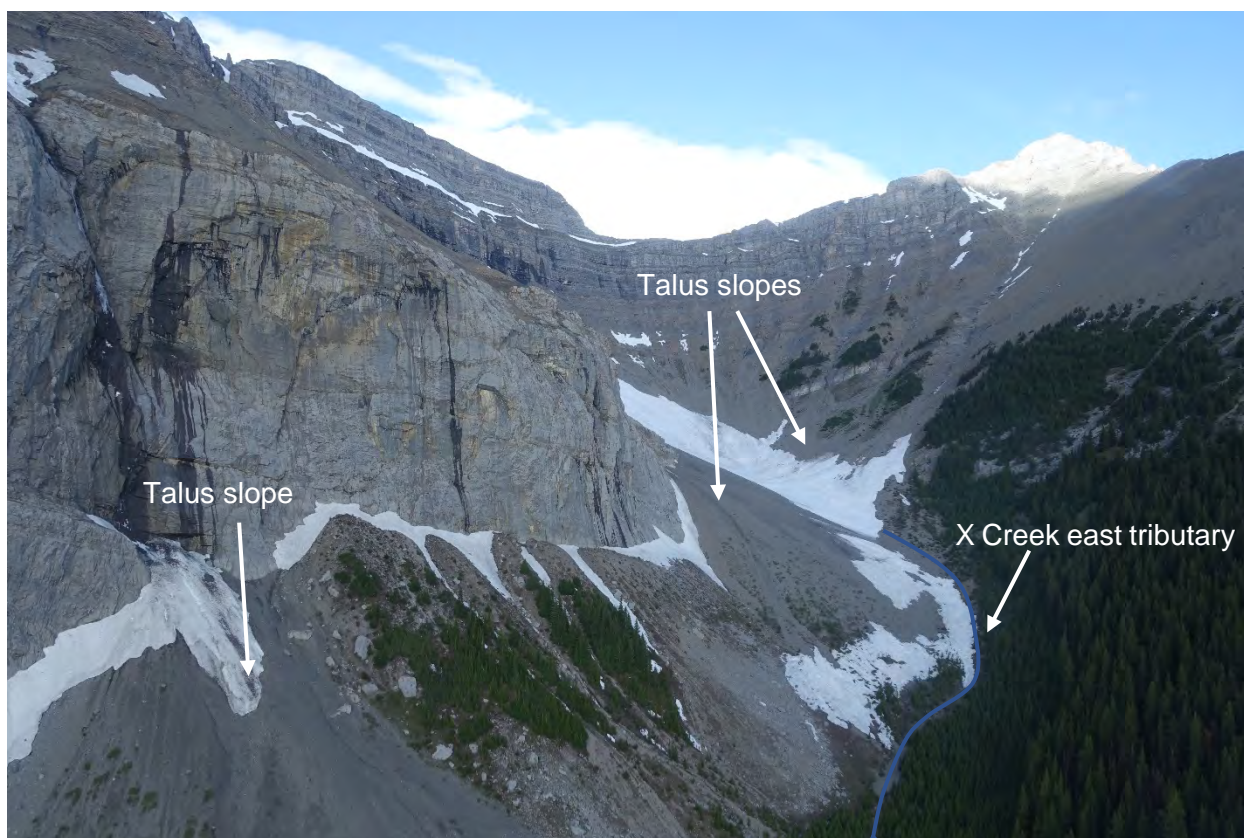


Figure 2-6. Extensive talus deposits in the upper X Creek east tributary. Photo: BGC, June 13, 2018.

The watersheds of Y and Z creeks are characterized by limited sediment supply sources, which is partially due to relative low rates of weathering and rock fall production, and partially because snow avalanches are able to transport loose channel debris to lower elevations. Y Creek stores higher volumes of debris in the upper watershed channel than Z Creek, due to the presence of a rock slide deposit of unknown age (Figure 2-7) that extends from the rock cliffs to an approximate elevation of 1800 m (approximately 250 m above the fan apex). The supply limitations in these watersheds reduce the maximum amount of debris that can be recruited in debris floods and debris flows from the watershed.

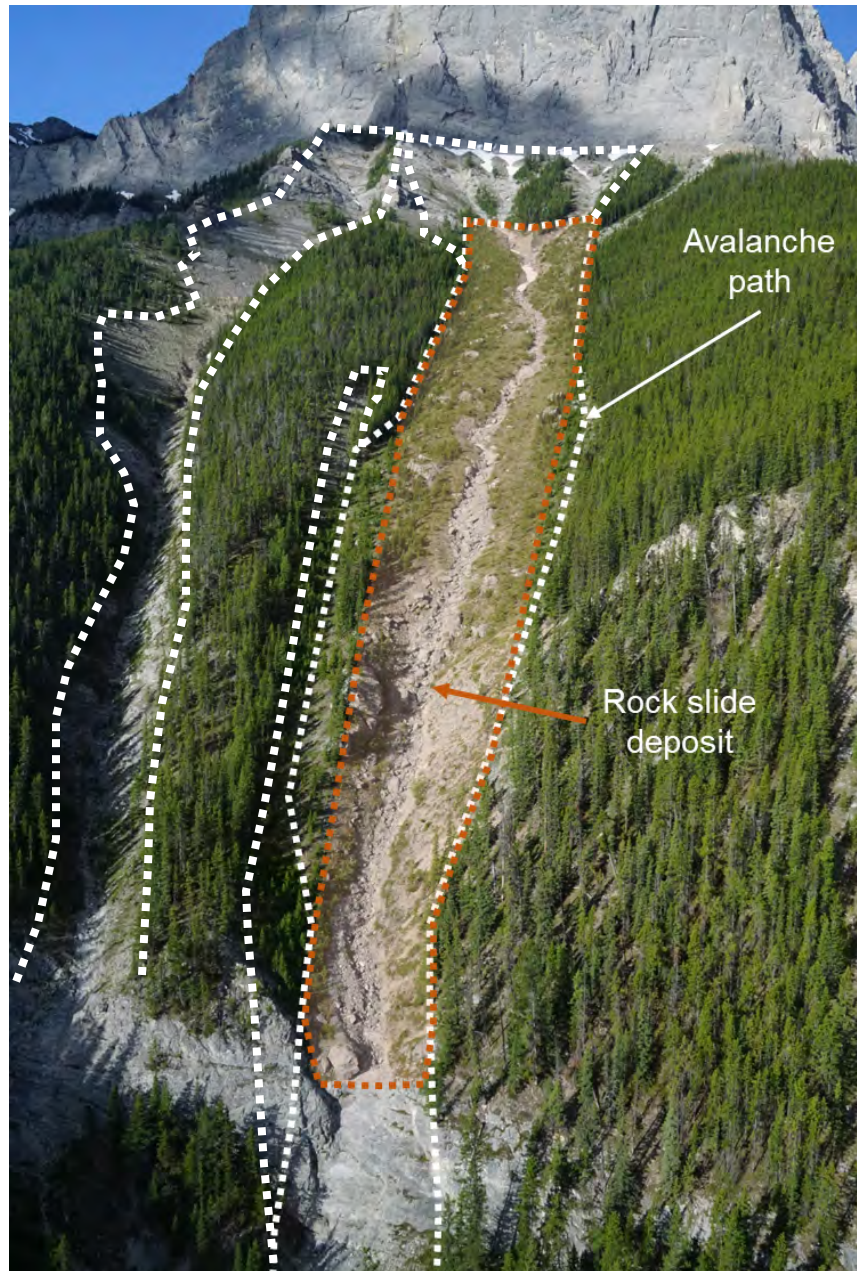


Figure 2-7. Aerial view of the upper Y Creek watershed showing three avalanche paths (delineated in white dashed lines) and a rock slide deposit. This channel has significantly more debris storage than Z Creek and can produce larger debris flows. Photo: BGC, June 12, 2018.

2.4.3. Fan Characteristics

The fans of X, Y, and Z creeks are shown on three drawings. Drawing 01 shows an overview of the fans in relation to the watersheds. Drawing 02 shows higher detail of the fans with the 2015 lidar DEM hillshade, while Drawing 03 shows the same area on the 2013 orthoimagery. The fan areas delineated on these drawings have been interpreted by BGC based on the lidar data; the exact fan boundary for all fans is difficult to define due to the re-grading that occurred as part of

the Peaks of Grassi development. Future landscape alterations, as well as additional assessments and major future debris flows or floods (and their associated sediment deposition and erosion), may change the fan boundaries in some areas.

The fan apex for all three streams is at approximately 1500 m elevation, which coincides with the approximate elevation of extensive surficial deposits (till, kame terrace, older fan deposits) along the Bow River Valley (Figure 2-5). The streams have eroded into these deposits and deposited this material, along with material sourced from the watershed, onto the fans. Y and Z creeks descend over waterfalls approximately 100 m upslope of the fan apex. Snow avalanche paths, as indicated by the lack of mature conifers on orthophotos, were mapped to extend all the way to the fan apices on all three creeks.

X Creek fan has a lobate appearance rather than a radial cone shape, as the fan gradually deposited in the low areas between various glacial landforms and bedrock ridges. This effect is referred to as a “telescoping” or “segmented” alluvial fan (Ryder, 1971; Bull, 1977). The X Creek fan surface has also been modified due to historical coal mining activity, particularly on the distal fan (Gadd, 2013). Coal mining ceased in the Bow River Valley in the mid-1970s. Trails, access roads and right-of-ways traverse the X Creek fan.

Y and Z creeks have created fans on a benched slope above the Peaks of Grassi development. This bench is interpreted to be a mixture of remnant kame terraces and glacially sculpted outcrops of sedimentary bedrock. Small gullies just beyond the toe of the Y Creek fan indicate that some flow from Y Creek goes over the “lip” of a 50 m long, 40% steep slope above the Peaks of Grassi subdivision (Drawing 02). It is not clear when the erosion of these gullies occurred.

2.4.4. Existing Mitigation

Flood diversion structures exist on the X, Y and Z creek fans, as shown on Figure 2-8. According to Canmore, the structures were constructed concurrently with the development in the late 1990s. The structures are constructed in V-shaped pairs, as shown in Figure 2-8. They consist of short, wooden walls that are between 0.4 and 0.8 m high, with riprap-lined ditches on the upstream side to convey surface flows and avoid erosion of the wall foundations (Figure 2-9). The walls are intended to direct and route flows into shallow riprap-lined channels, which lead to the storm drain system (Figure 2-10). The channels are between 26 and 50 m long, about 2 m wide and pass between houses. On the eastern Y Creek fan, one lot was left unoccupied adjacent to the channel.

After a July 2012 event on Y Creek (see Section 5.1.1), the eastern Y Creek wood wall was extended an additional 40 m to protect additional homes.

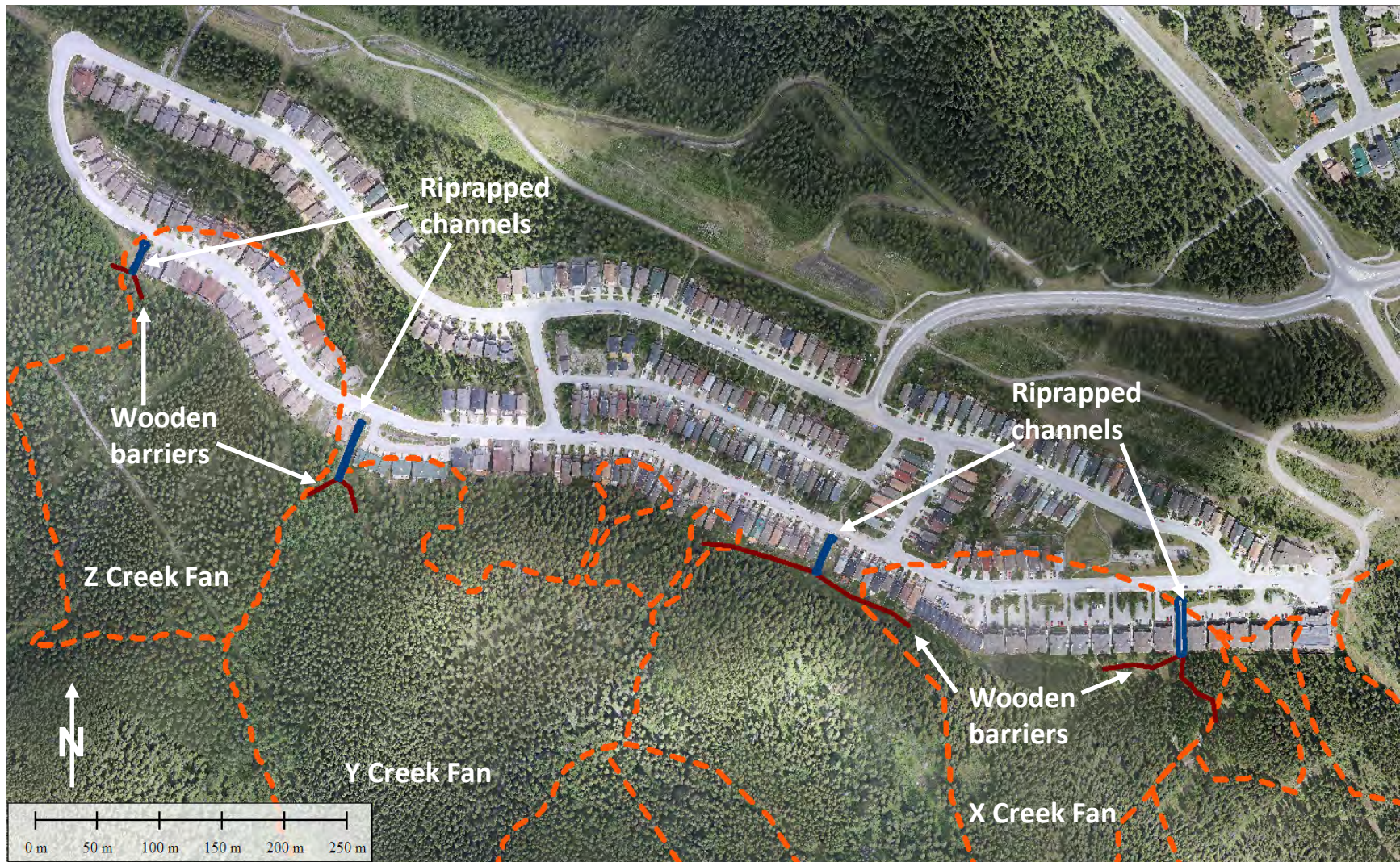


Figure 2-8. Locations of wooden walls (brown lines) and riprapped channels (blue outlines). Fans are outlined with dashed orange lines.



Figure 2-9. Two wooden walls on the western side of the Z Creek fan. The walls are aligned in a V shape, to funnel water into a riprap-lined ditch (Figure 2-10). BGC photo, June 7, 2018.



Figure 2-10. Looking downstream along the western Z Creek riprapped channel. Yellow arrow points to storm drain inlet at the far end. BGC photo, June 7, 2018.

BGC did not observe an incised or identifiable channel upslope of any of the wooden walls, with the exception of the gully upstream of the eastern Y Creek wall. There are also no easily identifiable channels observed on the lidar imagery (Drawing 02) for Y and Z creeks. This suggests that the flows are either depositional at the distal fan, or not sufficiently concentrated to causes incision.

2.5. Elements at Risk

Appendix E provides a detailed summary of elements at risk within the study area. The study area intersects the Peaks of Grassi development in Canmore. Existing development intersects the distal portions (situated away from the centre of the fan) of the mapped fan boundaries on Y and Z creeks. The mapped fan boundaries of X Creek intersect resort facilities at the distal edge of the fan. Land use in the surrounding area is a mix of residential (single family homes, duplex, and townhouses) and commercial (resort accommodations). 2014 Census summaries (Canmore 2015) indicate a population of approximately 927 residents.

The total estimated value of development in the study areas is \$151M in taxable building “improvements”, (Canmore 2018). Assessed building values do not necessarily correspond to replacement value, which may be higher.

Table 2-3 lists the elements at risk considered in this assessment. Table 2-3 does not include all elements that could suffer direct or indirect consequences due to a geohazard event and focuses on those that can be reasonably assessed based on the information available. Only building structures and persons within buildings were systematically included in the economic and safety risk analyses. The remaining elements were considered in terms of their location and characteristics within steep creek hazard areas, but vulnerability or risk was not quantified.

Table 2-3. List of elements at risk considered in the risk assessment.

Element at Risk	Description
Building Structures	Commercial, residential, transportation.
Persons	Persons located within buildings.
Lifelines	Sewerage, stormwater management, gas distribution, electrical power and telephone line distribution, roads ¹ .
Critical facilities	Facilities critical for function during a hazard event ² None Identified.
Business activity	Businesses located on the fan that have the potential to be directly impacted by geohazards, either due to building damage or interruption of business activity due to loss of access.
Cultural/ecological significance	Peaks of Grassi Park, Highline Trail, Powerline Trail.

Notes:

Local roads include: Kamenka Green, Lawrence Grassi Ridge, Peaks Drive, Shellian Lane, Three Sisters Drive, and Wilson Way. Further definition of critical facilities is provided in Appendix E.

2.6. Summary

X, Y, and Z Creeks are mountainous creeks in the Bow River Valley that are subject to steep creek hazards. Since deglaciation some 10,000 years ago, the creeks have formed fans from repeated steep creek processes and other geohazards, including floods, debris floods, debris flows, snow avalanches, rock fall, and rock slides. Steep creek hazards have in the past affected the Peaks of Grassi subdivision on the distal margins of the alluvial fans, although no debris flow has been recorded to have impacted the subdivision since its construction in the late 1990s.

The following section will explain the various methods used to decipher the frequency-magnitude relationships of floods, debris flows and debris floods on X, Y and Z creeks, and estimate their respective risk.



3. METHODS

3. METHODS

3.1. Introduction

This chapter summarizes the methods employed by BGC to determine the frequency and magnitude of steep creek hazards on X, Y and Z creeks, as well as the runout modeling methodology, risk assessment and mitigation design methods. Additional detail about the methods are provided in the following appendices:

- Appendix C – Test Pit Detailed Logs and Photograph Logs
- Appendix D – Test Pit Sample Testing Results
- Appendix E – Risk Assessment Methods.

3.2. Hazard Assessment Background

This section introduces steep creek hazard assessment for readers who may be new to this type of analysis. The specific hazard assessment methods are described in more detail in Sections 3.3 through 3.5.

3.2.1. Frequency-Magnitude Relationships

Frequency-magnitude (F-M) relations answers the question “how often and how big can steep creek hazard events become?”. The ultimate objective of an F-M analysis is to develop a graph that relates the return period of the hazard to its magnitude. Figure 3-1 shows this conceptually. The red line (i.e., event magnitude) levels off at some point because of either sediment supply or water limitations. This means that debris flows and debris floods from a given watershed have a maximum possible sediment volume and peak discharge.

Any F-M calculation that spans time scales of millennia necessarily includes some judgment and assumptions, both of which are subject to some degree of uncertainty. Quantification of this uncertainty is often difficult, and judgement is required to assess the appropriate degree of conservatism, particularly when life loss risk and mitigation design are involved. Design decisions are also complicated by a changing climate.

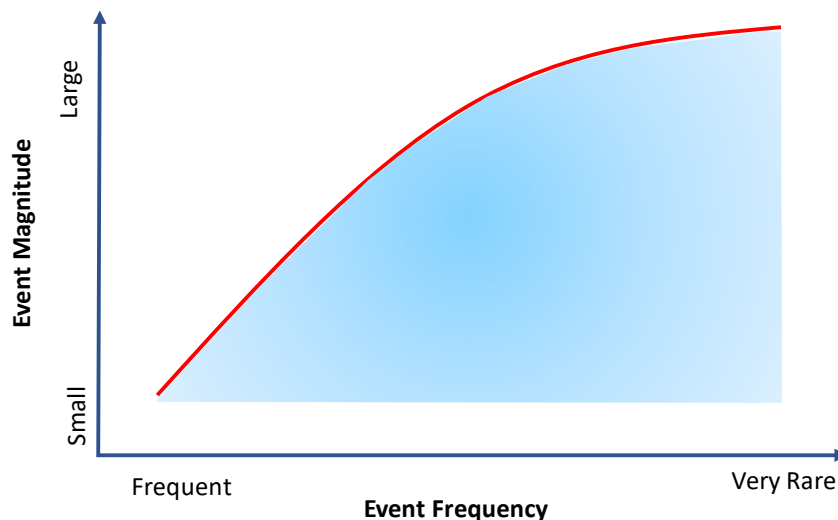


Figure 3-1. Conceptual frequency-magnitude curve.

Once events have been documented and their age and volume estimated, return period ranges need to be assigned to individual events that allow extrapolation and interpolation into annual probabilities beyond those extracted from the physical record. Such record extension is necessary to develop quasi-continuous event scenarios that then form the basis of numerical runoff modeling and the consequence analysis that forms part of the risk assessment.

The analysis described in this section is based on the best data available and is considered appropriate for the scale and level of detail of this assessment.

3.2.2. Return Period Classes

This report uses the terms “frequency”, “hazard probability” and “return period” interchangeably, depending on the context. Frequency is numerically equivalent to long-term hazard probability. It is defined as the annual probability of occurrence of a hazard scenario. Return period is the inverse of frequency, and it is defined as the average recurrence interval (in years) of a hazard scenario. For example, an annual frequency of 0.01 corresponds to a 100-year return period.

Five return period classes were defined for the work. These classes correspond to those recommended in the draft AEP guidelines (BGC, March 31, 2017) and are consistent with BGC’s previous Canmore work.

- 10 to 30 years
- 30 to 100 years
- 100 to 300 years
- 300 to 1000 years
- 1000 to 3000 years.

The residual risks associated with higher return periods (i.e., >3000 years) were not considered, as they are associated with very high uncertainty and are typically outside of the range of dating methods that can be applied to such steep creek hazard and risk studies.

3.2.3. Hazard Assessment Workflow

The flowchart shown in Figure 3-2 outlines the workflow for the hazard assessment portion of the project. The objective of the hazard assessment is to develop F-M relationships for peak discharge and debris-flood/debris-flow sediment volume. This, in turn, will form part of the input to the numerical model (FLO-2D), which then allows the simulation of clearwater floods, debris floods, and debris flows on each fan and for each return period.

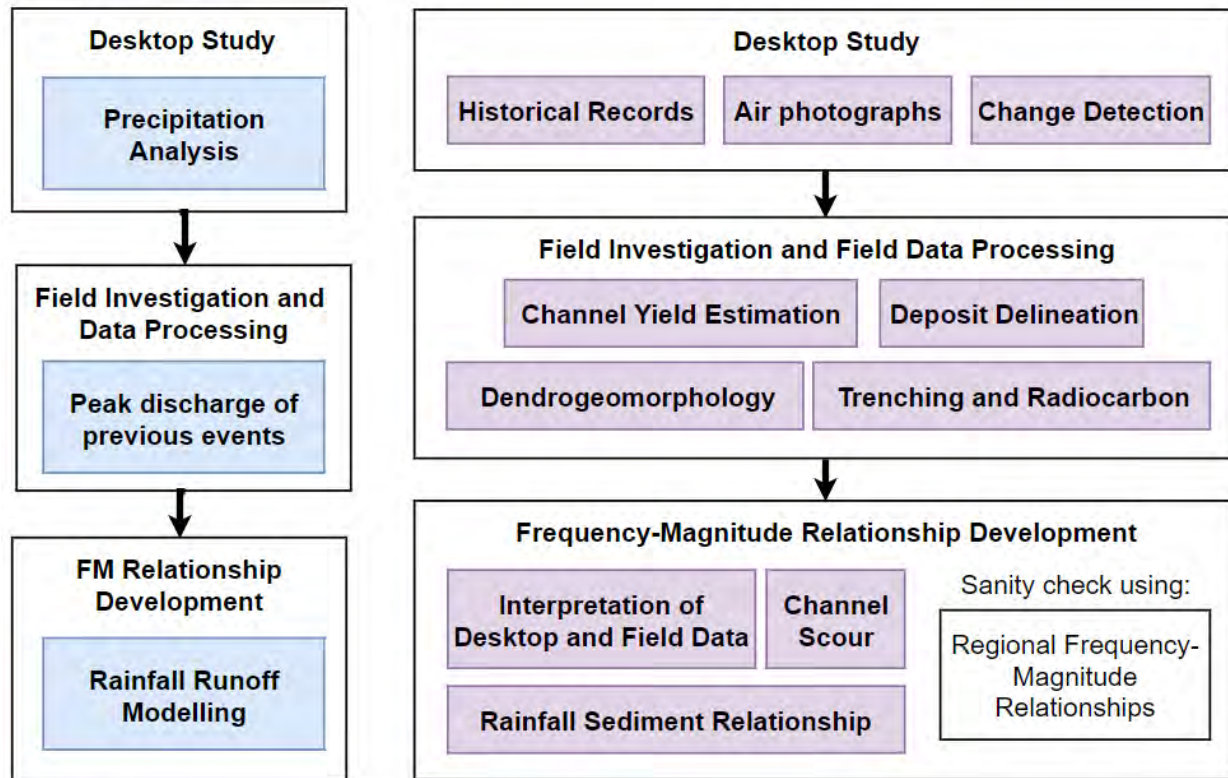


Figure 3-2. Workflow used to develop F-M relationships for X, Y and Z Creeks, for floods and debris floods (blue) and debris flows (purple).

The peak discharge assessment is presented in Section 3.3. The debris-flow sediment volume assessment is split into two sections: Section 3.4 addresses the desktop study, field investigation and data processing steps; and Section 3.5 addresses the F-M relationship.

3.3. Flood and Debris Flood Peak Discharge Assessment

3.3.1. Rainfall Analysis

Unlike debris flows, which may involve significant progressive sediment bulking³ due to entrainment of loose or poorly consolidated debris throughout their transport zone, floods and debris floods have a limited capacity of sediment entrainment and transport. Instead, the duration of runoff above a given entrainment threshold will determine the volume of debris transported in the event. Therefore, one of the first steps for assessing flood and debris flood sediment volume is to develop flood hydrographs for various return period events. This in turn requires an estimate of rainfall for various durations and return periods which is accomplished by frequency analyses of historical rainfall data from nearby climate stations.

The most relevant station with a long-term record is the Kananaskis climate station, located approximately 30 km east of X, Y, and Z creeks. This station has 12 years of recorded data with 15-minute precipitation reading intervals between 1982 to 1998 (not including 1983, 1989, 1992 and 1994), and an additional 62 years of data with daily precipitation reading intervals between 1940 and 2017.

The Kananaskis data were analyzed using a statistical computing software (R, Version 3.5.1, 2018), to assess the magnitude of 24-hour precipitation events with return periods ranging from 10 years to 3000 years. Daily rainfall values were converted to 24-hour maximum daily rainfall values by multiplication of a factor of 1.1, which is the average ratio between measured daily and 24-hour maximum rainfall values for the period 1982-1998 at the Kananaskis station (as calculated by BGC from the data). This adjustment is intended to correct for storms that may not occur within a midnight-to-midnight 24-hour period. The resulting 24-hour rainfall frequency analysis is illustrated in Figure 3-3 for the 74-year dataset. Results for three probability distributions are shown: GEV (linear moments), log Pearson Type III, and GEV (maximum likelihood estimates). Where the dataset exceeds 50 years, the GEV (lm) distribution is generally considered most accurate.

³ Note that, in its original meaning Costa (1985) used the term 'flow bulking' referred to the volumetric expansion of a debris flood by the incorporation of a significant volume of sediment. More recently, it has been used in the case of debris flows to scale the peak flow and volume in comparison with the peak flow of a clearwater flow of similar return periods. In this case, the peak flow and volume increase are caused by water addition due to temporary damming and release downstream, and/or in high flow velocities leading to incorporation of additional water and sediment in the channel and side slopes downstream. Bulking from these processes can increase peak flows by one to two orders of magnitude over the comparable clear water peak flows.

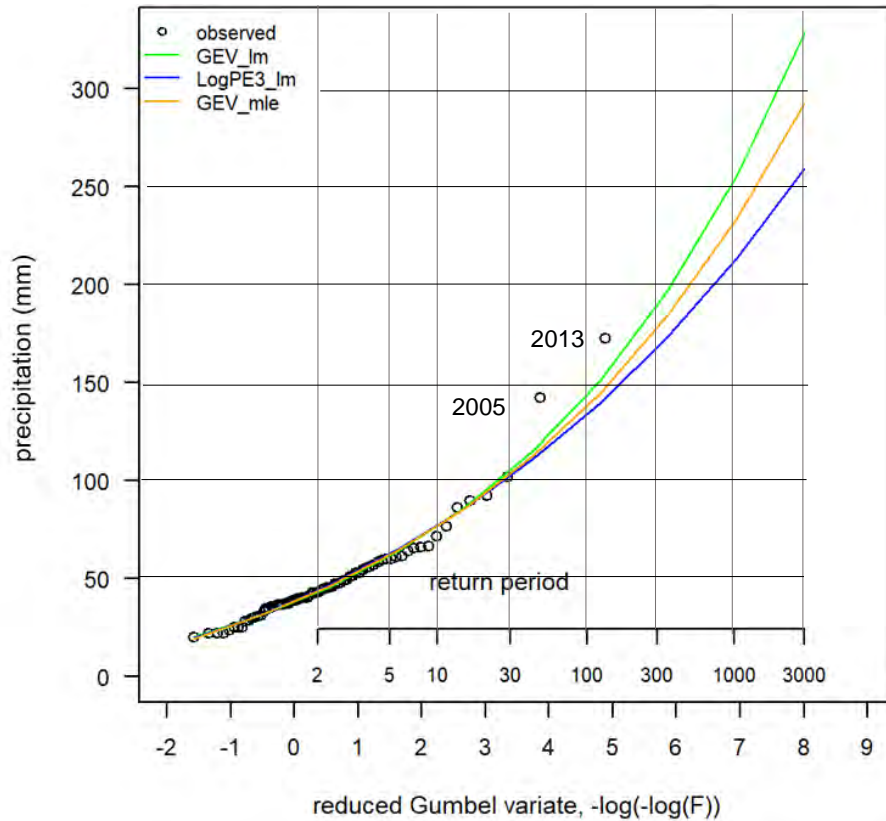


Figure 3-3. R-generated 24-hour rainfall frequency analysis of the Kananaskis climate station for the period 1940 to 2017 (R, Version 3.5.1).

The GEV (maximum likelihood estimates) distribution was selected to estimate the 24-hour rainfall for each return period, as summarized in Table 3-1. It is notable that the two largest events (June 18-21, 2013 and 2005) plot outside of the predicted range for all three distributions. This likely suggests a different meteorological signal of the triggering storm, and ideally should be analyzed separately. However, given that only two of such storms have been recorded, it is not suitable for statistical analysis. An alternative could be to exclude these two data points from the analysis, but critical information may be lost by doing so. It would also flatten the frequency curves, which, in light of the extreme nature of the 2005 and 2013 events would be unconservative.

Table 3-1. Summary of 24-hour rainfall at the Kananaskis (3053600) climate station using data from 1940 to 2017 with GEV distribution.

24-hour Maximum Precipitation (mm)	Return Period (Years)					
	10	30	100	300	1000	3000
Upper 95 th percentile	89	128	188	263	377	518
Best fit	77	103	138	178	232	292
Lower 95 th percentile	65	78	89	92	86	66

Note that all values reported in Table 3-1 are imputed based on the GEV distribution shown in Figure 3-3.

Although the gauge has a relatively long period of record (74 years), the uncertainty associated with the discharge estimates increases considerably for return periods that exceed the record length (i.e., 300-year, 1000-year and 3000-year return period estimates). This uncertainty is captured in the upper and lower 95th percentiles calculated for each return period event (Table 3-1). To confirm that the 3000-year return period precipitation event is reasonable, it was compared with the probable maximum precipitation (PMP) for the Elbow River basin (Kappel et al., 2018) and Cougar Creek (nhc, 2017), which were 294 to 376 mm and 400 mm respectively for the 24-hour event. The 24-hour, 3000-year return period estimate of 292 mm seems reasonable compared to these values, as one would expect an asymptotic decline in rainfall at the highest return periods due to meteorological limitations. Conversely, the upper 95th percentile estimates appear to be over-estimates. While the PMP does not have a statistically-based return period, it is generally associated with a return period of approximately 10,000 years.

3.3.2. Peak Discharge Estimation from Cross-Sections

The rainfall frequency analysis described in the previous section is the primary input for estimating peak discharges based on rainfall-runoff modelling. Calibration for such modelling can be provided by highwater marks in the channel. During the field work on May 8 and June 11 to 13, 2018, BGC observed high-water mark cross-sections on X, Y and Z creeks as follows:

- 3 sections on the X Creek east tributary
- 2 sections on the X Creek west tributary
- 2 sections on X Creek downstream of the tributary confluence
- 2 sections on Y Creek
- 3 sections on Z Creek.

The high-water marks on some of these sections are likely associated with the June 2013 event, and their locations are shown on Drawings 01 and 02. Where possible, bedrock-controlled cross-sections were measured, as they produce more reliable discharge estimates. In sections that are not bedrock controlled, subsequent erosion or aggradation after or during the June 2013 event may have caused inaccurate discharge values.

Channel depth, width, and gradient were measured at each of the high-water marks. Discharge calculations also depend on the Manning's *n* value, which is a measure of stream bed roughness. Manning's *n* value was calculated using the formula from Jarrett (1985) as shown in [Equation 3-1, who investigated roughness coefficients for steep cobble-boulder streams in Colorado with channel gradients up to 5%. Jarrett's formula is a function of channel slope and hydraulic radius:

$$n = 0.39s^{0.38}R^{-0.16} \quad \text{[Equation 3-1]}$$

where *s* is channel gradient (ft/ft) and *R* is the hydraulic radius⁴ (ft).

Jarrett's research focused on streams with channel gradients of less than 5%, while channel gradients at the measured cross-sections ranged from 18% to 45% and thus may not be readily

⁴ The ratio of the cross-sectional area of the channel to the wetted perimeter

applicable. Therefore, BGC also applied two additional discharge calculation methods: Prochaska, Santi, Higgins & Cannon (2008) and Zimmerman (2010). Estimates from all three methods are reported in the results sections.

3.3.3. Rainfall-Runoff Modelling

Rainfall-runoff modelling uses the results of the precipitation analysis (Section 3.3.1) to estimate clearwater peak flows for various return periods. Rainfall runoff is affected by several factors, including the extent and type of ground cover in the watershed, and the watershed size. The purpose of conducting the rainfall-runoff modelling was to develop a flood frequency analysis (FFA) for return periods ranging from 10 to 3000 years. An indirect method is required as streamflow is not gauged on any of the study creeks or other smaller watersheds in the Bow Valley.

Rainfall-runoff modeling was conducted using HEC-HMS (Version 4.2.1), a software developed by the US Army Corps of Engineers (USACE, 2015). HEC-HMS was selected because it is an industry standard rainfall-runoff modelling program, which has also been used to model other creeks in the Bow Valley (BGC March 7, 2014; October 31, 2014; November 16, 2015). Required inputs to HEC-HMS include:

- A storm hyetograph (rainfall distribution over time) or a 24-hour rainfall value and specified Soil Conservation Society (SCS) standard rainfall distribution. A specified hyetograph was used for the June 2013 storm model, and a Type 1 SCS 24-hour distribution was used for all other cases. The Type 1 distribution is similar to the available intensity-duration-frequency rainfall data for the Kananaskis climate station.
- The time of concentration or “lag time”: the time needed for water to flow from the most remote point in a watershed to the watershed outlet, estimated using the SCS lag time method.
- Initial abstraction (I_a) refers to all initial rainfall volume losses such as surface depression storage, vegetation interception, and infiltration. I_a was calculated assuming:

$$I_a = 0.05 \cdot \left(\frac{1000}{CN} - 10 \right) \quad \text{[Equation 3-2]}$$

as recommended by National Resource Conservation Service (NRCS) (Hawkins, Ward, Woodward & Van Mullem, 2010)

- The SCS runoff curve number (CN)⁵, a value that ranges between 0 and 100 and determines how much of the rainfall infiltrates and is being stored as soil moisture (i.e., does not contribute to the storm hydrograph and thus the effective runoff). The CN value is a function of soil type, ground cover and antecedent moisture condition which describes the soil moisture condition at the beginning of a storm. The SCS unit hydrograph method is highly dependent on the CN value; a higher CN value will cause a higher peak flow as less precipitation goes into soil storage (USDA, 1986).

⁵ SCS-CN is the Soil Conservation Service curve number which is dimensionless and lumps the effects of land use and hydrologic conditions on surface runoff. It relates direct surface runoff to rainfall.

The HEC-HMS model has previously been calibrated to the steep creeks in the Canmore area using peak flow estimates, as back-calculated from high water marks observed at a number of creeks following the June 2013 flood (e.g., Jura Creek; BGC, September 30, 2015). Those calibration efforts suggest that CN values of 65 and 79 are appropriate for vegetated and unvegetated rocky areas, respectively. The CN values listed in Table 3-2 represent a composite CN value for the respective watersheds. The resulting model inputs for each creek are summarized in Table 3-2.

Table 3-2. HEC-HMS model inputs for each creek.

Creek	CN value	Lag time (min)	Initial Abstraction (mm)
X Creek	71	16.8	5.2
Y Creek	68	6.5	6.0
Z Creek	66	6.5	5.8

The results of the rainfall-runoff modelling are presented in Sections 4.2.1, 5.2.1 and 6.2.1.

3.3.4. Impacts of Climate Change

To assess the potential impacts of climate change, the rainfall-runoff modelling was repeated with climate-change adjusted 24-hour rainfall estimates. This section describes the methods used for this analysis.

Climate change is expected to alter temperatures and precipitation in the future along with the magnitude and frequency of extreme precipitation events (Allan & Soden, 2008, Beniston & Stoffel, 2014). BGC used the University of Western Ontario’s IDF climate change tool (IDF_CC Tool 3.0) to evaluate the potential impacts of climate change on rainfall for a range of return periods. The tool was designed to analyze the effects of two Representative Carbon Pathway (RCP) scenarios (RCP 4.5 and 8.5) on rainfall events based on global climate model (GCM) outputs.

To estimate the future 24-hour rainfall totals for the study area, the IDF climate change tool uses an ensemble of 9 different bias-corrected GCMs from the Pacific Climate Impacts Consortium⁶ (PCIC) for the time period from 2050 to 2100. RCP 4.5 is a reasonably optimistic scenario that represents reaching a radiative forcing⁷ of 4.5 W/m² between now and the end of the century, accompanied by an increase in annual global temperature of 2°C over pre-industrial levels. The

⁶ The Pacific Climate Impacts Consortium (PCIC) is a climate service center out of the University of Victoria. PCIC focuses on climate studies and the impacts of a changing climate for the BC and Yukon regions.

⁷ Radiative forcing is the net radiative flux on the Earth’s atmosphere. It is expressed as power per area (Watts per square meter). Net radiative flux is the amount of energy absorbed by the Earth compared to the amount of energy redirected to space.

RCP 8.5 scenario assumes that only modest technological advances and improvements in energy efficiency are achieved (i.e., “business as usual”) and represents reaching a radiative forcing of 8.5 W/m² by the end of the century.

Table 3-3 summarizes the predicted 24-hour rainfall totals for the period from 2050 to 2100 for both RCP scenarios.

Table 3-3. Summary of the estimated 24-hour rainfall for a range of return periods at the Kananaskis (3053600) climate station in the period from 2050 to 2100, based on an ensemble of 9 GCMs.

Return Period (Years)	10	30	100	300 ¹	1000 ¹	3000 ¹
RCP 4.5 Maximum Precipitation (mm)	94	133	184	236	311	393
RCP 8.5 Maximum Precipitation (mm)	97	133	179	233	304	383

Note:

1. Statistically extrapolated using a logarithmic relationship between return period and 24-hour maximum precipitation.

It is notable that the results from the two scenarios are similar and, for some return periods, the RCP 8.5 is even below that of the RCP 4.5 scenario. Intuitively, one would expect that the change from the RCP 4.5 to 8.5 should be positive due to the more pronounced radiative forcing and higher moisture content in a warmer atmosphere. However, precipitation depends on moisture availability, which will not necessarily increase with radiative forcing.

The results of the climate change assessment for each creek are presented with the rainfall-runoff modelling in Sections 4.2.1, 5.2.1 and 6.2.1. The climate change assessment was used as an input for the rainfall-sediment analysis (Section 3.5.3).

3.4. Debris-flow/Debris-flood Assessment – Data Collection and Processing

The first step in the development of an F-M relationship for debris flows is a desktop study (analysis of historical records and air photographs, comparison of lidar datasets) followed by field investigations and data processing, as described in the following sections.

3.4.1. Historical Records

BGC reviewed several engineering reports in the hazard assessment of Cougar Creek (BGC, March 7, 2014) and identified previously reported debris flood and/or flood events on Cougar Creek in 1948, 1956, 1967, 1974, 1980, 1990, 1995, 2003, 2005, and 2012. Although flooding on Cougar Creek does not necessarily imply flooding on other creeks, this information helped guide the frequency analysis for other steep mountain creeks in the Bow Valley, including X, Y and Z creeks.

Canmore provided some information on general observations made by residents during 2012 and 2013 events that are discussed in more detail in Sections 4.1.1, 5.1.1, and 6.1.1.

3.4.2. Air Photo Interpretation

Air photos dating back to 1947 were interpreted for estimation of debris-flow frequencies. Depending on the resolution and quality of the photos and the thickness of the vegetation, it is sometimes possible to observe changes to the fan surface such as fresh debris lobes or channels. Other changes are also recorded, such as land use, road construction, logging and fire history. The photographs analyzed are listed in Table 3-4, and a comparison is shown on Drawing 04.

Table 3-4. Summary of reviewed historical air photographs.

Year	Roll	Photo #	Scale	Date
1947	A10908	110	1:40,000	May 11
	A11101	008		September 23
1950	AS 167 5101/02	14	1:40,000	September 23
1962	AS 830	50, 51	1: 31,680	September 18
1972	AS 1185 Line 67	4	1:21,120	July 8
1984	AS 3085	71, 72	1:20,000	August 22
1997	AS 4824	60, 61	1:15,000	July 19
2008	AS 5450	239	1:30,000	August 18
2013*	-	-	0.1 m	June 28

*2013 imagery was gathered by satellite method rather than traditional air photo method and as such does not have roll or photo number information. Scale is reported as the photo's pixel width.

3.4.3. Lidar Change Detection

Analysis of topographical change between lidar datasets involves aligning datasets and determining the Limit of Detectable change (LoD_{95%}). Change detection was attempted on X, Y and Z creeks, but the 2009 pre-event data set did not extend to the fan apex on any of the creeks. This meant that the bulk of the 2013 deposits were not included in the analysis area, and no additional analysis of the change detection results was undertaken.

3.4.4. Field Investigation

Fieldwork on X, Y and Z creeks was conducted on May 8, 2018 and from June 11 to 13, 2018 by BGC personnel (Matthias Jakob, Emily Moase, Christy Rouault, Midori Telles-Langdon, and Beatrice Collier-Pandya). Field work included test pitting, coring of trees for dendrogeomorphic analysis, and channel hikes to collect high water mark cross sections and channel sediment loads. The upper watersheds were traversed multiple times by helicopter and numerous photographs were taken to allow reconstruction of channel yield rates for sections that were inaccessible by foot.

3.4.5. Test Trenching and Radiocarbon Dating

Test trenching allows estimation of the thickness of past debris flows/debris floods, which are typically distinct from overlying and underlying deposits. It also permits for sampling of datable

organic materials found in paleosols (old soil layers) and embedded within the debris flow deposits. An approximate age can then be assigned to the deposit.

Radiocarbon dating involves measuring the amount of the radioisotope ^{14}C preserved in organic materials and using the rate of radioactive decay to calculate the age of a sample. This method requires the deposition and preservation of organic materials within the sedimentary stratigraphy of the fan. The age range of this method is from approximately 45,000 years to several decades. As such, the method is applicable to the time scale of post-glacial fan formation in western Canada.

Test pits were excavated by backhoe on the X, Y, and Z creek fans from June 11 to 13, 2018. Four test pits were dug on each fan typically to about 2 m deep, the pit walls were logged, and photos taken at each location. Access granted by Alberta Parks to the fan areas limited test pit locations to adjacent to main trails. Test pit locations are on Drawings 01, 02 and 03 and detailed test pit logs are in Appendix C.

Unit contacts and buried soils were examined for organic carbon for radiocarbon dating. Test pits and exposures were photographed. Radiocarbon samples were collected in plastic bags, air-dried, and then sent to Beta Analytic labs in Florida for age determination by Accelerator Mass Spectrometry (AMS). A total of 12 excavated test pits were described. Twenty-eight (28) samples were collected of which 17 were submitted for radiocarbon dating. Detailed results of the radiocarbon dating are in Appendix D. Four of the 28 samples contained tephra-like⁸ material and were submitted for tephrochronology testing at the University of Alberta.

Results from the radiocarbon were reviewed to identify unique events on each creek. Deposit areas for these events were estimated using scientific judgement, based on the existing terrain and possible flow-paths, and using measured unit thickness as a rough proxy for event size. Event volumes were calculated from the areas using the measured unit thicknesses from the test pits.

3.4.6. Dendrogeomorphology

Dendrogeomorphology (dendro) is a subdiscipline of dendrochronology, in which tree rings and tree growth are used to analyze historical landslide activity. Tree core samples were collected from 16 trees on X Creek, 8 trees on Y Creek and 13 trees on Z Creek for analysis. The sample locations are shown on Drawing 01, 02 and 03.

The analysis is based on two main characteristics of tree ring samples:

1. Tree age: the age of the tree determines the “minimum establishment date”: in other words, the approximate time when the tree started growing.
 - If lots of trees in one area all started growing around the same time, that may indicate that a stand-destroying event occurred recently, which cleared the original trees and left space for new trees to establish.

⁸ Tephra are volcanic ashes that were deposited during eruptions of upwind volcanoes. In the Canmore areas, tephra can be found from the Mount Meager eruption (southern BC, approximately 2600 years ago) and Crater Lake (Oregon, some 7700 years ago).

- The date is a minimum, because tree rings indicate the minimum age of the tree at the height where the coring was collected. Cores are usually collected at about chest height (1.2 m), so it may have taken the tree a few years to grow 1.2 m. In addition, several years may pass for a tree seed to establish on a freshly disturbed surface.
2. Special features (in conifers only): Features in the wood that may suggest landslide activity include scars, traumatic resin ducts, reaction wood and growth disturbances.
- Scars occur when a landslide or avalanche damages the bark or wood of a tree but does not kill the tree at impact. Figure 3-4 shows an example of a debris-flow scarred tree.
 - Traumatic resin ducts (TRDs) are small circles that appear within the wood, which indicate that the tree sustained physical damage during that year (similar to scar tissue).
 - Reaction wood appears when a tree has been knocked or tipped over by a landslide. Denser wood grows on the downslope side, to correct the growth of the tree and insure that it continues to grow vertically.
 - Growth disturbances occur when a landslide changes the conditions around the tree, such as the availability of light, water or nutrients. These changes may cause the tree to grow noticeably faster or slower.

Tree cores were extracted from living trees using 5 mm Mora increment borers. In the office, the samples were glued onto wooden mounting boards and sanded to facilitate ring and feature identification. Analysis was completed using a specialized scanner and WinDENDRO software (WinDENDRO, 2012). WinDENDRO is a semi-automatic image analysis program, which identifies tree rings and measures the width of the yearly growth. Once the tree ages were confirmed, the growth rings were analyzed to identify anomalies that may be associated with debris-flood, debris-flow or avalanche events. It can be difficult to differentiate between steep creek and avalanche processes, although sometimes, the location of the TRDs within the ring can indicate whether the damage occurred in the dormant period (winter) or the growing season (spring and summer).

Dendrogeomorphological analysis provided limited information on X, Y and Z creeks. The trees were generally less scarred and impacted than the trees in other areas that BGC had previously analyzed, and most of the scars were from forest fires rather than steep creek events. The weaker tree ring signals are likely caused by the lower event volumes on X, Y and Z creeks, compared to larger creeks like Three Sisters and Stoneworks. The results of the dendro analysis are presented in sections 4.1.4, 5.1.4 and 6.1.4, but were not used to develop F-M relationships.

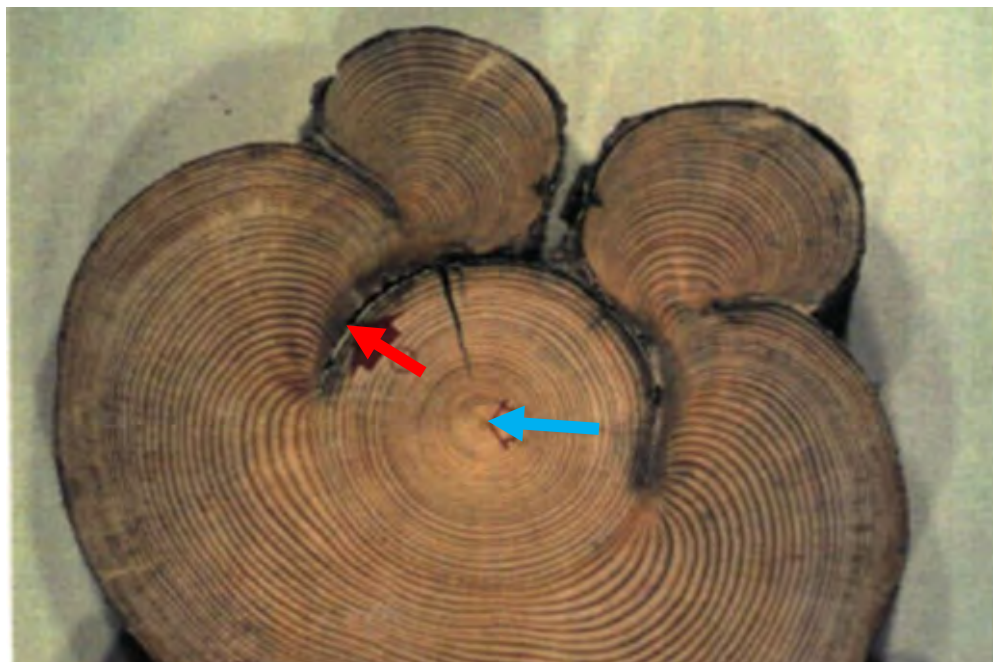


Figure 3-4. Impact scars on a spruce tree near Fergusson Creek in southwest BC showing an example of scars that can be dated precisely. The red arrow points at a scar, and the blue arrow points at the center of the tree (from Jakob, 1996).

3.4.7. Delineation of Previous Events

Several of the hazard assessment methods described can be used to estimate the inundation area of debris flows or debris floods, but hazard analysis depends on knowing the event volume, not just the event area. There are two main methods that can be used to estimate the volume of a steep creek event, given the deposit area: 1) thickness estimation, and 2) area-volume relationships.

Deposit thicknesses were used to estimate the volume of the 2013 events on X, Y and Z creeks. During field work, the deposit perimeters were hiked and delineated using handheld GPS units, and deposit thickness was estimated at regular intervals. Field delineations are more accurate than remote-sensing based delineations because deposits may be hidden under the tree canopy. The sediment volume was subsequently estimated by multiplying the delineated area by the thickness estimate for each deposit segment.

The second method involves using empirical area-volume formulae, which relate the area of a debris-flow or debris-flood deposit with its estimated volume. The debris flow formula in [Equation 3-3 was developed from a global dataset collected by Griswold and Iverson (2008), while the debris-flood relationship in [Equation 3-4 was developed by BGC using known event volumes (from detailed lidar change detection) and areas in the Bow Valley.

$$V = 0.12 A^{1.25} \quad \text{[Equation 3-3]}$$

$$V = \frac{1}{95} A^{1.5} \quad \text{[Equation 3-4]}$$

where V is sediment volume (m³) and A is deposit area (m²).

The 2013 event magnitude on all three creeks was estimated using both methods (thickness and area-volume). For the area-volume relationships, application of the debris flow relationship provided unrealistically high results, while the debris flood relationship provided unrealistically low results. We interpret the 2013 event as a multi-phase flow, with short debris-flow surges preceded and followed by lengthy periods of high bedload transport, due to the unusual length of the June 18 to 21 rainstorm. To overcome this issue, the two equations were combined. The debris flow equation was applied to the deposit areas that exhibited distinct debris flow characteristics such as deposited levees and well-defined lobes. The debris flood equation was applied for the deposits on the distal fan portions that displayed more diffusely deposited sediments. The volumes derived from both equations were then summed for a total deposit volume.

3.4.8. Channel Sediment Yield Estimation

The maximum available volume of erodible sediment in a watershed can be determined through field and desktop study where sediment yield is estimated at various cross sections along the length of the channel. Sediment yield is the amount of potentially erodible sediment stored in the bed and along the banks of a debris-flow prone channel. It is typically measured over relatively homogenous channel sections and expressed as a volume per metre channel length (Hung, Morgan, & Kellerhals, 1984). Channel yield rate estimates increase with the time after the last debris flow as more time means longer periods of potential debris accumulation.

Channel yield rates were estimated per unit metre for the entire length of Y and Z creeks, and for the X Creek West tributary, above the fans as summarized in Table 3-5. Yield rates were not estimated for the X Creek East tributary, because it is sediment-supply unlimited.

Table 3-5. Summary of channel yield hikes on X, Y and Z creeks.

Creek	Length of channel hiked above fan apex (m)	Number of reaches hiked	Upper limit of hike (elevation, m)	Length of channel yield inferred from remote sensing (m)
West X	-	-	1518	2340
Y	190	4	1690	1755
Z	740	10	1850	135

For each reach, the minimum and maximum erodible depths of material and the wetted length of the channel cross section were estimated. This method provides an upper credible limit to debris availability, which acts as a “reality check” to the later construction of the F-M curve. BGC also estimated the proportion of erodible material along the reach expressed in percent, based on field traverses and satellite imagery. The yield rates were then calculated as the product of the erodible depth, wetted length and proportion erodible. Sediment volumes were calculated by applying the yield rate to each reach. Best estimate yield rate and sediment volumes were calculated as the

average between the minimum and maximum estimates. Upper watershed yield rates were estimated via remote sensing techniques using air photographs, lidar data, and photographs taken during the helicopter flight on June 13, 2018. Yield rates were subjectively assigned a $\pm 25\%$ error since the bottom of the channel was not always visible.

Local point source failures were estimated by using lidar delineations, and field estimates of potential source and surficial material thicknesses. The total volume of material available in the watershed was calculated by summing the point sources and the sediment volumes along each channel reach.

3.5. Debris-flow Assessment – Frequency-Magnitude Analysis

3.5.1. Interpretation of Desktop and Field Data

Desktop and field analysis are critical for developing an understanding of the unique processes and hazards on each creek, but it can be challenging to translate qualitative observations into quantitative data points for a F-M plot. To construct an F-M relationship, the return period (frequency) and sediment volume (magnitude) of each data point must be estimated to the extent the various methods may allow. Many hazard assessment techniques only provide insight into the relative frequency *or* magnitude of debris flows, but not frequency *and* magnitude. Table 3-6 summarizes the frequency and magnitude information available from the desktop and field hazard assessment methods discussed to this point.

Table 3-6. Frequency and magnitude information that can be inferred from desktop and field hazard assessment methods.

Method	Frequency	Magnitude
Historical records	Event dates, but records may have been lacking or missed.	Not specified in most records due to challenges in quantification.
Air photo interpretation	Site specific but may provide dates for large events during air photo record (70 years).	Can be estimated indirectly from deposit delineations where they can be identified through tree canopies.
Lidar change detection	Not possible to apply due to limited 2009 lidar coverage.	
Test trenching and radiocarbon dating	Site specific but may provide dates for large events since deglaciation.	Can be estimated from delineations; significant uncertainty.
Dendro-geomorphology	Site specific but may provide dates for large events during tree ring record (~130 years in the case of this study).	Can be estimated from area delineations, if sufficient numbers of trees are affected.
Channel yield	Could only be assigned if recharge rates were known for multiple events over time.	Provides an upper bound sediment estimate and allows an estimate of volumes for events in near future.
Delineation of previous events	Frequency information from air photos, radiocarbon dating or dendrogeomorphological studies.	Estimated using thickness estimates or area-volume relationships.

Several of the methods summarized in Table 3-6 provide event magnitude information, and event dates, but not specific event frequencies. A technique called “magnitude cumulative frequency” (MCF) analysis can be used to estimate event frequency, given magnitude and the range of event dates.

3.5.2. Magnitude Cumulative Frequency (MCF) Analysis

Seismology has been the precursor to the use of regional magnitude-cumulative frequency curves (MCF) (Gutenberg and Richter, 1954). An inventory of sediment volumes of known dates in a given time interval T_i is ranked from largest to smallest. The incremental debris-flood frequency of rank i is determined as $1/T_i$ and the MCF then states the cumulative incremental frequencies as:

$$F_i = \sum_{i=1}^n f_i \quad \text{[Equation 3-5]}$$

where f_i is the incremental frequency of an event of rank i and F_i is the annual debris-flood frequency of an event of greater than volume V_i . The MCF curve is then produced by plotting F_i against V_i .

The use of MCF assumes that all events are known, and volumes can be combined in reasonable volume classes, or that the dataset is stratified into classes where confidence exists that all such events have been included. The latter is believed to be the case at X, Y and Z creeks, where return period classes are believed to span ranges of respective volumes. Furthermore, the selection of different plotting methods (cumulative vs. non-cumulative, linear and logarithmic binning, different bin sizes and choice of trend lines for extrapolations) can bias the results (Brardinoni and Church, 2004). The MCF technique is very sensitive to the number of events, as adding events will invariably decrease the individual return periods for events smaller than those newly added.

On X, Y and Z creeks, MCF analysis was used to estimate event frequency for the identified radiocarbon events. MCF analysis could not be applied to the air photo or dendrogeomorphology techniques, because magnitude information could not be reconstituted.

3.5.3. Rainfall Sediment Relationship

In addition to the frequency and magnitude information that was obtained from the desktop and field data, a rainfall-sediment relationship was also developed for debris flow and debris flood events. This analysis uses data from previous events in similar watersheds to answer the question: “for a given volume of rain, how much sediment would we expect to see mobilized in this watershed”?

The initial dataset from the rainfall-sediment relationship was extracted from the August 2005 storms in Switzerland. Rickenmann and Koschni (2010) compiled a database which included 33 debris flow and 39 fluvial sediment transport events. Sediment volumes were determined using lidar change detection, or by tracking the amount of material removed from catchment basins. Rainfall volume was determined from a combination of gauge and radar data.

As part of BGC's 2014 and 2015 Canmore studies, these data were combined with additional cases from the 2013 Bow Valley event to develop a debris-flood-specific relationship. This relationship was suitable for watersheds with larger watershed areas (> 5km²) and unlimited sediment supply, such as Cougar Creek, Three Sisters Creek and Stoneworks Creek in Canmore, and Exshaw Creek, Jura Creek and Heart Creek in the Municipal District of Bighorn. Additional information about the debris-flood relationship is available in BGC's reports (March 7, 2014; October 31, 2014; November 16, 2015).

However, the original debris-flood rainfall-sediment relationship is not considered valid for X, Y and Z creeks since they are subject to debris flows at higher return periods, have smaller watersheds and are sediment supply-limited. For this reason, a new relationship was developed, using the following dataset:

- 14 debris flow cases from the Rickenmann and Koschni dataset. Watershed areas range between 0.3 and 9.4 km², with an average of 3.3 km²; channel gradients range between 12% and 40% (average of 31%).
- 19 cases from the Rickenmann and Koschni dataset that were classified as "debris flow (fluvial transport)". Watershed areas range between 0.3 and 15.0 km², with an average value of 4.1 km²; channel gradients range between 8% and 40% (average of 26%).
- 7 debris flow cases from the Bow Valley from BGC's data. Watershed areas range between 0.5 to 2.6 km², with an average of 1.0 km², and channel gradients range between 17% and 40% (average 24%).

Regression analysis yielded the following formula:

$$\log V_S = 0.6881 \log V_R + 0.301, R^2 = 0.20 \quad \text{[Equation 3-6]}$$

where V_S is the total sediment volume displaced and V_R is the total rainfall. This relationship is considered valid for smaller watersheds that are prone to debris floods at lower return periods, and debris flows at higher return periods. The relationship has a low R^2 value which indicates substantial scatter around the best fit line but was found to be statistically significant at a p-value of 0.004. The data and the regression line are shown in Figure 3-5.

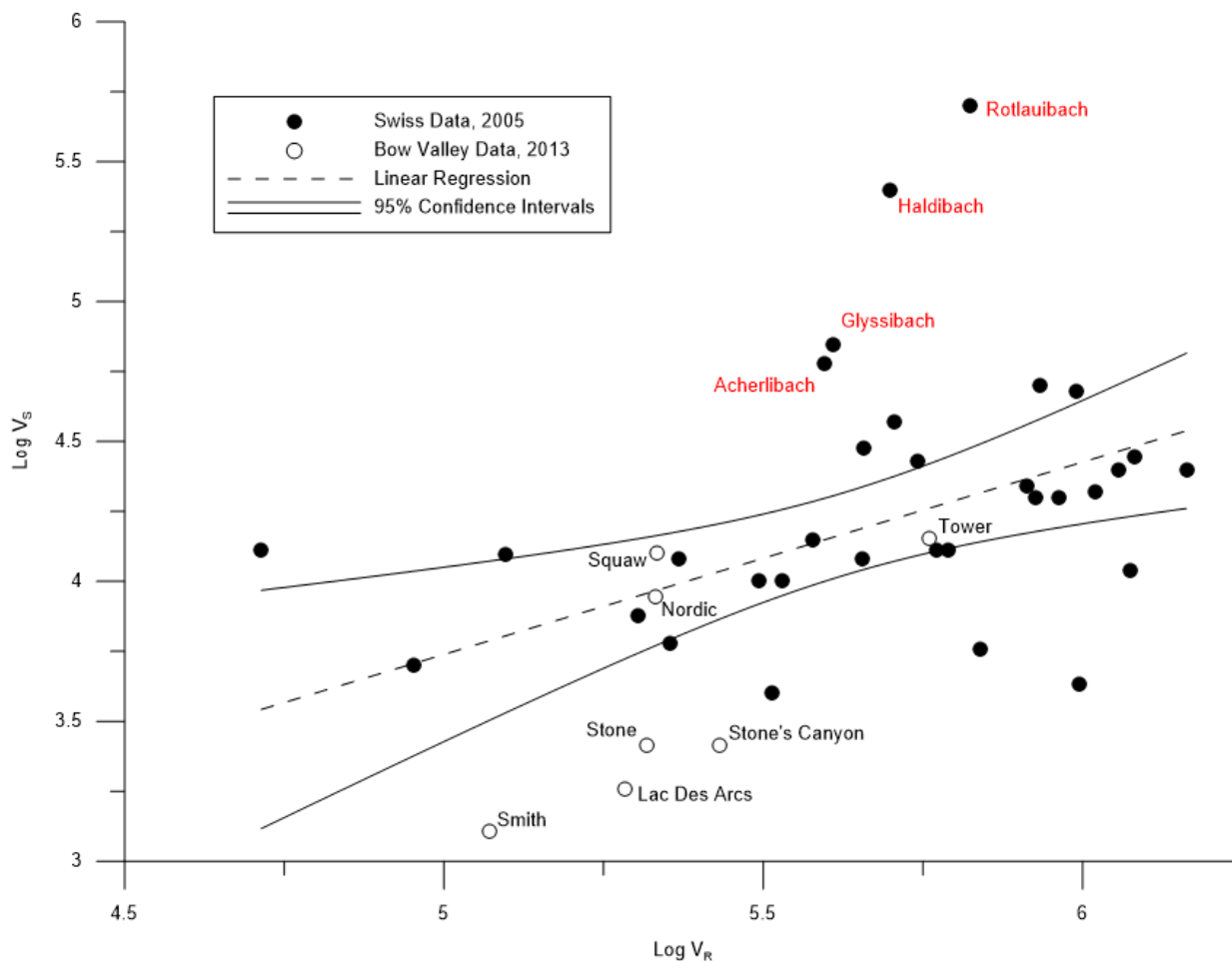


Figure 3-5. Sediment and runoff data from the Swiss and Bow Valley datasets. Datasets compiled by Rickenmann and Koschni (2010) and BGC, respectively. Red text labels indicate outliers in the Swiss dataset (discussed in text) and black lines show the confidence interval⁹.

The dataset includes some obvious outliers, shown with red labels in Figure 3-5. These cases all involved landslide-associated sediment input which increased the sediment yield, but otherwise did not have unusual watershed areas and channel gradients. Although these cases severely decreased the R^2 value of the relationship, BGC did not have a strong basis to exclude them. Landslides may contribute to the sediment volumes of X, Y and Z creeks, and inclusion of the red cases might better represent the natural variability of steep creek watersheds.

On the lower end, several of the Canmore cases are also outliers. Sediment volume for these creeks were estimated from lidar change detection, and high detection limits and small deposit volumes might mean that sediment volumes were underestimated. We would also expect to see

⁹ Confidence intervals are a statistical tool for showing variability in a dataset. A 95% confidence interval means that, if the same population were sampled on numerous occasions and interval estimates are made on each occasion, the resulting intervals would bracket the true population parameter in approximately 95% of the cases.

comparatively smaller sediment volumes from the small watersheds during the June 2013 event, due to long duration and low intensity of the storm. Water travels faster through smaller watersheds, allowing less time for runoff to accumulate and increase the discharge. In other words, the data may be accurately representing natural steep creek variability, at the opposite end of the spectrum from the Swiss data.

It is worthwhile to compare the bedrock geology in the Swiss dataset with the Canmore data to determine if a combined dataset is justified. In general, the Swiss dataset contains a mix of conglomerates, limestones, dolomites, marl, schists and phyllites as well as loose Quaternary deposits. This contrasts the Canmore data that consists entirely of sedimentary rocks. Rickenmann and Koschni (2010) used a geological index in their analysis with the attempt to improve predictions of debris-flow volumes. They found that the inclusion of the lithology-based index did not improve the predictive performance of their model. Other workers who have attempted to include geological factors (D'Agostino et al., 1996) also concluded that adding a geological index does not substantially improve event magnitude prediction. Given the relative similarities of bedrock geology as far as sedimentary rocks is concerned and the fact that geology does not appear to improve the Swiss relationship, BGC believes that application of the combined Swiss-Canmore dataset is appropriate.

BGC recognizes that a much steeper regression line through the data may be credible if emphasis would be placed on the red-marked creeks in Figure 3-5. However, the Swiss landslide cases are outliers, both in terms of the typical behaviour of those catchments, and in terms of the typical behaviour of Swiss catchments in general (pers. comm. Dr. Rickenmann, 2016). Furthermore, none of the Canmore debris flow data plot above the 95% confidence limit, and only one creek in the Bow Valley (Squaw Creek) plots above the best-fit regression line. For this reason, BGC felt that a steeper relationship would reflect the upper credible limit of sediment transport, whereas our objective was to develop a best estimate. The outlier points were included in the best estimate relationship (rather than discarded), but we felt that developing a steeper fit would yield overly-conservative results.

Using a relationship as shown in Figure 3-5 that has a low coefficient of determination (R^2) can be problematic, especially in cases where both the predictor (independent) and dependent variables have some unquantifiable error. The R^2 value can be improved (from 0.20 to 0.31) by deleting outliers, but BGC chose not to do this, given the rationale mentioned above. An alternative to a regression analysis is a functional analysis as discussed by Mark and Church (1977). A functional analysis is preferable in situations where an unbiased estimate of parameters of physical relationships are the objective. However, successful application of this technique requires information on error variances or ratio of error variances of the variables which is not achievable in the case of the three study creeks.

These considerations imply that the predictions achieved with Equation 3-6 are associated with considerable error. To overcome this issue, BGC used additional volume estimates from test trenching and compared the derivative F-M relationship with a regional approach (Jakob et al. 2016), which allows added confidence in the overall results.

As a final check of the impact of using Equation 3-6 given its low coefficient of determination, BGC deleted the rainfall-sediment relationship from each F-M analysis and estimated the impact on the predicted sediment volumes. We found that deletion of the rainfall-sediment data has only minor effects on the volume estimates. For example, for X, Y and Z creeks, for the 1000-year return period, the changes amounted to 2%, 12% and -17%, respectively. These changes, if modeled would likely be well within the expected error range in flow distribution and intensity given all other modeling inputs.

3.5.4. Development of Local Frequency-Magnitude Relationships

Local F-M relationships were developed for X, Y and Z creeks using the following data sources:

- MCF analysis based on radiocarbon event delineations and the maximum credible channel yield estimate
- The rainfall-sediment relationship, based on rainfall volumes bulked with snowmelt
- The 2013 event, with the magnitude estimated based on field delineations and the debris area-volume relationship (see Section 3.4.7), and the frequency estimated using the rainfall-sediment relationship (about 100 years)¹⁰.

MCF analysis, radiocarbon delineations, channel yield estimation and 2013 volume estimation have been described in previous sections.

For the rainfall-sediment relationship, the rainfall volumes were determined as follows:

- Precipitation estimates (in mm) from the rainfall analysis (Table 3-1) were multiplied by the watershed area to estimate the total rainfall volume falling on the watershed for each return period. To account for significant uncertainty in analysis, and to acknowledge that future climates are likely to change precipitation rates and volumes, precipitation estimates for the RCP 4.5 scenario were used.
- The rainfall volumes were bulked by a snowmelt factor, which was determined for each watershed by estimating the amount of snowmelt contribution during the 2013 event, based on measurements of snowpack loss over the event (Table 3-7). The snowmelt factor is intended to account for water contribution from melting snow in the upper watershed during a storm, such as occurred during the 2013 event. Due to the large uncertainty in the factor, a sensitivity check was performed to confirm that the F-M results are not highly sensitive to the snowmelt factor.
- [Equation 3-6 was used to calculate sediment volume (V_S), given rainfall volume (V_R).
- At lower return periods, the rainfall-sediment relationship was truncated at the credible limit of debris flows, based on judgement. On X Creek, the relationship was truncated at 30 years and on Y and Z Creeks, the relationship was truncated at 100 years.

¹⁰ The estimated return period of the 2013 event on X, Y and Z creeks is significantly lower than the estimated return period for larger Bow Valley creeks, because of the long duration of the storm, smaller watershed sizes and lower lag times for X, Y and Z creeks. Rainfall passes through small watersheds much quicker than larger watersheds, limiting the amount of flow concentration that can occur.

Table 3-7. Snowmelt factors for the three watersheds.

Watershed	Snowmelt factor
X Creek	1.18
Y Creek	1.16
Z Creek	1.07

The F-M analysis yielded nine or ten data points for each creek: one point from the 2013 event estimate; four or five points from the MCF analysis; and four or five points from the rainfall-sediment relationship. Figure 3-6 shows an example from Y Creek, highlighting the source of each of the data points. A regression line was fit to the points, and the regression equation was used to develop the sediment volume estimates for each return period.

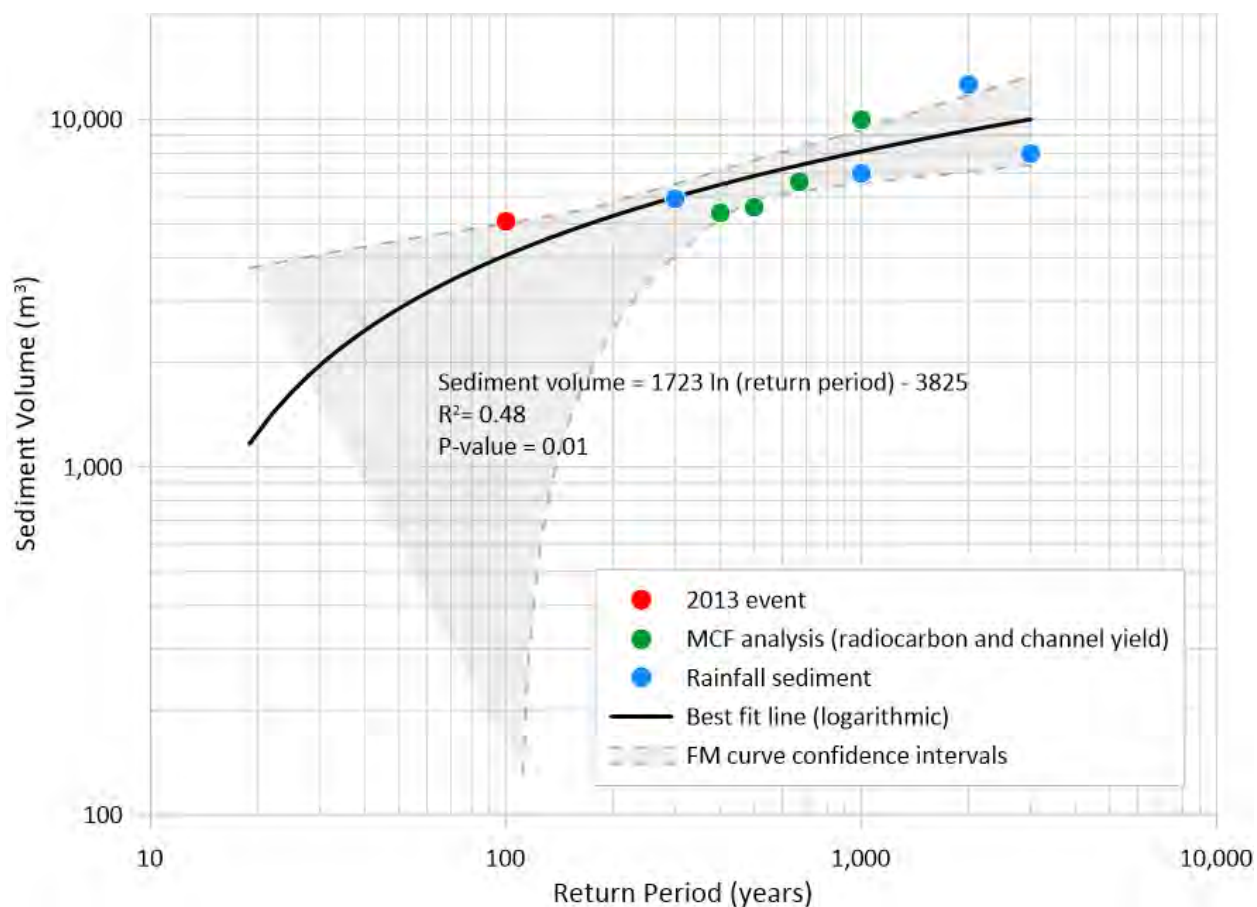


Figure 3-6. Example frequency-magnitude curve for Y Creek, showing the three data sources differentiated. The confidence intervals appear narrow due to the log-log scale.

3.5.5. Comparison with Regional Sediment Frequency-Magnitude Relationships

BGC used regional sediment F-M relationships to evaluate and “reality check” the site-specific relationships that were developed as part of this work. The regional relationships involve a few key assumptions:

1. That watersheds with similar watershed areas or fan areas will produce similar sediment volumes at similar return periods.
2. That the behaviour of smaller watersheds can be predicted from the behaviour of large watersheds (or vice versa) by scaling based on watershed area or fan area

The regional relationships were used as a comparison tool, rather than as a direct input to the F-M analysis because they do not account for site-specific geomorphological characteristics and are meant as a regional scoping tool rather than as a replacement for detailed fan hazard and risk assessments. Watershed-specific idiosyncrasies may include: watersheds that transition between process types; sites with extremely high or low sediment supply; and periglacial influences. Where possible, site-specific assessment is preferable.

Jakob, McDougall, Bale & Friele (2016) provides additional detail about the rationale for and development of regional relationships. In addition, the paper presents two relations: one for debris-flows in southwestern British Columbia and one for debris-floods in the Bow Valley. Because X, Y and Z creeks do not fit into either of these categories, several additional regional relations were developed for comparison with the site-specific F-M curves. The regional relations were developed using the following workflow:

- A dataset of F-M curves was collected, including eighteen creeks and 76 individual F-M data points (return period and sediment volume). The dataset also included the watershed area and fan area for each site.
- Two separate corrections were applied to the data. The first correction involved dividing the sediment volume by the watershed area, and the second involved dividing the sediment volume by the fan area. This correction provided a dataset that was independent of study area scale; it could be used to answer the question: “for a given return period, how much sediment can be expected per square kilometer of watershed or fan?”

$$V_{s-c} = \frac{\text{Sediment volume}}{\text{Watershed area}} \text{ or } V_{s-c} = \frac{\text{Sediment volume}}{\text{Fan area}}$$

where V_{s-c} is the corrected sediment volume.

- The two corrected datasets were filtered into three subsets, according to the following cases:
 - Case 1: all watershed areas < 5 km²
 - Case 2: all watersheds in the Bow Valley
 - Case 3: all watersheds < 5 km² in the Bow Valley
- For each case, a logarithmic regression line was fit to the data, and an equation was developed. The equation was in the form:

$$V_{s-c} = a \times \ln(\text{Return period}) + b$$

where a and b are the regression coefficients. This produced six different relationships, which could be used to calculate V_{s-c} from return period.

- The six relationships were solved for each return period, for each study creek, producing 30 frequency/magnitude data points per site. A regression was fit to these points to create

one overall regional F-M relation for the site, which could be compared to the F-M curve developed from site-specific data.

Figure 3-7 shows an example regional F-M curve for X Creek. The regional curves are compared with the site-specific curves in Sections 4.2.2, 5.2.2 and 6.2.2.

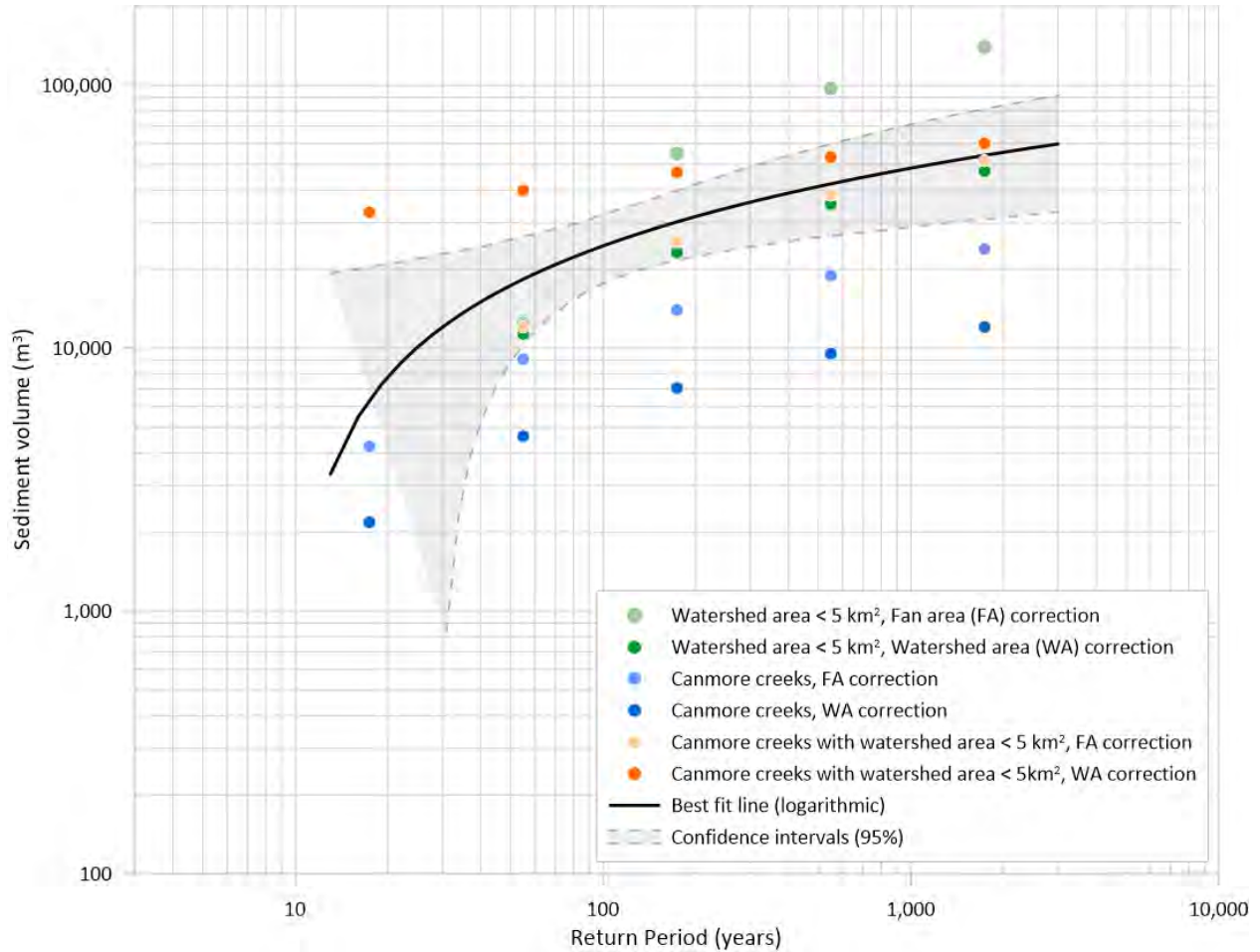


Figure 3-7. Regional F-M curve for X Creek, based on a regression fit to three different regional cases, using two different correction factors (six data subsets in total).

3.5.6. Debris Flow Peak Discharge Assessment

Once debris flow sediment volumes have been estimated for each return period, empirical relationships can be used to calculate the corresponding peak discharge. Three empirical relationships have been developed for granular debris flows, by Mizuyama, Kobashi & Ou (1992, [Equation 3-7]), Jakob (1996, [Equation 3-8]) and Rickenmann (1999, [Equation 3-9]).

$$Q_{max} = (0.077 V)^{0.752} \quad \text{[Equation 3-7]}$$

$$Q_{max} = (0.036 V)^{0.901} \quad \text{[Equation 3-8]}$$

$$Q_{max} = 0.1 V^{5/6} \quad \text{[Equation 3-9]}$$

The average of the three equations was used for modelling. It should be noted that these relationships provide very high peak discharge estimates, because they assume that the total flow volume comes down within a single surge. This is a conservative assumption, but it's consistent with worldwide observations and the literature.

3.5.7. Error and Uncertainty

Frequency-magnitude relationships are associated with substantial uncertainty, as it is very difficult to estimate a F-M relation using nine or ten scattered data points. Limitations and uncertainty include:

- The MCF analysis is dependent on the number of known (dated) event. Additional events will skew the F-M relationship. Given the limited number of test pits and thicknesses of known debris flows, it is extremely likely that several previous events were missed. Arguably mostly small events were missed as the larger ones can be recognized (and dated) more easily. Inclusion of additional small hypothetical events will pull this subset of data points downwards, which will also pull the overall regression downwards. Excluding these small events results in a more conservative final F-M relationship than had those data points been included.
- The F-M relation of debris flows and debris floods is likely to change in the future. This change is complex. In sediment supply-limited watersheds, an increase in hydro-climatic extremes would likely result in more frequent sediment movements, but with reduced sediment loads as the supply cannot keep up with the sediment transport. Climate change may also lead to increasing rates of weathering and, in areas underlain by permafrost, lead to higher rates of rock fall frequency due to the loss of interstitial ice that acts as a cohesive agent. Neither process has been studied in the study area watersheds and their influence on channel recharge is thus speculative. Adjusting the F-M curve towards higher frequencies is expected, but towards higher magnitudes is less clear. By using the climate-change adjusted runoff-sediment relationship, BGC is instilling an element of conservatism as the blue points in Figure 3-6 have shifted slightly upwards compared to reliance on historical data only.
- A further element of conservatism is instilled by allowing for snowmelt. Snowmelt may or may not be a factor depending on the seasonality of the debris flows or debris floods. Clearly not all debris flows and debris floods will occur during times of remaining watershed snow and thus the inclusion of snowmelt for all cases is conservative. A sensitivity check showed that the F-M results were not highly sensitive to the snowmelt factor.

In summary, elements of conservatism have been included in each of the elements included in the F-M analysis. To avoid overconservative assumptions, BGC checked the validity of the final F-M curve by comparing the book ends to the curve (i.e., the estimated volumes of the 2013 event and the maximum debris flow or debris flood amounts as estimated from yield rates with point source failures). This comparison added confidence that the final F-M relationships are indeed realistic while being modestly conservative given the gamut of uncertainties involved in the disparate analytical tools. Instilling further elements of conservatism such as using the upper

error bounds of the F-M relationships does not appear to be warranted and may result in overly conservative debris flow and debris floods volumes, hence overly conservative risk assessment results and ultimately possibly overly conservative (and thus expensive) mitigation design.

3.6. Hydrodynamic Modelling and Hazard Mapping

Numerical modelling of debris floods and debris flows is the basis for the delineation of hazard intensity zones which serves as input to the quantitative debris-flood and debris-flow risk assessment (QRA).

3.6.1. Model Selection – FLO-2D

Modelling was completed using FLO-2D, a two-dimensional, volume conservation hydrodynamic model. FLO-2D can be used to model clearwater flows, sediment transport and debris flows, which allows its application for X, Y and Z creeks, because they are subject to this process continuity. By comparison, models like DAN-3D are only suitable for debris flow modelling, so the use of multiple modelling packages would have been required. In addition, FLO-2D has been used to model steep creek hazards for other Canmore creeks, so its use on this project is consistent with the other Canmore and Bow Valley studies. It is also a FEMA approved model which lends additional legitimacy of the model. Lastly, comparisons between FLO-2D and other debris flow models (i.e., RAMMs), has shown that it yields reasonable results once calibrated with known events (Cesca and D'Agostino, 2008).

In FLO-2D, flow progression is controlled by topography and flow resistance. The governing equations include the continuity equation and the two-dimensional equation of motion (dynamic wave momentum equation). The two-dimensional representation of the motion equation is defined using a finite difference grid system and is solved by computing average flow velocity across a grid element boundary one direction at a time with eight potential flow directions. Pressure, friction, convective, and local accelerations components in the momentum equation are retained.

3.6.2. Two-part Modelling Approach

Steep creek hazard events can include a range of behaviours, from debris-flow surges to more watery afterflows. Modelling these behaviours can be challenging due to the way that FLO-2D addresses sediment dilution. If a short pulse of sediment is added to a model that includes much larger volumes of clearwater, the sediment concentration quickly dilutes to below 20%, which is the FLO-2D threshold for flow governed by rheological parameters. This dilution prevents the sediment from depositing, resulting in unrealistically high debris flow runout distances and lower-than-expected flow depths.

To address this issue, each event was modelled in two parts. The first part uses a short-duration, high-sediment volume hydrograph to represent the debris-flow and sediment transport portion of the event, with debris-flow rheological parameters to control the flow behaviour. The second part uses a 24-hour hydrograph based on the rainfall runoff modelling to simulate a flow phase with a

sediment concentration less than 20%. This could represent a hyperconcentrated after-flow, debris flood or bedload transport event¹¹.

At high return periods (> ~100 years), risk to development is controlled by debris-flow impact (model part one), due to the higher velocities and forces. At low return periods (< ~ 100 years), the debris may deposit prior to reaching the development. Then, the main damage is caused by flooding and remobilization of sediment during the debris-flood phase (model part two). Therefore, modelling both event phases should allow for better assessment of the overall hazard.

3.6.3. Basic Setup and Input Parameters

The models are run on a grid created from a DEM constructed from 2015 lidar. Grid spacing varies for each creek as the fan areas are different sizes and the number of cells is not to exceed about 30,000 cells to ensure reasonable processing times for the models. X Creek used a 5 m grid spacing, and Y and Z Creeks used a 3 m grid spacing. This means that an elevation is averaged for each cell from the DEM.

Appropriate boundaries and boundary conditions were selected for each creek to best show how the flows would interact with the topography and development. Manning’s n values were input for all cells depending whether the cell was in the built environment or on the fan. A hydrograph for the inflow cell at the apex of the fan was specified depending on the return period being modelled.

Table 3-8 summarizes the basic input parameters that were used to set up the models.

Table 3-8. FLO-2D basic input parameters.

Parameter		Value
Manning’s n	Undeveloped areas	0.075
	Streets	0.025
Floodplain Limiting Froude number	Floods and debris floods	1.1
	Debris flows	1.3
Sediment concentration (by volume)	Floods and debris floods	<20%
	Debris flows	50%
Surface detention ¹²		0.03 m

The effects of infiltration were tested for both the debris-flow and flood models, using parameters recommended by the FLO-2D developer for alluvial fans (pers. comm., J. O’Brien). As with other fans in the Canmore area, infiltration had a very limited impact on the model results and was

¹¹ It is not a given that both (the short-lived debris flow peak and the longer runoff hydrograph) occur in unison. For example, an isolated thunderstorm could result in a high volume of rain falling over a short period which would result in an event characterized by a short-lived debris-flow surge but not the long-lived afterflow. The likelihood of both events occurring increases at higher return periods, due to the higher probability of coincidental high precipitation cells embedded in larger long-duration storms.

¹² The surface detention parameter limits the minimum flow depth of modelled flow. It is intended to account for flow storage in shallow depressions.

therefore not included in the final models. This means that the model results are conservative, because they assume high antecedent moisture levels.

In addition to debris modelling, FLO-2D also has several features that facilitate modelling flows through urban environments, such as the Peaks of Grassi development on the edge of the X, Y and Z creek fans. Table 3-9 summarizes the components that were used.

Table 3-9. Components used to model the built environment.

Feature	Description	Application on XYZ
Levees	Use to block flow through a grid element, up to a certain flow depth	The levee tool was used to model the wooden walls that are installed in four locations on the upstream side of the Peaks of Grassi development.
Area Reduction Factors (ARFs)	Used to block flow through grid elements that are occupied by buildings or other structures	ARFs were applied to grid cells that are entirely occupied by buildings on the X, Y and Z creek fans. The use of ARFs meant that flow was concentrated through the narrow gaps between the houses, which is a realistic representation of what could happen in a steep creek event.
Storm drains	Used to model storm drain systems, rather than single hydraulic structures such as culverts	BGC integrated the Peaks of Grassi storm drain system in to the Y and Z Creek FLO-2D models. However, given that the storm drains blocked during the 2012 event, the storm drains were only used during the 10-30 year flood models, with the assumption that the drains would block during higher return periods.

3.6.4. Sediment Model Setup and Calibration

In FLO-2D, sediment and water inputs are defined using inflow hydrographs, which can be assigned to grid cells at the fan apex. The peak discharge of the hydrograph is changed between model scenarios to model different event sediment volumes; the sediment volumes are determined using the F-M relationships for each creek. The debris-flow input hydrographs use a constant hydrograph shape and sediment concentration (50%), and the length of the hydrograph is adjusted to match the estimated sediment volume and peak discharge. In general, because of the high peak discharges, the hydrographs are very short (<10 minutes). The inflow hydrograph parameters are summarized in Table 3-10.

Table 3-10. Simulated debris-flow and sediment transport scenarios on X, Y and Z Creeks.

Return period	Sediment volume (m ³)			Peak discharge at fan apex (m ³ /s)		
	X Creek	Y Creek	Z Creek	X Creek	Y Creek	Z Creek
10 to 30	1,000	1,100	-	20	5	-
30 to 100	7,000	3,100	900	140	10	5
100 to 300	14,000	5,100	2,400	250	110	10
300 to 1000	21,000	7,000	3,900	350	140	86
1000 to 3000	28,000	9,000	5,400	440	170	110

Debris-flow modelling also requires the definition of rheological parameters, which inform the flow behaviour of the water and debris slurry. In FLO-2D, the main rheological parameters are viscosity and yield stress. These parameters can be modified during model calibration in order to achieve the best possible match with the behaviour of known events. Neither variable is directly measured from observed events.

For X, Y and Z creeks, the June 2013 event was used for calibration. BGC used the event delineations shown on Drawings 02, 03 and 05 and flow depths from field observations to calibrate the models. The calibration models were based on the post-event topography (dated 2015), because pre-event topography (2009) was not available for the full extent of the fans¹³. The final rheological parameters are presented in Table 3-11.

Table 3-11. Rheological parameters used for Bow Valley debris-flow models.

Viscosity Coefficient	Viscosity Exponent	Yield Stress Coefficient	Yield Stress Exponent
0.0360	22.1	0.181	25.7

These parameters match the Aspen Pit 1 rheology recommended in the FLO-2D reference manual (FLO-2D, 2017), and have also been used for modelling debris flows in the northern Italian Dolomites with similar geological and morphological characteristics as the Bow River valley (Cesca & D'Agostino, 2008).

3.6.5. Flood Model Setup and Calibration

The flood or debris-flood model phase also requires input hydrographs, but not sediment volumes or rheological parameters. Hydrographs were defined for a 24-hour event, using the water volumes and peak discharges that were determined from the rainfall-runoff modelling. Table 3-12 summarizes the debris-flood input hydrograph parameters.

Table 3-12. Simulated flood scenarios on X, Y and Z Creeks.

Return period	Water volume (m ³)			Peak discharge (m ³ /s)		
	X Creek	Y Creek	Z Creek	X Creek	Y Creek	Z Creek
72 hr 2013 event	404,000	64,000	34,000	8.5	1.3	0.7
24 hr 2013 event	179,000	28,000	15,000	8.5	1.3	0.7
10 to 30	101,000	15,000	8,000	12.8	2.8	1.5
30 to 100	150,000	23,000	12,000	19.4	4.3	2.3
100 to 300	223,000	35,000	18,000	29.3	6.6	3.5
300 to 1000	331,000	52,000	28,000	44.4	10.0	5.3
1000 to 3000	492,000	78,000	41,000	67.1	15.3	8.1

¹³ A sensitivity check was performed on Y Creek, using an altered version of the 2015 topography in attempt to remove the 2013 deposit. The topography change did not have a substantial impact on the runoff results. Nonetheless, an exact match between the observed and modelled flows cannot be expected.

The debris-flood models were calibrated using the highest intensity, 24-hour portion of the June 2013 72-hour hydrograph.

3.6.6. Hazard Mapping

FLO-2D model outputs include grid cells showing the velocity, depth, and extent of debris-flow and debris-flood inundation. Hazard mapping is used to translate these results into inputs that can be used for the risk assessment. This is done using the flow intensity index (I_{DF}), which is a measure of the potential destructiveness of the modelled events, at all locations within the study area. Flow intensity was defined as an index according to Jakob, Stein, and Ulmi (2012) as:

$$I_{DF} = d \times v^2 \quad \text{[Equation 3-10]}$$

where d is flow depth (m) and v is flow velocity (m/s). I_{DF} values in certain ranges have implications for potential building damage, as shown in Table 3-13.

Table 3-13. Definitions and colour coding for debris flow creeks.

Impact Intensity	Colour	Building Damage Potential	Description
< 1	Yellow	Minor	Slow flowing shallow and deep water with little or no debris. High likelihood of water damage. Potentially dangerous to people in buildings, on foot or in vehicles in areas with higher water depths.
1 to 10	Orange	Major	Potentially fast flowing but mostly shallow water with debris. Moderate likelihood of building structure damage and high likelihood of major sediment and/or water damage. Potentially dangerous to people on the first floor or in the basement of buildings, on foot or in vehicles.
10 to 100	Red	Severe	Fast flowing and deep water and debris. High likelihood of moderate to major building structure damage and severe sediment and water damage. Very dangerous to people in buildings, on foot or in vehicles.
>100	Dark Red	Destruction	Very fast flowing and deep water and debris. High likelihood of severe building structure damage and severe sediment and water damage. Extremely dangerous to people in buildings, on foot or in vehicles.

Interpreted hazard maps showing I_{DF} values at all locations within the study area were developed for X, Y and Z creeks, for each return period class. In addition, spatial impact probabilities were used to assign likelihoods to different avulsion scenarios. In general, the current main flow path was assigned a spatial impact probability of 70%, main avulsion paths were assigned spatial probabilities between 20% and 40%, and other fan areas were assigned spatial probabilities of 10%. Additional detail for each creek is provided in the results chapters.

3.7. Risk Assessment Methods

3.7.1. Introduction

Quantitative risk assessment (QRA) involves estimating the likelihood that a hazard occurs, impacts elements at risk, and causes consequences. Vulnerability estimation involves estimating the likelihood of consequences, given that a hazard occurs and impacts elements at risk. The key difference between vulnerability and risk estimation is that vulnerability estimates assume impact, whereas risk additionally provides estimates of the likelihood of impact.

The analysis methods are described in detail in Appendix E. The primary objective of the risk assessment is to support risk management decision making. Importantly, the assessment does not consider all possible risks that could be associated with a debris flow or debris flood. The risk assessment considers key risks that can be systematically estimated, compared to risk tolerance standards, and then used to optimize mitigation strategies. These mitigation strategies, once implemented, would also reduce relative levels of risk for a broader spectrum of elements than those explicitly considered in this report.

This assessment also assesses risk of debris flows or debris floods separately for each creek. While it is possible that events may occur independently, multiple events could occur on the same day. Each of the watersheds studied are unique and produce different types of steep creek hazard events and have different times of runoff concentration. Separate assessment of risk for each creek (e.g., not combined risk) is a simplification that reflects the level of information available.

3.7.2. Safety Risk

Safety risk was estimated from two perspectives: risk to individuals and groups.

Individual safety risk considers the risk to a particular individual exposed to hazard and is independent of the number of persons exposed to risk. BGC compared the individual risk estimate results to geohazard tolerance criteria adopted by Canmore for previous risk assessments completed for other creeks impacting the town. The applied criteria for individual geohazard risk tolerance are as follows (Canmore Municipal Development Plan, 2016):

- Maximum 1:10,000 (1×10^{-4}) risk of fatality per year for existing developments
- Maximum 1:100,000 (1×10^{-5}) risk of fatality per year for new developments.

For context, the risk tolerance threshold of 10^{-4} (1/10,000) for existing development is comparable to the lowest background risk of death that Canadians face, on average, throughout their lives. This tolerance threshold is also similar to the average Canadian's annual risk of death due to motor vehicle accidents, 1/12,500, for the year 2008 (Statistics Canada, 2012).

Group safety considers the collective risk to all individuals exposed to hazard and is proportional to the number of persons exposed to risk. For risk to groups, estimated risks were compared to group risk tolerance criteria formally adopted in Hong Kong (Geological Engineering Office (GEO), 1998) and Canmore (Canmore, 2016), and informally applied in Australia (AGS, 2007) and District of North Vancouver (DNV) (DNV, 2009a; 2009b). Group risk tolerance criteria reflect society's general intolerance of incidents that cause higher numbers of fatalities. Group risk tolerance

thresholds based on criteria adopted in Canmore (Canmore, 2016) are shown on an Frequency-Number of Fatalities (F-N) curve in Figure 3-8. Three zones can be defined as follows:

- Unacceptable – where risks are generally considered unacceptable by society and require mitigation.
- As Low as Reasonably Practicable (ALARP) or “Tolerable”– where risks are generally considered tolerable by society only if risk reduction is not feasible or if costs are grossly disproportionate to the improvement gained (this is referred to as the ALARP principle).
- Acceptable – where risks are broadly considered acceptable by society and do not require mitigation.

Where N was calculated to be less than one (e.g., the probability of at least one fatality is not zero, but one fatality is not expected for any single scenario), only individual safety risk estimates were reported.

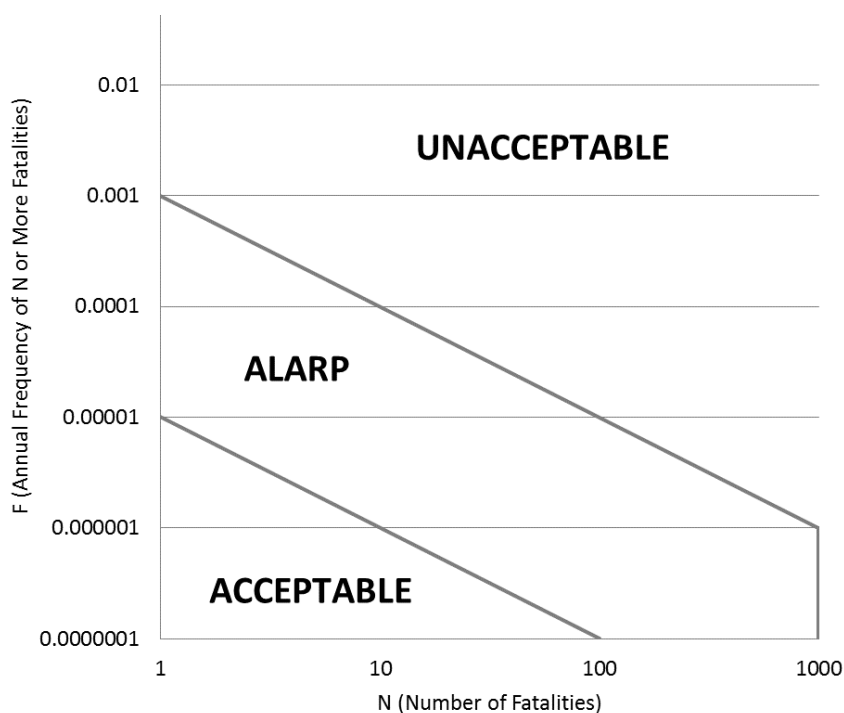


Figure 3-8. Group risk tolerance criteria as defined by GEO (1998) and accepted by Canmore municipal policy (2016).

3.7.3. Economic Risk

Economic risk considers direct building damage costs and interruption of business activity. Building damage costs were estimated based on the criteria presented in Appendix E. In summary, the proportion of building damage was estimated based on vulnerability criteria related to the hazard intensity index (I_{DF}).

BGC mapped the distribution of business activity by estimating the total annual revenue for the parcels within the study area containing commercial development based on data obtained from commercial data provider Hoovers (2013).

As a proxy for level of business impact, BGC summed the annual revenue estimated for parcels impacted by a debris-flow/debris-flood scenario. Additional factors such as indirect losses, damages to business equipment or inventory, interruption of transportation corridors, or effects of prolonged outage, were not estimated.

3.7.4. Critical facilities

No facilities from the Hoovers (2013) dataset were defined as critical within the study area.

3.7.5. Lifelines

As noted in Section 2.5, assessment of lifelines was limited to identifying their location within steep creek hazard areas. In the emergency response period, evacuation and road closures may also extend beyond the areas directly impacted.

3.8. Conceptual Mitigation Design

Mitigation can be used to reduce risk by reducing either the magnitude, intensity or probability of the hazard, or the severity of the consequences (Hung et. al., 1987; VanDine, 1996). This section describes the general techniques that can be used for debris-flow and debris-flood mitigation.

There are a wide variety of debris-flow and debris-flood mitigation techniques:

- Mitigation can be structural or non-structural
 - Structural measures involve construction of barriers, channels, or slope stabilization
 - Non-structural measures involve temporary or permanent removal of elements at risk from hazardous areas or changing people's behavior to reduce vulnerability
- Structural measures can be located in the watershed, in the channel, on the fan, or in the community
- Structural measures in Canada are often located at the fan apex or on the fan, because the channel and upper watershed are typically inaccessible.

Figure 3-9 shows selected examples of structural mitigation measures. These measures are often combined to create a "functional chain" of mitigation (Hübl & Fiebiger, 2005). The most effective mitigation systems include a range of different techniques, to provide redundancy and optimize risk reduction. Selection of appropriate mitigation depends on several factors, including:

- The budget and any funding-related conditions
- The timeline for design and construction
- Land use or zoning restrictions
- Maintenance considerations, including capability for long-term maintenance, and options for debris disposal
- Social and cultural implications
- Environmental concerns, such as fish-bearing streams or wildlife corridors.



Figure 3-9. Examples mitigation structures: (a) earth-fill retention berm, Glyssibach, Brienz, Switzerland; (b) stone diversion berm, Trachtbach, Brienz, Switzerland; (c) conveyance channel with earthfill berms, Rennebach, Austria; (d) log crib check dams, Gesäuse, Austria; and (e) flexible debris net, Cougar Creek, Canmore, Alberta. Photograph (d) by M. Jakob, other photographs by E. Moase.

Non-structural measures for debris flow and debris flood risk management typically include the following options:

- **Education** – Provide training for residents and workers who are commonly exposed to hazards. Training topics include: how to interpret hazard maps and identify areas exposed to hazards; causes and triggers of events; measures that individual property owners can take to protect themselves; emergency preparedness; and actions to take during an event. This can reduce the vulnerability of individuals to hazardous events.
- **Emergency Management Planning** – Develop plans to respond during or immediately after an event. This would typically involve plans for evacuation, checking in with neighbors, and staging of equipment and materials. This can reduce the consequences of a hazard event and improve resilience of the community.
- **Temporary Evacuation** – This can include precautionary evacuation from hazard zones during periods of heavy rainfall. This method can reduce safety risk but does not reduce property damage. This method can be difficult to implement effectively because of large uncertainties in predicting events, the possibility of frequent false alarms, and the requirement for occupants to evacuate quickly and without assistance.
- **Development Restrictions** – This involves creation of zones where future development is not allowed. This should be based on hazard maps that are updated as conditions and topography change. Particularly, construction of structural mitigation measures can change the debris flow and debris flood impact location and extents.
- **Relocation** – Remove buildings from hazard zones. This can eliminate safety and economic risk from hazard sources, but the costs and trade-offs can be prohibitive.

Use of non-structural measures depends on the type and value of elements at risk, the regulatory and governmental context, and triggers and thresholds for warning system design. Non-structural mitigation could be used in combination with structural mitigation measures to improve risk reduction.

3.9. Summary

This section summarized the different techniques that were applied for X, Y and Z creeks to: (a) estimate the frequency and magnitude of steep creek hazards; (b) numerically simulate the hazards; (c) quantify the life loss and economic risks; and (d) develop conceptual mitigation options. Subsequent sections provide the results of the hazard assessment, risk assessment and mitigation design results for each of the three creeks.



4. X CREEK RESULTS

4. X CREEK RESULTS

This section describes the results of the hazard and risk assessments for X Creek, as well as the proposed conceptual mitigation.

4.1. Previous Events on X Creek

4.1.1. Documented Events

BGC is aware of one documented event on X Creek, in 2013, as summarized in BGC's event forensic memo (December 2, 2013).

Between June 19 and 21, 2013, the southwestern Alberta mountain front was affected by heavy rainfall combined with snowmelt at higher elevations which initiated flooding, debris floods and debris flows on the Bow River and its tributaries. On X Creek, a debris flow deposited material on the fan, but no flows were reported to have reached the Peaks of Grassi development or any other developments downstream.

4.1.2. Assessment of the June 2013 Event

The June 2013 event on X Creek was a debris flow which diluted into a debris flood in the lower fan portions. The debris flow originated in the steeper west tributary of the watershed, with very limited sediment and water input from the larger east tributary. Near the fan apex, the deposit shows typical debris flow morphology, including small levees and lobes. Indicators of high velocities and impact forces, including damage to trees immediately below the fan apex, were observed in the field. The distal sediment deposit is much finer-grained and less continuous (only located in flat areas and in hollows), suggesting a debris flood process (Figure 4-1). A minor avulsion occurred during the 2013 event, which directed flow along the Highline Trail and eroded a channel through the forest (Figure 4-2).

The sediment volume that deposited on the fan during the 2013 event on X Creek is estimated to be about 9,600 m³. This volume was estimated through a combination of field delineations, field deposit estimates and area-volume relationships, as described in Section 3.4.

BGC used a variety of information sources to estimate the peak discharge of the June 2013 event on X Creek, as discussed in Section 3.3. The results of this assessment are summarized in Table 4-1, and the location of the high-water mark cross-sections are shown on Drawing 02.



Figure 4-1. Shallow debris deposits from the June 2013 event on the distal areas on the X Creek fan. BGC photograph, June 11, 2018.



Figure 4-2. Erosion from the trail avulsion on X Creek. BGC photograph, June 13, 2018.

Table 4-1. Comparison of estimated peak discharge values for the June 2013 event on X Creek, using rainfall-runoff modelling and high-water mark cross-sections.

Method	Location	Cross-section peak discharge estimates using different calculation methods (m ³ /s)			Peak Discharge Best Estimate (m ³ /s)
		Jarrett (1984)	Zimmerman (2010)	Prochaska et al. (2008)	
Rainfall-runoff modelling	Fan apex	N/A			9
High-water mark cross-sections	X-01 (Mainstem)	15	33	43	15 – 45
	X-02 (East tributary)	0.3	0.4	2	< 2
	X-03 (East tributary)	0.6	0.6	4	1 – 4
	X-04 (East tributary)	0.9	0.8	5	1 – 5
	X-05 (Paleochannel)	5	9	16	5 – 15
	X-06 (Mainstem)	30	53	72	30 – 70
	X-07 (West tributary)	30	69	56	30 – 70

As seen in the table, the rainfall-runoff modelling suggested a peak discharge of 9 m³/s and the cross sections give peak discharge values of 15 to 70 m³/s on the mainstem of the creek. BGC estimates that the actual peak discharge (including water and sediment) at the fan apex was about 30 m³/s, based on the following:

- Rainfall runoff modelling likely underestimated the peak discharge because it doesn't account for orographic effects, antecedent rainfall, snowmelt inputs or additional volume due to sediment bulking
- General agreement between sections X-01, X-06 and X-07, given a velocity of about 3 to 4 m/s.

The 2013 event on X Creek is estimated to have a return period of about 100 years.

4.1.3. Air Photograph Interpretation

Air photo and satellite images between 1947 and 2013 were examined to search for evidence of past debris flows or sediment transport events on X Creek. Before the 2013 debris flow, no conclusive evidence of debris flow activity (e.g., tree breaks, fresh vegetation, etc.) was observed in the air photo record. However, a lighter shade of vegetation is apparent along the X Creek channel across the fan on all air photos (Drawing 04) and is most apparent in the 1947 air photo. This change in vegetation may represent recurring sediment transport events in the X Creek fan channel. Additionally, fresh avalanche tracks were observed in the lower watershed in 1947, 1962 and 1997. Overall, the air photo and satellite records indicate that no debris flows of sufficient magnitude to disturb tree cover occurred between 1947 and 2013.

These observations support the supposition that small debris flows or sediment transport events may occur several times a century on X Creek with magnitudes in the hundreds to low thousands of cubic metres.

4.1.4. Dendrogeomorphology

Results for the 16 samples on X creek are presented in Table 4-2 and tree locations are shown on Drawing 01, 02 and 03.

Table 4-2. Summary of X Creek dendro sample features.

Sample	Tree type	Minimum establishment date (first ring)	Features ¹⁴
X-01	Pine	1894	Moderate TRDs in 1954
X-02	Engelmann Spruce	1923	Faint TRDs
X-03	Engelmann Spruce	1954	Moderate to strong TRDs in 1956, 1963, 1964, 1965, 1968, 1971, 1972, and 2010
X-04	Engelmann Spruce	1921	Sustained growth reduction starting in 2002, moderate to strong TRDs in 2002, 2003, 2005, 2012, and 2015
X-05	Engelmann Spruce	1926	Moderate TRDs in 1948
X-06	Engelmann Spruce	1906	Moderate to strong TRDs in 1998, 2002, 2008, and 2012
X-07	Engelmann Spruce	1811	Scar in 1892, moderate TRDs in 1828, 1850, 1888, 1911, and 1973, sustained growth acceleration starting in 1898
X-08	Engelmann Spruce	1947	Faint TRDs
X-09	Engelmann Spruce	1930	Moderate TRDs in 1967
X-10	Engelmann Spruce	1929	Moderate to strong TRDs in 1955, 1957, and 1970
X-11	Pine	1956	Faint TRDs
X-12	Engelmann Spruce	1874	Moderate to strong TRDs in 1896, 1898, 1901, 1906, 1965, and 2011
X-13	Engelmann Spruce	1941	Moderate TRDs in 2014 and 2015
X-14	Engelmann Spruce	1919	Reaction wood in 1922
X-15	Engelmann Spruce	1939	Moderate to strong TRDs in 1958, 1959, 1966, and 1995
X-16	Engelmann Spruce	1934	Faint TRDs

The scar on sample X-07 corresponds to historical forest fire events in the area and the moderate to strong TRD features do not show up in enough trees at the same to outline any event. In addition, the minimum establishment ages do not suggest that a consistent stand replacing event occurred within the tree ring record. With few anomalies and no agreement between samples, the

¹⁴ Traumatic resin ducts (TRDs) are small circles that appear within the wood, which indicate that the tree sustained physical damage during that year (similar to scar tissue).

X Creek tree samples provide limited information to outline any historical events and there were no events from the air photo interpretation to corroborate with. Therefore, dendrogeomorphology was not used in to develop the F-M relationships.

4.1.5. Radiocarbon Dating

Radiocarbon sample dates and test pit logs were used to estimate sediment volumes for four different events, which are summarized in Table 4-3 and shown in Figure 4-3. Radiocarbon results are expressed in years before present (BP), where “present” is taken to be the year 1950. The radiocarbon results showed a minimum event return period of 500 years and a thickness of units in the test pits of 0.5 to 0.7 m. An accurate aggradation rate for the fan could not be estimated as it was challenging to line up events across the test pits. This is most likely due to the fingering nature of the deposits on the fan. Detailed results of the radiocarbon dating are provided in Appendix D.

Table 4-3. Sediment volumes estimated from radiocarbon dates and test pit logging.

Event Date (years BP)	Sample	Estimated Deposit Area (m ²)			Measured Unit Thickness (m)	Best Estimate Volume (m ³)
		Minimum	Maximum	Best estimate		
9200	TP-X-01, G3	32,000	81,000	56,500	0.4	22,600
6400	TP-X-02, G3	41,000	80,000	60,500	0.7	42,350
5100	TP-X-03, G2	43,000	80,000	61,500	0.6	36,900
430	TP-X-04, G1	30,000	114,000	72,000	0.5	36,000

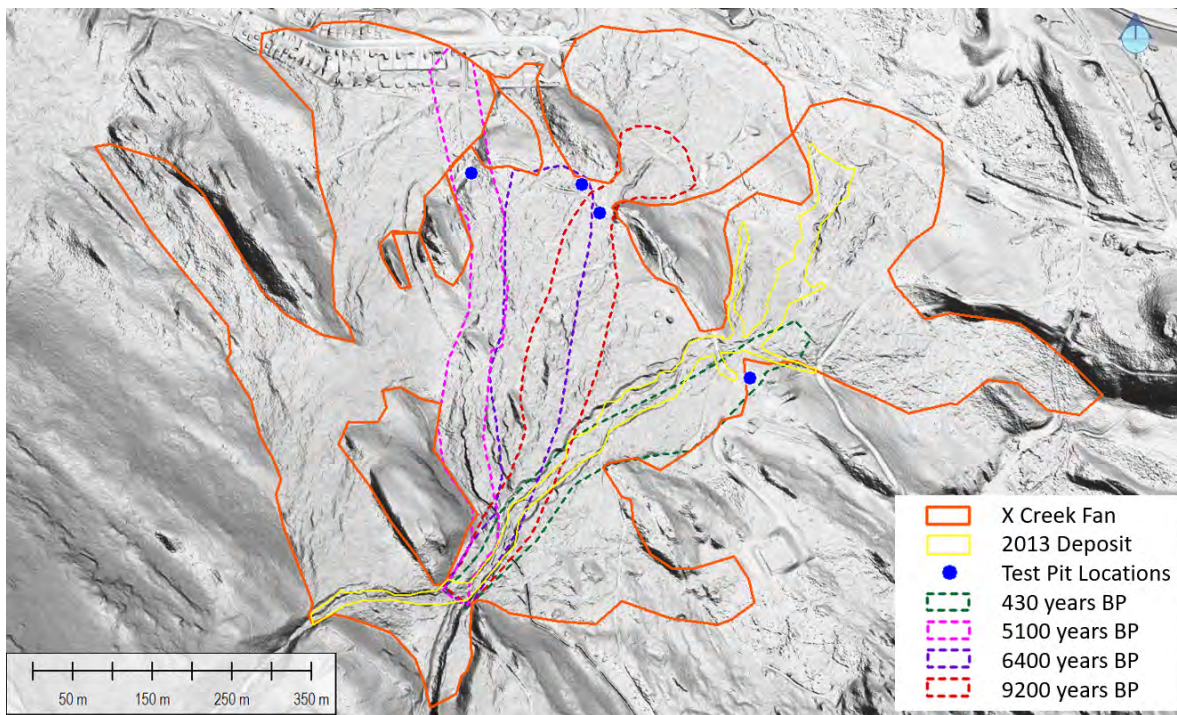


Figure 4-3. Deposit delineations from radiocarbon sample dates and test pit locations.

4.2. Frequency Magnitude Relationship

4.2.1. Flood Peak Discharge

The flood peak discharge results were estimated using rainfall-runoff modelling and are summarized in Table 4-4.

Table 4-4. Estimated peak discharge for X Creek based on historical precipitation at Kananaskis climate station and under possible climate change conditions.

Return Period (years)	Historical Peak Discharge (m ³ /s)	2050-2100 RCP 4.5		2050-2100 RCP 8.5	
		Peak Discharge (m ³ /s)	Percent increase from historical (%)	Peak Discharge (m ³ /s)	Percent increase from historical (%)
10	10	14	40	14	40
30	16	24	50	24	50
100	26	40	54	38	46
300	38	57	50	56	47
1000	55	82	49	80	50
3000	76	111	46	107	41

The historical peak discharge estimates were used for flood modelling.

4.2.2. Debris-flow Sediment Volume and Peak Discharge

The interpreted F-M relationship for X Creek is shown in Figure 4-4, and the estimated sediment volumes and peak discharges for each return period are provided in Table 4-5. The error bars for the data points shown on Figure 4-4 were developed through a combination of geoscientific judgement based on the understanding of the respective geomorphological processes and specific error estimations related to the individual analytical methods.

Table 4-5. Interpreted sediment transport magnitudes for each return period scenario on X Creek.

Return Period (years)	Sediment Volume (m ³)	Peak Discharge at fan apex (m ³ /s)	Event types
10 to 30	1,000	20	Debris flood
30 to 100	7,000	140	Debris flow
100 to 300	14,000	250	Debris flow
300 to 1000	21,000	350	Debris flow
1000 to 3000	28,000	440	Debris flow

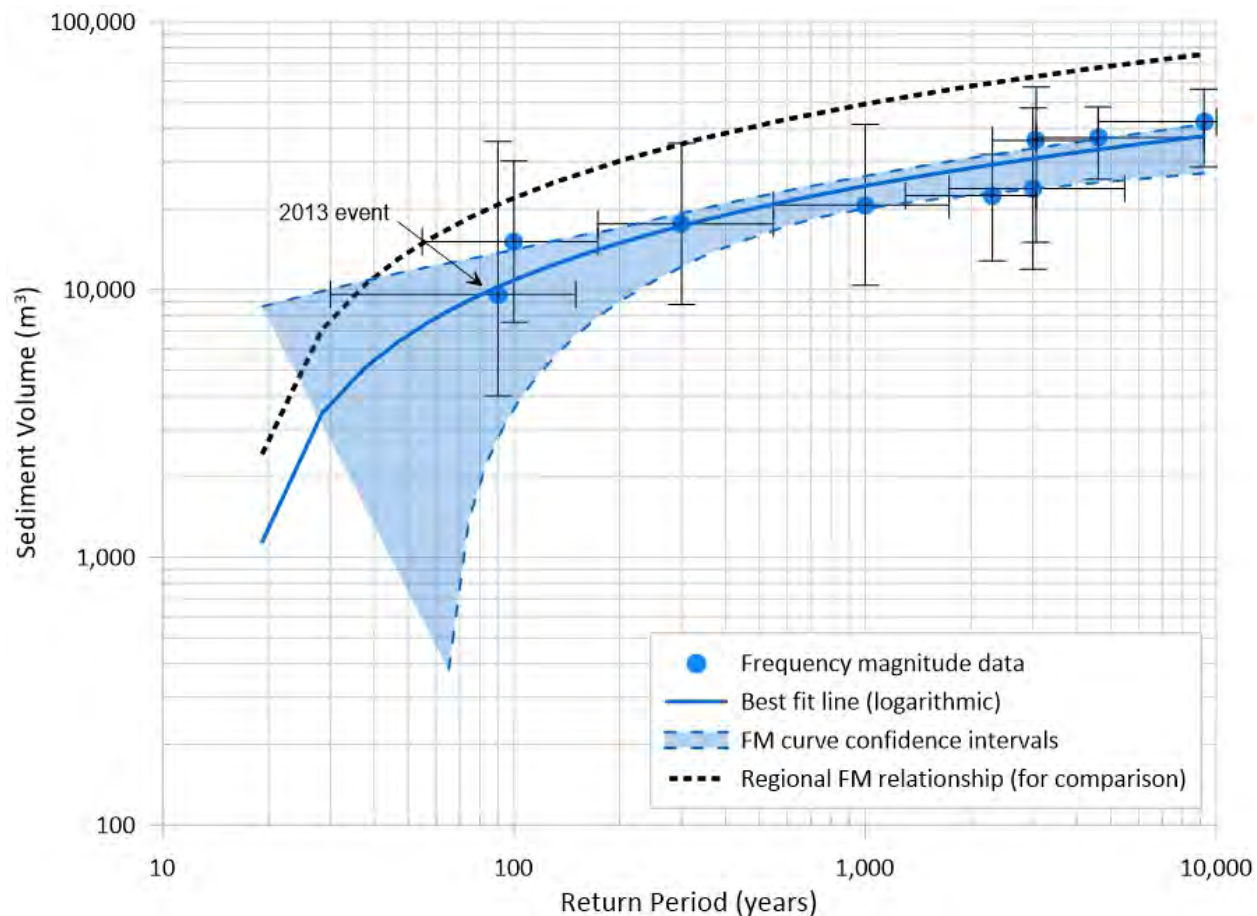


Figure 4-4. Interpreted F-M relationship for X Creek (blue), compared with the regional F-M relationship (black).

The following additional qualitative observations help to interpret steep creek hazards on X Creek:

- Debris flows on X Creek have an interpreted return period of approximately 100 years. Sediment transport in the form of bedload transport or small debris floods occurs more frequently.
- The regional F-M relationship predicts larger sediment volumes than the site-specific F-M relationship, likely because the regional relationship was developed for debris-flow watersheds and X Creek is a debris-flow and debris-flood watershed (see Figure 2-4).
- The frequency of steep creek hazards on X Creek may increase in the future, due to climate change. This may not be accompanied by a decrease in debris volumes as the watershed is supply-unlimited.
- A stand-replacing wildfire would likely increase the frequency and magnitude of debris flows in the few years after the fire and until pioneer vegetation has replaced the burned areas. Should a watershed-wide wildfire occur, additional protection may become necessary.

- The best estimate F-M curve shown in Figure 4-4 attempts to strike a balance between expected climate-change effects (higher frequency-lower magnitude) and the potential for stand-replacing wildfires associated with future higher temperatures and/or beetle infestations (higher frequency-higher initial magnitude).

4.2.3. Peak Discharge of Debris Flows Compared to Debris Floods

Peak discharges from debris flows are much higher than those of clearwater floods and debris flows. First, most debris flows are initiated by landslides impacting the main channel at some oblique angle and transferring their momentum to the main channel where a process known as undrained loading leads to liquefaction of all channel materials overlying bedrock which then mobilize abruptly. Then, as the debris flow moves downstream, it progressively bulks through entrainment of channel debris and creek flows. Debris flows can travel faster than the clearwater flows, resulting in a disproportionately high bulking factor¹⁵. As a result, volume bulking by at least one order of magnitude (x10) has been often reported in the literature. A summary is provided by Hungr et al. (2005). The volumetric bulking is associated with a corresponding increase in peak discharge as the rising volume will occupy an increasingly larger cross-section, and at velocities well in excess of those observed in clearwater floods (Iverson, 2012). Iverson and Ouyang (2015) found that debris-flow mass and momentum grows simultaneously when rapid debris loading over a wet alluvial channel surface produces large positive pore pressures. These elevated pore pressure fields encourage bed sediment scour, lead to friction reduction and unleash a positive feedback through further momentum increase. Recent advances in this science are summarized in Jakob (2018).

In some cases, debris flows can also be generated due to landslide dam outbreak floods. BGC did consider dam breaks at the study creeks, but because the mainstem channels are so steep, a landslide dam would impound a relatively small volume of water and as such is not considered as a dominating trigger event for debris flows.

The empirical relations used by BGC to estimate peak discharge are global equations, repeated by workers in Japan, Canada, Switzerland and elsewhere. There are no geomechanical reasons why there should be significant differences in these relations despite different hydroclimatic and geomorphic environments, as long as one can claim the debris flow is either coarse granular (with a steep bouldery frictional front that results in high peak flows) or is muddy without a steep bouldery front. The latter is more typical for volcanic debris flows or those in fine-grained sedimentary or weak metamorphic rocks.

¹⁵ The “bulking factor” is defined, in this context as the ratio between the clearwater flood discharge and the debris flow peak discharge. It largely depends on the amount of debris stored in a given channel, the availability of water in the stream or on the eroded side slopes, channel length and the capability of the debris flow to erode all the of the loose channel fill.

4.3. Numerical Debris-Flow Modelling and Hazard Mapping

X Creek floods and debris flows were modelled using FLO-2D, following the procedures outlined in Section 3.6. Assuming sufficient antecedent rainfall, even frequent flood events have the potential to reach the developed areas, but the flow depths and velocities would be quite low (less than 1 m deep, less than 2 m/s, I_{DF} less than $10 \text{ m}^3/\text{s}^2$). Debris flows with a return period greater than about 100 years may reach the limits of the present development, if an avulsion occurs. Table 4-6 summarizes the range of predicted impact intensities at the urban development interface for the different return periods.

Table 4-6. Impact intensities at urban development on the X Creek fan.

Return Period (years)	Governing process at the development interface	Number of Occupied Parcels with	
		$I_{DF} < 1$	$I_{DF} = 1 - 10$
10 to 30	Floods and debris floods - avulsion	2*	Impact not anticipated
30 to 100	Floods and debris floods - avulsion	2*	
100 to 300	Debris flow – avulsion	7*	2*
300 to 1000	Debris flow – avulsion	7*	2*
1000 to 3000	Debris flow - avulsion	97*	4*

* Indicates that impact is only anticipated in the event of an avulsion, which was assigned a 10% or 30% probability, depending on the area.

The FLO-2D numerical modelling results were processed for each return period to create interpreted hazard maps of flow intensity, which are presented on Drawing 06. The wooden walls were included in the model and had an impact on the flows, but these differences cannot be explicitly seen in the drawings because the flows were categorized by intensity category (i.e., $I_{DF} < 1$, 1-10 and 10-100). Drawing 09 shows the composite hazard map for the X, Y and Z creeks study area.

4.4. Risk Analysis

This section summarizes results of the X Creek risk assessment based on the methods described in Appendix E. As described in Section 3.7.2, safety risk is estimated separately for individuals and groups (societal risk). The results presented are the combined annual risk from all debris-flow scenarios, given that some parcels may be impacted by more than one scenario.

4.4.1. Individual Risk

There are no instances where estimated individual risk exceeds 1:10,000 risk of fatality per year for occupied residential buildings for X Creek. At three parcels estimated individual risk exceeds 1:100,000. Drawing 10 shows residential lots where BGC’s best-estimate of individual risk (PDI) exceeds 1:100,000 risk of fatality per year assuming full-time occupancy. Lots not coloured did not exceed $PDI = 1:100,000$.

4.4.2. Group Risk

Figure 4-5 presents the results of group risk analysis on an F-N curve. Estimated overall group debris-flow risk plots well into the ALARP range when compared to the international risk tolerance standards described in Section 3.7.2. Table 4-7 lists the range of expected fatalities for each main debris flow scenario for X Creek. It is important to note that the debris-flow return periods listed in Table 4-7 indicate the recurrence interval of the scenario, not the likelihood of fatalities (which is lower, as shown on Figure 4-5).

Table 4-7. Estimated life loss for each scenario on X Creek.

Scenario	Frequency (1:years)	Estimated Number of Fatalities (N)
1	1:10 to 1:30	<1
2	1:30 to 1:100	<1
3	1:100 to 1:300	<1
4	1:300 to 1:1000	<1
5	1:1000 to 1:3000	2

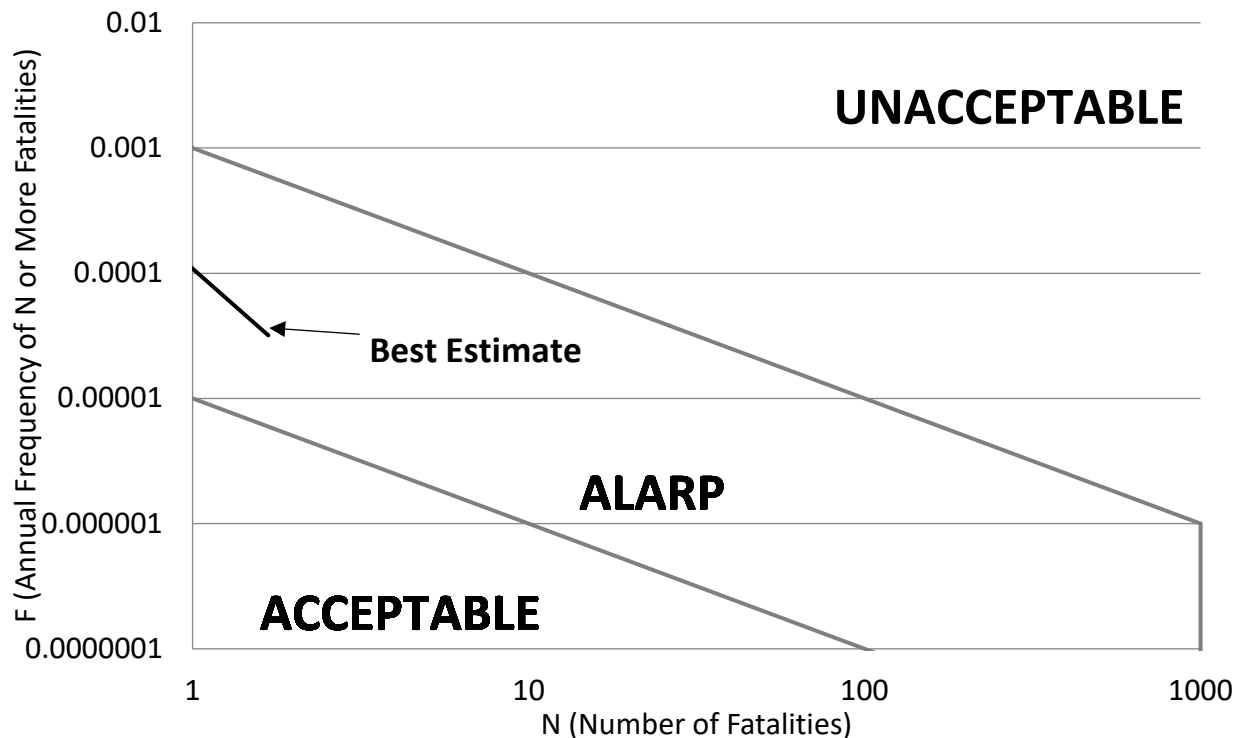


Figure 4-5. F-N curve showing the results of the X Creek risk analysis for groups.

4.4.3. Economic Risk

This section describes economic risk from building damage and interruption to business activity.

4.4.3.1. Building Damage

Table 4-8 summarizes the total building damage cost estimates for each scenario. For reference, total estimated building value for the X Creek fan is approximately \$51 million. Average annualized building damage is approximately \$13,000 based on the scenario damage costs listed in Table 4-8. Estimated building damage costs are based only on a portion of assessed building values and do not include damage to contents or inventory. In addition, costs of cleanup and recovery are not included.

Table 4-8. Summary of estimated building damage at X Creek.

Scenario	Frequency (1:years)	Building Damage Cost (\$)
1	1:10 to 1:30	36,000
2	1:30 to 1:100	36,000
3	1:100 to 1:300	1,155,000
4	1:300 to 1:1000	1,155,000
5	1:1000 to 1:3000	2,132,000

Life loss and economic risk on X Creek are controlled by the mid-creek avulsion scenario, which is estimated to start occurring around the 100-year return period. Since only a portion of the flow is expected to avulse, the I_{DF} category is similar on the distal fan for the 100 to 300-year and the 300 to 1000-year events, leading to similar life loss risk and building damage estimates.

4.4.3.2. Business Activity

Table 4-9 summarizes business activity impacts for business located within the study area. BGC mapped the distribution of business activity in the study area by estimating the total annual revenue for each parcel identified as containing businesses.

Based on the data available, it is not possible to determine the vulnerability of businesses to complete loss of function, and associated economic cost, due to debris flow impacts. For example, a retail store could suffer loss of inventory and business function, whereas a business generating revenue elsewhere could suffer office-related damages without necessarily losing their source of revenue.

As a proxy for level of business impact, BGC summed the annual revenue estimated for parcels impacted by a debris-flow scenario. Additional factors such as indirect losses, damages to business equipment or inventory, interruption of transportation corridors, or effects of prolonged outage were not estimated.

Table 4-9. Summary of business consequence estimates on X Creek.

Scenario	Frequency (1:years)	Number of Businesses Affected	Number of Employees Affected	Annual Business Revenue (\$M)
1	1:10 to 1:30	3	91	4.5
2	1:30 to 1:100	3	91	4.5
3	1:100 to 1:300	4	93	4.6
4	1:300 to 1:1000	4	93	4.6
5	1:1000 to 1:3000	5	94	4.7

Note: Three of the businesses are located in the same building.

4.4.4. Lifelines

Drawing 06 shows the location of lifelines in relation to steep creek hazard scenarios. Table 4-10 lists roads directly impacted by debris-flow scenarios. In the emergency response period, evacuation and road closures may also extend beyond the areas directly impacted.

Table 4-10. Summary of roads and bridges potentially impacted by debris flow scenarios on X Creek.

Lifeline		Scenario				
		1	2	3	4	5
Roads	Lawrence Grassi Ridge					✓
	Shellian Lane					✓
	Three Sisters Drive			✓	✓	✓
	Wilson Way			✓	✓	✓

4.5. Conceptual Mitigation Design

The X Creek risk assessment has shown that the current steep creek hazard risk is tolerable for individual risk, and within the ALARP (as low as reasonably possible) zone for group risk. In addition, the expected annualized economic losses are about \$13,000. According to the ALARP principle (see Section 3.7.2), additional measures should be implemented if practicable and cost effective. Potential measures could include:

- Monitoring and channel works to reduce avulsion potential** – The majority of the risk on X Creek comes from avulsion scenarios in which flows spill out of the existing channel and impact a portion of the fan away from the existing channel. Channel works to reduce avulsion potential at critical channel areas could be a cost-effective option for managing risk. The channel should be visually monitored on a periodic basis to identify potential avulsion locations. Monitoring visits could occur on an annual basis, as well as after significant flow events. The focus should be on the west bank of X Creek, from the apex of the west tributary to the mid-fan. Issues observed during the monitoring could be managed using hand tools or tracked equipment to modify the channel and bank to limit

the likelihood of avulsions. Minor modifications may include moving or realigning obstructions such as trails and bridges; even these small features can cause avulsions, as occurred with the trail avulsion during the June 2013 event. More substantial channel works could involve shifting material from the channel bed to the banks, to build up the banks and increase the capacity of the main channel.

- **Education and local protection guidance for homeowners** – In the event of an avulsion, the intensity of debris flows at the development interface on X Creek would be less than $10 \text{ m}^3/\text{s}^2$ ($I_{DF} < 10$), which corresponds to a vulnerability of 1-2% for people in buildings. Life loss risk under these conditions could be reduced by limiting or avoiding occupancy of basements and upslope ground floor areas during periods of heavy rain. To limit economic damages, individual properties owners could construct permanent or temporary barriers to protect ground-level windows and doors from water and debris entry. Hazard awareness education could involve information flyers that are mailed to homeowners, as well as public meetings.
- **Installation of additional wooden walls** – The existing wooden walls upstream of the Peaks of Grassi development do not extend across the entire development interface, as shown on Figure 2-8. The walls could be extended or modified to divert flows. Upgrades to existing drainage channels or installation of additional channels may be needed to manage the concentrated flows.

Table 4-11 presents a comparison of these options.

Table 4-11. Comparison of X Creek mitigation options.

Criteria	Monitoring and channel works	Hazard awareness education	Additional wooden walls
Cost*	Low to moderate - Depends on the scale of the work	Low – guidance could be shared at an information session or by mail	Moderate – similar order of magnitude as the 2012 wall upgrades on Y Creek
Risk reduction	Should be able to considerably reduce the risk of avulsion, but requires periodic review and maintenance	Depends on the resident, including degree of advance preparation and long-term memory about the recommendations	Would reduce flow intensity, even if broken or damaged in the event; design should consider potential risk transfer caused by flow diversion
Impact to wildlife	Limited, depends on scale of work	No impact	Some impact, would need to consult with AEP to limit impact to wildlife
Impact to residents	Very limited, depends on scale of work	Success of the measure depends on resident involvement	Limited impact

* Cost comparison categories are approximate, as follows: Low means <\$10,000; Moderate means \$10,000 - \$100,000 and High means >\$100,000.

The comparison above suggests that a combination of channel monitoring and works to reduce avulsion potential, and hazard awareness education is likely preferable on X Creek. BGC is

available to support Canmore with identifying the preferred risk management solution for the community.

4.6. Summary

The X Creek fan is a large, telescoping fan complex that is subject to debris floods, debris flows and avulsions. Debris flows have an estimated minimum return period of about 30 to 100 years, and smaller sediment transport events may occur more frequently.

Because of limited development on the X Creek fan, the life loss risks are tolerable or within the ALARP zone. Avulsion potential controls the risk to development. In other words, a debris flood or debris flow needs to occur *and* avulse towards the development, before it poses a safety or economic risk. Risk could be managed by channel works to reduce avulsion potential and hazard awareness education for residents living in the hazard zone.



5. Y CREEK RESULTS

5. Y CREEK RESULTS

This section describes the results of the hazard and risk assessments for Y Creek, as well as the proposed conceptual mitigation.

5.1. Previous Events on Y Creek

5.1.1. Documented Events

BGC is aware of two documented events on Y Creek, in 2012 and 2013.

On July 13, 2012, a heavy rainstorm in the watershed resulted in overland flooding to the usually dry gullies on the eastern side of the Y Creek fan (Town of Canmore, 2012). The existing diversion structures were not long enough to capture the flow, which resulted in the flooding of several backyards. Residents directed the flows between homes to minimize damage to the structures and prevent basement flooding. Because of the volume of water and steep grades, a large quantity of landscape material was washed from the yards and onto the street where it was carried to downstream sewers. The stormwater drainage system plugged, resulting in flooding of the street (Canmore, 2012). Following this event, the existing diversion structure was extended by about 40 m to the west, to protect an additional five homes. This work was completed before spring 2013, and the extension was designed by ISL Engineering and Land Services Ltd.

Between June 19 and 21, 2013, southwestern Alberta was affected by heavy rainfall combined with snowmelt at higher elevations which initiated flooding, debris floods and debris flows on the Bow River and its tributaries. On Y Creek, a debris flow deposited material on the fan and muddy water descended to the diversion structures protecting the development. According to videos and reports from the Town of Canmore, the diversion structures were not overtopped and directed flow to the riprapped channel as designed with no damage to residences (Figure 5-1).

5.1.2. Assessment of the June 2013 Event

The June 2013 event on Y Creek was a debris flow which diluted into a debris flood in the lower fan portions. Near the fan apex, the deposit shows typical debris flow morphology, including small levees and lobes. Indicators of high velocities and impact forces, including super-elevation around the bed at the fan apex, and damage to trees immediately below the fan apex were observed in the field. The distal sediment deposit is much finer-grained and less continuous (only located in flat areas and in hollows), suggesting a debris flood process.

The sediment volume that deposited on the fan during the 2013 event on Y Creek is estimated to be about 4,200 m³. This was estimated through a combination of field delineations, field deposit estimates and area-volume relationships, as described in Section 3.4.

BGC used a variety of data sources and techniques to estimate the peak discharge of the June 2013 event on Y Creek, as discussed in Section 3.3. The results of this assessment are summarized in Table 5-1.



Figure 5-1. Water flowing along the eastern Y Creek diversion wall during the June 2013 event, shown looking upstream (left) and east along the wall (right). Images are stills from a video provided by the Town of Canmore, dated June 19, 2013 at 10:20 am.

Table 5-1. Comparison of estimated peak discharge values for the June 2013 event on Y Creek, using rainfall-runoff modelling and high-water mark cross-sections.

Method	Location	Cross-section peak discharge estimates using different calculation methods (m ³ /s)			Peak Discharge Best Estimate (m ³ /s)
		Jarrett (1984)	Zimmerman (2010)	Prochaska et al. (2008)	
Rainfall-runoff modelling	Fan apex	N/A			1.4
High-water mark cross-sections	Y-01	9.2	14	14.2	10 – 15
	Y-02	30	(not credible)	38	30 – 40
	Y-03	6	15	11	5 – 15
Super-elevation assessment	Fan apex bend	N/A			25
Video reconstruction	East wooden wall	1.3	1.5	N/A	1.4

The rainfall-runoff modelling suggested a peak discharge of 1.4 m³/s and peak discharge values derived from cross-sections and back-calculated velocities yield between 6 and 38 m³/s. This discrepancy is expected as rainfall-runoff modelling does not account for sediment bulking and additional water entrainment associated with debris flow activity. BGC estimates that the actual (best estimate) peak discharge (including water and sediment) of the debris flow at the fan apex was about 25 m³/s, based on the following:

- Several of the cross-sections did not have bedrock control, so additional erosion could have occurred in the measured section since the event peak. This would result in an over-estimate of the discharge.
- Section Y-03 was estimated from lidar and field photographs based on vegetation trim-lines. Vegetation has likely re-established in the five years since the event.

The 2013 event on Y Creek is estimated to have a return period of about 100 years.

5.1.3. Air Photograph Interpretation

Air photo and satellite images between 1947 and 2013 were examined to search for evidence of past debris flows or sediment transport events on Y Creek. No conclusive evidence of debris flow activity (e.g., tree breaks, fresh vegetation, etc.) was observed in the air photo record. However, shallow debris flow deposits can be obscured by tree cover, as was observed in the 2013 satellite image. A swath of a lighter shade of vegetation is apparent on the 1947, 1950 and 1962 air photos on the west edge of the fan (Drawing 04). This vegetation is most obvious on the 1962 air photographs and may represent a debris flow or avalanche path that occurred prior to 1947 that was subsequently re-vegetated by deciduous trees. Additionally, fresh avalanche tracks were observed in the lower watershed in 1962 and 1997. Overall, the air photo and satellite records indicate that no debris flows of sufficient magnitude and intensity to snap trees and leave a visible path from the air occurred between 1947 and 2013.

5.1.4. Dendrogeomorphology

Results for the 8 samples on Y creek are presented in Table 5-2 and tree locations are shown on Drawing 01, 02 and 03.

The scar on sample Y-08 corresponds to historical forest fires in the area in the late 1800s, and the moderate to strong traumatic resin duct features do not show up in enough trees at the same time to outline any event. In addition, the minimum establishment ages do not suggest that a consistent stand replacing event occurred within the tree ring record. With few anomalies and no agreement between samples, the Y Creek tree samples provide limited information to outline any historical events and there were no analogous events deducted from air photo interpretation. Therefore, results from the dendrogeomorphological analysis were not used to develop the F-M relationship for Y Creek.

Table 5-2. Summary of Y Creek dendro sample features.

Sample	Tree type	Minimum establishment date (first ring)	Features
Y-01	Engelmann Spruce	1918	Faint TRDs
Y-02	Engelmann Spruce	1927	Moderate TRDs in 1944 and 1970
Y-03	Engelmann Spruce	1925	Faint TRDs
Y-04	Engelmann Spruce	1937	Faint TRDs
Y-06	Engelmann Spruce	1918	Faint TRDs
Y-07	Engelmann Spruce	1933	Faint TRDs
Y-08	Engelmann Spruce	1927	Scar in 1989, reaction wood starting in 1954, moderate to strong TRDs in 1952, 1970, 1996, and 2013
Y-09	Engelmann Spruce	1957	Reaction wood starts in 1968, moderate TRDs in 1970

5.1.5. Radiocarbon Dating

Radiocarbon sample dates and test pit logs were used to estimate sediment volumes for four different events, which are summarized in Table 5-3 and shown in Figure 5-2. The radiocarbon results showed a minimum event return period of 300 years and a thickness of units in the test pits of 0.4 to 0.9 m. Detailed results of the radiocarbon dating are provided in Appendix D.

Table 5-3. Sediment volumes estimated from radiocarbon dates and test pit logging.

Event Date (years BP)	Sample	Estimated Deposit Area (m ²)	Measured Unit Thickness (m)	Estimated Deposit Volume (m ³)
2000	TP-BGC18-Y-01-G1	14,000	0.9	12,600
900	TP-BGC18-Y-02-G2	11,000	0.6	6,600
700	TP-BGC18-Y-03-G2	14,000	0.4	5,600
200	TP-BGC18-Y-04-G1	12,000	0.9	5,400

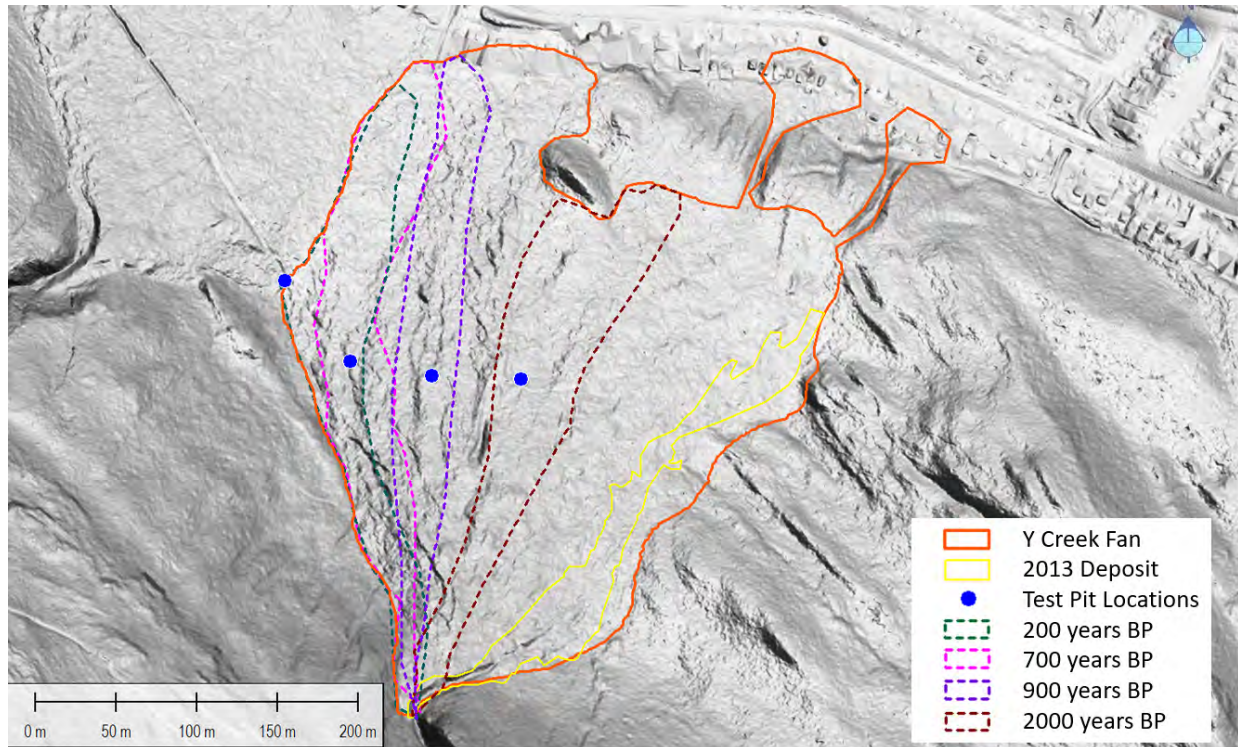


Figure 5-2. Deposit delineations from radiocarbon sample dates and test pit locations. Note that these delineations are very approximate given the low number of test pits that were possible due to access restrictions.

5.2. Frequency Magnitude Relationship

This section summarizes the site-specific F-M relationship that was developed for Y Creek.

5.2.1. Flood Peak Discharge

The flood peak discharge results were estimated using rainfall-runoff modelling and are summarized in Table 5-4.

Table 5-4. Estimated peak discharge for Y Creek based on historical precipitation at Kananaskis Climate Station including climate change effects.

Return Period (years)	Historical Peak Discharge (m ³ /s)	2050-2100 RCP 4.5		2050-2100 RCP 8.5	
		Peak Discharge (m ³ /s)	Percent increase from historical (%)	Peak Discharge (m ³ /s)	Percent increase from historical (%)
10	2	3	50	3	50
30	4	5	25	5	25
100	6	9	50	9	50
300	9	13	44	13	44
1000	13	19	46	18	38
3000	17	26	53	25	47

The historical peak discharge estimates were used for flood modelling.

5.2.2. Debris-flow Sediment Volume and Peak Discharge

The interpreted F-M relationship for Y Creek is shown in, and the estimated debris-flow sediment volumes and peak discharges for each return period are provided in Table 5-5. The error bars for the data points shown on Figure 5-3 were developed through a combination of judgement and error estimations from the analysis methods.

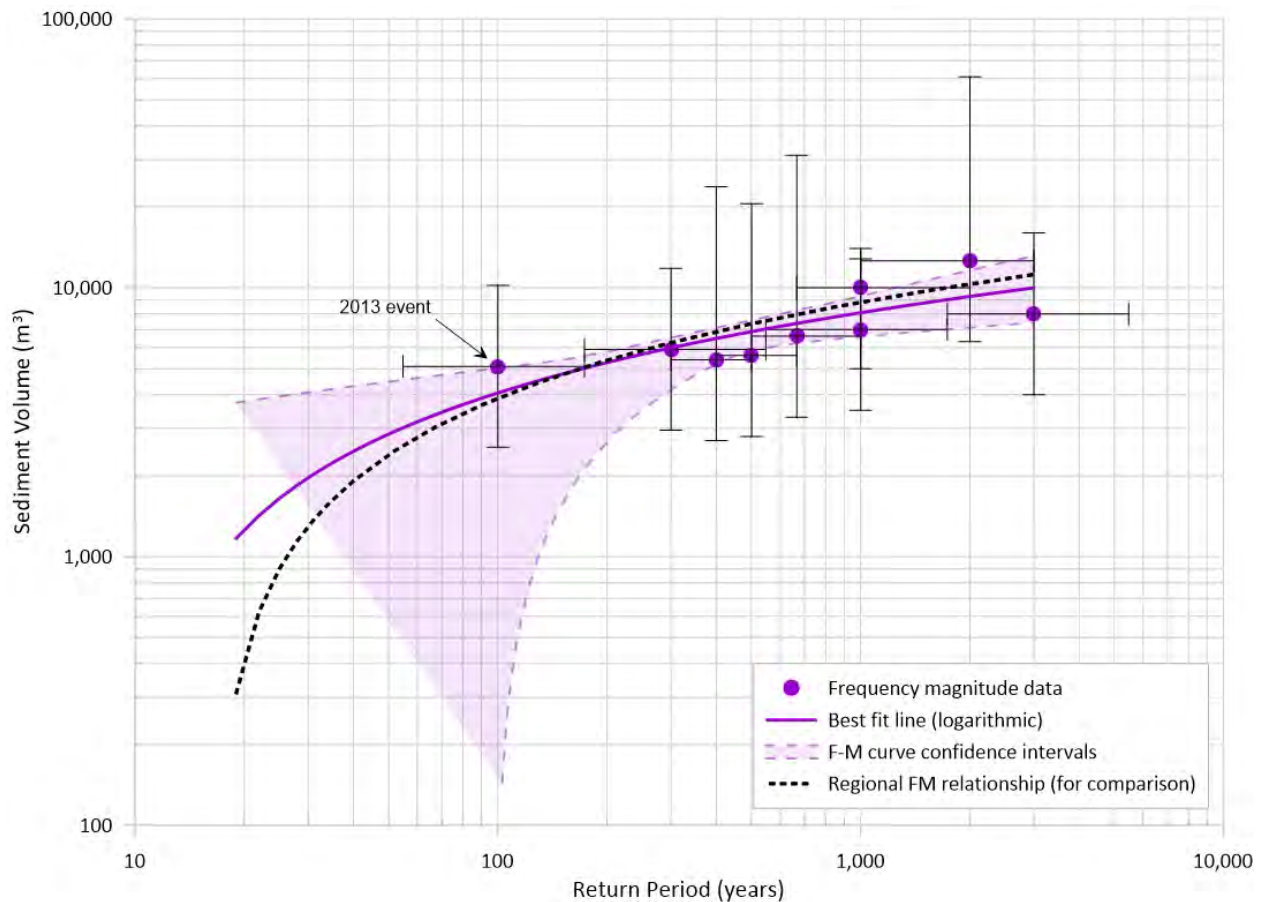


Figure 5-3. Interpreted F-M relationship for Y Creek (purple), compared with the regional F-M relationship (black).

Table 5-5. Interpreted sediment magnitudes for each return period scenario on Y Creek.

Return period (years)	Sediment Volume (m ³)	Peak Discharge at fan apex (m ³ /s)	Event types
10 to 30	1,100	5	Debris flood
30 to 100	3,100	10	Debris flood
100 to 300	5,100	110	Debris flow
300 to 1000	7,000	140	Debris flow
1000 to 3000	9,000	170	Debris flow

The following additional qualitative observations help to interpret steep creek hazards on Y Creek:

- Debris flows on Y Creek have an interpreted return period of approximately 100 years. Sediment transport in the form of bedload transport or small debris floods occurs more frequently.
- Y Creek shows good agreement between the interpreted site-specific F-M relationship and the regional F-M relationship.
- The frequency of steep creek hazards on Y Creek may increase in the future, due to climate change. This may be accompanied by a decrease in debris volumes as the watershed is supply-limited.
- A stand-replacing wildfire would likely increase the frequency and magnitude of debris flows in the few years after the fire and until pioneer vegetation has replaced the burned areas. Should a watershed-wide wildfire occur, additional protection may become necessary.
- The best estimate F-M curve shown in Figure 5-3 attempts to strike a balance between expected climate-change effects (higher frequency-lower magnitude) and the potential for stand-replacing wildfires associated with future higher temperatures and/or beetle infestations (higher frequency-higher initial magnitude).

5.3. Numerical Debris-Flow Modelling and Hazard Mapping

Y Creek floods and debris flows were modelled using FLO-2D, following the process outlined in Section 3.6. Assuming sufficient antecedent rainfall, even frequent flood events have the potential to reach the developed areas, but the flow depths and velocities would be quite low (less than 1 m deep, less than 2 m/s, I_{DF} less than $10 \text{ m}^3/\text{s}^2$). Debris flows with a return period greater than about 300 years may reach the limits of the present development. Table 5-6 summarizes the predicted impact intensities at the development interface.

Table 5-6. Impact intensities at urban development on the Y Creek fan.

Return Period (years)	Governing process at development interface	Number of Occupied Parcels with	
		$I_{DF} < 1$	$I_{DF} = 1 - 10$
10 to 30	Floods and debris floods	79	0
30 to 100	Floods and debris floods	81	0
100 to 300	Floods and debris floods	120	0
300 to 1000	Debris flow	116	10
1000 to 3000	Debris flow	95	48

The FLO-2D numerical modelling results were processed for each return period to create interpreted hazard maps of flow intensity, which are presented on Drawing 07. The wooden walls were included in the model and had an impact on the flows, but these differences cannot be explicitly seen in the drawings because the flows were categorized by intensity category (i.e., $I_{DF} < 1$, 1-10 and 10-100). Drawing 09 shows the composite hazard map for the X, Y and Z creeks study area.

5.4. Risk Analysis

This section summarizes results of the Y Creek risk assessment based on the methods described in Appendix E. As described in Section 3.7.2, safety risk is estimated separately for individuals and groups (societal risk). The results presented are the combined annual risk from all debris-flow scenarios, given that some parcels may be impacted by more than one scenario.

5.4.1. Individual Risk

There are no instances where estimated individual risk exceeds 1:10,000 risk of fatality per year for occupied residential buildings for Y Creek. At eight parcels, estimated individual risk exceeds 1:100,000. Drawing 10 shows residential lots where BGC's best-estimate of individual risk (PDI) exceeds 1:100,000 risk of fatality per year assuming full-time occupancy. Lots not coloured did not exceed PDI = 1:100,000.

5.4.2. Group Risk

Figure 5-4 presents the results of group risk analysis on an F-N curve. Estimated overall group debris-flow risk plots well into the ALARP range when compared to the international risk tolerance standards described in Section 3.7.2. Table 5-7 lists the range of expected fatalities for each main debris flow scenario for Y Creek. It is important to note that the debris-flow return periods listed in Table 5-7 indicate the recurrence interval of the scenario, not the likelihood of fatalities (which is lower, as shown on Figure 5-4).

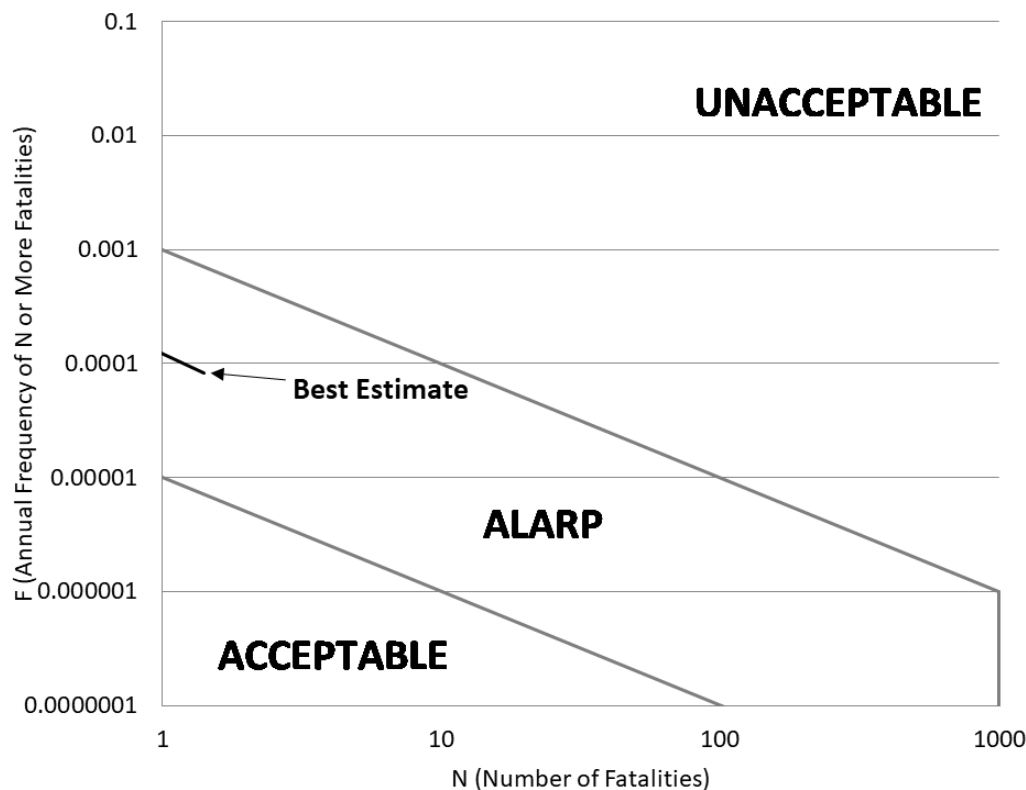


Figure 5-4. F-N curve showing the results of the Y Creek risk analysis for groups.

Table 5-7. Estimated life loss for each scenario on Y Creek.

Scenario	Frequency (1:years)	Estimated Number of Fatalities (N)
1	1:10 to 1:30	0
2	1:30 to 1:100	<1
3	1:100 to 1:300	<1
4	1:300 to 1:1000	<1
5	1:1000 to 1:3000	1

5.4.3. Economic Risk

This section describes economic risk from building damage and interruption to business activity.

5.4.3.1. Building Damage

Table 5-8 summarizes the total building damage cost estimates for each scenario. For reference, total estimated building value for Y Creek is approximately \$56 million. Average annualized building damage is approximately \$16,000 based on the scenario damage costs listed in Table 5-8. Estimated building damage costs are based only on a portion of assessed building values and do not include damage to contents or inventory. In addition, costs of cleanup and recovery are not included.

Table 5-8. Summary of estimated building damage at Y Creek.

Scenario	Frequency (1:years)	Building Damage Cost (\$)
1	1:10 to 1:30	101,000
2	1:30 to 1:100	115,000
3	1:100 to 1:300	502,000
4	1:300 to 1:1000	1,623,000
5	1:1000 to 1:3000	4,271,000

5.4.3.2. Business Activity

Table 5-9 summarizes business activity impacts for business located within the study area.

Table 5-9. Summary of business consequence estimates on Y Creek.

Scenario	Frequency (1:years)	Number of Businesses Affected	Number of Employees Affected	Annual Business Revenue (\$M)
1	1:10 to 1:30	1	2	0.2
2	1:30 to 1:100	1	2	0.2
3	1:100 to 1:300	2	14	3.2
4	1:300 to 1:1000	2	14	3.2
5	1:1000 to 1:3000	2	14	3.2

5.4.4. Lifelines

Drawing 07 shows the location of lifelines in relation to steep creek hazard scenarios. Table 5-10 lists roads directly impacted by debris-flow scenarios. In the emergency response period, evacuation and road closures may also extend beyond the areas directly impacted.

Table 5-10. Summary of roads and bridges potentially impacted by debris flow scenarios of Y Creek.

Lifeline		Scenario				
		1	2	3	4	5
Roads	Kamenka Green			✓	✓	✓
	Lawrence Grassi Ridge	✓	✓	✓	✓	✓
	Peaks Drive	✓	✓	✓	✓	✓
	Wilson Way	✓	✓	✓	✓	✓

5.5. Conceptual Mitigation Design

The Y Creek risk assessment has shown that the current steep creek hazard risk is tolerable for individual risk, and within the ALARP (as low as reasonably possible) zone for group risk. In addition, the expected annualized economic losses are about \$16,000. According to the ALARP principle (see Section 3.7.2), additional measures should be implemented if practicable. Potential measures could include:

- Education and local protection guidance for homeowners** – The intensity of debris flows at the development interface on Y Creek would be less than 10 m³/s² (IDF < 10), which corresponds to a vulnerability of 1-2% for people in buildings. Life loss risk under these conditions could be reduced by limiting or avoiding occupancy of basements and upslope ground floor areas during periods of heavy rain. To limit economic damages, individual properties owners could construct permanent or temporary barriers to protect ground-level windows and doors from water and debris entry. Hazard awareness education could involve information flyers that are mailed to homeowners, as well as public meetings.

- **Reinforce and increase the height of the existing wooden wall** – Numerical modelling suggests that the existing wooden wall behind 931 to 949 Wilson Way could be overtopped by flows above the 100-year return period. Increasing the height and impact resistance of this wall could reduce the risk for the houses. Wooden walls are a suitable option on Y Creek, due to the low flow depths and velocities of debris flows on the distal fan. This option increases the diverted flow discharge and volume, and may transfer risk to homes that are along or downstream of the drainage channel. Risk transfer should be assessed during design, and upgrades to existing drainage channels or installation of additional channels may be needed to manage the concentrated flows.
- **Installation of additional wooden walls** – The existing wooden walls upstream of the Peaks of Grassi development do not extend across the entire development interface, as shown on Figure 2-8. Additional wooden walls could be constructed to detain and attenuate debris. Wooden walls may be preferable in undeveloped areas because they have a small footprint, can be routed around trees, and can be constructed in offset segments to allow wildlife passage.
- **Construction of earthfill berms** – Earthfill berms could also be used to similar effect as the wooden walls, but with a longer design life. Berms could be constructed from the fan sediment and revegetated after construction to limit the long-term disturbance. However, berm construction would cause significant short-term disturbance and would require tree-felling, due to the larger footprint.

Figure 5-5 shows potential alignments for structural mitigation measures, and Table 5-11 presents a comparison of these options.

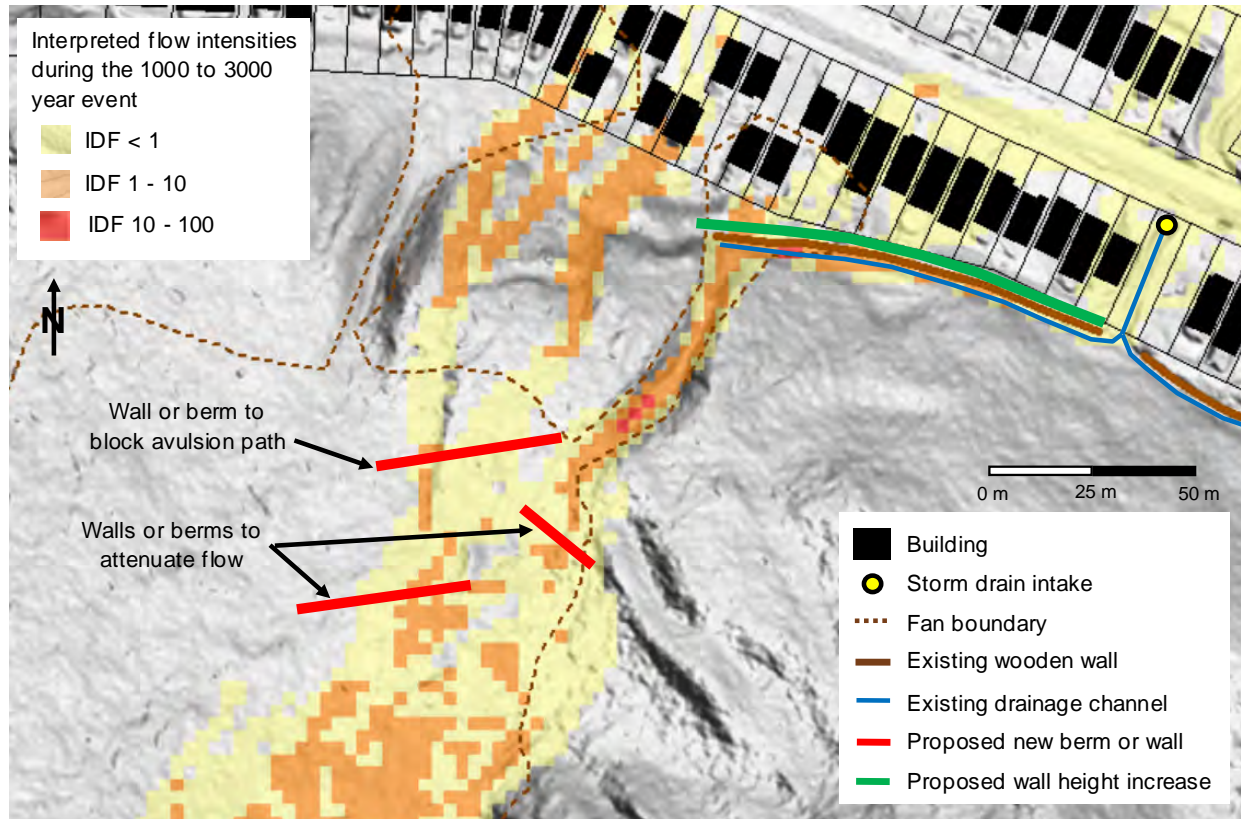


Figure 5-5. Proposed locations for structural mitigation measures on Y Creek.

Table 5-11. Comparison of Y Creek mitigation options.

Criteria	Hazard awareness education	Reinforce existing wall	Additional wooden walls	Earthfill berms
Cost*	Low – guidance could be shared at an information session or by mail	Moderate to high	Moderate to high – depending on the extent and location of the walls	Moderate to high – depending on the extent and location of the berms
Risk reduction	Depends on the resident, including degree of advance preparation and long-term memory about the recommendations	Reduces likelihood that existing wall is overtopped; Risk transfer should be assessed	Would reduce flow intensity, even if broken or damaged in the event	Would reduce flow intensity, even if eroded or overtopped
Impact to wildlife and vegetation	No impact	Very limited	Some impact, would need to consult with AEP to optimize alignment	Significant impact during construction, some impact once constructed
Impact to residents	Success of the measure depends on resident involvement	Low, except during construction	Low	Low

* Cost comparison categories are approximate, as follows: Low means <\$10,000; Moderate means \$10,000 - \$100,000 and High means >\$100,000.

The comparison above suggests that the preferred option may be increasing and reinforcing the existing wooden wall, in combination with hazard awareness education. BGC is available to support Canmore with identifying the preferred risk management solution for the community.

5.6. Summary

Y Creek is a sediment supply limited watershed that is subject to debris flows. Debris flows have an estimated minimum return period of about 30 to 100 years, and smaller sediment transport events may occur more frequently.

Because development is located at the far edge of the fan, the life loss risks on Y Creek are tolerable and within the ALARP zone. Events larger than about the 100-year return period could cause damage to properties below the main channel, including the area that was affected in 2012 and 2013, and shallow flooding may occur in this area even during more frequent events (see Drawings 07 and 09). Average annualized building damage is about \$16,000 per year. Risk can be managed by increasing and reinforcing the existing wooden diversion wall and hazard awareness education for residents living in the hazard zone.



6.0 Z CREEK RESULTS

6. Z CREEK RESULTS

This section describes the results of the hazard and risk assessments for Z Creek, as well as the proposed conceptual mitigation.

6.1. Previous Events on Z Creek

6.1.1. Documented Events

BGC is aware of one documented event on Z Creek, in 2013.

Between June 19 and 21, 2013, the southwestern Alberta mountain front was affected by heavy rainfall combined with snowmelt at higher elevations which initiated flooding, debris floods and debris flows on the Bow River and its tributaries. On Z Creek, a small debris flood deposited material on the fan, but no flows were reported to have reached the Peaks of Grassi development.

6.1.2. Assessment of the June 2013 Event

The June 2013 event on Z Creek was a debris flood that deposited sediment at the fan apex and on the mid-fan. The deposit lacks the levee and lobe features which would indicate a debris flow event. The deposit did reach within 110 m of the development.

The sediment volume that deposited on the fan during the 2013 event on Z Creek is estimated to be about 500 m³. This volume was estimated through a combination of field delineations, field deposit estimates and area-volume relationships, as described in Section 3.4.

BGC used a variety of data sources and techniques to estimate the peak discharge of the June 2013 event on Z Creek, as discussed in Section 3.3. The results of this assessment are summarized in Table 6-1.

Table 6-1. Comparison of estimated peak discharge values for the June 2013 event on Z Creek, using rainfall-runoff modelling and high-water mark cross-sections.

Method	Location	Cross-section peak discharge estimates using different calculation methods (m ³ /s)			Peak Discharge Best Estimate (m ³ /s)
		Jarrett (1984)	Zimmerman (2010)	Prochaska et al. (2008)	
Rainfall-runoff modelling	Fan apex	N/A			0.8
High-water mark cross-sections	Z-01	0.8	0.9	(not credible – not a debris flow)	<1
	Z-02	5	9		5 – 10
	Z-03*	3	4		3 - 5

* Section geometry measured from 2015 lidar, flow depths estimated from satellite orthoimagery.

The rainfall-runoff modelling suggested a peak discharge of 0.8 m³/s and peak discharge values derived from cross-sections and back-calculated velocities yield between 1 and 10 m³/s. BGC estimates that the actual (best estimate) peak discharge (including water and sediment) at the fan apex was about 1 m³/s, based on the good agreement between the rainfall-runoff modelling and section Z-01. Sections Z-02 and Z-03 were located significantly upstream of the fan apex and

may have had snow at the channel base at the time of the event. The 2013 event on Z Creek is estimated to have a return period of about 100 years, based on the 24-hour rainfall volume.

6.1.3. Air Photograph Interpretation

Air photo and satellite images between 1947 and 2013 were examined to search for evidence of past debris flows or sediment transport events on Z Creek. No conclusive evidence of debris flow activity (e.g., tree breaks, fresh vegetation, etc.) was observed in the air photo record. However, shallow debris flow deposits can be obscured by tree cover, as was observed in the 2013 satellite image. Fresh avalanche tracks were observed in the lower watershed in 1962 and 1997. Overall, the air photo and satellite records indicate that no debris flows or debris floods of sufficient magnitude to disturb tree cover occurred between 1947 and 2013.

6.1.4. Dendrogeomorphology

Results for the 13 samples on Z creek are presented in Table 6-2 and tree locations are shown on Drawing 01, 02 and 03.

Table 6-2. Summary of Z Creek dendro sample features.

Sample	Tree type	Minimum establishment date (first ring)	Features
Z-01	Engelmann Spruce	1973	Reaction wood starting in 1984
Z-02	Engelmann Spruce	1943	Faint TRDs
Z-03	Engelmann Spruce	1948	Sustained growth acceleration starting in 1999, moderate TRDs in 1999 and 2001
Z-04	Engelmann Spruce	1876	Sustained growth acceleration starting in 1898, moderate to strong TRDs in 1902 and 1932
Z-05	Engelmann Spruce	1890	Sustained growth acceleration starting in 1898, moderate to strong TRDs in 1897, 1910, and 1911
Z-06	Engelmann Spruce	1899	Faint TRDs
Z-07	Engelmann Spruce	1852	Sustained growth acceleration starting in 1900, strong TRDs in 1899
Z-08	Engelmann Spruce	1901	Faint TRDs
Z-09	Engelmann Spruce	1853	Scar in 1895, sustained growth acceleration starting in 1898, moderate to strong TRDs in 1899, 1902, 1921, 1923, 1947
Z-10	Engelmann Spruce	1914	Faint TRDs
Z-11	Engelmann Spruce	1867	Scar in 1900 and 1914, reaction wood starting in 1901, sustained growth acceleration starting in 1903
Z-12	Engelmann Spruce	1890	Sustained growth acceleration starting in 1898, moderate to strong TRDs in 1902, 1925, 1961, and 1971
Z-13	Engelmann Spruce	1941	Moderate TRDs in 2002

The scars on samples Z-09 and Z-11 corresponds to historical forest fire events in the area, and the traumatic resin duct (TRD) features do not show up on enough trees at the same time to outline any event. In addition, the minimum establishment ages do not suggest that a consistent stand replacing event occurred within the tree-ring record. With few anomalies and no agreement between samples, the Z Creek tree samples provide limited information to outline any historical events and there were no events from the air photo interpretation to corroborate with. Therefore, dendrogeomorphology was not used in the development of the F-M relationships.

6.1.5. Radiocarbon Dating

Radiocarbon sample dates and test pit logs were used to estimate sediment volumes for three different events, which are summarized in Table 6-3 and shown in Figure 6-1. The radiocarbon results showed a minimum event return period of 400 years and a thickness of units in the test pits of 0.3 to 0.6 m. Detailed results of the radiocarbon dating are in Appendix D.

Table 6-3. Sediment volumes estimated from radiocarbon dates and test pit logging.

Event Date (years BP)	Sample	Estimated Deposit Area (m ²)	Measured Unit Thickness (m)	Estimated Deposit Volume (m ³)
8700	TP-BGC18-Z-03-G2	10,000	0.5	5,000
3100	TP-BGC18-Z-02-G2	14,000	0.3	4,200
1900	TP-BGC18-Z-01-G2	13,000	0.6	7,800

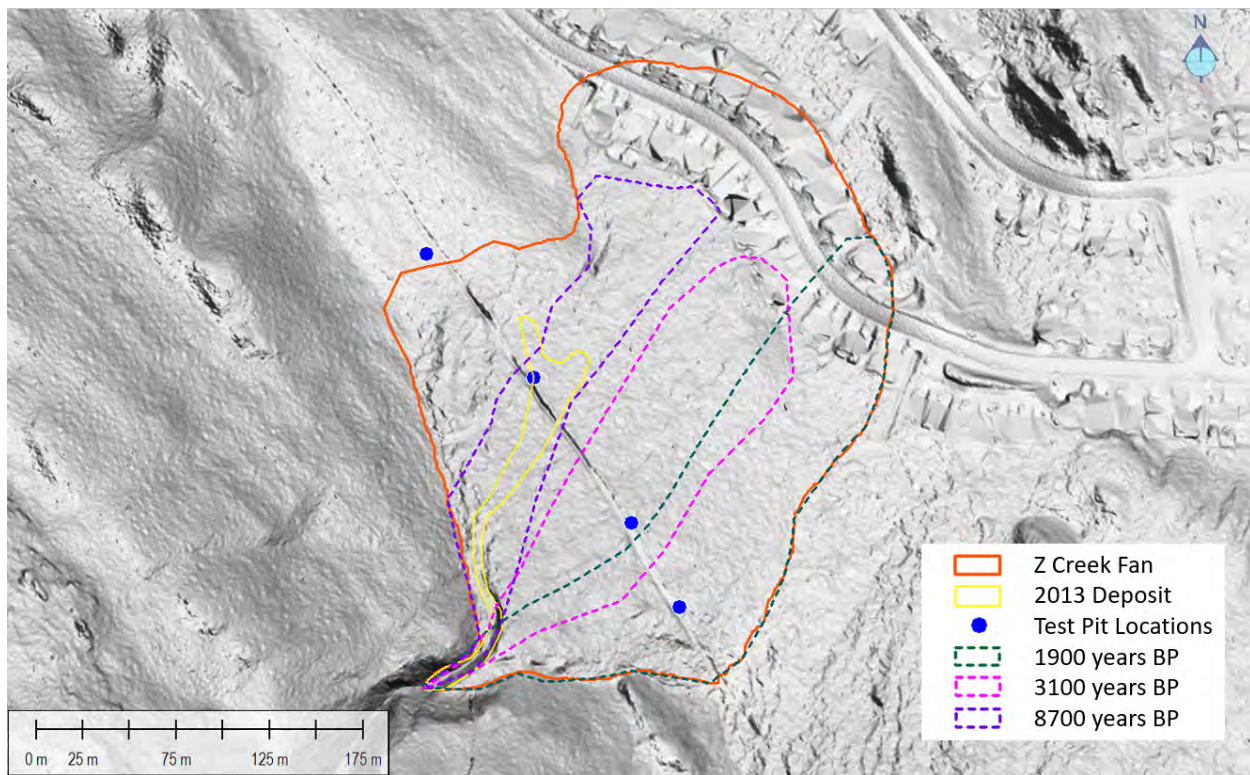


Figure 6-1. Deposit delineations from radiocarbon sample dates and test pit locations.

6.2. Frequency Magnitude Relationship

This section summarizes the site-specific F-M relationship that was developed for Z Creek.

6.2.1. Flood Peak Discharge

The flood peak discharge results were estimated using rainfall-runoff modelling and are summarized in Table 6-4.

Table 6-4. Estimated peak discharge for Z Creek based on historical precipitation at Kananaskis Climate Station and under possible climate change conditions.

Return Period (years)	Historical Peak Discharge (m ³ /s)	2050-2100 RCP 4.5		2050-2100 RCP 8.5	
		Peak Discharge (m ³ /s)	Percent Increase (%)	Peak Discharge (m ³ /s)	Percent Increase (%)
10	1	2	100	2	100
30	2	3	50	3	50
100	3	5	66	5	66
300	5	7	40	7	40
1000	7	10	43	10	43
3000	9	13	44	13	44

The historical peak discharge estimates were used for flood modelling.

6.2.2. Debris-flow Sediment Volume and Peak Discharge

The interpreted F-M relationship for Z Creek is shown in, and the estimated debris-flow sediment volumes and peak discharges for each return period are provided in Table 6-5. Sediment transport is not expected to occur on Z Creek below the 30-year return period. The error bars for the data points shown on Figure 6-2 were developed through a combination of judgement and error estimations from the analysis methods.

Table 6-5. Interpreted debris flow magnitudes for each return period scenario on Z Creek.

Return period (years)	Sediment Volume (m ³)	Peak Discharge at fan apex (m ³ /s)	Event types
30 to 100	900	5	Debris flood
100 to 300	2,400	10	Debris flood
300 to 1000	3,900	86	Debris flow
1000 to 3000	5,400	110	Debris flow

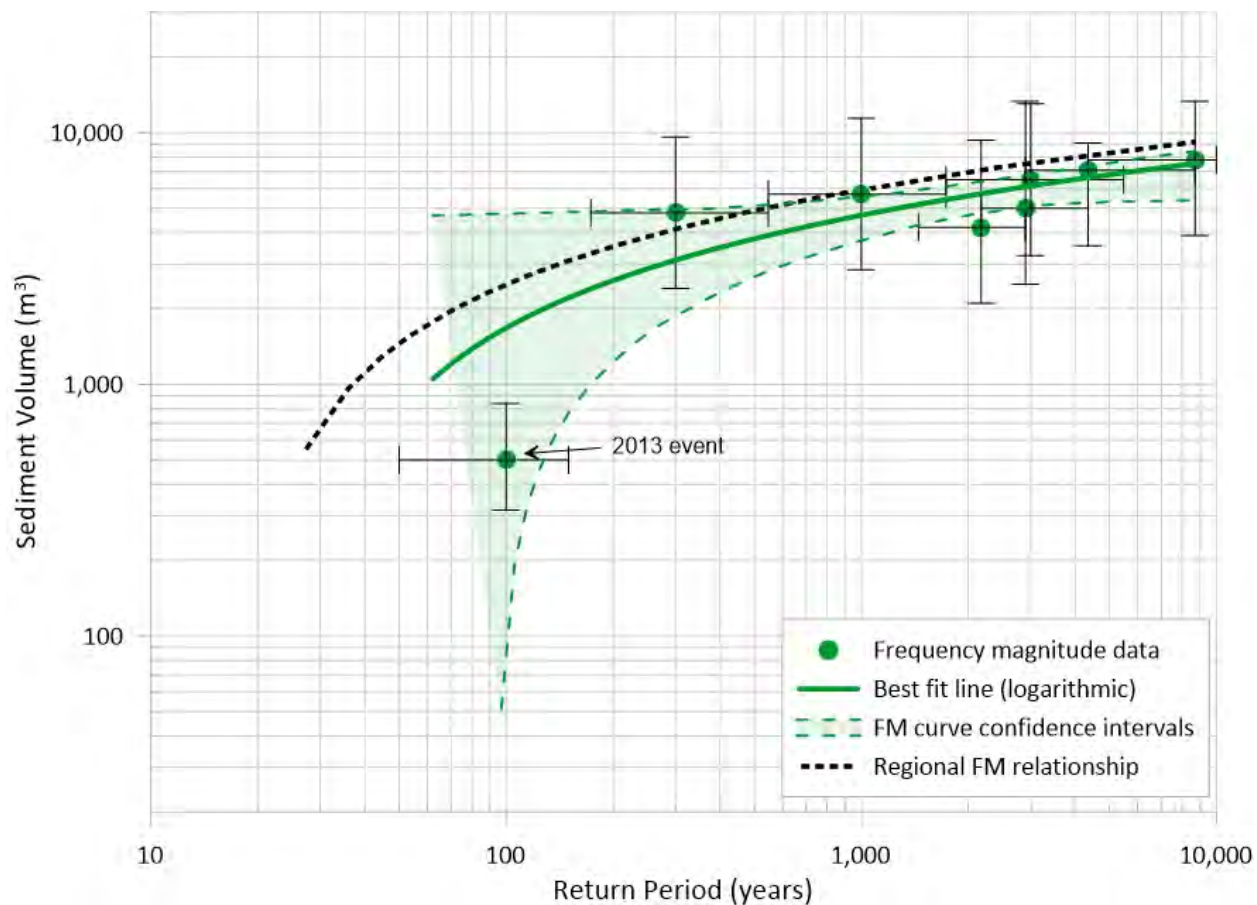


Figure 6-2. Interpreted F-M relationship for Z Creek (green), compared with the regional F-M relationship (black).

The 2013 event is associated with a comparatively small sediment volume and peak discharge, due to the long duration of the June 2013 storm.

The following additional qualitative observations help to interpret steep creek hazards on Z Creek:

- Debris flows on Z Creek have an interpreted return period of approximately 300 years. Sediment transport in the form of bedload transport or small debris floods occurs more frequently.
- Z Creek shows good agreement between the interpreted site-specific F-M relationship and the regional F-M relationship.
- The frequency of steep creek hazards on Z Creek may increase in the future, due to climate change. This may be accompanied by a decrease in debris volumes as the watershed is supply-limited.
- A stand-replacing wildfire would likely increase the frequency and magnitude of debris flows in the few years after the fire and until pioneer vegetation has replaced the burned areas. Should a watershed-wide wildfire occur, additional protection may become necessary.

- The best estimate F-M curve shown in Figure 6-2 attempts to strike a balance between expected climate-change effects (higher frequency-lower magnitude) and the potential for stand-replacing wildfires associated with future higher temperatures and/or beetle infestations (higher frequency-higher initial magnitude).

6.3. Numerical Debris-Flow Modelling and Hazard Mapping

6.3.1. Modelling and Hazard Mapping Results

Z Creek floods and debris flows were modelled using FLO-2D, following the process outlined in Section 3.6. Assuming sufficient antecedent rainfall, even frequent flood events have the potential to reach the developed areas, but the flow depths and velocities would be quite low (less than 1 m deep, less than 2 m/s, I_{DF} less than $10 \text{ m}^3/\text{s}^2$). Debris flows with a return period greater than about 100 years may reach the limits of the present development. Table 6-6 summarizes the predicted impact intensities at the development interface.

Table 6-6. Impact intensities at urban development on the Z Creek fan.

Return Period (years)	Governing process	Number of Occupied Parcels with	
		IDF < 1	IDF = 1 – 10
10 to 30	Floods and debris floods	46	0
30 to 100	Floods and debris floods	46	0
100 to 300	Debris flow	84	6
300 to 1000	Debris flow	68	22
1000 to 3000	Debris flow	67	23

The FLO-2D numerical modelling results were processed for each return period to create interpreted hazard maps of flow intensity, which are presented on Drawing 08. The wooden walls were included in the model and had an impact on the flows, but these differences cannot be explicitly seen in the drawings because the flows were categorized by intensity category (i.e., $I_{DF} < 1$, 1-10 and 10-100). Drawing 09 shows the composite hazard map for the X, Y and Z creeks study area.

6.3.2. Interaction with Stones Canyon Creek

Stones Canyon Creek lies to the west of Z Creek and is also subject to debris flows (BGC 2015). As part of the 2015 work, a frequency-magnitude relationship was compiled for Stones Canyon Creek, and numerical modelling was completed for three debris flow scenarios: an event similar to the 2013 event; a less than 300-year return period event; and a greater than 300-year return period event. Drawing 07 in BGC’s (2015) report demonstrates that debris flow intensities in the west corner of the existing Peaks of Grassi development for the return period class considered are estimated as less than one ($I_{DF} < 1 \text{ m}^3/\text{s}^2$). At return periods greater than 300 years, BGC models suggest that the impact intensity will likely increase to values $> 1 \text{ m}^3/\text{s}^2$. For convenience, the results from the Stones Canyon Creek modeling was added to Drawing 09. Note that the

Stones Canyon Creek modeling was commensurate with a Class 2 assessment according to the Draft Alberta Guidelines for Steep Creek Risk Assessments. This means that the return period classes of 300 to 1000 and 1000 to 3000 years were not modeled. Due to the larger risk potential for the combined X, Y and Z creeks, BGC's conducted a Class 4 study for those creeks.

The numerical modeling conducted for Z-Creek demonstrates that overland flow associated with a debris flow or a high runoff event may reach a small overlapping area of the Stones Creek Canyon fan, in the northwestern edge of the Peaks of Grassi Development. This overlapping area is subject to flow intensities of well below $1 \text{ m}^3/\text{s}^2$, which is expected given the findings of the test trenching program conducted by BGC in 2015 for the proposed Hillcroft development that demonstrated a low degree of geomorphic activity (BGC, 2015). The model results imply that life loss risks to existing and future development in the northwestern edge of the Peaks of Grassi development are negligible, and that nuisance flooding rather than structural impact to buildings can be expected.

One other question is if the northwestern fan edge of Z Creek be subject to higher impact intensities should Z-Creek and Stones Canyon Creek witness simultaneous debris flows or flood events. To answer this question, BGC investigated the flow intensities from Z Creek. In areas that overlap with Stones Canyon Creek, flow intensities on Z Creek are less than $0.1 \text{ m}^3/\text{s}^2$, and often less than $0.01 \text{ m}^3/\text{s}^2$. This suggests that the hazard contribution from Z Creek to the proposed Hillcroft development is negligible in this area. In addition, the assumption of simultaneous flow occurrence is extremely conservative as it presumes that the peak flow velocities and flow depths are reached exactly at the same time. In reality, even if a debris flow or flood occurs on Z-Creek and Stones Canyon Creek on the same day, it is very unlikely that they occur precisely at the same time due to differences in watershed area, triggering mechanism and travel time. To calculate the true hazard probability of a combined event, one would have to estimate the conditional probability of simultaneous occurrence and multiply it by the hazard probability, which then yields a lower value for the original hazard probability. In short, BGC does not expect that the hazard overlap area on the Northwestern corner of the Peaks of Grassi Development result in substantially higher risk, even in the case of simultaneous flood/debris flow events.

The final question pertains to future mitigation on Stones Canyon Creek. BGC (2016) proposed a berm to protect any future development on the western end of the Lawrence Grassi Ridge. The preliminary alignment would run in north-south direction and flank Wilson Way on the truncated Stones Canyon Creek fan. BGC does not expect that this berm would alter the flow behaviour, hazard or risks in the runout area of Z Creek overland flow, as it would be located above the expected Z-creek flow elevation and parallel to the direction of flows from Z Creek.

In summary, overland flow on Z-Creek can potentially interact with Stones Canyon Creek on the latter's distal fan but the expected intensities, even in the very unlikely event of exactly simultaneous debris flow or flood occurrence, are too low to pose a credible life loss risk. Given that the hazard relates to nuisance flooding and not debris flow or debris flood impact, the Town of Canmore will be managing overland flooding via their Draft Engineering Design Guidelines (Canmore, 2019) that considers local site grades and drainage. BGC does not expect any risk

transfer from a deflection berm on Stones Canyon Creek fan, should it be built at some time in the future.

6.4. Risk Analysis

This section summarizes results of the Z Creek risk assessment based on the methods described in Appendix E. As described in Section 3.7.2, safety risk is estimated separately for individuals and groups (societal risk). The results presented are the combined annual risk from all debris-flow scenarios, given that some parcels may be impacted by more than one scenario.

6.4.1. Individual Risk

Estimated individual risk was estimated at 1.2×10^{-4} for four occupied residential parcels at Z creek. This effectively equals Canmore’s individual risk tolerance threshold of 1:10,000 risk of fatality per year. Estimated individual risk exceeds 1:100,000 at 17 parcels; Drawing 10 shows residential lots where BGC’s best-estimate of individual risk (PDI) exceeds 1:10,000 and 1:100,000 risk of fatality per year assuming full-time occupancy. Lots not coloured did not exceed PDI = 1:100,000.

6.4.2. Group Risk

Table 6-7 lists the range of expected fatalities (N) for each main debris flow scenario for Z Creek. As N was less than one for all scenarios, group risk is acceptable. An F-N plot is not presented for this scenario, because the minimum N value on the F-N plot is one.

Table 6-7. Estimated life loss for each scenario on Z Creek.

Scenario	Frequency (1:years)	Estimated Number of Fatalities (N)
1	1:10 to 1:30	0
2	1:30 to 1:100	0
3	1:100 to 1:300	<1
4	1:300 to 1:1000	<1
5	1:1000 to 1:3000	<1

6.4.3. Economic Risk

This section describes economic risk from building damage and interruption to business activity.

6.4.3.1. Building Damage

Table 6-8 summarizes the total building damage cost estimates for each scenario. For reference, total estimated building value for Z Creek is approximately \$44 million. Average annualized building damage is approximately \$21,000 based on the scenario damage costs listed in Table 6-8. Estimated building damage costs are based only on a portion of assessed building

values and do not include damage to contents or inventory. In addition, costs of cleanup and recovery are not included.

Table 6-8. Summary of estimated building damage at Z Creek.

Scenario	Frequency (1:years)	Building Damage Cost (\$)
1	1:10 to 1:30	88,000
2	1:30 to 1:100	219,000
3	1:100 to 1:300	902,000
4	1:300 to 1:1000	2,706,000
5	1:1000 to 1:3000	2,960,000

6.4.3.2. Business Activity

Table 6-9 summarizes business activity impacts for business located within the study area.

Table 6-9. Summary of business consequence estimates on Z Creek.

Scenario	Frequency (1:years)	Number of Businesses Affected	Number of Employees Affected	Annual Business Revenue (\$M)
1	1:10 to 1:30	1	5	0.5
2	1:30 to 1:100	1	5	0.5
3	1:100 to 1:300	5	14	3.5
4	1:300 to 1:1000	5	14	3.5
5	1:1000 to 1:3000	5	14	3.5

6.4.4. Lifelines

Drawing 08 shows the location of lifelines in relation to steep creek hazard scenarios. Table 6-10 lists roads directly impacted by debris-flow scenarios. In the emergency response period, evacuation and road closures may also extend beyond the areas directly impacted.

Table 6-10. Summary of roads and bridges impacted by debris flow scenarios of Z Creek.

Lifeline		Scenario				
		1	2	3	4	5
Roads	Lawrence Grassi Ridge	✓	✓	✓	✓	✓
	Wilson Way	✓	✓	✓	✓	✓

6.4.5. Discussion

The Z Creek life loss results are the “opposite” of the X and Y Creek results; for Z Creek, individual risk is intolerable (or at the threshold), while group risk is acceptable, while X and Y Creeks have

tolerable individual risk and group risk in the ALARP zone. There are two factors that contribute to this difference:

1. There is a larger at-risk population on X and Y creeks (larger N value), compared to Z Creek, because of the higher development density (see Drawing 10). This pushes the N value on X and Y Creeks just above one, which is the threshold for ALARP.
2. High vulnerability values were used for individual risk, compared to group risk. This is standard practice in BGC's risk assessments for Canmore, but it means that individual risk and group risk will not necessarily have equivalent results.

6.5. Conceptual Mitigation Design

6.5.1. Risk Summary and Design Event

Unlike on X and Y creeks, the individual life loss risk on Z Creek is intolerable according to Canmore's policy, *although it is effectively at the threshold (1.2×10^{-4} for 4 parcels) given the uncertainty involved in the study*. Group risk is considered acceptable, because N is less than 1 for all scenarios. Annualized economic losses are expected to be about \$21,000.

For the parcels with PDI > 1:10,000, Table 6-11 shows the breakdown of PDI by return period scenario. The PDI for each scenario are 'partial' risk estimates that contribute (sum) to the total risk of all scenarios.

Table 6-11. PDI by scenario, for parcels on Z Creek with PDI > 1:10,000

Scenario	PDI
1 – 10 to 30 years	0
2 – 30 to 100 years	0
3 – 100 to 300 years	8.4×10^{-5}
4 – 300 to 1000 years	2.9×10^{-5}
5 – 1000 to 3000 years	8.4×10^{-6}
Total	1.2×10^{-4}

The table shows that Scenario 3 (100 to 300-year return period) is the largest contributor to individual life loss risk on Z Creek. In addition, only a minor reduction in individual life loss risk is required to achieve tolerable safety risk, especially because group risk is already acceptable. For these reasons, BGC has used the 100 to 300-year event as the mitigation design event on Z Creek for the conceptual options presented in this report.

The 100 to 300-year event has the following characteristics at the development interface:

- Flow depths between about 0.4 and 0.6 m
- Flow velocities between about 1.2 and 2 m/s.

6.5.2. Debris-flow Mitigation Concept

Potential mitigation measures that could be implemented at Z Creek include:

- **Education and guidance for homeowners** – The intensity of debris flows at the development interface on Z Creek would be less than $10 \text{ m}^3/\text{s}^2$ ($\text{IDF} < 10$), which corresponds to a vulnerability of 1-2% for people in buildings. Life loss risk under these conditions could be reduced by limiting or avoiding occupancy of basements and upslope ground floor areas during periods of heavy rain. To limit economic damages, individual properties owners could construct permanent or temporary barriers to protect ground-level windows and doors from water and debris entry. Hazard awareness education could involve information flyers that are mailed to homeowners, as well as public meetings.
- **Reinforce, increase height, and extend existing wooden wall** – Extend the existing wooden wall that is currently located behind 1129 Wilson Way by approximately 100 m toward the southeast across the full width of modelled flows (Figure 6-3). The existing wall height and impact resistance may need to be increased to resist the design flows. The proposed alignment is favourable because of the 6% gradient along the path, which would allow some portion of the flow to be diverted, rather than stalling or ponding upstream of the wall. Although this should be further reviewed during future design stages, risk transfer appears tolerable because the walls return water to Wilson Way near the location it would arrive to without the diversion. Wooden walls are expected to be suitable due to the expected flow velocity and shallow flow depth. Earthfill berms could be used instead of wood. Earthfill berms could be designed to resist larger flows than wooden walls and may be less of a barrier to wildlife, but earthfill berm would have a larger footprint, require erosion protection that is typically expensive, and cause more disturbance during construction. The location of the wall is favorable because debris-flow depths and velocities decrease with distance from the fan apex. Evaluation of the storm drain intake and storm drain channel should occur in parallel with wall design, as upgrades to these elements may reduce downstream flood damage.
- **Debris flow net in Z Creek canyon** – Construct a flexible debris flow net across Z Creek in its confined reach immediately above the fan apex (Figure 6-4). The net could be up to 6 m tall and on the order of 15 m wide, which would allow the net to be anchored directly into the side walls without posts. The net would be suspended on cables anchored into steeply dipping shale bedrock that is exposed in the sidewalls. A single net would likely have a sediment storage capacity that is less than $1,000 \text{ m}^3$ due to the steep channel (20 degrees) and confined canyon walls, which is less than half of the design event. This would significantly reduce the debris reaching the Z Creek fan but would not eliminate the hazard. Multiple nets could be used to increase sediment storage capacity, although this would complicate access to the nets. Accessing the net(s) for construction, maintenance, and sediment removal will be challenging and will require construction of an access road. Flexible debris flow nets would typically be damaged or destroyed by snow avalanche impacts because avalanche velocity is typically much higher than debris flow velocity. An assessment of potential snow avalanche impact forces at the proposed location should be

completed before this option is selected for debris flow mitigation. An advantage of using a flexible net is that water will be able to pass below the net in the natural channel.

- **Other debris retention in Z Creek canyon** - Construct a series of check dams or a debris basin across Z Creek immediately above or at the fan apex area (Figure 6-4). These structures could be constructed with earthworks (e.g. excavation, earthfill, riprap, stone pitching) or concrete, and would require an access road for construction, maintenance, and sediment removal. The function of these structures would be similar to the flexible debris flow net. Advantages of these types of structures compared to flexible debris net include their ability to resist snow avalanche impact and they could be designed to retain up to the design debris volume. Disadvantages include that these structures would likely be more expensive than flexible debris nets and would have a larger footprint and area of disturbance.

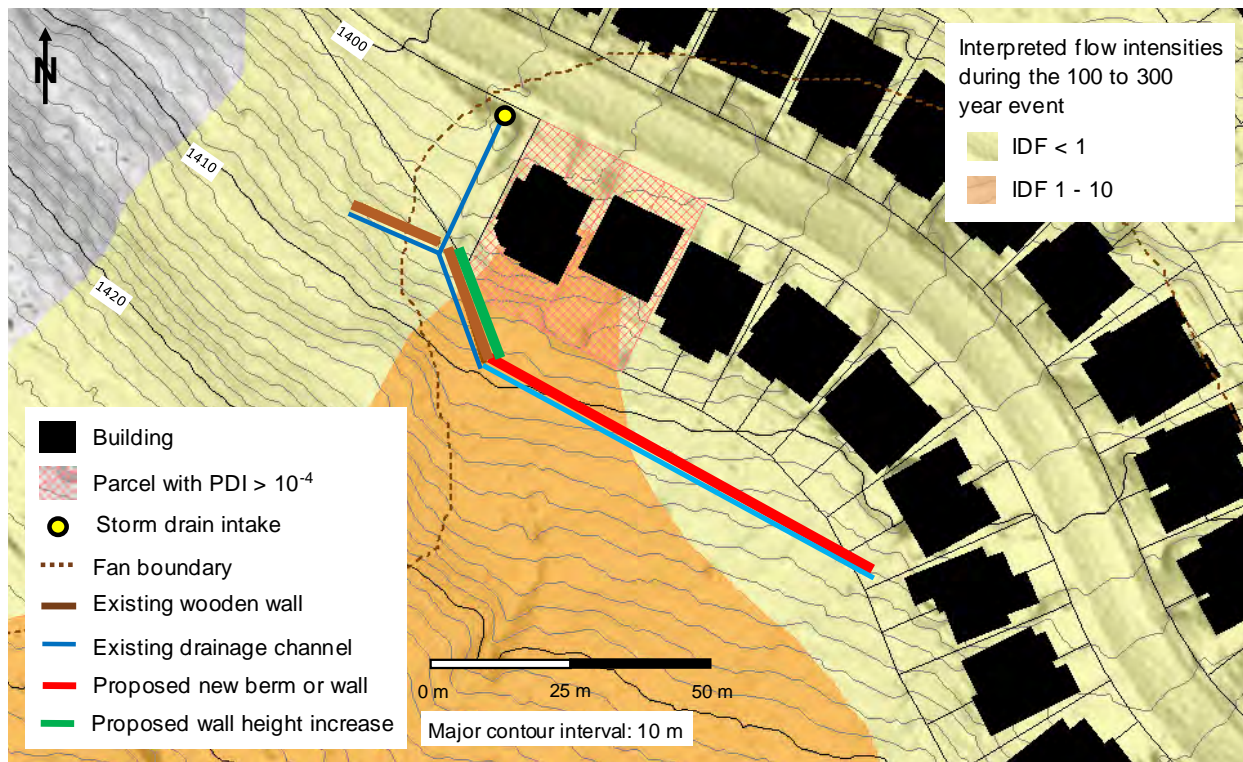


Figure 6-3. Proposed locations for diversion berms or walls on the lower Z Creek fan.

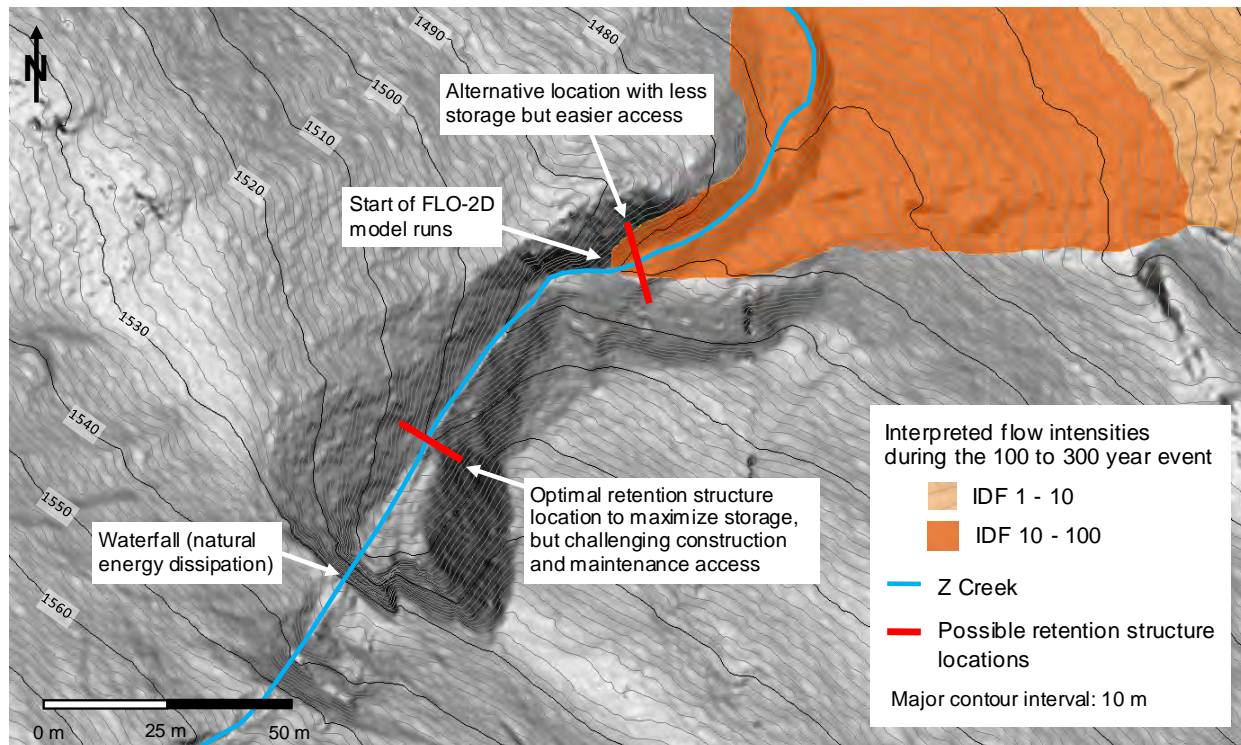


Figure 6-4. Z Creek fan apex area, showing possible location of debris flow net and other debris retention measures.

Table 6-12. Comparison of Z Creek mitigation options.

Criteria	Hazard awareness education	Reinforce and extend wall	Flexible debris flow nets	Earthfill or concrete debris retention
Cost*	Low – guidance could be shared at an information session or by mail	Moderate to high	High	High to very high
Risk reduction	Depends on the resident, including degree of advance preparation and long-term memory about the recommendations	Moderate - Reduces likelihood that existing wall is bypassed; Risk transfer should be assessed	Moderate to high – a single net would likely be overtopped, and may be damaged by snow avalanche	High – can be designed to retain design volume and resist snow avalanche impact.
Impact to wildlife and vegetation	None	Low	May disrupt wildlife passage; less disturbance area than earthfill or concrete option.	Relatively large disturbance area
Impact to residents	Success of the measure depends on resident involvement	Low, except during construction	Low	Low

* Cost comparison categories are approximate, as follows: Low means <\$10,000; Moderate means \$10,000 - \$100,000; High to means \$100,000 - \$1,000,000; Very High means > \$1,000,000.

Reinforcing and extending the existing wooden wall, in combination with hazard awareness education is likely capable of reducing risk to a tolerable level. Debris flow nets or other debris retention designs near the fan apex area could further reduce risk, although with high maintenance cost, construction cost, and environmental disturbance. BGC is available to support Canmore with identifying the preferred risk management solution for the community.

6.6. Summary

Z Creek is a small debris-flow prone watershed situated above the western end of the Peaks of Grassi development. Debris flows could occur with a minimum return period of about 300 years, though floods with some sediment transport events could occur more frequently. A range of techniques, including rainfall-runoff analysis, air photograph interpretation and radiocarbon dating were used to develop an F-M relationship, which suggested that debris flows in excess of 5,000 m³ could occur on Z Creek.

A quantitative risk assessment demonstrated that annual individual life loss risk on Z Creek is at the tolerable risk threshold for existing development (1:10,000) for four parcels, according to Canmore policy. Group risk is considered acceptable, and expected annualized economic damages are about \$21,000 per year. The risk could be managed by a combination of structural and non-structural measures, including extending the existing system of wooden diversion walls and channels to divert flows away from buildings at risk.



7.0 CONCLUSIONS

7. CONCLUSIONS

7.1. Limitations

This assessment is based on the current number of dwellings and observed geomorphological conditions on the X, Y and Z creek fans and the surrounding area. Estimated risk levels assume current conditions. Debris fans and the processes in their watersheds are dynamic, and hazard and risk will change to some degree when floods or debris flows avulse out of the existing channel or erode new channels. Similarly, any man-made alterations of the landscape through fill placements, cut-slopes or road constructions may change the distribution and intensity of debris flow and flood hazards and thus change the fan's risk profile. Modifications to development will also change the risk by changing the number and location of persons exposed to hazard. As such, to assure consistency of this report with current conditions, BGC recommends that the risk assessment be updated following debris flows or changes to the existing development.

7.2. Conclusions

This integrated steep creek assessment focused on X, Y, and Z creeks. The conclusions of the hazard and risk assessment portions of the study can be summarized as follows:

7.2.1. Hazard Assessment

1. X, Y and Z creeks are subject to debris floods at lower return periods, and debris flows at higher return periods. Sediment transport occurred on all three creeks during the June 2013 event.
 - The June 2013 event is associated with a lower return period on X, Y and Z creeks (about 100 years) compared to other, larger Canmore creeks, due to their smaller watersheds and decreased lag times.
2. Detailed assessment of the June 2013 event provided the following estimates of sediment volume and peak discharge:
 - a. X Creek: 9,600 m³ of sediment and a peak discharge of 30 m³/s, in the form of a debris flow from the west tributary
 - b. Y Creek: 4,200 m³ of sediment and a peak discharge of 25 m³/s, in the form of a debris flow
 - c. Z Creek: 500 m³ of sediment and a peak discharge of 1 m³/s, as a small debris flood or bedload transport event
3. F-M relationships were developed for each of the creeks, up to the 1000 to 3000-year return period. The 1000 to 3000-year events on each creek are expected to involve:
 - a. X Creek: 28,000 m³ of sediment and a peak discharge of 440 m³/s
 - b. Y Creek: 9,000 m³ of sediment and a peak discharge of 170 m³/s
 - c. Z Creek: 5,400 m³ of sediment and a peak discharge 110 m³/s.

7.2.2. Risk Assessment

1. The risk assessment identified that individual risk on Z Creek is at the threshold between tolerable and intolerable, according to the targets adopted by Canmore. The group risk on Z Creek plots in the acceptable zone.
2. On X and Y creeks, individual risk is tolerable, but group risk is in the ALARP zone.
3. Expected annualized economic damages are \$13,000 per year on X Creek, \$16,000 per year on Y Creek and \$21,000 per year on Z Creek.

7.2.3. Risk Reduction

X, Y and Z creek risks are either at the threshold for individual life loss risk for existing development (in the case of Z Creek), or within the ALARP zone for group risk (in the case of X and Y creeks). This means that mitigation is not a necessity, but rather a beneficial measure if life loss were considered the only criterion to motivate structural mitigation measures.

BGC considered the following mitigation concepts:

1. A general homeowner education program for residents of the Peaks of Grassi neighbourhood. This would help build community awareness of and resilience for steep creek hazards.
2. On X Creek, the risks arise from the avulsion potential, which could be managed through monitoring and channel works.
3. On Y Creek, the risks are posed by a debris flow travelling along the main flow path and over-topping the existing wooden wall. Risk could be managed by increasing the height and resistance of the existing wall, and possibly by adding additional structures upstream.
4. On Z Creek, the risks also arise from the main flow path. The existing wooden wall could be extended to redirect flows through an expanded channel.

Canmore will decide whether and which of these mitigation options are practical, given the broader context of hazards and challenges affecting the community.

8. CLOSURE

We trust the above satisfies your requirements at this time. Should you have any questions or comments, please do not hesitate to contact us.

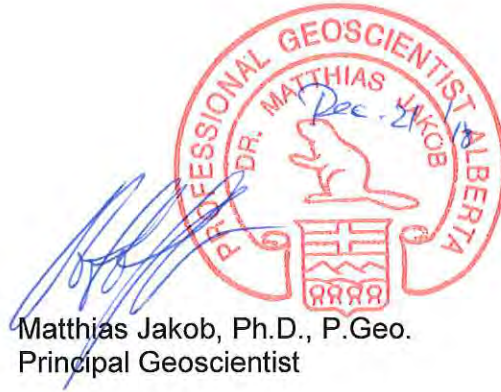
Yours sincerely,

BGC ENGINEERING INC.

per:



Emily Moase, M.Sc., P.Eng.
Geological Engineer



Matthias Jakob, Ph.D., P.Geo.
Principal Geoscientist



Kris Holm, M.Sc., P.Geo.
Senior Geoscientist



Beatrice Collier-Pandya, B.Sc., EIT
Geological Engineer-In-Training

Reviewed by:

Hamish Weatherly, M.Sc., P.Geo.
Principal Hydrologist

MJ/HW/mjp/mm

REFERENCES

- Allan, R.P. & Soden, B.J. (2008). Atmospheric warming and the amplification of precipitation extremes. *Science*, 321(5895), 1481-1484.
- Australian Geomechanics Society (2007). A National Landslide Risk Management Framework for Australia. *Australian Geomechanics*, 42, 1-36. Retrieved from <https://australiangeomechanics.org/wp-content/uploads/2010/11/LRM2007-Framework.pdf>
- Barnett, D.N., Brown, S.J., Murphy, J.M., Sexton, D.M.H., & Webb, M.J. (2006). Quantifying uncertainty in changes in extreme event frequency in response to doubled CO₂ using a large ensemble of GCM simulations. *Climate Dynamics*, 26(5), 489-511.
- Beniston, M., and Stoffel, M. (2014). Assessing the impacts of climatic change on mountain water resources. *Science of the Total Environment*, 493. DOI <http://dx.doi.org/10.1016/j.scitotenv.2013.11.122>
- BGC Engineering Inc. (2013a, December 2). Pigeon Creek, forensic analysis and short-term debris flood mitigation [Memo]. Prepared for the Town of Canmore.
- BGC Engineering Inc. (2013b, December 2). Stone Creek, forensic analysis and short-term debris flow mitigation [Memo]. Prepared for the Town of Canmore.
- BGC Engineering Inc. (2013c, December 2). *Stoneworks Creek, forensic analysis and short-term debris flood mitigation* [Memo]. Prepared for the Town of Canmore.
- BGC Engineering Inc. (2013d, December 2). *X, Y, and Z Creeks, forensic analysis* [Memo]. Prepared for the Town of Canmore.
- BGC Engineering Inc. (2013a, December 11). *Cougar Creek, 2013 forensic analysis and short-term debris flood mitigation* [Report]. Prepared for the Town of Canmore. BGC Doc. No. TC13-004.
- BGC Engineering Inc. (2013b, December 22). *Three Sisters Creek, forensic analysis and short-term debris flood mitigation* [Memo]. Prepared for the Town of Canmore.
- BGC Engineering Inc. (2013, December 18). *Echo Canyon Creek, forensic analysis and long-term debris flow mitigation concepts* [Memo]. Prepared for the Town of Canmore.
- BGC Engineering Inc. (2014, January 3). *Stewart Creek, forensic analysis and conceptual debris flood mitigation* [Memo]. Prepared for the Town of Canmore.
- BGC Engineering Inc. (2014, March 7). *Cougar Creek, debris flood hazard assessment* [Report]. Prepared for the Town of Canmore. BGC Doc. No. TC13-010.
- BGC Engineering Inc. (2014, June 11). *Cougar Creek debris-flood risk assessment* [Report]. Prepared for the Town of Canmore. BGC Doc. No. TC14-001
- BGC Engineering Inc. (2014, August 1). *Cougar Creek forensic analysis, hydroclimatic analysis of the June 2013 Storm* [Report]. Prepared for the Town of Canmore. BGC Doc. No. TC13-005.
- BGC Engineering Inc. (2014, October 31). *Three Sisters Creek debris-flood hazard assessment* [Report]. Prepared for the Town of Canmore.
- BGC Engineering Inc. (2015, January 20). *Three Sisters Creek debris-flood risk assessment* [Report]. Prepared for the town of Canmore. BGC Doc. No. TC14-007.

- BGC Engineering Inc. (2015, May 21). *Cougar Creek baseline debris-flood risk assessment update* [Letter report]. Prepared for the Town of Canmore.
- BGC Engineering Inc. (2015, September 30). *Exshaw and Jura Creek debris-flood hazard and risk assessment and preliminary mitigation design – completion report* [Letter report]. Prepared for the Municipal District of Bighorn.
- BGC Engineering Inc. (2015, October 23). *Stone Creek debris-flow risk assessment* [Report]. Prepared for the Town of Canmore.
- BGC Engineering Inc. (2015, October 28). *Stones Canyon Creek Development Level 2 debris-flow risk assessment* [Report]. Prepared for Hillcroft Developments Ltd.
- BGC Engineering Inc. (2015, November 16). *Stoneworks Creek debris flood hazard assessment* [Report]. Prepared for the Town of Canmore. BGC Doc. No. TC15-001.
- BGC Engineering Inc. (2016, September 27). *Pigeon Creek debris-flood risk assessment* [Report]. Prepared for the Town of Canmore.
- BGC Engineering Inc. (2016, September 30). *Stoneworks Creek debris-flood risk assessment* [Report]. Prepared for the Town of Canmore.
- BGC Engineering Inc. (2017, March 31). *Draft guidelines for steep creek risk assessments in Alberta* [Report]. Prepared for Alberta Environment and Parks.
- Brardinoni, F. and Church, M. (2004). Representing the magnitude-frequency relation: Capilano river basin. *Earth Surface Processes and Landforms* 29: 115-124.
- Bull, W.B. (1977). The alluvial fan environment. *Progress in Physical Geography* 1: 222-270. doi:10.1177/030913337700100202
- Canadian Standards Association. (1997). *Risk Management: Guidelines for Decision Makers* (CAN/CSA Q850-97). Mississauga, ON: CSA Group.
- Cesca, M. and D'Agostino, V. (2008). Comparison between FLO-2D and RAMMS in debris-flow modelling: a case study in the Dolomites. *Monitoring, Simulation Prevention and Remediation of Dense Debris Flows II, WIT Transactions on Engineering Science*, 60, 197-206.
- D'Angostino V., Cerato, M., Coali, R. 1996. Il trasporto solido di eventi estremi nei torrenti del Trentino Orientale. Schutz des Lebensraumes vor Hochwasser, Muren, Massenbewegungen und Lawinen, Vo. 1, Interpretation 1996, Tagungsband, Garmisch-Partenkirchen: Germany; 377-386 (in Italian).
- District of North Vancouver (2009a, November 10). *Report to Council: Natural Hazards Risk Tolerance Criteria; District of North Vancouver, British Columbia*. District of North Vancouver, BC.
- District of North Vancouver (2009b). *Report to Council No. 11.5225.00/000.000 dated November 10, 2009*. District of North Vancouver, BC.
- Environment and Climate Change Canada. (n.d.). *Historical Data – Kananaskis* [Data]. Extracted June 1, 2018 from the Environment and Climate Change Canada Canadian Historical Data website:
http://climate.weather.gc.ca/historical_data/search_historic_data_e.html
- Environment and Climate Change Canada. (2011). *1981-2010 Climate Normals & Averages* [Data]. Extracted June 1, 2018 from the Environment and Climate Change Canada

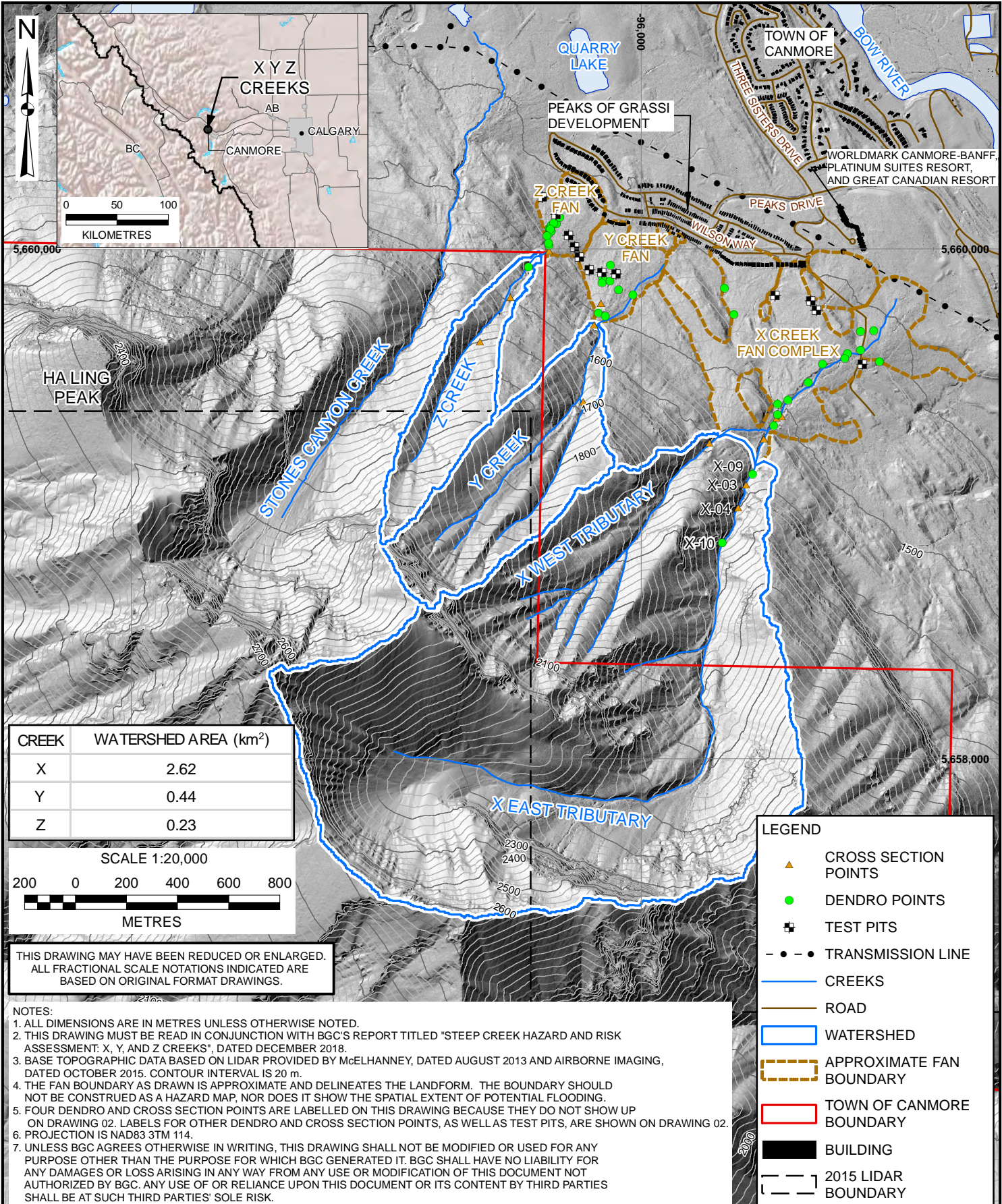
- Canadian Climate Normals website:
http://climate.weather.gc.ca/climate_normals/index_e.html
- FLO-2D Software, Inc. (2017). FLO-2D Reference Manual. Build No. 16 January 2017.
- Gadd, B. (2013). Brief History of Coal-mining in the Bow Valley. Available online from:
<http://www.bengadd.com/BenGaddDownloads.htm>, March 2013.
- Geotechnical Engineering Office. (1998). *Landslides and boulder falls from natural terrain: interim risk guidelines* (GEO Report No. 75). Hong Kong.
- Griswold, J.P., & Iverson, R.M. (2008). *Mobility statistics and automated hazard mapping for debris flows and rock avalanches* (US Geological Survey Scientific Investigations Report 2007-5276). Reston, Virginia: US Geological Survey.
- Gutenberg, B. & Richter, C.F. (1954). *Seismicity of the Earth* (2nd ed.). Princeton, N.J.: Princeton University Press.
- Hawkins, R.H., Ward, T.J., Woodward, E. & Van Mullem, J.A. (2010, June-July). Continuing Evolution of Rainfall-Runoff and the Curve Number Precedent. *2nd Joint Federal Interagency Conference*. Paper presented at the meeting of Advisory Committee on Water Information. Retrieved from
https://acwi.gov/sos/pubs/2ndJFIC/Contents/10E_Hawkins.pdf.
- Holm, K., Jakob, M., Scordo, E., Strouth, A., Wang, R. & Adhikari, R. (2016, October). Identification, prioritization, and risk reduction: steep creek fans crossed by highways in Alberta. *GeoVancouver 2016*. Paper presented at the meeting of the Canadian Geotechnical Society, Vancouver, British Columbia.
- Hong Kong Geotechnical Engineering Office (GEO). (1998). *Landslides and Boulder Falls from Natural Terrain: Interim Risk Guidelines*. Geo Report 175, Geotechnical Engineering Office, Civil Engineering Department, Hong Kong Special Administrative Region, 184 pp.
- Hoovers. (2013). *Company Lead List: Complete Gold* [Data]. Obtained October 9, 2013, from Hoovers, a Dunn and Bradstreet (D&B) Company.
- Hungr, O., Morgan, G.C. & Kellerhals, R. (1984). Quantitative analysis of debris torrent hazards for design of remedial measures. *Canadian Geotechnical Journal*, 21, 663–677.
doi:10.1139/t84-073
- Hungr, O., Bovis, M., McDougall, S. 2005. Debris flow entrainment. In: Jakob, M. and Hungr, O. (eds). *Debris flows and related phenomena*. Springer Heidelberg, p. 135-155.
- Hungr, O., Leroueil, S., & Picarelli, L. (2014). The Varnes classification of landslide types, an update. *Landslides*, 11, 167–194. <https://doi.org/10.1007/s10346-013-0436-y>
- Iverson, R.M. (2012). Elementary theory of bed-sediment entrainment by debris flows and avalanches, *J. Geophys. Res.*, 117, F03006, doi: 10.1029/2011JF002189.
- Iverson, R. M., and C. Ouyang (2015), Entrainment of bed material by Earth-surface mass flows: Review and reformulation of depth-integrated theory, *Rev. Geophys.*, 53, 27–58, doi:10.1002/2013RG000447
- Jakob, M. (1996). *Morphometric and geotechnical controls of debris flow frequency and magnitude in southwestern British Columbia* (Ph.D. thesis). Department of Geography, University of British Columbia, Vancouver, B.C.

- Jakob, M., Stein, D., and Ulmi, M. (2012). Vulnerability of buildings to debris flow impact. *Natural Hazards: Journal of International Society for the Prevention and Mitigation of Natural Hazards*, 60(2), 241-261.
- Jakob, M., McDougall, S., Bale, S., Friele, P. (2016, October). Regional debris-flow and debris-flood frequency-magnitude curves. *GeoVancouver 2016*. Paper presented at the meeting of the Canadian Geotechnical Society, Vancouver, British Columbia.
- Jakob, M. 2018. Debris flow hazard and risk assessment – a practitioner’s view. Invited paper for the 7th International Conference on Debris-Flow Hazards Mitigation, Boulder Colorado, June 2019. Jarrett, R.D., (1985). *Determination of roughness coefficients for streams in Colorado*. (USGS Water Resources Investigations Report 85-4004). Lakewood, Colorado: United States Geological Survey and State of Colorado, Department of Natural Resources, Colorado Water Conservation Board.
- Kappel, B., Abbas, S., Figliuzzi, S., Guangul, S., Sabol, G. (2018). Updating PMP for the Elbow River: Complex Terrain, Unique Solutions. Canadian Dam Association Bulletin, Winter 2018, 10-25.
- Lau, C.A., (2017). *Channel scour on temperate alluvial fans in British Columbia* (Master’s thesis). Simon Fraser University, Burnaby, British Columbia. Retrieved from http://summit.sfu.ca/system/files/iritems1/17564/etd10198_CLau.pdf
- Li, Y., Szeto, K., Stewart, R., Theriault, J., Chen, L., Kochtubajda, B., Liu, A., Boodoo, S., Goodson, R., Mooney, C., Kurkute, S. (2017) A Numerical Study of the June 2013 Flood-Producing Extreme Rainstorm over Southern Alberta. *Journal of Hydrometeorology*, 18, 2057-2078.
- Mark, D.M. and Church, M. 1977. On the misuse of regression in earth science. *Mathematical Geology*, 9 (1): 63-75.
- Mizuyama, T., Kobashi, S. and Ou, G. (1992). Prediction of debris flow peak discharge. *Interpraevent, International Symposium, Bern, Switzerland, Tagespublikation*, 4: 99-108.
- Natural Regions Committee. (2006). *Natural Regions and Subregions of Alberta* [D.J. Downing and W.W. Pettapiece]. Edmonton, AB: Government of Alberta. Pub. No. T/852.
- Pierson, T.C. (2005). Hyperconcentrated flow – transitional process between water flow and debris flow. In: Jakob, M. and Hungr, O. (eds). *Debris flows and related phenomena*. Springer Heidelberg, p.159-196.
- Pomeroy, J., Fang, X., Marks, D. (2016). The cold rain-on-snow event of June 2013 in the Canadian Rockies – characteristics and diagnosis. *Hydrological Processes*, 30, 2899-2914.
- Porter, M. & Morgenstern, N. (2013). *Landslide Risk Evaluation: Canadian Technical Guidelines and Best Practices related to Landslides: a national initiative for loss reduction* (Geological Survey of Canada Open File 7312). Ottawa, ON: Geological Survey of Canada
- Prochaska, A.B., Santi, P., Higgins, J.D., Cannon, S.H. (2008). A study of methods to estimate debris flow velocity. *Landslides*, 5(4), 431-444. <https://doi.org/10.1007/s10346-008-0137-0>
- R (Version 3.5.1) [Computer software]. Retrieved from <https://www.r-project.org/>
- WinDENDRO (Version 2012b) [Computer software]. Quebec, CA: Regent Instruments Inc.
- Rickenmann, D. (1999). Empirical Relationships for Debris Flows. *Natural Hazards* 19: 47-77.

- Rickenmann, D. & Koschni, A. (2010). Sediment load due to fluvial transport and debris flows during the 2005 flood events in Switzerland. *Hydrological Processes*, 24, 993-1007.
- Ryder, J.M. (1971). The stratigraphy and morphology of paraglacial alluvial fans in southwestern British Columbia. *Canadian Journal of Earth Sciences*, 8(2), 279-298.
<https://doi.org/10.1139/e71-027>
- Statistics Canada. (2012, July). Mortality, Summary List of Causes 2009 [Data]. Catalogue no. 84F0209X. Retrieved from <https://www150.statcan.gc.ca/n1/en/pub/84f0209x/84f0209x2009000-eng.pdf?st=rnvjX35L>
- Teufel, B., Diro, G., Whan, K., Milrad, S., Jeong, D., Ganji, A., Huziy, O., Winger, K., Gyakum, J., Elia, R., Zwiers, F., Sushama, L. (2017). Investigation of the 2013 Alberta flood from weather and climatic perspectives. *Climate Dynamics*, 48, 2881-2899.
- Town of Canmore. (2012). Request for Decision – Peaks of Grassi Drainage Diversion. Agenda # G-1, October 16, 2012.
- Town of Canmore. (2015). 2014 Municipal Census [Data], dated February 24, 2015. Retrieved from <https://www.canmore.ca/census-documents/119-census-2014-final-report>
- Town of Canmore. (2016). Canmore Municipal Development Plan, Bylaw 2016-03, dated September 27, 2016.
- Town of Canmore. (2018). 2017 assessment data, provided June 28, 2018.
- United States Army of Corps Engineers. (2015). Hydrologic Engineering Centre-Hydrologic Modeling System (HEC-HMS) (Version 4.2.1) [Computer software]. Davis, CA.
- United States Department of Agriculture. (1986). *Urban Hydrology for Small Watersheds* (Technical Release 55). Washington, DC.
- VanDine, D.F. (2012). *Risk Management – Canadian Technical Guidelines and Best Practices Related to Landslides* (Open File 6996). Ottawa, ON: Geological Survey of Canada.
- Zimmermann, A. (2010). Flow resistance in steep streams: an experimental study. *Water Resources Research*, 46(9). <https://doi.org/10.1029/2009WR007913>

DRAWINGS

X:\Projects\1261025\GIS\Production\Report\20180626_Steep_Creek_Hazard_and_Risk_Assessment_X_Y_and_Z_Creeks\01_X_Y_and_Z_Creek_Watersheds_and_Fans.mxd Date: Wednesday, December 19, 2018 Time: 2:35 PM



THIS DRAWING MAY HAVE BEEN REDUCED OR ENLARGED.
ALL FRACTIONAL SCALE NOTATIONS INDICATED ARE
BASED ON ORIGINAL FORMAT DRAWINGS.

NOTES:

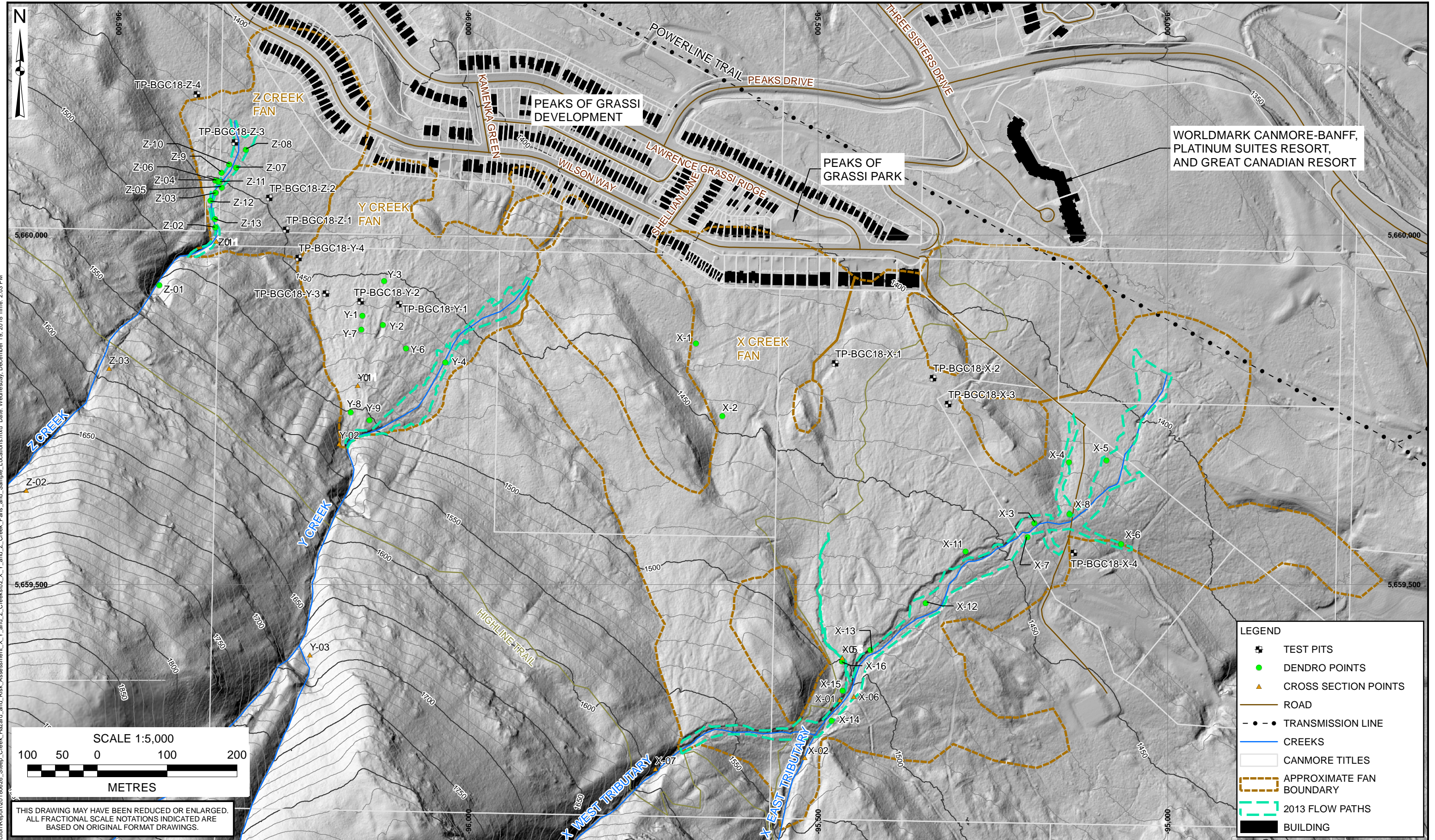
1. ALL DIMENSIONS ARE IN METRES UNLESS OTHERWISE NOTED.
2. THIS DRAWING MUST BE READ IN CONJUNCTION WITH BGC'S REPORT TITLED "STEEP CREEK HAZARD AND RISK ASSESSMENT: X, Y, AND Z CREEKS", DATED DECEMBER 2018.
3. BASE TOPOGRAPHIC DATA BASED ON LIDAR PROVIDED BY McELHANNEY, DATED AUGUST 2013 AND AIRBORNE IMAGING, DATED OCTOBER 2015. CONTOUR INTERVAL IS 20 m.
4. THE FAN BOUNDARY AS DRAWN IS APPROXIMATE AND DELINEATES THE LANDFORM. THE BOUNDARY SHOULD NOT BE CONSTRUED AS A HAZARD MAP, NOR DOES IT SHOW THE SPATIAL EXTENT OF POTENTIAL FLOODING.
5. FOUR DENDRO AND CROSS SECTION POINTS ARE LABELLED ON THIS DRAWING BECAUSE THEY DO NOT SHOW UP ON DRAWING 02. LABELS FOR OTHER DENDRO AND CROSS SECTION POINTS, AS WELLAS TEST PITS, ARE SHOWN ON DRAWING 02.
6. PROJECTION IS NAD83 3TM 114.
7. UNLESS BGC AGREES OTHERWISE IN WRITING, THIS DRAWING SHALL NOT BE MODIFIED OR USED FOR ANY PURPOSE OTHER THAN THE PURPOSE FOR WHICH BGC GENERATED IT. BGC SHALL HAVE NO LIABILITY FOR ANY DAMAGES OR LOSS ARISING IN ANY WAY FROM ANY USE OR MODIFICATION OF THIS DOCUMENT NOT AUTHORIZED BY BGC. ANY USE OF OR RELIANCE UPON THIS DOCUMENT OR ITS CONTENT BY THIRD PARTIES SHALL BE AT SUCH THIRD PARTIES' SOLE RISK.

SCALE:	1:20,000
DATE:	DEC 2018
DRAWN:	LL, BMB
CHECKED:	BCP
APPROVED:	MJ

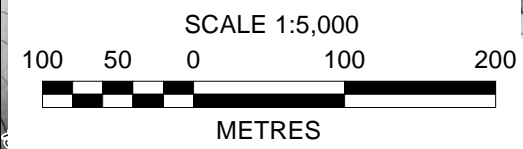
BGC ENGINEERING INC.
AN APPLIED EARTH SCIENCES COMPANY

CLIENT:
Town of CANMORE

PROJECT: STEEP CREEK HAZARD AND RISK ASSESSMENT: X, Y, AND Z CREEKS	
TITLE: X, Y, AND Z CREEKS WATERSHEDS AND FAN	
PROJECT No.: 1261025	DWG No.: 01



X:\Projects\1261025\GIS\Production\Report\1261025_Steep_Creek_Hazard_and_Risk_Assessment_X_Y_and_Z_Creeks\02_X_Y_and_Z_Creek_Fans_and_Sample_Locations.mxd Date: Wednesday, December 19, 2018 Time: 2:03 PM



THIS DRAWING MAY HAVE BEEN REDUCED OR ENLARGED.
ALL FRACTIONAL SCALE NOTATIONS INDICATED ARE
BASED ON ORIGINAL FORMAT DRAWINGS.

NOTES:

1. ALL DIMENSIONS ARE IN METRES UNLESS OTHERWISE NOTED.
2. THIS DRAWING MUST BE READ IN CONJUNCTION WITH BGC'S REPORT TITLED "STEEP CREEK HAZARD AND RISK ASSESSMENT: X, Y, AND Z CREEKS", AND DATED DECEMBER 2018.
3. BASE TOPOGRAPHIC DATA BASED ON LIDAR PROVIDED BY AIRBORNE IMAGING, DATED OCTOBER 2015. CONTOUR INTERVAL IS 10 m.
4. THE FAN BOUNDARY AS DRAWN IS APPROXIMATE AND DELINEATES THE LANDFORM. THE BOUNDARY SHOULD NOT BE CONSTRUED AS A HAZARD MAP, NOR DOES IT SHOW THE SPATIAL EXTENT OF POTENTIAL FLOODING. FAN BOUNDARIES WITHIN DEVELOPED AREAS ARE VERY APPROXIMATE AS THEY HAVE BEEN ALTERED BY THE DEVELOPMENTS.
5. PROJECTION IS NAD83 3TM 114.
6. UNLESS BGC AGREES OTHERWISE IN WRITING, THIS DRAWING SHALL NOT BE MODIFIED OR USED FOR ANY PURPOSE OTHER THAN THE PURPOSE FOR WHICH BGC GENERATED IT. BGC SHALL HAVE NO LIABILITY FOR ANY DAMAGES OR LOSS ARISING IN ANY WAY FROM ANY USE OR MODIFICATION OF THIS DOCUMENT NOT AUTHORIZED BY BGC. ANY USE OF OR RELIANCE UPON THIS DOCUMENT OR ITS CONTENT BY THIRD PARTIES SHALL BE AT SUCH THIRD PARTIES' SOLE RISK.

SCALE:	1:5,000
DATE:	DEC 2018
DRAWN:	JDC, BMB
CHECKED:	BCP
APPROVED:	MJ

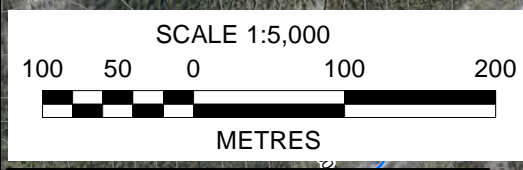
BGC ENGINEERING INC.
AN APPLIED EARTH SCIENCES COMPANY

CLIENT: **Town of CANMORE**

PROJECT:	STEEP CREEK HAZARD AND RISK ASSESSMENT: X, Y, AND Z CREEKS	
TITLE:	X, Y, AND Z CREEK FANS AND SAMPLE LOCATIONS	
PROJECT No.:	1261025	DWG No.: 02



X:\Projects\1261025\5\Production\Report\20180626_Steep_Creek_Hazard_and_Risk_Assessment_X_Y_and_Z_Creeks\03_Orthophoto_X_Y_and_Z_Creek_Fans.mxd Date: Wednesday, December 19, 2018 Time: 2:03 PM



THIS DRAWING MAY HAVE BEEN REDUCED OR ENLARGED.
ALL FRACTIONAL SCALE NOTATIONS INDICATED ARE
BASED ON ORIGINAL FORMAT DRAWINGS.

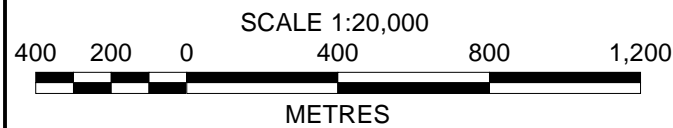
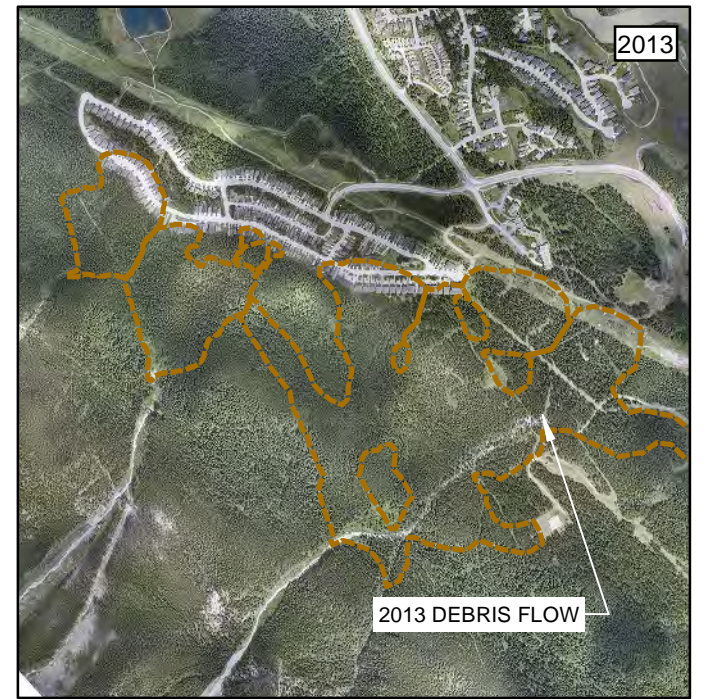
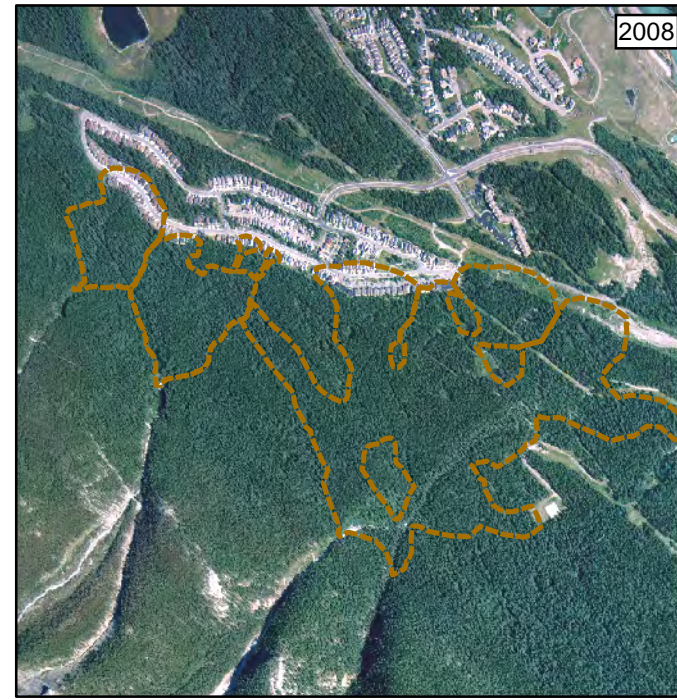
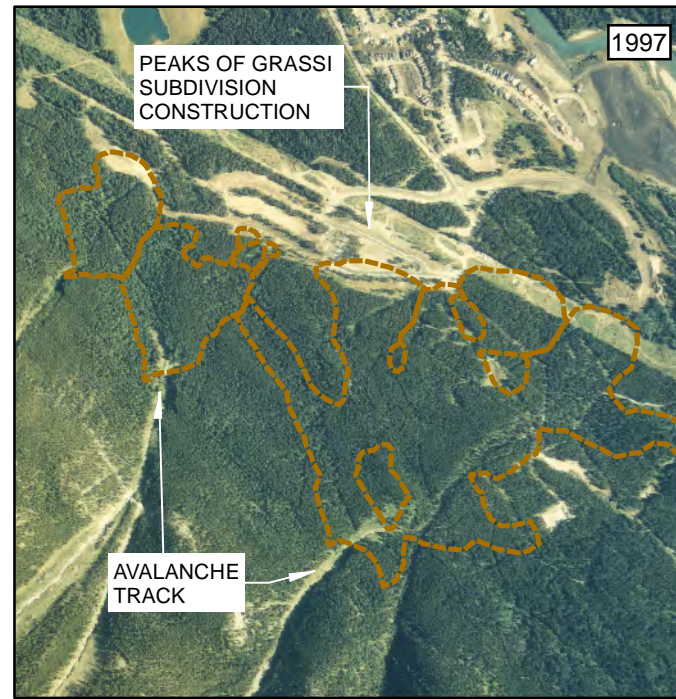
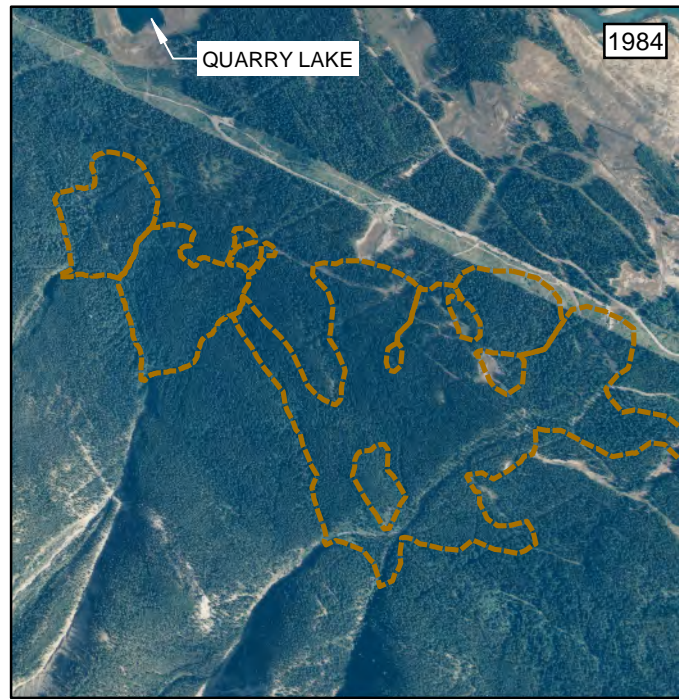
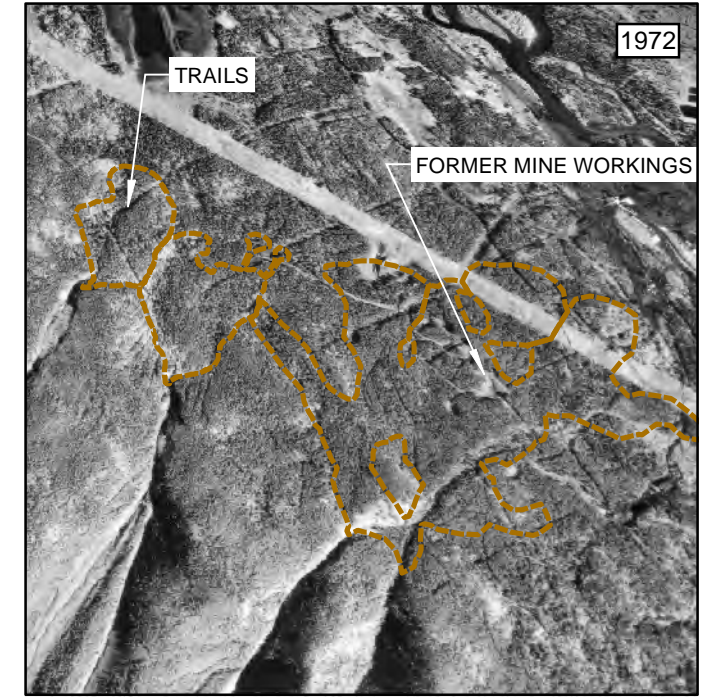
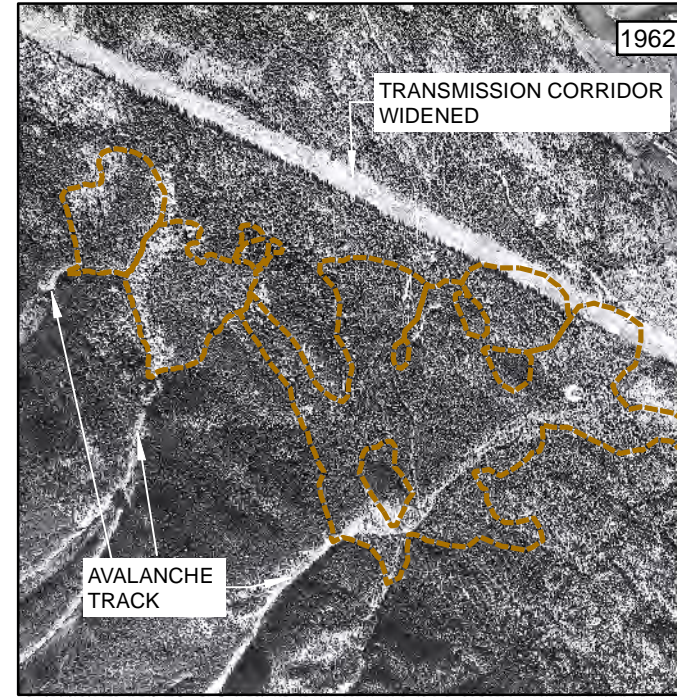
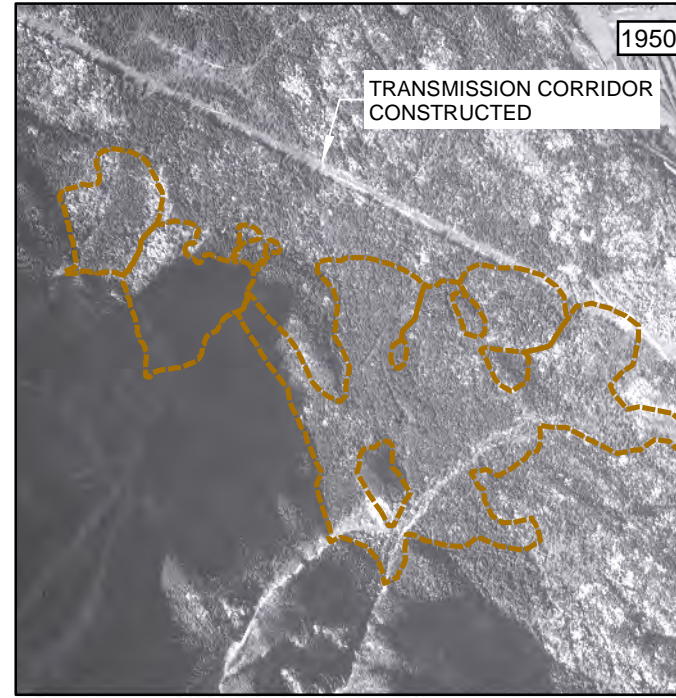
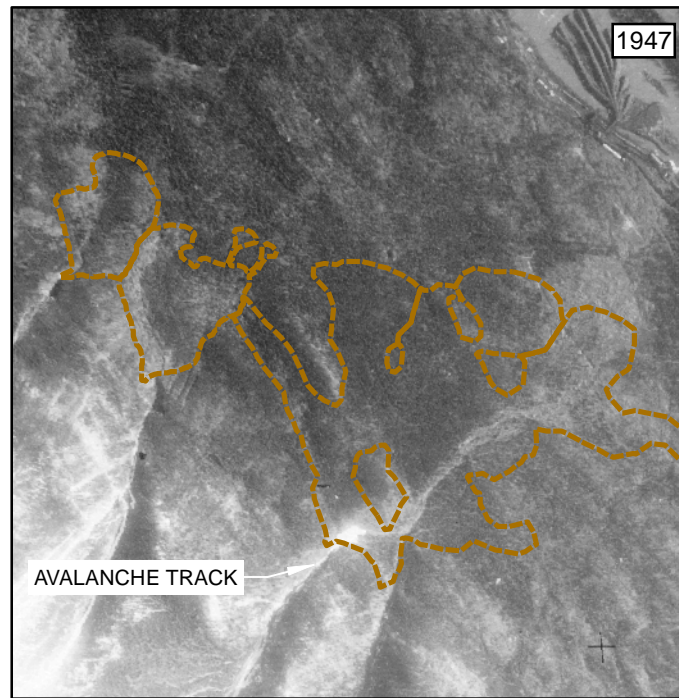
NOTES:
 1. ALL DIMENSIONS ARE IN METRES UNLESS OTHERWISE NOTED.
 2. THIS DRAWING MUST BE READ IN CONJUNCTION WITH BGC'S REPORT TITLED "STEEP CREEK HAZARD AND RISK ASSESSMENT: X, Y, AND Z CREEKS", AND DATED DECEMBER 2018.
 3. BASE TOPOGRAPHIC DATA BASED ON LIDAR PROVIDED BY AIRBORNE IMAGING, DATED OCTOBER 2015. CONTOUR INTERVAL IS 10 m.
 4. THE FAN BOUNDARY AS DRAWN IS APPROXIMATE AND DELINEATES THE LANDFORM. THE BOUNDARY SHOULD NOT BE CONSTRUED AS A HAZARD MAP, NOR DOES IT SHOW THE SPATIAL EXTENT OF POTENTIAL FLOODING. FAN BOUNDARIES WITHIN DEVELOPED AREAS ARE VERY APPROXIMATE AS THEY HAVE BEEN ALTERED BY THE DEVELOPMENTS.
 5. PROJECTION IS NAD83 3TM 114.
 6. UNLESS BGC AGREES OTHERWISE IN WRITING, THIS DRAWING SHALL NOT BE MODIFIED OR USED FOR ANY PURPOSE OTHER THAN THE PURPOSE FOR WHICH BGC GENERATED IT. BGC SHALL HAVE NO LIABILITY FOR ANY DAMAGES OR LOSS ARISING IN ANY WAY FROM ANY USE OR MODIFICATION OF THIS DOCUMENT NOT AUTHORIZED BY BGC. ANY USE OF OR RELIANCE UPON THIS DOCUMENT OR ITS CONTENT BY THIRD PARTIES SHALL BE AT SUCH THIRD PARTIES' SOLE RISK.

SCALE:	1:5,000
DATE:	DEC 2018
DRAWN:	JDC, BMB
CHECKED:	BCP
APPROVED:	MJ

BGC ENGINEERING INC.
AN APPLIED EARTH SCIENCES COMPANY

CLIENT: **Town of CANMORE**

PROJECT:	STEEP CREEK HAZARD AND RISK ASSESSMENT: X, Y, AND Z CREEKS FANS	
TITLE:	ORTHOPHOTO OF X, Y, AND Z CREEK FANS	
PROJECT No.:	1261025	DWG No: 03



THIS DRAWING MAY HAVE BEEN REDUCED OR ENLARGED.
ALL FRACTIONAL SCALE NOTATIONS INDICATED ARE
BASED ON ORIGINAL FORMAT DRAWINGS.

LEGEND
 APPROXIMATE FAN BOUNDARY

NOTES:
 1. ALL DIMENSIONS ARE IN METRES UNLESS OTHERWISE NOTED.
 2. THIS DRAWING MUST BE READ IN CONJUNCTION WITH BGC'S REPORT TITLED "STEEP CREEK HAZARD AND RISK ASSESSMENT: X, Y, AND Z CREEKS", AND DATED DECEMBER 2018.
 3. BASE TOPOGRAPHIC DATA BASED ON AIR PHOTOS PROVIDED BY ALBERTA AIR PHOTO LIBRARY AND NATIONAL AIR PHOTO LIBRARY. THE AIR PHOTOS DATED 1947 PROVIDED BY NATIONAL AIR PHOTO LIBRARY. THE AIR PHOTOS DATED 1949, 1950, 1962, 1972, 1984, 1997, AND 2008 PROVIDED BY ALBERTA AIR PHOTO LIBRARY. THE ORTHOPHOTO DATED 2013 PROVIDED BY TOWN OF CANMORE.
 4. THE FAN BOUNDARY AS DRAWN IS APPROXIMATE AND DELINEATES THE LANDFORM. THE BOUNDARY SHOULD NOT BE CONSTRUED AS A HAZARD MAP, NOR DOES IT SHOW THE SPATIAL EXTENT OF POTENTIAL FLOODING.
 5. PROJECTION IS NAD83 3TM 114.
 6. UNLESS BGC AGREES OTHERWISE IN WRITING, THIS DRAWING SHALL NOT BE MODIFIED OR USED FOR ANY PURPOSE OTHER THAN THE PURPOSE FOR WHICH BGC GENERATED IT. BGC SHALL HAVE NO LIABILITY FOR ANY DAMAGES OR LOSS ARISING IN ANY WAY FROM ANY USE OR MODIFICATION OF THIS DOCUMENT NOT AUTHORIZED BY BGC. ANY USE OF OR RELIANCE UPON THIS DOCUMENT OR ITS CONTENT BY THIRD PARTIES SHALL BE AT SUCH THIRD PARTIES' SOLE RISK.

SCALE:	1:20,000
DATE:	DEC 2018
DRAWN:	JDC. BMB
CHECKED:	BCP
APPROVED:	MJ

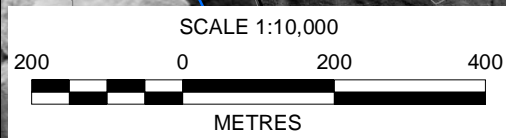
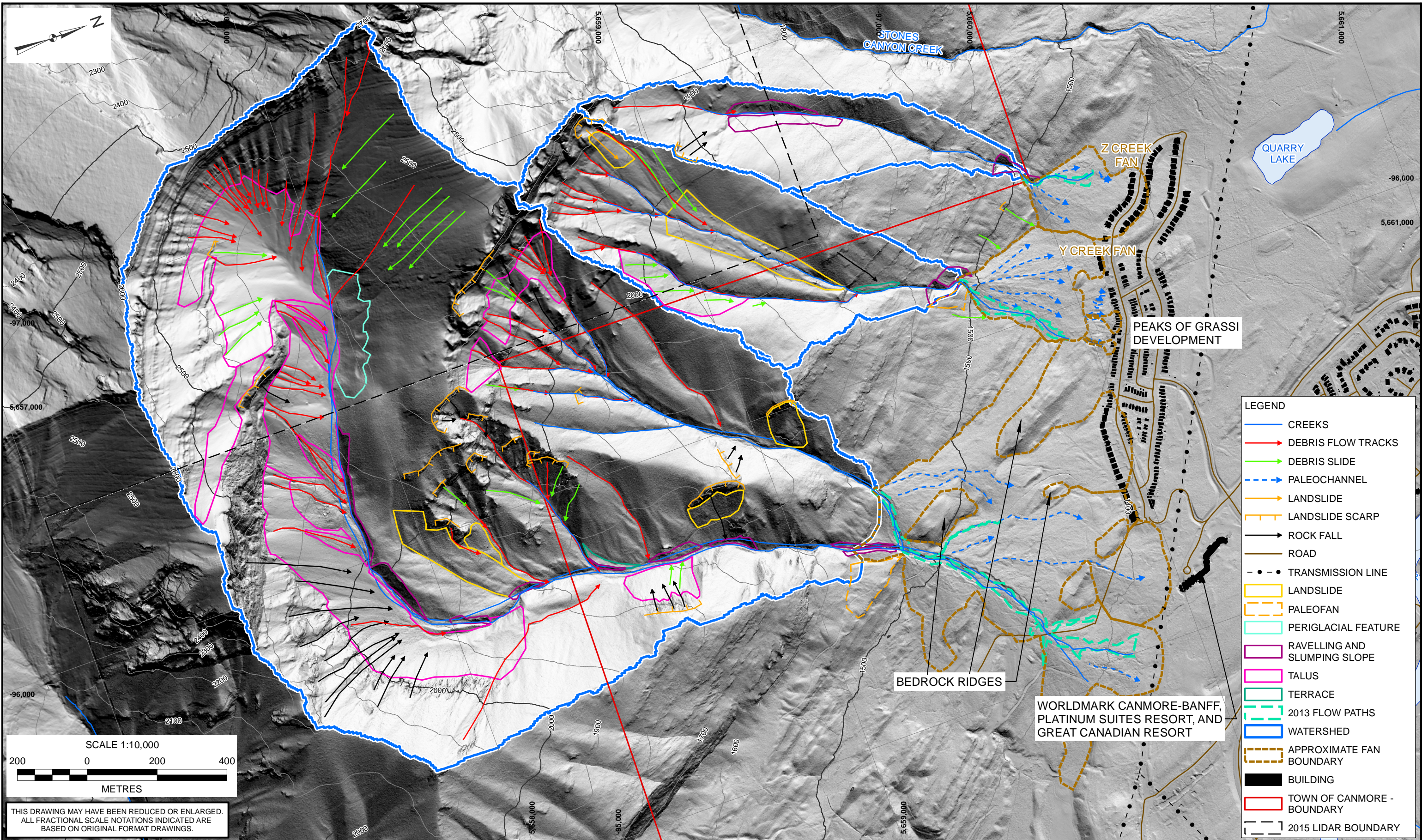
BGC ENGINEERING INC.
 AN APPLIED EARTH SCIENCES COMPANY

CLIENT:

PROJECT: STEEP CREEK HAZARD AND RISK ASSESSMENT: X, Y, AND Z CREEKS	
TITLE: X, Y, Z CREEKS AIR PHOTO COMPARISON	
PROJECT No.: 1261025	DWG No.: 04

X:\Projects\1261025\Production\Report\20180626_Steep_Creek_Hazard_and_Risk_Assessment_X_Y_and_Z_Creeks_Airphoto_Comparison.mxd Date: Wednesday, December 19, 2018 Time: 2:27 PM

X:\Projects\1261025\GIS\Production\Report\20180626_Steep_Creek_Hazard_and_Risk_Assessment_X_Y_and_Z_Creeks_Geomorphic_Map_of_Study_Area.mxd Date: Wednesday, December 19, 2018 Time: 2:06 PM



THIS DRAWING MAY HAVE BEEN REDUCED OR ENLARGED.
ALL FRACTIONAL SCALE NOTATIONS INDICATED ARE
BASED ON ORIGINAL FORMAT DRAWINGS.

LEGEND	
	CREEKS
	DEBRIS FLOW TRACKS
	DEBRIS SLIDE
	PALEOCHANNEL
	LANDSLIDE
	LANDSLIDE SCARP
	ROCK FALL
	ROAD
	TRANSMISSION LINE
	LANDSLIDE
	PALEOFAN
	PERIGLACIAL FEATURE
	RAVELLING AND SLUMPING SLOPE
	TALUS
	TERRACE
	2013 FLOW PATHS
	WATERSHED
	APPROXIMATE FAN BOUNDARY
	BUILDING
	TOWN OF CANMORE - BOUNDARY
	2015 LIDAR BOUNDARY

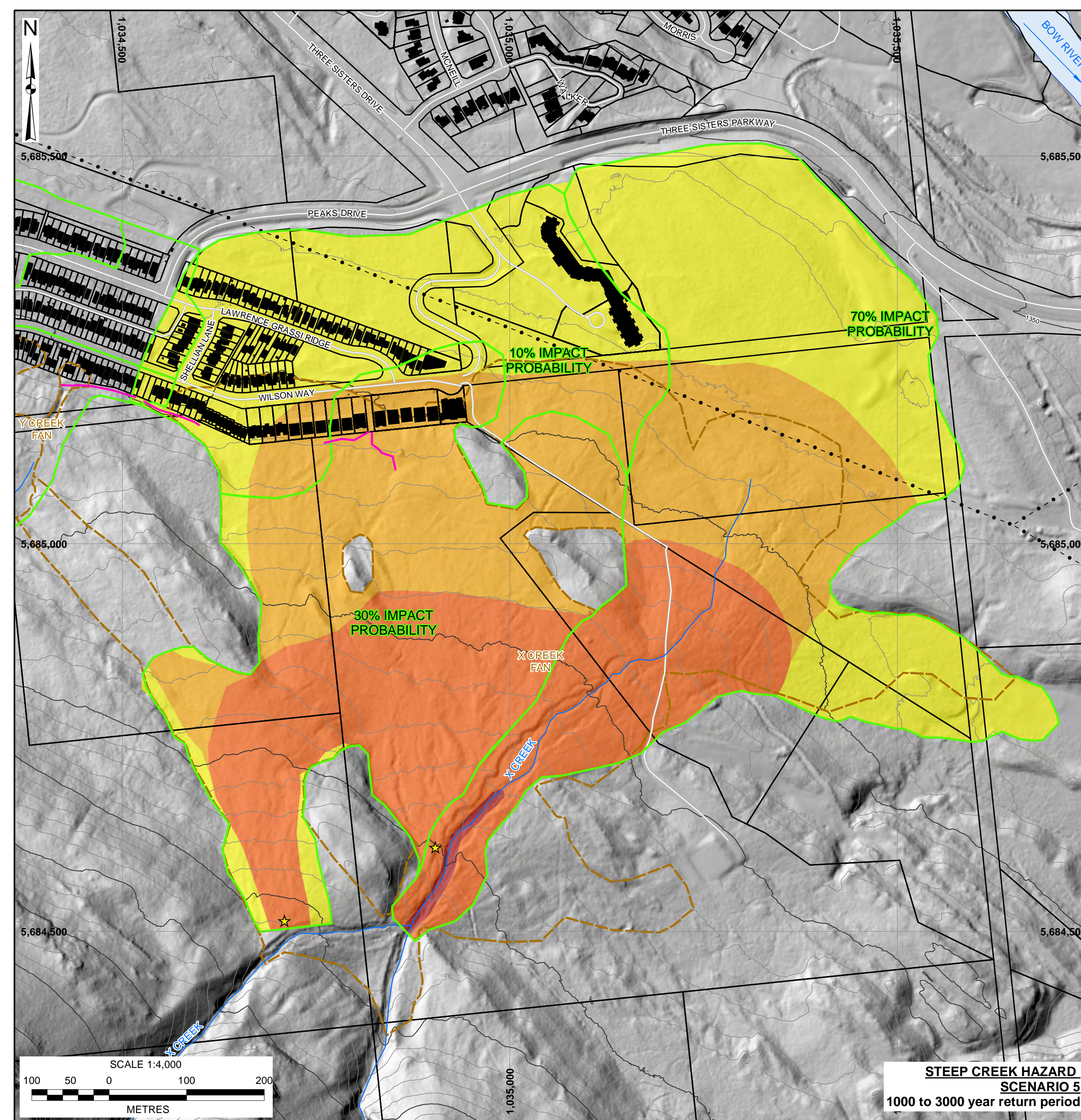
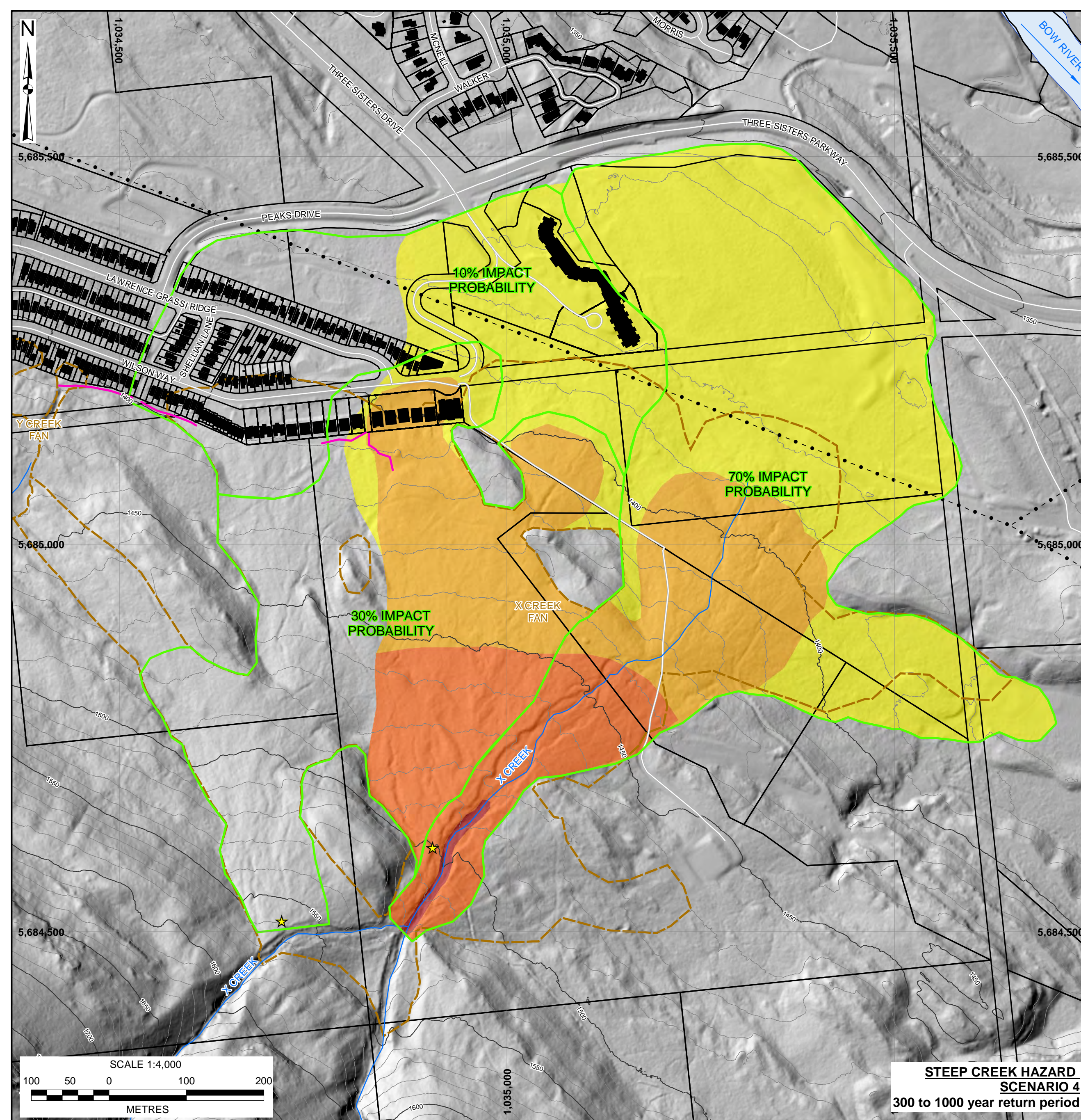
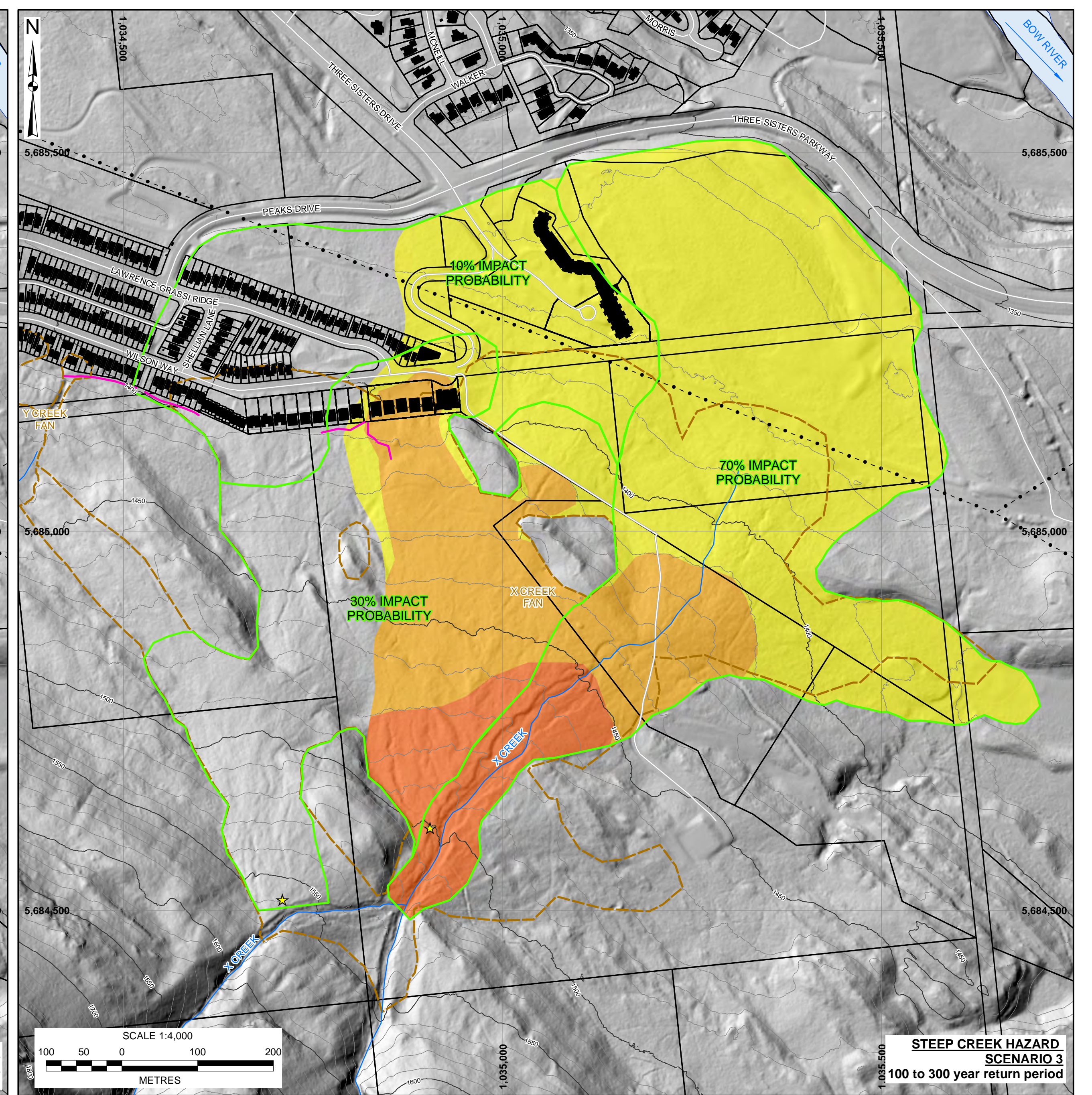
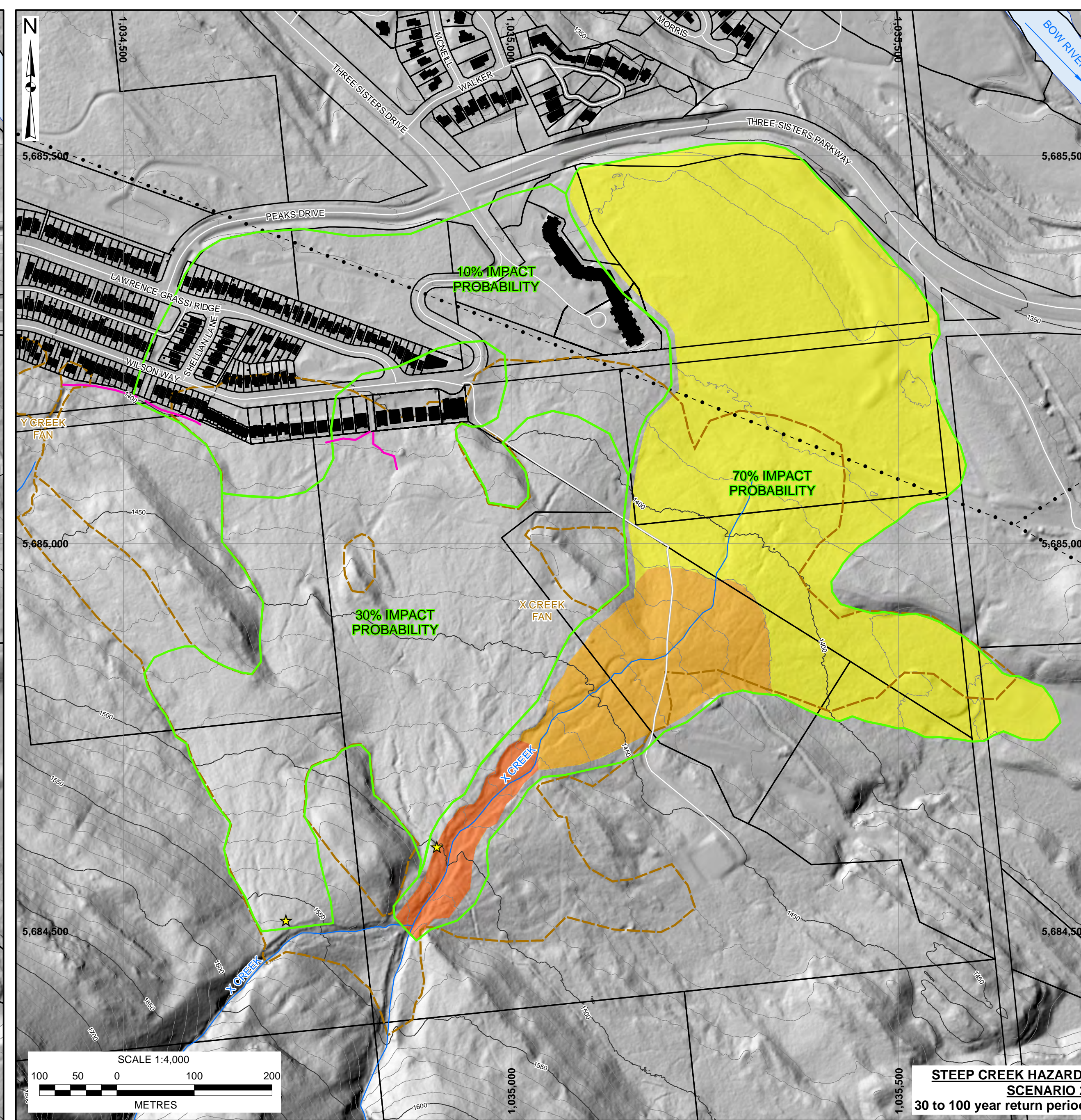
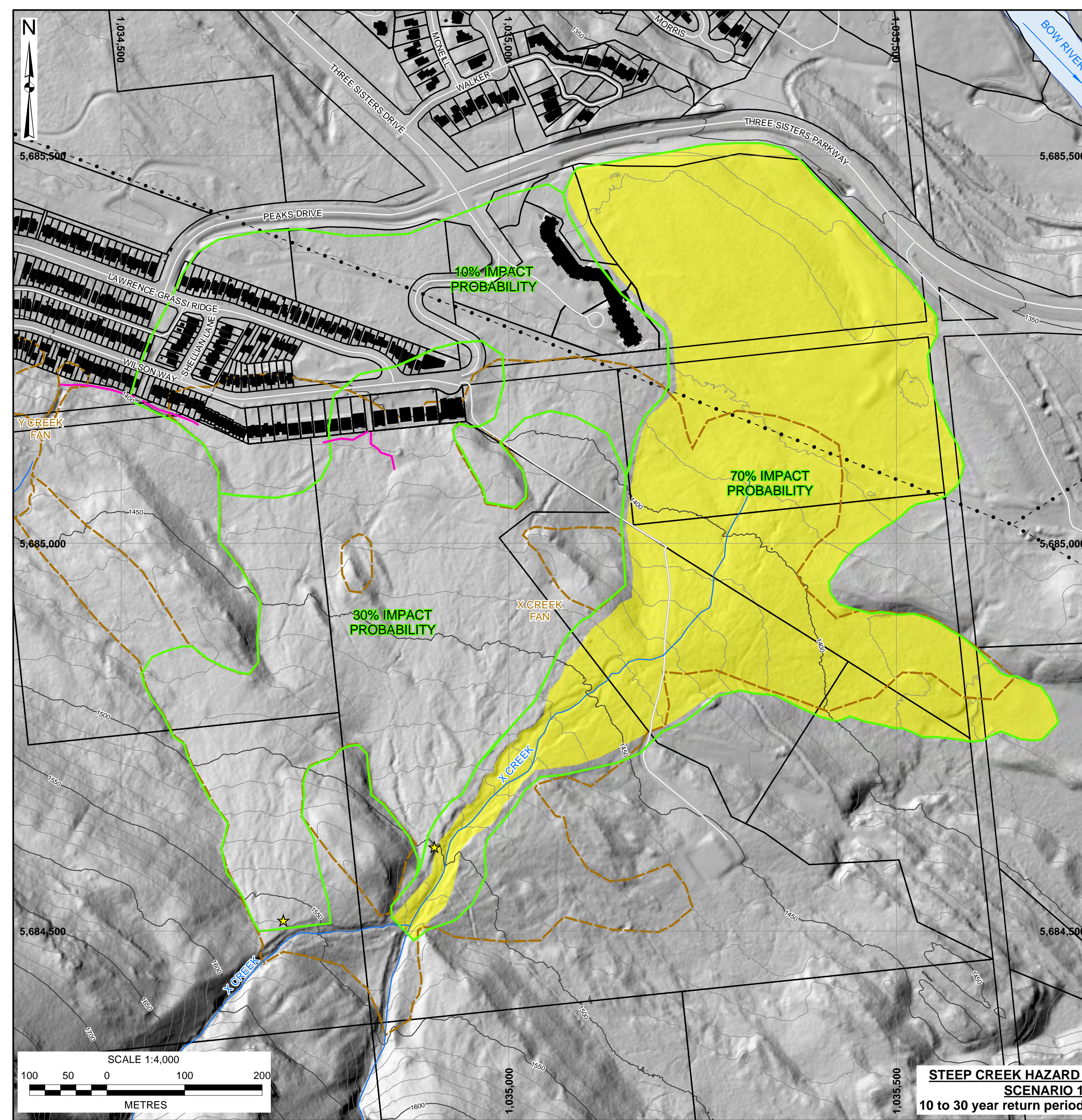
NOTES:
 1. ALL DIMENSIONS ARE IN METRES UNLESS OTHERWISE NOTED.
 2. THIS DRAWING MUST BE READ IN CONJUNCTION WITH BGC'S REPORT TITLED "STEEP CREEK HAZARD AND RISK ASSESSMENT: X, Y, AND Z CREEKS", DATED DECEMBER 2018.
 3. BASE TOPOGRAPHIC DATA BASED ON LIDAR PROVIDED BY MCELHANNEY, DATED AUGUST 2013 AND AIRBORNE IMAGING, DATED OCTOBER 2015. CONTOUR INTERVAL 100m.
 4. PROJECTION IS NAD 83 3TM 114.
 5. THE FAN BOUNDARY AS DRAWN IS APPROXIMATE AND DELINEATES THE LANDFORM. THE BOUNDARY SHOULD NOT BE CONSTRUED AS A HAZARD MAP, NOR DOES IT SHOW THE SPATIAL EXTENT OF POTENTIAL FLOODING.
 6. UNLESS BGC AGREES OTHERWISE IN WRITING, THIS DRAWING SHALL NOT BE MODIFIED OR USED FOR ANY PURPOSE OTHER THAN THE PURPOSE FOR WHICH BGC GENERATED IT. BGC SHALL HAVE NO LIABILITY FOR ANY DAMAGES OR LOSS ARISING IN ANY WAY FROM ANY USE OR MODIFICATION OF THIS DOCUMENT NOT AUTHORIZED BY BGC. ANY USE OF OR RELIANCE UPON THIS DOCUMENT OR ITS CONTENT BY THIRD PARTIES SHALL BE AT SUCH THIRD PARTIES' SOLE RISK.

SCALE:	1:10,000
DATE:	DEC 2018
DRAWN:	JDC, BMB
CHECKED:	BCP
APPROVED:	MJ

BGC ENGINEERING INC.
 AN APPLIED EARTH SCIENCES COMPANY

CLIENT:

PROJECT:	STEEP CREEK HAZARD AND RISK ASSESSMENT: X, Y, AND Z CREEKS	
TITLE:	X, Y, AND Z CREEKS GEOMORPHIC MAPPING	
PROJECT No.:	1261025	DWG No.: 05



LEGEND

- ★ POTENTIAL AVULSION ZONE
- WOODEN WALL
- SPATIAL IMPACT PROBABILITY ZONE
- INTENSITY INDEX (m²/s²)
- IDF < 1
- IDF 1 to 10
- IDF 10 to 100
- IDF > 100
- ▭ PARCEL
- BUILDING
- APPROXIMATE MODERN FAN BOUNDARY
- ROAD
- TRANSMISSION LINE
- CREEK
- APPROXIMATE MODERN FAN BOUNDARY

THIS DRAWING MAY HAVE BEEN REDUCED OR ENLARGED.
ALL FRACTIONAL SCALE NOTATIONS INDICATED ARE
BASED ON ORIGINAL FORMAT DRAWINGS.

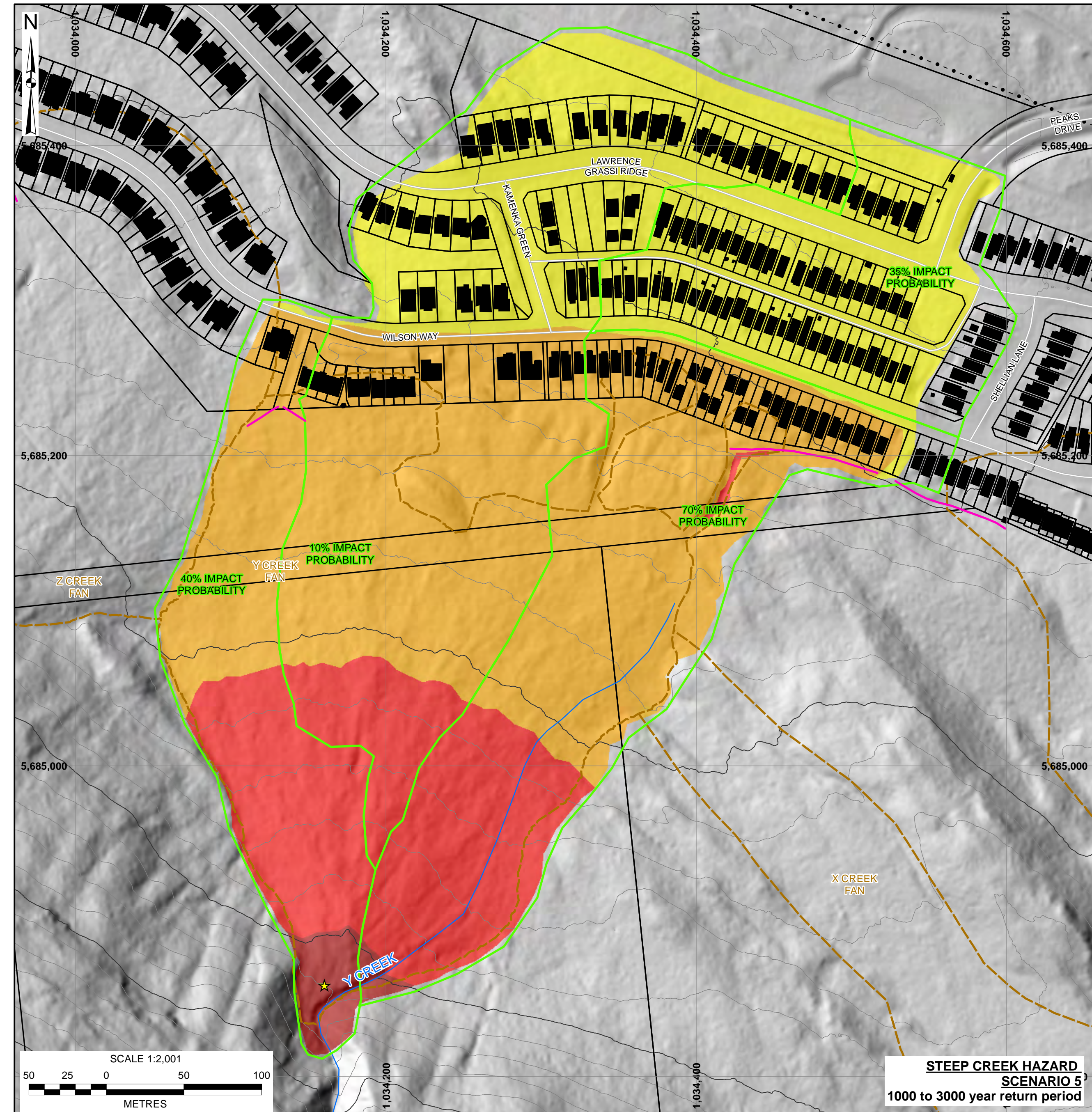
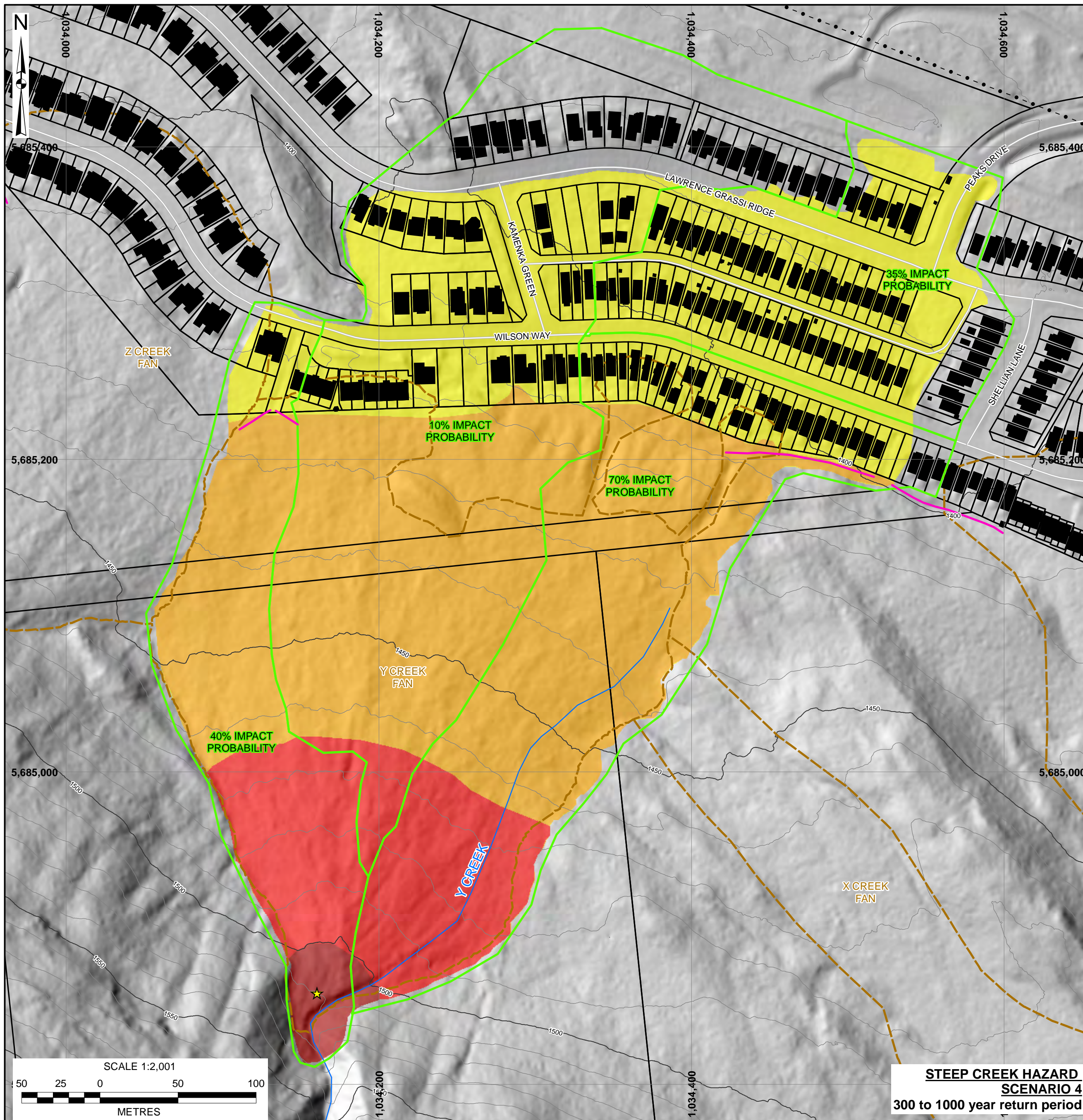
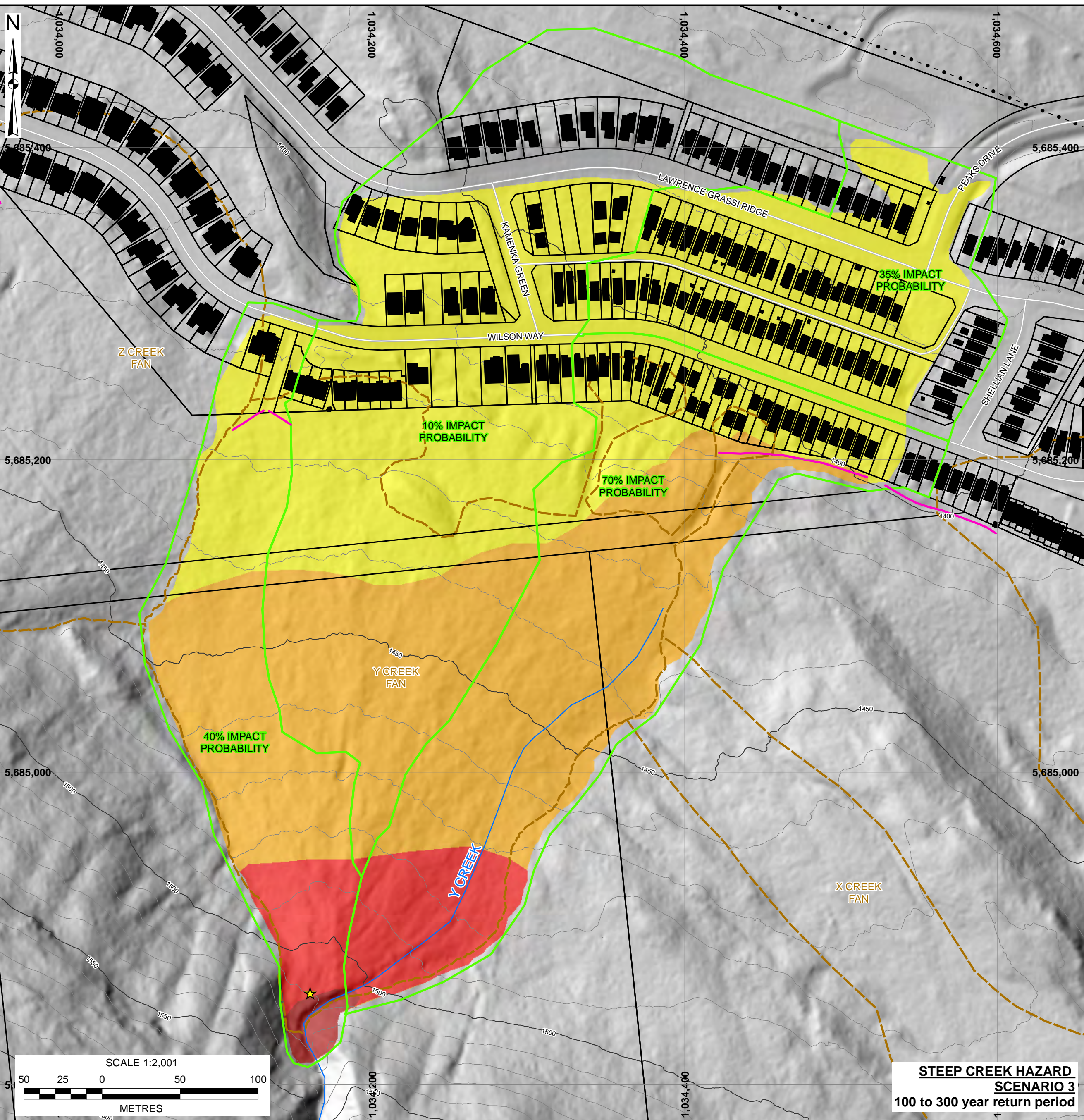
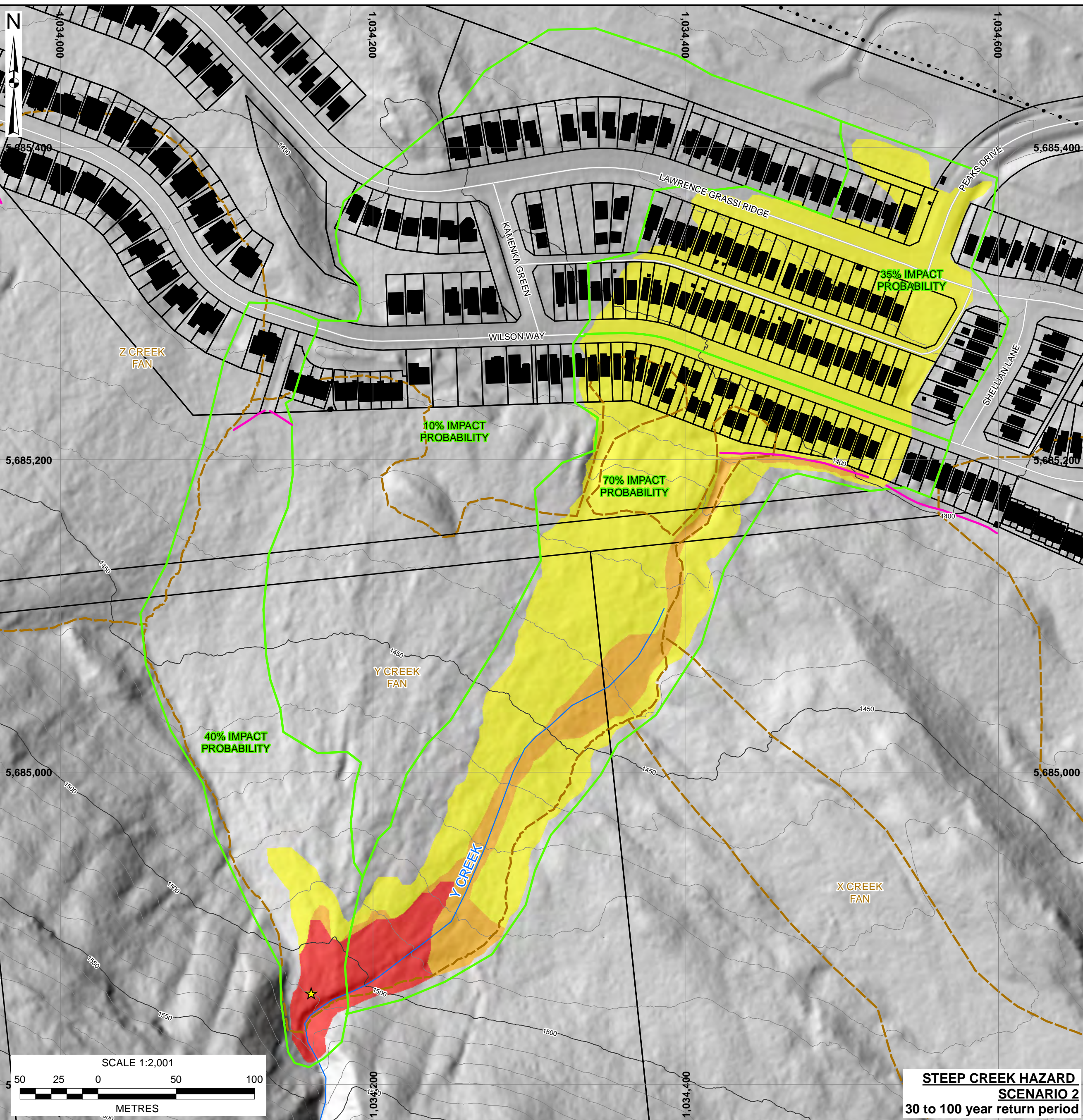
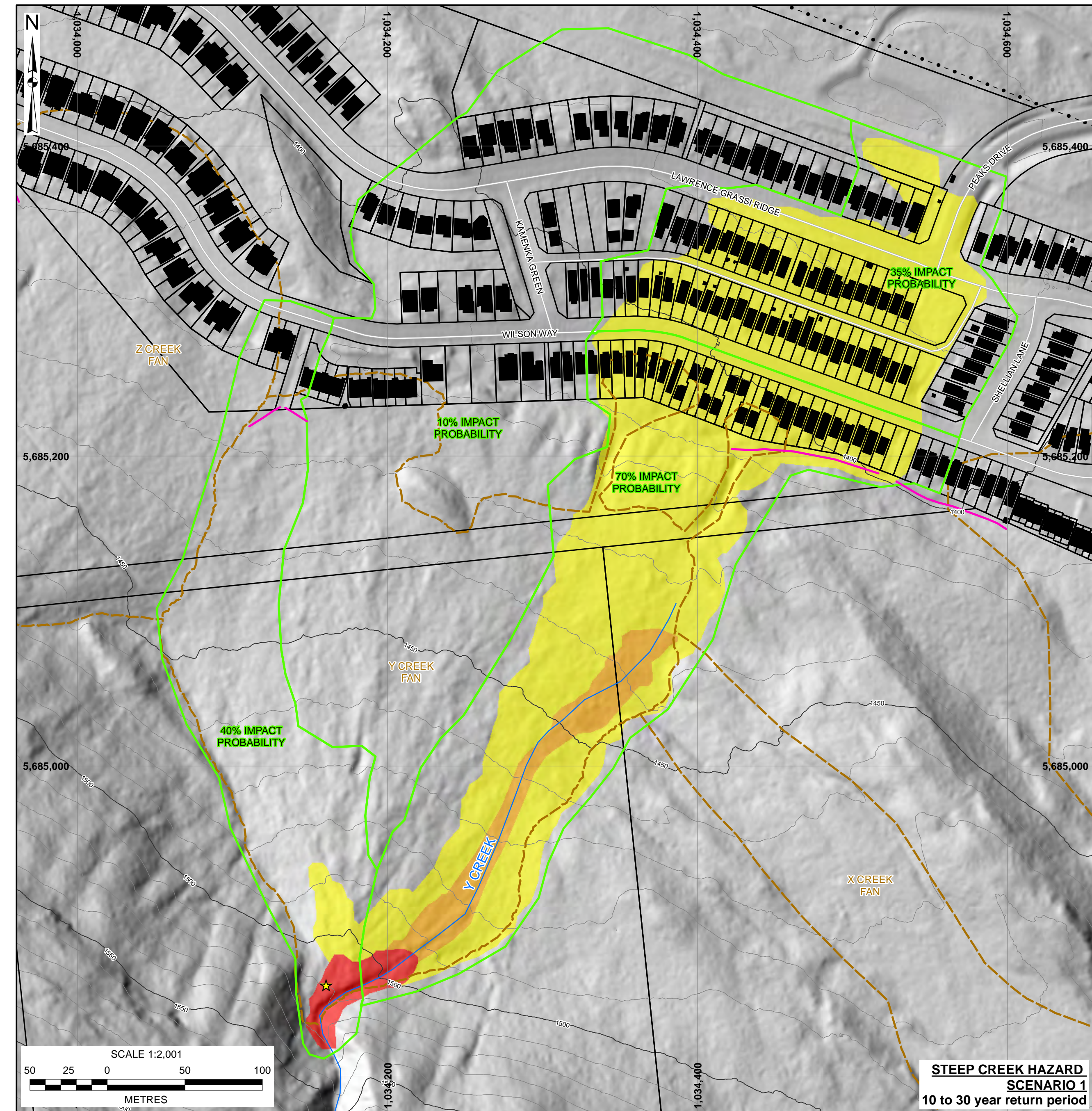
- NOTES:**
1. THE STEEP CREEK HAZARD INTENSITY AND SPATIAL IMPACT PROBABILITY ZONES SHOWN ON THIS MAP ARE INTERPRETATIONS, BASED ON NUMERICAL MODELLING RESULTS, FIELD RECONNAISSANCE, CURRENT TOPOGRAPHY AND JUDGEMENT.
 2. THIS MAP SHOULD NOT BE RELIED UPON AT A SCALE LARGER THAN (MORE DETAILED) THAN SHOWN ON THIS MAP.
 3. THIS MAP REPRESENTS A SNAPSHOT IN TIME BASED ON EXISTING CONDITIONS DESCRIBED IN THE REPORT. FUTURE CHANGES (DEVELOPMENT, MITIGATION, GEOHAZARD EVENTS) MAY WARRANT RE-DRAWING OF CERTAIN AREAS.
 4. ALL DIMENSIONS ARE IN METRES UNLESS OTHERWISE NOTED.
 5. THIS DRAWING MUST BE READ IN CONJUNCTION WITH BGC'S REPORT TITLED "STEEP CREEK HAZARD AND RISK ASSESSMENT: X, Y AND Z CREEKS" AND DATED DECEMBER 2018.
 6. BASE TOPOGRAPHIC DATA BASED ON LIDAR PROVIDED BY McELHANNAY, DATED AUGUST 2013. CONTOUR INTERVAL IS 10 m.
 7. WATERCOURSES, WATERBODIES AND ROADS WERE OBTAINED FROM CANVEC PROVIDED BY NATURAL RESOURCES CANADA.
 8. MODERN FAN BOUNDARIES DO NOT ALWAYS MATCH MODEL RESULTS AS FLOODING CAN EXCEED THE GEOMORPHIC FAN BOUNDARIES.
 9. PROJECTION IS NAD 83 UTM ZONE 10N. VERTICAL DATUM IS CGVD28.
 10. UNLESS BGC AGREES OTHERWISE IN WRITING, THIS DRAWING SHALL NOT BE MODIFIED OR USED FOR ANY PURPOSE OTHER THAN THE PURPOSE FOR WHICH BGC GENERATED IT.
BGC SHALL HAVE NO LIABILITY FOR ANY DAMAGES OR LOSS ARISING IN ANY WAY FROM ANY USE OR MODIFICATION OF THIS DOCUMENT
NOT AUTHORIZED BY BGC. ANY USE OF OR RELIANCE UPON THIS DOCUMENT OR ITS CONTENT BY THIRD PARTIES SHALL BE AT SUCH THIRD PARTIES' SOLE RISK.

SCALE:	1:4,000
DATE:	DEC 2018
DRAWN:	LL
CHECKED:	EM
APPROVED:	

BGC ENGINEERING INC.
AN APPLIED EARTH SCIENCES COMPANY

CLIENT: TOWN OF CANMORE

PROJECT:	STEEP CREEK HAZARD AND RISK ASSESSMENT: X, Y AND Z CREEKS		
TITLE:	X CREEK DEBRIS FLOW AND DEBRIS FLOOD RUNOUT AND INTENSITY		
PROJECT No.:	1261 025	DWG No.:	
			06



- LEGEND**
- ★ POTENTIAL AVULSION ZONE
 - WOODEN WALL
 - SPATIAL IMPACT PROBABILITY ZONE
 - INTENSITY INDEX (m³/s²)
 - IDF < 1
 - IDF 1 TO 10
 - IDF 10 TO 100
 - IDF > 100
 - ▭ PARCEL
 - ▭ BUILDING
 - APPROXIMATE MODERN FAN BOUNDARY
 - ROAD
 - TRANSMISSION LINE
 - CREEK
 - APPROXIMATE MODERN FAN BOUNDARY

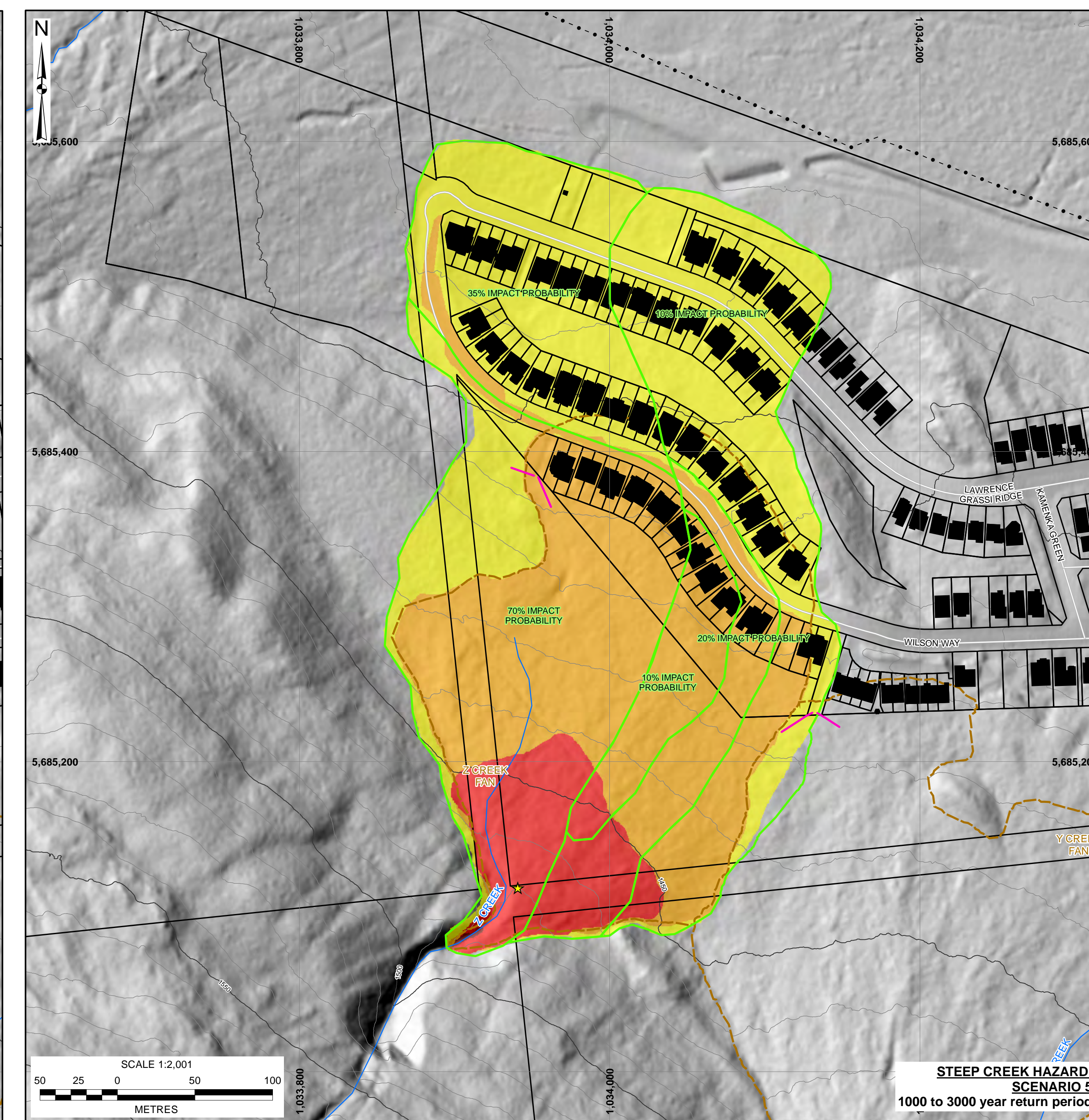
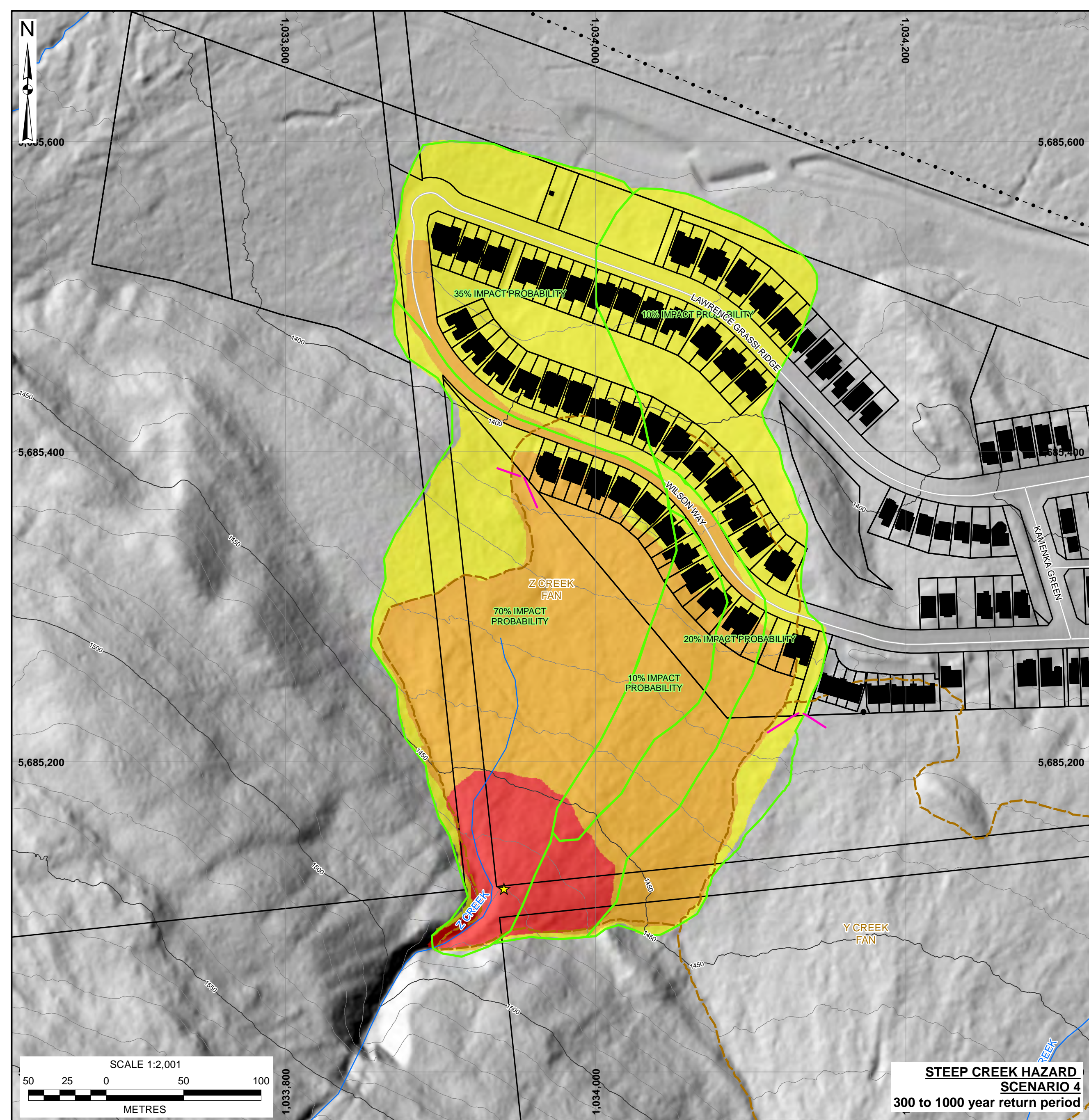
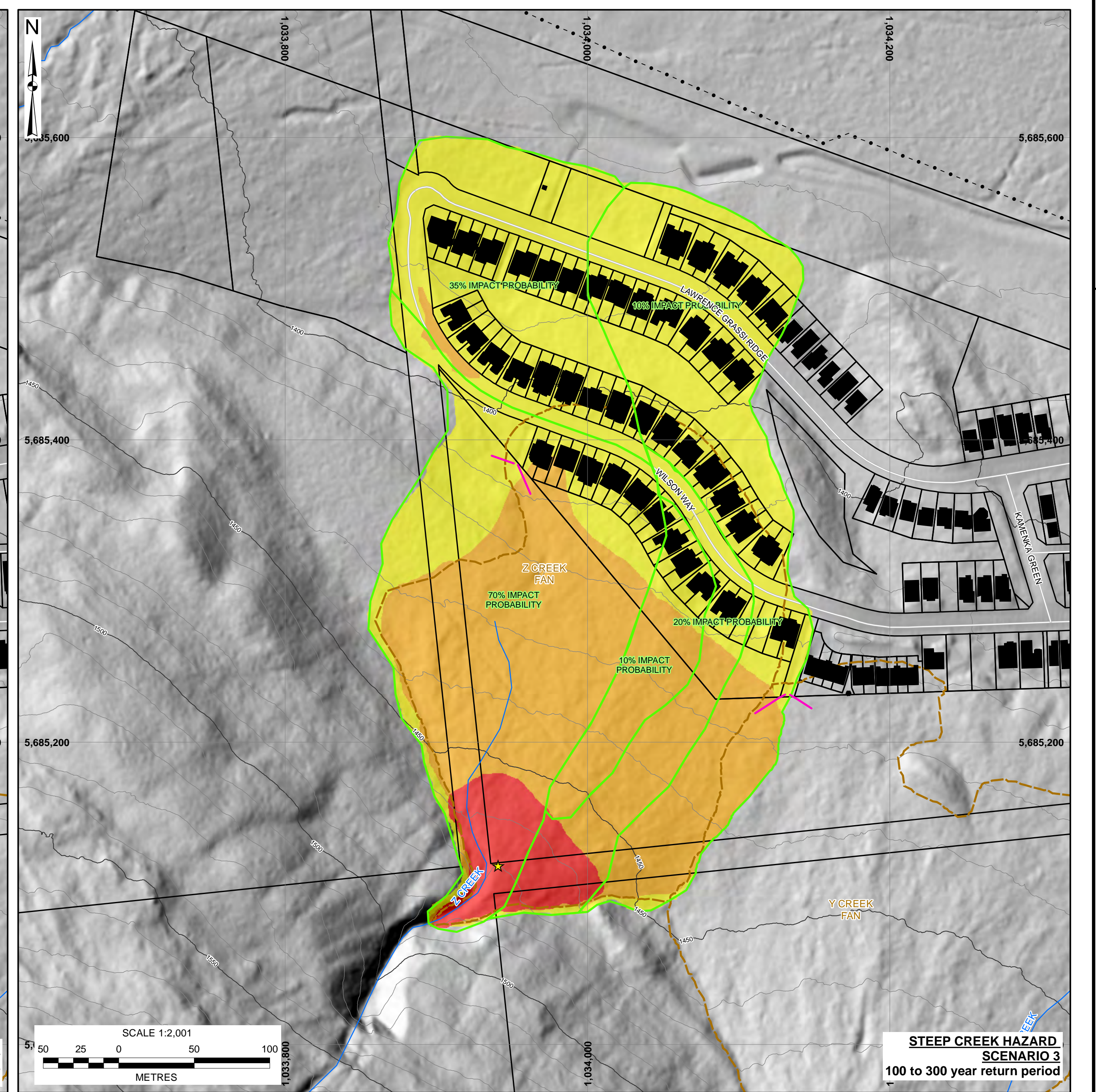
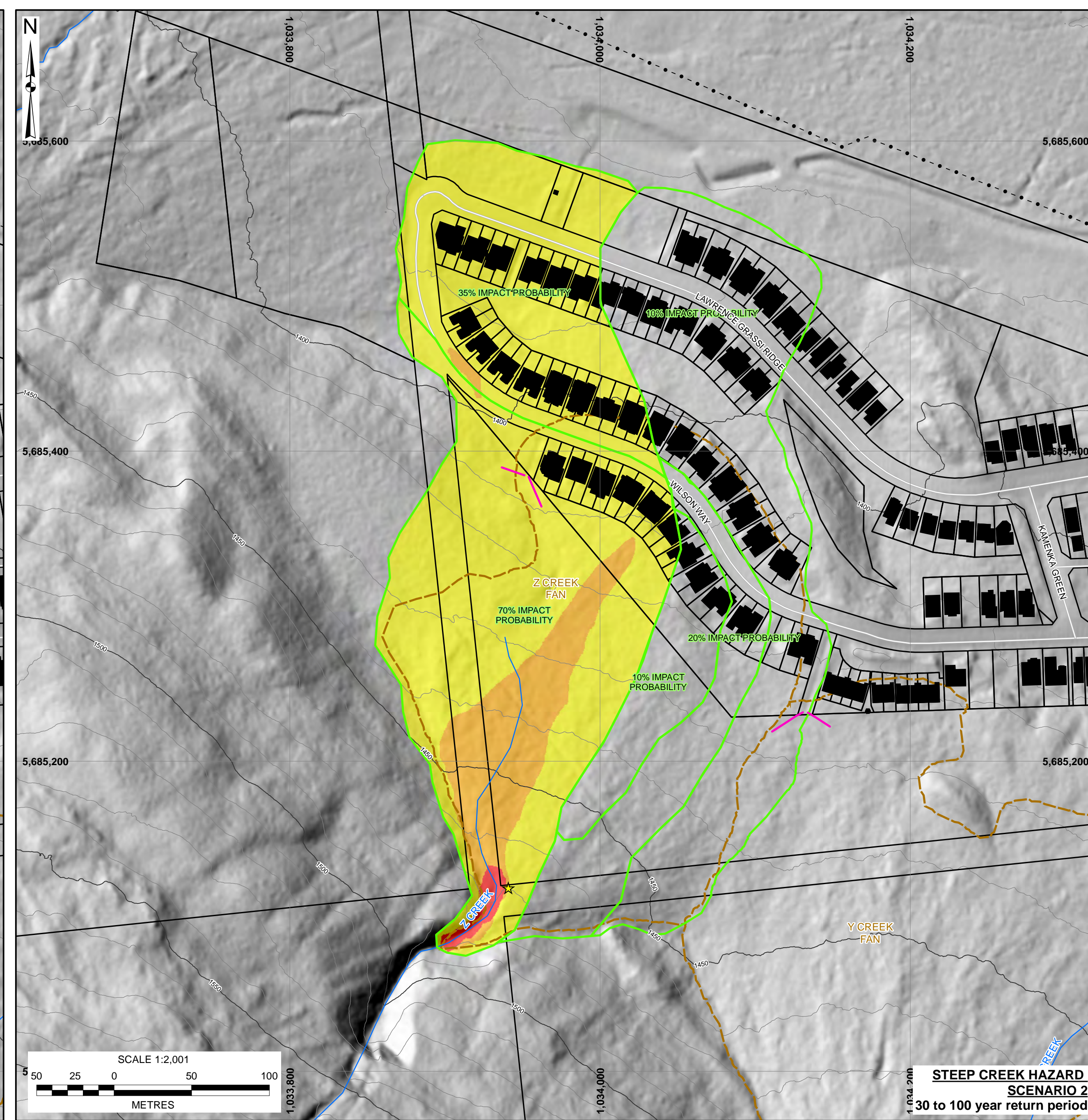
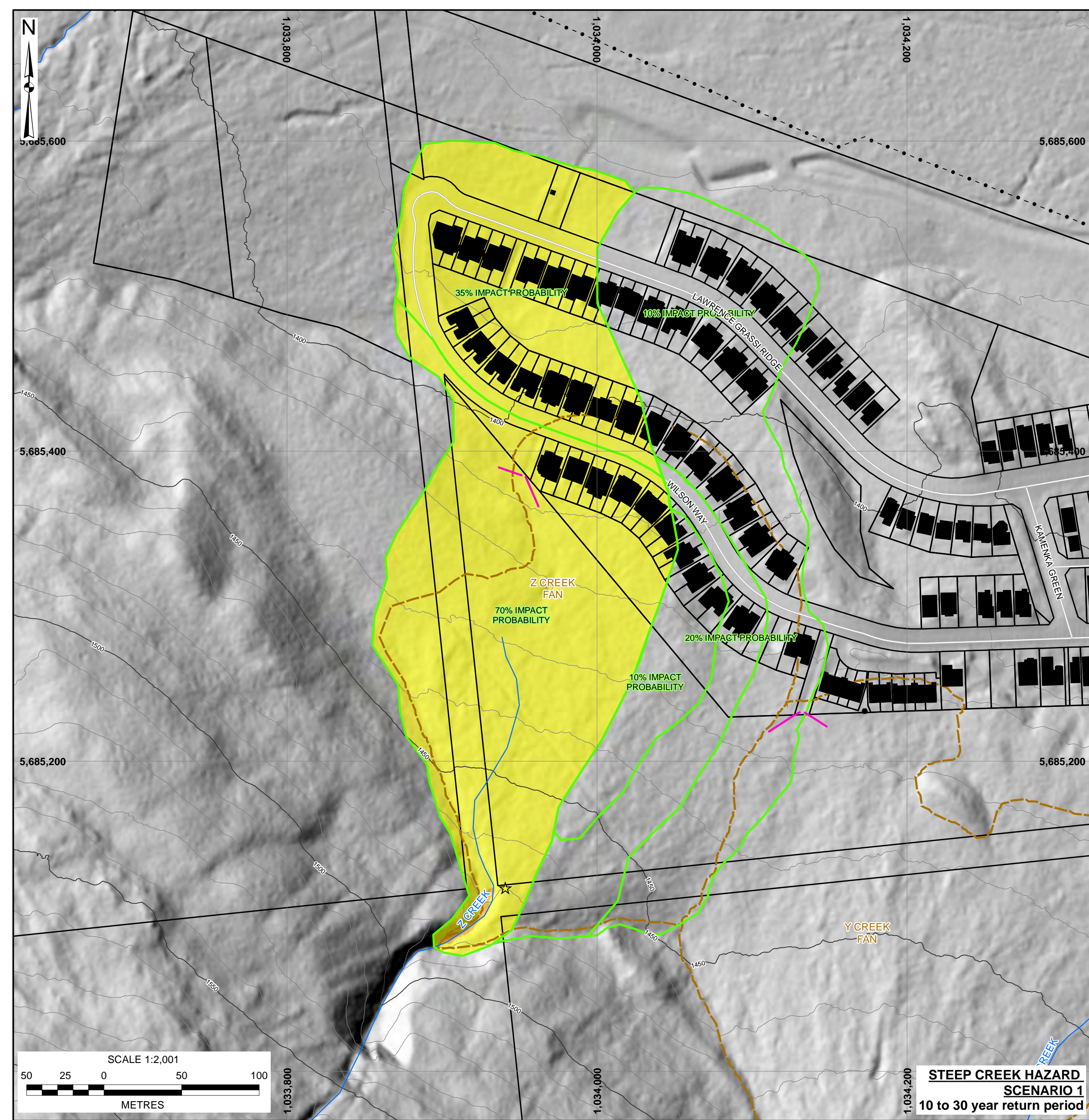
THIS DRAWING MAY HAVE BEEN REDUCED OR ENLARGED.
ALL FRACTIONAL SCALE NOTATIONS INDICATED ARE
BASED ON ORIGINAL FORMAT DRAWINGS.

- NOTES:**
1. THE STEEP CREEK HAZARD INTENSITY AND SPATIAL IMPACT PROBABILITY ZONES SHOWN ON THIS MAP ARE INTERPRETATIONS, BASED ON NUMERICAL MODELLING RESULTS, FIELD RECONNAISSANCE, CURRENT TOPOGRAPHY AND JUDGEMENT.
 2. THIS MAP SHOULD NOT BE RELIED UPON AT A SCALE LARGER THAN (MORE DETAILED) THAN SHOWN ON THIS MAP.
 3. THIS MAP REPRESENTS A SNAPSHOT IN TIME BASED ON EXISTING CONDITIONS DESCRIBED IN THE REPORT. FUTURE CHANGES (DEVELOPMENT, MITIGATION, GEOHAZARD EVENTS) MAY WARRANT RE-DRAWING OF CERTAIN AREAS.
 4. ALL DIMENSIONS ARE IN METRES UNLESS OTHERWISE NOTED.
 5. THIS DRAWING MUST BE READ IN CONJUNCTION WITH BGC'S REPORT TITLED "STEEP CREEK HAZARD AND RISK ASSESSMENT: X, Y AND Z CREEKS" AND DATED DECEMBER 2018.
 6. BASE TOPOGRAPHIC DATA BASED ON LIDAR PROVIDED BY McELHANNAY, DATED AUGUST 2013. CONTOUR INTERVAL IS 10 m.
 7. WATERCOURSES, WATERBODIES AND ROADS WERE OBTAINED FROM CANVEC PROVIDED BY NATURAL RESOURCES CANADA.
 8. MODERN FAN BOUNDARIES DO NOT ALWAYS MATCH MODEL RESULTS AS FLOODING CAN EXCEED THE GEOMORPHIC FAN BOUNDARIES.
 9. PROJECTION IS NAD 83 UTM ZONE 10N. VERTICAL DATUM IS CGVD28.
 10. UNLESS BGC AGREES OTHERWISE IN WRITING, THIS DRAWING SHALL NOT BE MODIFIED OR USED FOR ANY PURPOSE OTHER THAN THE PURPOSE FOR WHICH BGC GENERATED IT.
BGC SHALL HAVE NO LIABILITY FOR ANY DAMAGES OR LOSS ARISING IN ANY WAY FROM ANY USE OR MODIFICATION OF THIS DOCUMENT
NOT AUTHORIZED BY BGC. ANY USE OF OR RELIANCE UPON THIS DOCUMENT OR ITS CONTENT BY THIRD PARTIES SHALL BE AT SUCH THIRD PARTIES' SOLE RISK.

SCALE:	1:2,000		PROJECT:	STEEP CREEK HAZARD AND RISK ASSESSMENT: X, Y AND Z CREEKS		
DATE:	DEC 2018		TITLE:	Y CREEK DEBRIS FLOW AND DEBRIS FLOOD RUNOUT AND INTENSITY		
DRAWN:	LL	CLIENT:	TOWN OF CANMORE		PROJECT No.:	1261 025
CHECKED:	EM				DWG No.:	07
APPROVED:						

X:\Projects\1261025\GIS\Production\Report\1261025_Slip, Steep Creek Hazard and Risk Assessment_X, Y and Z Creeks\07_Y_Creek_Debis Flow and Details_Flood, Debris Flow and Details_10-5.mxd, Wednesday, December 19, 2018 Time: 3:51 PM

THIS DRAWING IS 100% AT FULL SIZE. ALL SCALES REFERENCED TO FULL SIZE.



LEGEND	
★	POTENTIAL AVULSION ZONE
—	WOODEN WALL
—	SPATIAL IMPACT PROBABILITY ZONE
INTENSITY INDEX (m ³ /s ²)	
Yellow	IDF < 1
Orange	IDF 1 to 10
Red	IDF 10 to 100
Dark Red	IDF > 100
Black outline	PARCEL
Orange dashed line	APPROXIMATE MODERN FAN BOUNDARY
Black outline	BUILDING
Grey line	ROAD
Blue dashed line	TRANSMISSION LINE
Blue line	CREEK
Orange dashed line	APPROXIMATE MODERN FAN BOUNDARY

THIS DRAWING MAY HAVE BEEN REDUCED OR ENLARGED. ALL FRACTIONAL SCALE NOTATIONS INDICATED ARE BASED ON ORIGINAL FORMAT DRAWINGS.

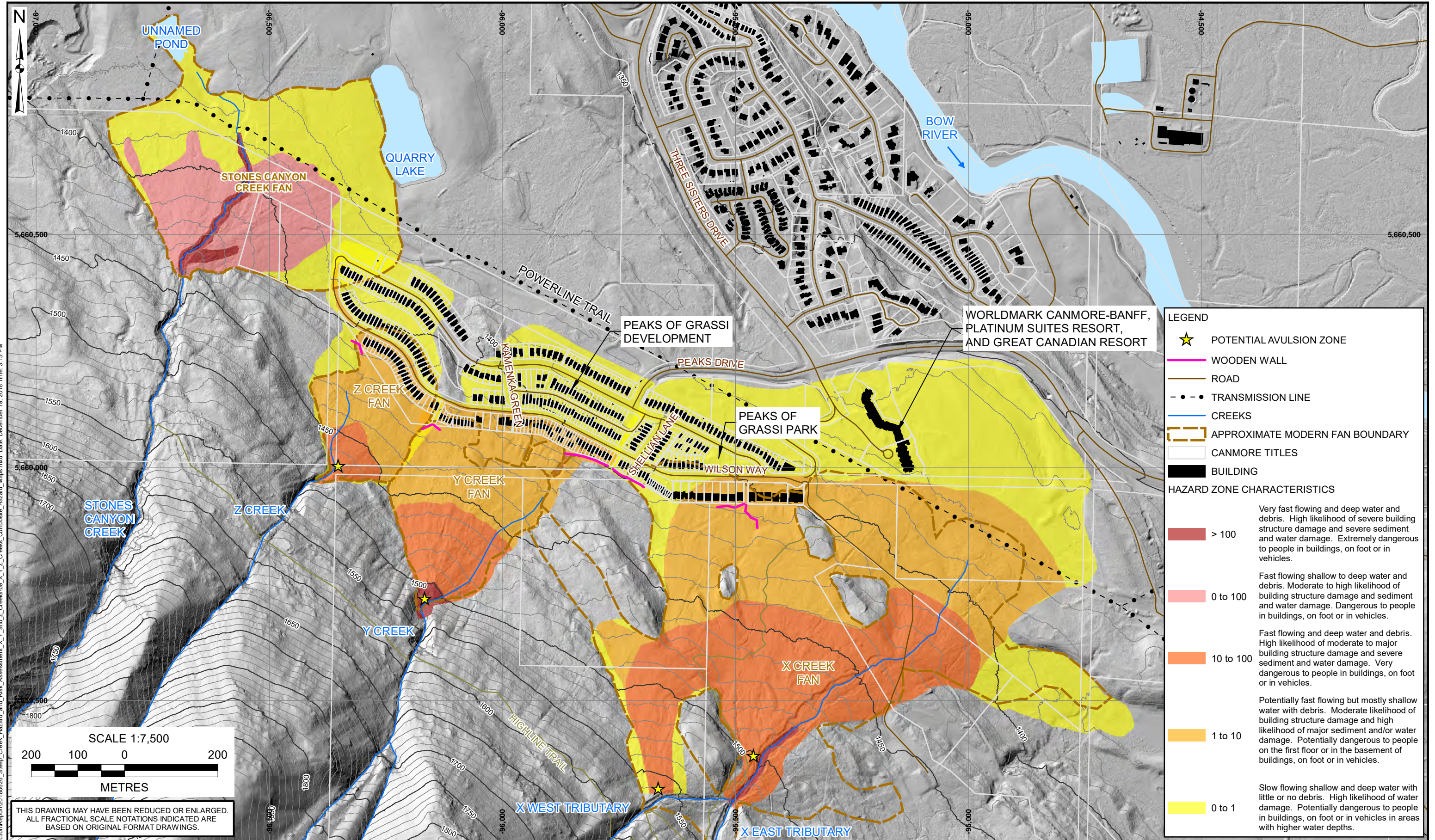
- NOTES:
1. THE STEEP CREEK HAZARD INTENSITY AND SPATIAL IMPACT PROBABILITY ZONES SHOWN ON THIS MAP ARE INTERPRETATIONS, BASED ON NUMERICAL MODELLING RESULTS, FIELD RECONNAISSANCE, CURRENT TOPOGRAPHY AND JUDGEMENT.
 2. THIS MAP SHOULD NOT BE RELIED UPON AT A SCALE LARGER THAN (MORE DETAILED) THAN SHOWN ON THIS MAP.
 3. THIS MAP REPRESENTS A SNAPSHOT IN TIME BASED ON EXISTING CONDITIONS DESCRIBED IN THE REPORT. FUTURE CHANGES (DEVELOPMENT, MITIGATION, GEOHAZARD EVENTS) MAY WARRANT RE-DRAWING OF CERTAIN AREAS.
 4. ALL DIMENSIONS ARE IN METRES UNLESS OTHERWISE NOTED.
 5. THIS DRAWING MUST BE READ IN CONJUNCTION WITH BGC'S REPORT TITLED "STEEP CREEK HAZARD AND RISK ASSESSMENT: X, Y AND Z CREEKS" AND DATED DECEMBER 2018.
 6. BASE TOPOGRAPHIC DATA BASED ON LIDAR PROVIDED BY McELHANNAY, DATED AUGUST 2013. CONTOUR INTERVAL IS 10 m.
 7. WATERCOURSES, WATERBODIES AND ROADS WERE OBTAINED FROM CANVEC PROVIDED BY NATURAL RESOURCES CANADA.
 8. MODERN FAN BOUNDARIES DO NOT ALWAYS MATCH MODEL RESULTS AS FLOODING CAN EXCEED THE GEOMORPHIC FAN BOUNDARIES.
 9. PROJECTION IS NAD 83 UTM ZONE 10N. VERTICAL DATUM IS CGVD28.
 10. UNLESS BGC AGREES OTHERWISE IN WRITING, THIS DRAWING SHALL NOT BE MODIFIED OR USED FOR ANY PURPOSE OTHER THAN THE PURPOSE FOR WHICH BGC GENERATED IT. BGC SHALL HAVE NO LIABILITY FOR ANY DAMAGES OR LOSS ARISING IN ANY WAY FROM ANY USE OR MODIFICATION OF THIS DOCUMENT. NOT AUTHORIZED BY BGC. ANY USE OF OR RELIANCE UPON THIS DOCUMENT OR ITS CONTENT BY THIRD PARTIES SHALL BE AT SUCH THIRD PARTIES' SOLE RISK.

SCALE:	1:2,000
DATE:	DEC 2018
DRAWN:	LL
CHECKED:	EM
APPROVED:	

BGC ENGINEERING INC.
AN APPLIED EARTH SCIENCES COMPANY

CLIENT: TOWN OF CANMORE

PROJECT:	STEEP CREEK HAZARD AND RISK ASSESSMENT: X, Y AND Z CREEKS		
TITLE:	Z CREEK DEBRIS FLOW AND DEBRIS FLOOD RUNOUT AND INTENSITY		
PROJECT No.:	1261 025	DWG No.:	08

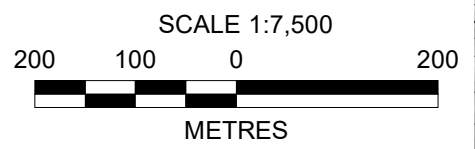


LEGEND

- ★ POTENTIAL AVULSION ZONE
- WOODEN WALL
- ROAD
- · - · TRANSMISSION LINE
- CREEKS
- APPROXIMATE MODERN FAN BOUNDARY
- CANMORE TITLES
- BUILDING

HAZARD ZONE CHARACTERISTICS

> 100	Very fast flowing and deep water and debris. High likelihood of severe building structure damage and severe sediment and water damage. Extremely dangerous to people in buildings, on foot or in vehicles.
0 to 100	Fast flowing shallow to deep water and debris. Moderate to high likelihood of building structure damage and severe sediment and water damage. Dangerous to people in buildings, on foot or in vehicles.
10 to 100	Fast flowing and deep water and debris. High likelihood of moderate to major building structure damage and severe sediment and water damage. Very dangerous to people in buildings, on foot or in vehicles.
1 to 10	Potentially fast flowing but mostly shallow water with debris. Moderate likelihood of building structure damage and high likelihood of major sediment and/or water damage. Potentially dangerous to people on the first floor or in the basement of buildings, on foot or in vehicles.
0 to 1	Slow flowing shallow and deep water with little or no debris. High likelihood of water damage. Potentially dangerous to people in buildings, on foot or in vehicles in areas with higher water depths.



THIS DRAWING MAY HAVE BEEN REDUCED OR ENLARGED. ALL FRACTIONAL SCALE NOTATIONS INDICATED ARE BASED ON ORIGINAL FORMAT DRAWINGS.

NOTES:

1. THE STEEP CREEK HAZARD INTENSITY AND SPATIAL IMPACT PROBABILITY ZONES SHOWN ON THIS MAP ARE INTERPRETATIONS, BASED ON NUMERICAL MODELLING RESULTS, FIELD RECONNAISSANCE, CURRENT TOPOGRAPHY AND JUDGEMENT.
2. ALL DIMENSIONS ARE IN METRES UNLESS OTHERWISE NOTED.
3. THIS DRAWING MUST BE READ IN CONJUNCTION WITH BGC'S REPORT TITLED "STEEP CREEK HAZARD AND RISK ASSESSMENT: X, Y, AND Z CREEKS", AND DATED DECEMBER 2018.
4. BASE TOPOGRAPHIC DATA BASED ON LIDAR PROVIDED BY McELHANNEY, DATED AUGUST 2013. CONTOUR INTERVAL IS 10 m.
5. THE FAN BOUNDARY AS DRAWN IS APPROXIMATE AND DELINEATES THE LANDFORM. THE BOUNDARY SHOULD NOT BE CONSTRUED AS A HAZARD MAP, NOR DOES IT SHOW THE SPATIAL EXTENT OF POTENTIAL FLOODING. FAN BOUNDARIES WITHIN DEVELOPED AREAS ARE VERY APPROXIMATE AS THEY HAVE BEEN ALTERED BY THE DEVELOPMENTS.

6. HAZARD ZONES FOR STONES CANYON CREEK OBTAINED FROM BGC'S REPORT TITLED "STONES CANYON CREEK, LEVEL 2 DEBRIS-FLOW RISK ASSESSMENT" FOR HILLCROFT DEVELOPMENTS LTD, DATED OCTOBER 2015.
7. PROJECTION IS NAD83 3TM 114. VERTICAL DATUM IS CGVD28.
8. UNLESS BGC AGREES OTHERWISE IN WRITING, THIS DRAWING SHALL NOT BE MODIFIED OR USED FOR ANY PURPOSE OTHER THAN THE PURPOSE FOR WHICH BGC GENERATED IT. BGC SHALL HAVE NO LIABILITY FOR ANY DAMAGES OR LOSS ARISING IN ANY WAY FROM ANY USE OR MODIFICATION OF THIS DOCUMENT NOT AUTHORIZED BY BGC. ANY USE OF OR RELIANCE UPON THIS DOCUMENT OR ITS CONTENT BY THIRD PARTIES SHALL BE AT SUCH THIRD PARTIES' SOLE RISK.

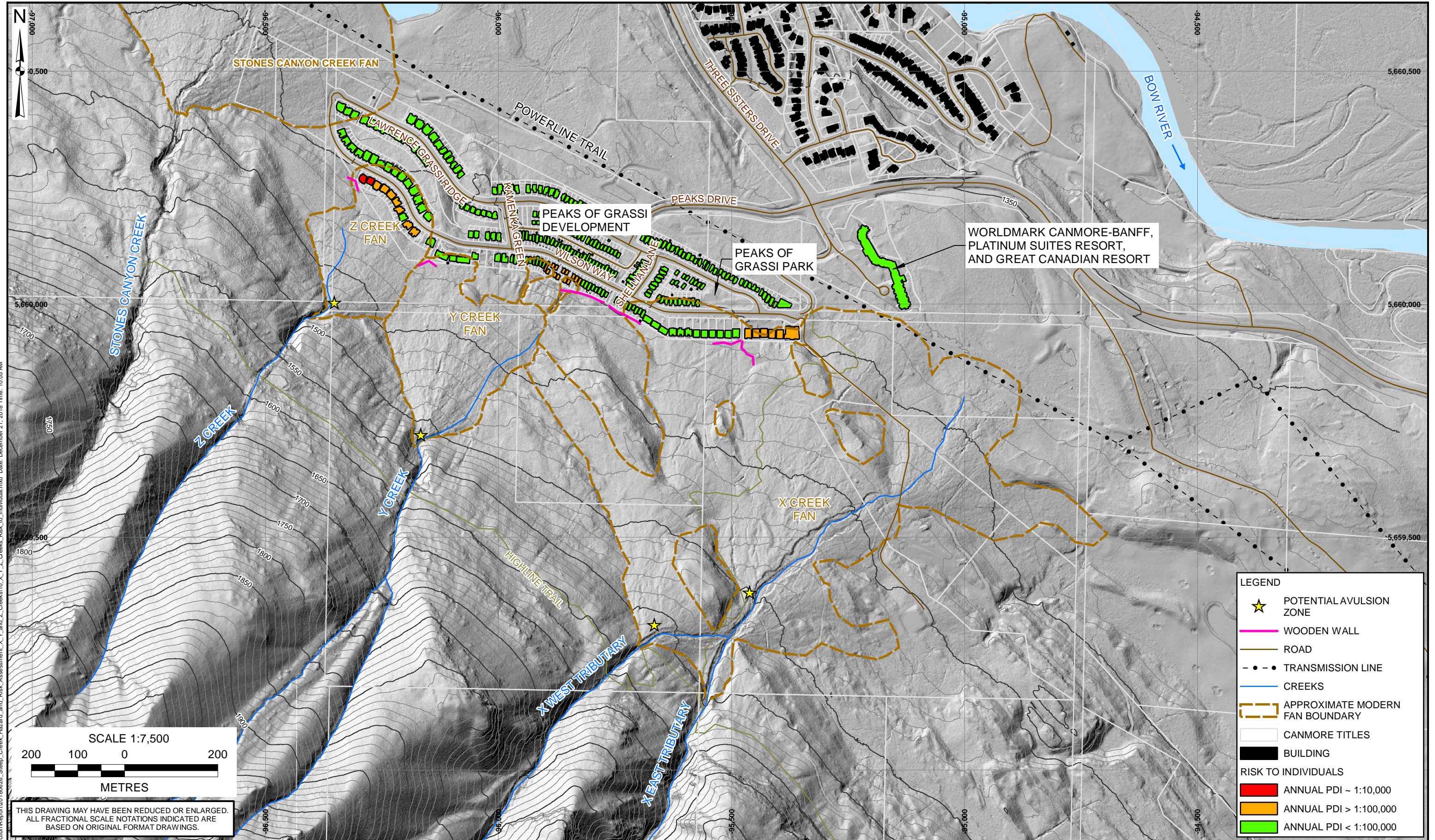
SCALE:	1:7,500
DATE:	DEC 2018
DRAWN:	BMB, LL
CHECKED:	EM
APPROVED:	MJ

BGC ENGINEERING INC.
AN APPLIED EARTH SCIENCES COMPANY

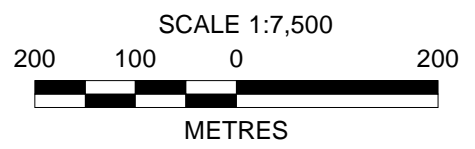
CLIENT: **Town of CANMORE**

PROJECT:	STEEP CREEK HAZARD AND RISK ASSESSMENT: X, Y, AND Z CREEKS	
TITLE:	COMPOSITE HAZARD MAP	
PROJECT No.:	1261025	DWG No.:
		09

X:\Projects\1261025\GIS\Production\Report\1261025_Steep_Creek_Hazard_and_Risk_Assessment_X_Y_and_Z_Creeks_Composite_Hazard_Map.mxd Date: December 19, 2018 Time: 3:15 PM



X:\Projects\1261025\GIS\Production\Report\20180626_Steep_Creek_Hazard_and_Risk_Assessment_X_Y_and_Z_Creeks\10_X_Y_Z_Creeks_Risk_to_Individual.mxd Date: December 21, 2018 Time: 10:05 AM



THIS DRAWING MAY HAVE BEEN REDUCED OR ENLARGED.
ALL FRACTIONAL SCALE NOTATIONS INDICATED ARE
BASED ON ORIGINAL FORMAT DRAWINGS.

NOTES:

1. THE STEEP CREEK HAZARD INTENSITY AND SPATIAL IMPACT PROBABILITY ZONES SHOWN ON THIS MAP ARE INTERPRETATIONS, BASED ON NUMERICAL MODELLING RESULTS, FIELD RECONNAISSANCE, CURRENT TOPOGRAPHY AND JUDGEMENT.
2. ALL DIMENSIONS ARE IN METRES UNLESS OTHERWISE NOTED.
3. THIS DRAWING MUST BE READ IN CONJUNCTION WITH BGC'S REPORT TITLED "STEEP CREEK HAZARD AND RISK ASSESSMENT: X, Y, AND Z CREEKS", AND DATED DECEMBER 2018.
4. BASE TOPOGRAPHIC DATA BASED ON LIDAR PROVIDED BY AIRBORNE IMAGING, DATED OCTOBER 2015. CONTOUR INTERVAL IS 10 m.
5. THE FAN BOUNDARY AS DRAWN IS APPROXIMATE AND DELINEATES THE LANDFORM. THE BOUNDARY SHOULD NOT BE CONSTRUED AS A HAZARD MAP, NOR DOES IT SHOW THE SPATIAL EXTENT OF POTENTIAL FLOODING. FAN BOUNDARIES WITHIN DEVELOPED AREAS ARE VERY APPROXIMATE AS THEY HAVE BEEN ALTERED BY THE DEVELOPMENTS.
6. PROJECTION IS NAD83 3TM 114. VERTICAL DATUM IS CGVD28.
7. UNLESS BGC AGREES OTHERWISE IN WRITING, THIS DRAWING SHALL NOT BE MODIFIED OR USED FOR ANY PURPOSE OTHER THAN THE PURPOSE FOR WHICH BGC GENERATED IT. BGC SHALL HAVE NO LIABILITY FOR ANY DAMAGES OR LOSS ARISING IN ANY WAY FROM ANY USE OR MODIFICATION OF THIS DOCUMENT NOT AUTHORIZED BY BGC. ANY USE OF OR RELIANCE UPON THIS DOCUMENT OR ITS CONTENT BY THIRD PARTIES SHALL BE AT SUCH THIRD PARTIES' SOLE RISK.

SCALE: 1:7,500
DATE: DEC 2018
DRAWN: BMB, LL
CHECKED: EM
APPROVED: MJ

BGC ENGINEERING INC.
AN APPLIED EARTH SCIENCES COMPANY

CLIENT: **Town of CANMORE**

PROJECT: STEEP CREEK HAZARD AND RISK ASSESSMENT: X, Y, AND Z CREEKS
TITLE: RISK TO THE INDIVIDUAL
PROJECT No.: 1261025
DWG No.: 10

LEGEND

- ★ POTENTIAL AVULSION ZONE
- WOODEN WALL
- ROAD
- · - · - TRANSMISSION LINE
- CREEKS
- APPROXIMATE MODERN FAN BOUNDARY
- CANMORE TITLES
- BUILDING

RISK TO INDIVIDUALS

- ANNUAL PDI ~ 1:10,000
- ANNUAL PDI > 1:100,000
- ANNUAL PDI < 1:100,000

APPENDIX A - STEEP CREEK PROCESS TYPES

APPENDIX A – STEEP CREEK PROCESS TYPES

A.1. STEEP CREEK PROCESS TYPES

Steep mountain creeks (here-in defined as having channel gradients steeper than 5%) are typically subject to a spectrum of mass movement processes that range from clear water floods to debris floods to hyper-concentrated flows to debris flows in order of increasing sediment concentration. In this report, they are referred to collectively as hydrogeomorphic¹ floods or processes. There is a continuum between these processes in space and time with floods transitioning into debris floods and eventually debris flows through progressive sediment entrainment. Conversely, dilution of a debris flow through partial sediment deposition and tributary injection of water can lead to a transition towards hyper-concentrated flows and debris floods and eventually floods.

In western Canada, most infrastructure on such creeks have been designed for clearwater floods with return periods of up to 200 years (100 years in Alberta). This design does not account for hydrogeomorphic processes such as debris floods and debris flows in which parts of or the entire channel bed sediments are mobilized and lead to erosion of channel bed and banks and debris inundation on terminal alluvial fans (Jakob et al., 2016).

Ignoring the specific hydrogeomorphic processes that act on steep creeks can and has led to a plethora of problems, many of which are caused by the fact that culverts and sometimes bridges have not been designed for heavy sediment loads or severe bank erosion. When such culverts are overwhelmed, blockage and re-direction of waters and sediment can occur.

A.1.1. Steep Creeks

Hydrogeomorphic floods are a phenomenon of steep channels. The morphology and processes in steep channels have been described by Church (2010, 2013). Sediment transfer occurs by a continuum of processes ranging from fluvial transport (bedload and suspended load) through debris floods to debris flows. These phenomena are transitional within time and space along the channel, depending on the sediment-water mixture. To understand the significance of these different modes of sediment transfer, it is useful to consider the characteristic anatomy of a steep channel system. Steep mountain slopes deliver sedimentary debris to the upper channels by rock fall, rock slides, debris avalanches, debris flows, slumps and raveling. Landslides may create temporary dams that pond water: when the dam breaks, a debris flow may be initiated in the channel. Debris flows and debris floods characteristically gain power and material as they move downstream, debouching onto a terminal fan where the channel enters the main valley floor. Here sediment is deposited and widespread damage may occur (Jakob et al. 2016).

¹ Hydrogeomorphology is an interdisciplinary science that focuses on the interaction and linkage of hydrologic processes with landforms or earth materials and the interaction of geomorphic processes with surface and subsurface water in temporal and spatial dimensions (Sidle and Onda, 2004).

The following subsections adapted from Jakob et al. (2016) provide a summary of debris flow and debris flood processes.

Figure A-1 summarizes the different hydrogeomorphic processes by their appearance in plan form, velocity and sediment concentration.

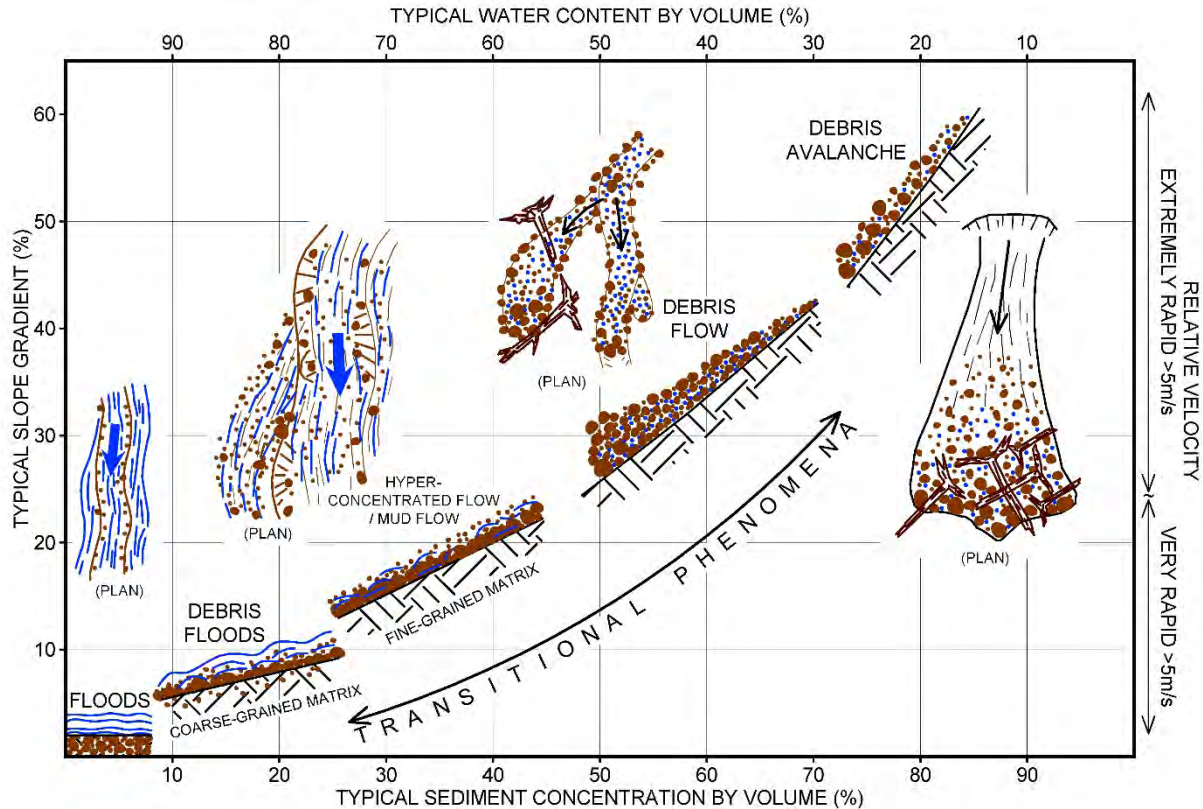


Figure A-1. Hydrogeomorphic process classification by sediment concentration, slope, velocity and planform appearance.

A.2. DEBRIS FLOWS

‘Debris flow’, as defined by Hungr et al. (2014), is a very rapid, channelized flow of saturated debris containing fines (i.e., sand and finer fractions) with a plasticity index of less than 5%. Debris flows originate from single or distributed source areas in debris mobilized by the influx of ground- or surface water. Liquefaction occurs shortly after the onset of landsliding due to turbulent mixing of water and sediment, and the slurry begins to flow downstream, ‘bulking’ by entraining additional water and channel debris.

Sediment bulking is the process by which rapidly flowing water entrains bed and bank materials either through erosion or preferential “plucking” until a certain sediment conveyance capacity (saturation) is reached. At this time, further sediment entrainment may still occur through bank undercutting and transitional deposition of debris with a zero net change in sediment concentration. The volume of the flowing mass is thereby increased (bulked). Bulking may be limited to partial channel substrate mobilization of the top gravel layer, or – in the case of debris

flows – may entail entrainment of the entire loose channel debris. Scour to bedrock in the transport zone is expected in the latter case.

Unlike debris avalanches, which travel on unconfined slopes, debris flows travel in confined channels bordered by steep slopes. In this environment, the flow volume, peak discharge, and flow depth increase, and the debris becomes sorted along the flow path. Debris-flow physics are highly complex and video recordings of events in progress have demonstrated that no unique rheology can describe the range of mechanical behaviours observed (Iverson, 1997). Flow velocities typically range from 1 to 10 m/s, although very large debris flows from volcanic edifices, often containing substantial fines, can travel at more than 20 m/s along much of their path (Major et al., 2005). The front of the rapidly advancing flow is steep and commonly followed by several secondary surges that form due to particle segregation and upwards or outwards migration of boulders. Hence, one of the distinguishing characteristics of coarse granular debris flows is vertical inverse grading, in which larger particles are concentrated at the top of the deposit. This characteristic behaviour leads to the formation of lateral levees along the channel that become part of the debris flow legacy. Similarly, depositional lobes are formed where frictional resistance from coarse-grained or large organic debris-rich fronts is high enough to slow and eventually stop the motion of the trailing liquefied debris. Debris-flow deposits remain saturated for some time after deposition, but become rigid once seepage and desiccation have removed pore water.

Typical debris flows require a channel gradient of at least 27% (15°) for transport over significant distances (Takahashi 1991) and have volumetric sediment concentrations in excess of 50%. Between the main surges a fluid slurry with a hyperconcentration (>10%) of suspended fines occurs. Transport is possible at gradients as low as 20% (11°), although some type of momentum transfer from side-slope landslides is needed to sustain flow on those slopes. Debris flows may continue to run out onto lower gradients even as they lose momentum and drain: the higher the fines content, and hence the slower the sediment-water mixture loses its water content, the lower the ultimate stopping angle. The silt-clay fraction is thus the most important textural control on debris-flow mobility. The surface gradient of a debris-flow fan approximates the stopping angle for flows issuing from the drainage basin.

Due to their high flow velocities, peak discharges are at least an order of magnitude larger than those of comparable return period floods. Further, the large caliber of transported sediment and wood means that debris flows are highly destructive along their channels and on fans.

Channel banks can be severely eroded during debris flows, although lateral erosion is often associated with the trailing hyperconcentrated flow phase that is characterized by lower volumetric sediment concentrations. The most severe damage results from direct impact of large clasts or coarse woody debris against structures that are not designed for the impact forces. Even where the supporting walls of buildings may be able to withstand the loads associated with debris flows, building windows and doors are crushed and debris may enter the building, leading to extensive damage to the interior of the structure (Jakob et al., 2012). Similarly, linear infrastructure such as roads and railways are subject to complete destruction. On fans, debris flows tend to

deposit their sediment rather than scour. Therefore, exposure or rupture of buried infrastructure such as telecommunication lines or pipelines is very rare. However, if a linear infrastructure is buried in a recent debris deposit, it is likely that over time or during a significant runoff event, the tractive forces of water will erode through the debris until an equilibrium slope is achieved, and the infrastructure thereby becomes exposed. This necessitates understanding the geomorphic state of the fans being traversed by a buried linear infrastructure.

Avulsions are likely in poorly confined channel sections, particularly on the outside of channel bends where debris flows tend to superelevate. Sudden loss of confinement and decrease in channel slope cause debris flows to decelerate, drain their inter-granular water, and increase shearing resistance, which slow the advancing bouldery flow front and block the channel. The more fluid afterflow (hyperconcentrated flow) is then often deflected by the slowing front, leading to secondary avulsions and the creation of distributary channels on the fan. Because debris flows often display surging behaviour, in which bouldery fronts alternate with hyperconcentrated afterflows, the cycle of coarse bouldery lobe and levee formation and afterflow deflection can be repeated several times during a single event. These flow aberrations and varying rheological characteristics pose a particular challenge to numerical modelers seeking to create an equivalent fluid (Iverson, 2014).

A.3. DEBRIS FLOODS AND HYPERCONCENTRATED FLOWS

A 'debris flood' is "a very rapid surging flow of water heavily charged with debris in a steep channel" (Hungre et al., 2014). Transitions from floods to debris floods occur at minimum volumetric sediment concentrations of 3 to 10%, the exact value depending on the particle size distribution of the entrained sediment and the ability to acquire yield strength². Because debris floods are characterized by heavy bedload transport, rather than by a more homogenous mixture of suspended sediments typical of hyperconcentrated flows (Pierson, 2005), the exact definition of sediment concentration depends on how sediment is transported in the water column. Debris floods typically occur on creeks with channel gradients between 5 and 30% (3-17°).

The term "debris flood" is similar to the term "hyperconcentrated flow", defined by Pierson (2005) on the basis of sediment concentration as "a type of two-phase, non-Newtonian flow of sediment and water that operates between normal streamflow (water flow) and debris flow (or mudflow)". Debris floods (as defined by Hungre et al., 2014) have lower sediment concentrations than hyperconcentrated flows (as defined by Pierson). Thus, there is a continuum of geomorphic events that progress from floods to debris floods to hyperconcentrated flows to debris flows, as volumetric sediment concentrations increase. Some creeks are hybrids, which implies that the dominant process oscillates between debris floods and debris flows.

Due to their initially relatively low sediment concentration, debris floods are more erosive along channel banks and beds than debris flows; the latter can reach a sediment saturation point

² The yield strength is the internal resistance of the sediment mixture to shear stress deformation; it is the result of friction between grains and cohesion (Pierson 2005).

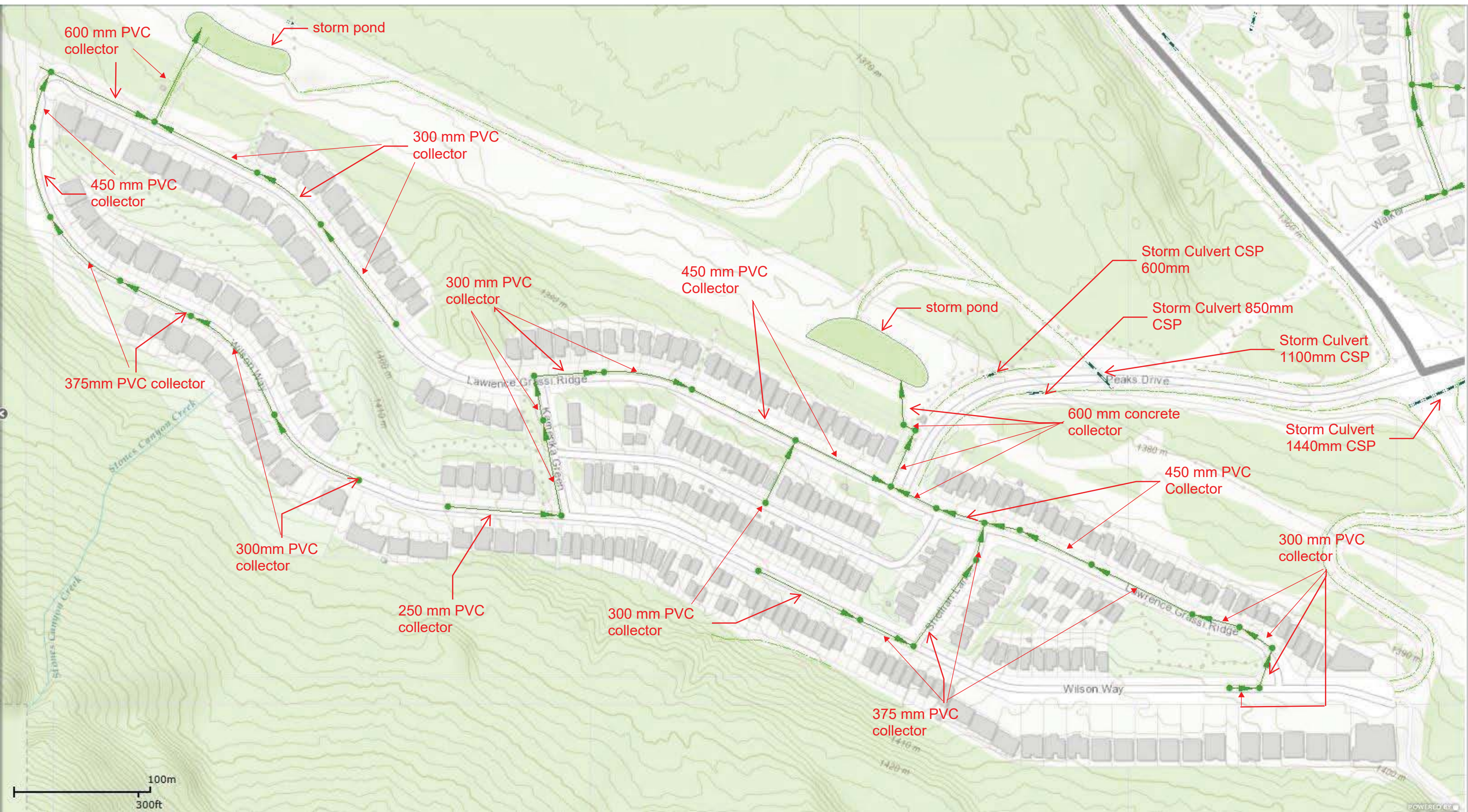
whereby bank or bed erosion is significantly reduced. Bank erosion and excessive amounts of bedload introduce large amounts of sediment to the fan where they accumulate (aggrade) in channel sections with decreased slope. In fact, debris floods can be initiated on the fan itself through rapid bed erosion and entrainment of bank materials. Because typical long-duration storm hydrographs fluctuate several times over the course of the storm, several cycles of aggradation and remobilization of deposited sediments on channel and fan reaches can be expected during the same event (Jakob et al., 2016).

Debris floods can be triggered by a variety of processes. One trigger is transition from a debris flow when lower stream channel gradients are encountered. Another trigger is exceedance of a critical shear stress threshold of the channel bed and full bed mobilization (Church, 2013). More uncommon triggers are landslide dam, beaver dam or glacial lake outburst floods as well as the failure of man-made dams (Jakob and Jordan, 2001; Jakob et al., 2016).

REFERENCES

- Church M. 2010. Mountains and montane channels. Chapter 2 in Burt, T., Allison, R., editors, *Sediment Cascades*. Oxford, Wiley-Blackwell: 17-53.
- Church M. 2013. Steep headwater channels. Chapter 9.28 in Shroder, J.F. (eds.) *Treatise on Geomorphology*, vol. 9, Wohl, E. (ed.), *Fluvial Geomorphology*. San Diego, Academic Press: 528-549.
- Hungr O, Leroueil S, and Picarelli L. 2014. The Varnes classification of landslide types, an update. *Landslides* **11**: 167-194.
- Iverson RM. 1997. The physics of debris flows. *Reviews of Geophysics* **35**(3): 245-296.
- Iverson RM. 2014. Debris flows: behaviour and hazard assessment. *Geology Today* **30**(1): 15-20.
- Jakob M, Clague J and Church M. 2016. Rare and dangerous: recognizing extra-ordinary events in stream channels. *Canadian Water Resources Journal*. doi:10.1080/07011784.2015.1028451
- Jakob M, Stein D, and Ulmi M. 2012. Vulnerability of buildings to debris flow impact. *Natural Hazards* **60**(2): 241-261.
- Jakob M and Jordan P. 2001. Design floods in mountain streams – the need for a geomorphic approach. *Canadian Journal of Civil Engineering* **28**(3): 425-439.
- Major J, Pierson T, and Scott K. 2005. Debris flows at Mount St. Helens, Washington, USA. *In: Debris-flow Hazards and Related Phenomena*. Edited by M. Jakob, O. Hungr. Springer, Berlin Heidelberg, pp. 685-731.
- Pierson TC. 2005. Distinguishing between debris flows and floods from field evidence in small watersheds. Fact Sheet 2004-3142. U.S. Geological Survey.
- Takahashi T. 1991. *Debris Flows*. Rotterdam, Balkema.

APPENDIX B - PEAKS OF GRASSI STORMWATER DRAINAGE SYSTEM



600 mm PVC collector

storm pond

300 mm PVC collector

450 mm PVC collector

450 mm PVC Collector

Storm Culvert CSP 600mm

Storm Culvert 850mm CSP

Storm Culvert 1100mm CSP

300 mm PVC collector

storm pond

600 mm concrete collector

Storm Culvert 1440mm CSP

375mm PVC collector

Lawrence Grassi Ridge

450 mm PVC Collector

300 mm PVC collector

300mm PVC collector

250 mm PVC collector

300 mm PVC collector

375 mm PVC collector

Wilson Way

100m
300ft

POWERED BY

APPENDIX C - TEST PIT DETAILED LOGS AND PHOTOGRAPH LOGS

Project: X Y and Z Creeks Steep Creek Hazard and Risk Assessment

Location : Canmore, AB

Project No. : 1261025

Survey Method : GPS
Coordinates : 11U 614754mE 5658511mN
Ground Elevation (m) 1421
Datum : NAD83

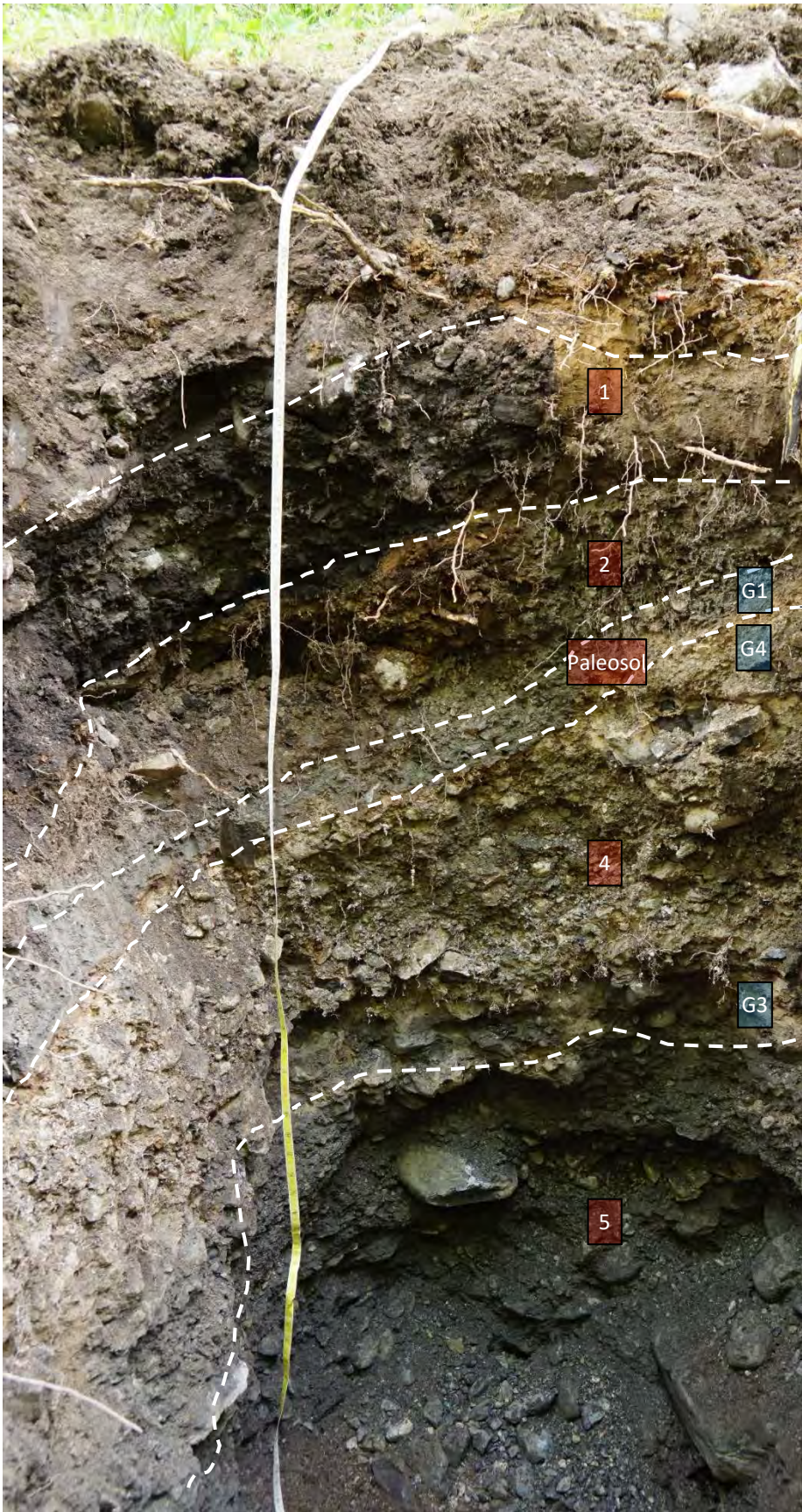
Start Date : 11 Jun 18
Finish Date: 11 Jun 18
Final Depth of Pit (m) : 2.0
Logged by : MJ
Reviewed by : N/A

Depth (m)	Symbol	Sample Material for Dating	Sample Age	Lithologic Description
0				Duff layer removed
				UNIT 1: DEBRIS FLOW DEPOSIT Matrix supported debris flow diamicton, angular to subangular.
				Oxidized, silty sand UNIT 2: DEBRIS FLOW DEPOSIT
1		G1 Sent for tephra testing, no glass (1.0 m)	No date	PALEOSOL Light grey, sandy silt
		G4 Organic Sediment (1.1 m)	9187 BP	BURN Oxidized soil UNIT 4: Matrix supported, Dmax = 0.4 m, sandy gravels.
		G3 Organic Sediment (1.6 m)	38470 BP	UNIT 5: DEBRIS FLOW DEPOSIT Matrix supported debris flow diamicton.
2				END OF TEST PIT AT 2.0 m
3				
4				
5				

CANMORE (STRAT_CO) CANMORE.GDL BGC.GDT 8/9/18

TP-BGC18-X-01

- 1 Unit Location Marker
- G1 Grab Sample Marker



0 mbgs

0.5

Oxidized soil layer

1.0

Oxidized soil layer

1.5

2.0

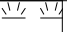



Project: X Y and Z Creeks Steep Creek Hazard and Risk Assessment

Location : Canmore, AB

Project No. : 1261025

Survey Method : GPS
Coordinates : 11U 614891mE 5658497mN
Ground Elevation (m) 1424
Datum : NAD83

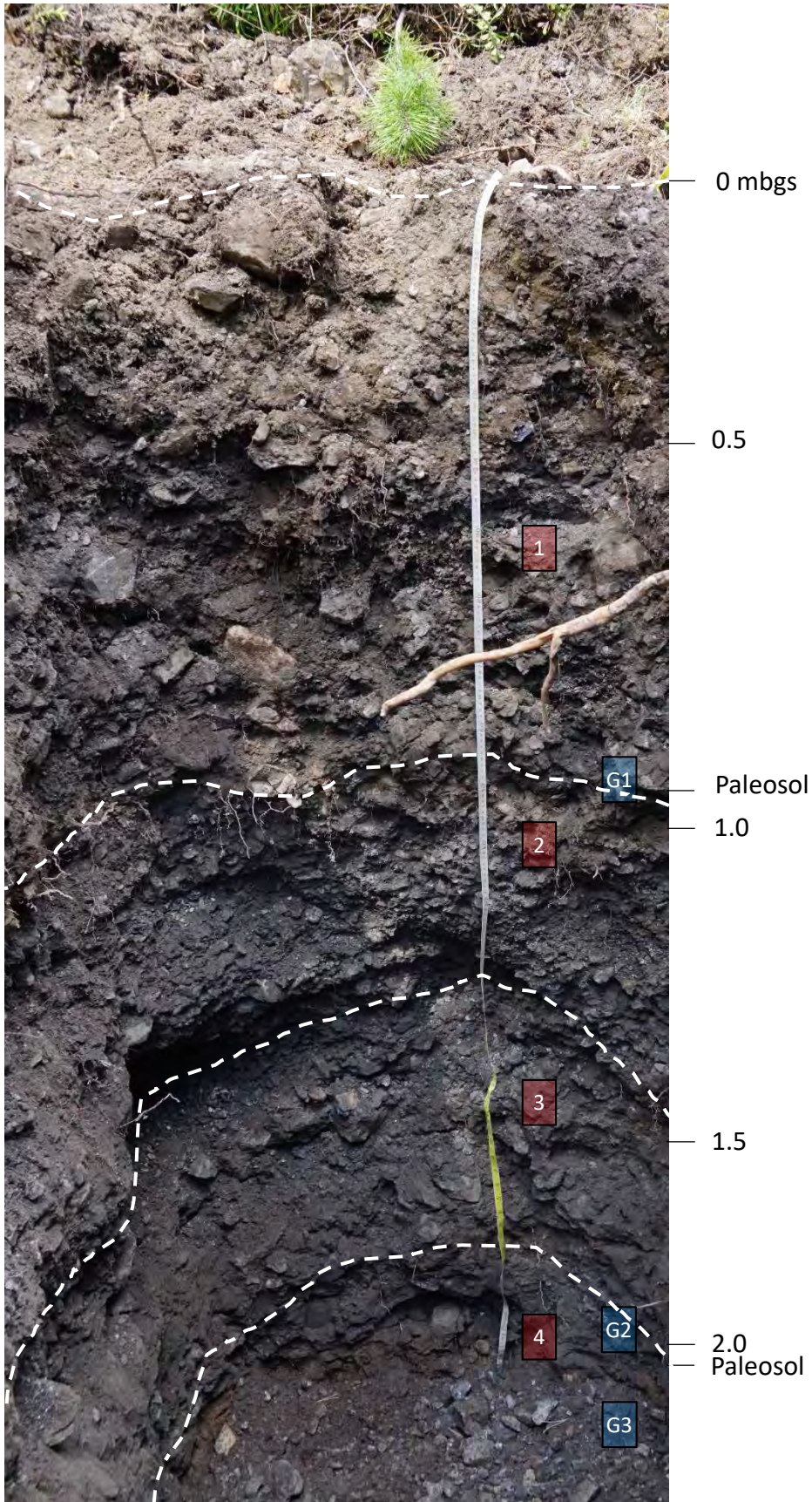
Start Date : 11 Jun 18
Finish Date: 11 Jun 18
Final Depth of Pit (m) : 2.3
Logged by : MJ
Reviewed by : N/A

Depth (m)	Symbol	Sample Material for Dating	Sample Age	Lithologic Description
0				Duff layer removed
0.9		G1 Sent for tephra testing, no glass (0.9 m)	No date	UNIT 1: DEBRIS FLOW DEPOSIT Undifferentiated matrix support debris flow diamicton, Dmax = 90 x 50 x 30 cm, D50 = 10 cm. Discontinuous fine sand lense at 0.4 m depth, < 10 cm thick.
1.0				PALEOSOL Light grey silt, continuous around entire pit, 2 to 4 cm thick, sharp upper contact, diffuse lower contact.
1.5				UNIT 2: DEBRIS FLOW DEPOSIT Matrix supported, non-cohesive debris flow layer, Dmax = 30 cm, D50 = 5 cm, diffuse lower layer.
2.0		G2 Wood (2.0 m) G3 Paleosol (2.0 m)	144 BP 6441 BP	UNIT 3: DEBRIS FLOW DEPOSIT Debris flow diamicton, lightly cohesive, Dmax = 25 cm, D50 = 5 cm.
2.2				PALEOSOL 2 to 5 cm thick COLLUVIUM END OF TEST PIT AT 2.2 m
3				
4				
5				

CANMORE (STRAT_CO) CANMORE.GDL BGC.GDT 8/9/18

TP-BGC18-X-02

- 1 Unit Location Marker
- G1 Grab Sample Marker



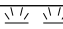




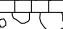
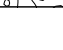
Project: X Y and Z Creeks Steep Creek Hazard and Risk Assessment

Location : Canmore, AB

Project No. : 1261025

Survey Method : GPS
Coordinates : 11U 614911mE 5658460mN
Ground Elevation (m) 1428
Datum : NAD83

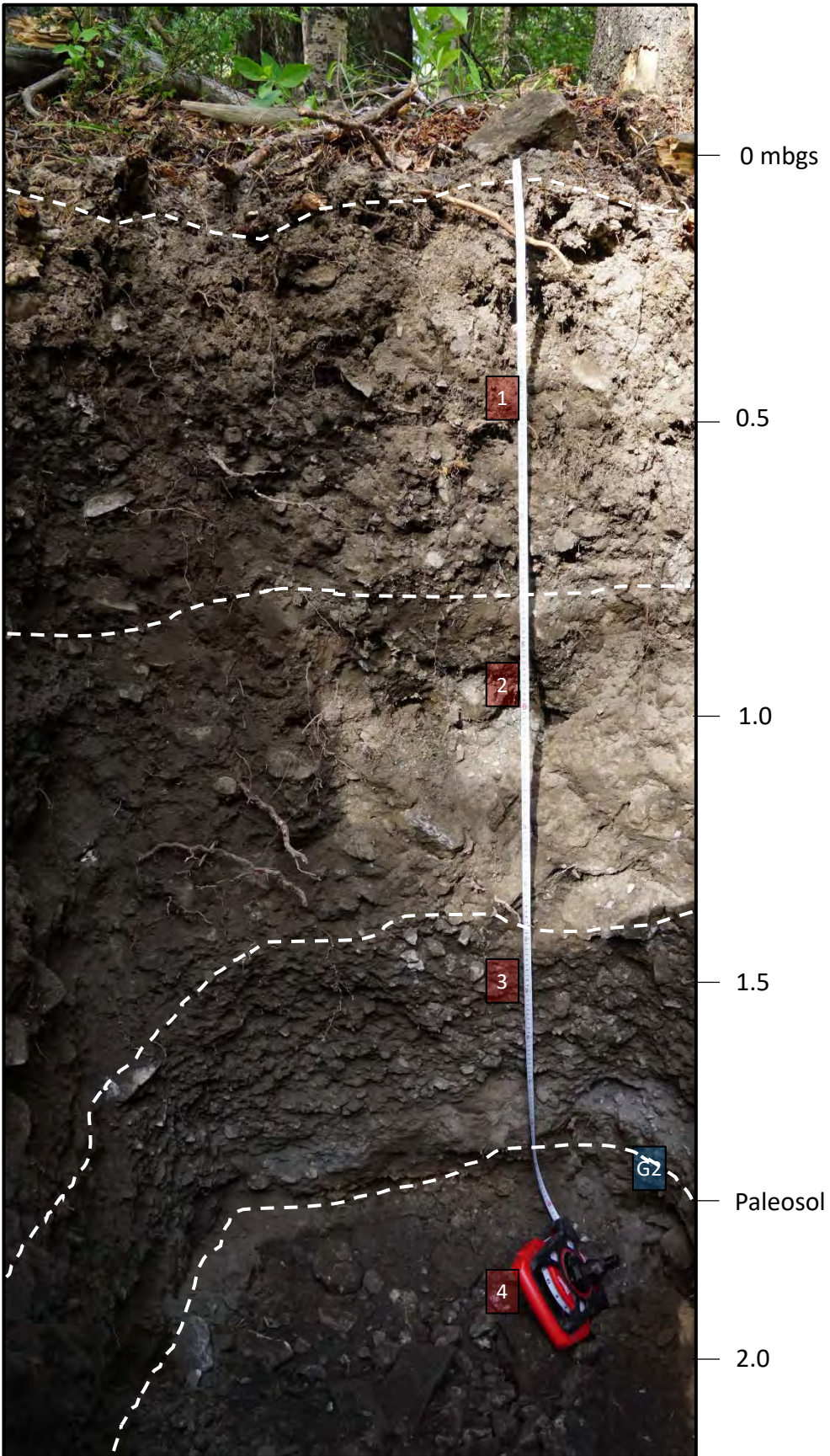
Start Date : 11 Jun 18
Finish Date: 11 Jun 18
Final Depth of Pit (m) : 2.1
Logged by : MJ
Reviewed by : N/A

Depth (m)	Symbol	Sample Material for Dating	Sample Age	Lithologic Description
0				Duff layer removed
				UNIT 1: DEBRIS FLOW DEPOSIT Angular debris, matrix supported, debris flow diamicton, Dmax = 100 x 50 x 40 cm, D50 = 5 cm.
1				SAND Discontinuous sand layer, fine wet sand.
				UNIT 2: DEBRIS FLOW DEPOSIT Debris flow diamicton, Dmax = 15 cm, D50 = 3 cm.
				UNIT 3: DEBRIS FLOW DEPOSIT Debris flow diamicton, poorly defined contact between Unit 2 and Unit 3, slight change in cohesion, Dmax = 15 cm, D50 = 3 cm, sharp lower contact.
2		G2 Charcoal (1.9 m)	5132 BP	PALEOSOL Sharp upper and lower contacts
				UNIT 4: DEBRIS FLOW DEPOSIT Debris flow diamicton.
				END OF TEST PIT AT 2.1 m
3				
4				
5				

CANMORE (STRAT_CO) CANMORE.GDL BGC.GDT 8/9/18

TP-BGC18-X-03

- 1 Unit Location Marker
- G1 Grab Sample Marker



Project: X Y and Z Creeks Steep Creek Hazard and Risk Assessment

Location : Canmore, AB

Project No. : 1261025

Survey Method : GPS
Coordinates : 11U 615110mE 5658255mN
Ground Elevation (m) 1435
Datum : NAD83

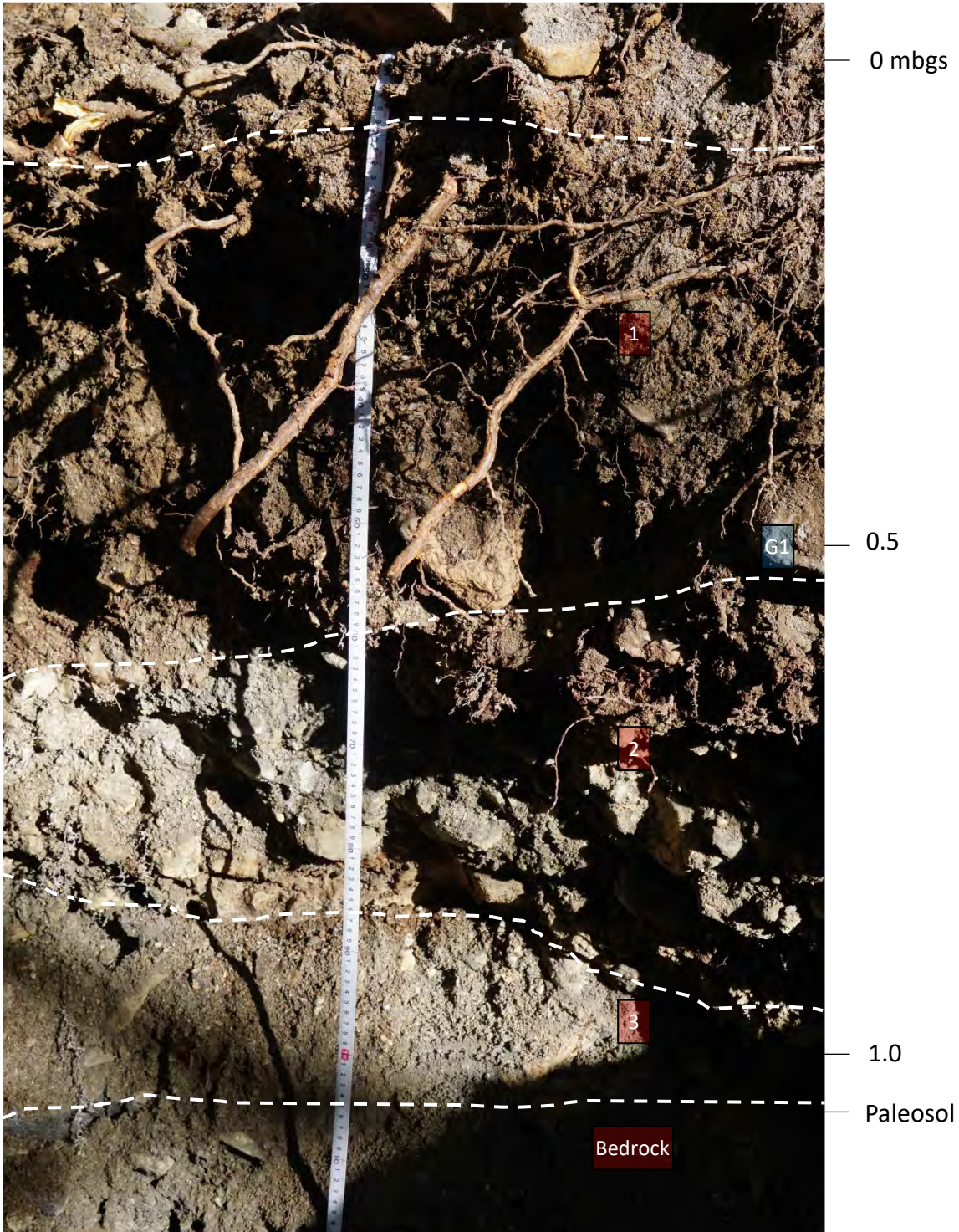
Start Date : 11 Jun 18
Finish Date: 11 Jun 18
Final Depth of Pit (m) : 1.5
Logged by : MJ
Reviewed by : N/A

Depth (m)	Symbol	Sample Material for Dating	Sample Age	Lithologic Description
0				Duff layer removed
				UNIT 1: DEBRIS FLOW DEPOSIT Debris flow diamicton, dark brown, moist, Dmax = 20 cm, D50 = 3 cm, well defined lower contact.
		G1 Organic Sediment (0.5 m)	428 BP	UNIT 2: DEBRIS FLOW DEPOSIT Light grey, subrounded to subangular, debris flow to debris flood, Dmax = 1 cm, D50 = 1 cm.
1				GRAVEL Peak gravel contact
				UNIT 3: DEBRIS FLOW DEPOSIT Debris flow diamicton, partially cemented above bedrock contact.
				BEDROCK Shale bedrock
				END OF TEST PIT AT 1.5 m
2				
3				
4				
5				

CANMORE (STRAT_CO) CANMORE.GDL BGC.GDT 8/9/18

TP-BGC18-X-04

- 1 Unit Location Marker
- G1 Grab Sample Marker



Project: X Y and Z Creeks Steep Creek Hazard and Risk Assessment

Location : Canmore, AB

Project No. : 1261025

Survey Method : GPS
Coordinates : 11U 614130mE 5658571mN
Ground Elevation (m) 1457
Datum : NAD83

Start Date : 12 Jun 18
Finish Date: 12 Jun 18
Final Depth of Pit (m) : 2.7
Logged by : MJ
Reviewed by : N/A

Depth (m)	Symbol	Sample Material for Dating	Sample Age	Lithologic Description
0				Duff layer removed
				UNIT 1: DEBRIS FLOW DEPOSIT Debris flow diamicton, brown B-horizon with apparent cohesion, Dmax = 40 cm, D50 = 5 cm.
1		G1 Organic Sediment (0.9 m)	2037 BP	PALEOSOL Well developed paleosol UNIT 2: DEBRIS FLOW DEPOSIT Debris flow diamicton, well drained, cohesionless, Dmax = 20 cm, D50 = 1 cm.
				GRAVEL Peagravel within Unit 2
2		G2 Charcoal (1.8 m)	2805 BP	UNIT 2: DEBRIS FLOW DEPOSIT Debris flow diamicton, well drained, cohesionless, Dmax = 20 cm, D50 = 1 cm. PALEOSOL Organic rich soil UNIT 3: DEBRIS FLOW DEPOSIT
3				END OF TEST PIT AT 2.7 m
4				
5				

CANMORE (STRAT_COI) CANMORE.GDL BGC.GDT 8/9/18

TP-BGC18-Y-01

1

Unit Location Marker

G1

Grab Sample Marker

0 mbgs

0.5

1

Paleosol
1.0

G1

2

1.5

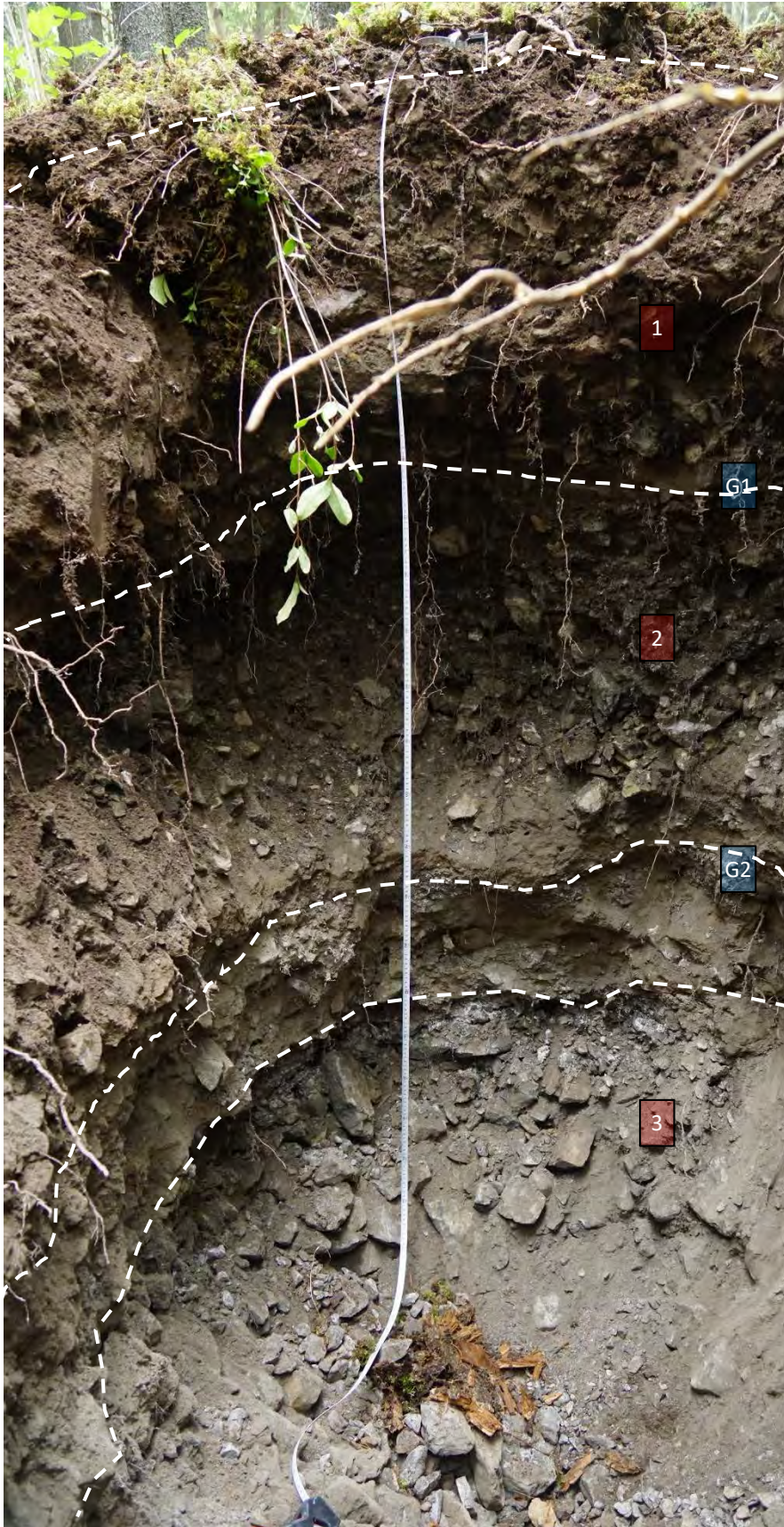
Paleosol

G2

2.0

3

2.5



Project: X Y and Z Creeks Steep Creek Hazard and Risk Assessment

Location : Canmore, AB

Project No. : 1261025

Survey Method : GPS
Coordinates : 11U 614071mE 5658573mN
Ground Elevation (m) 1459
Datum : NAD83

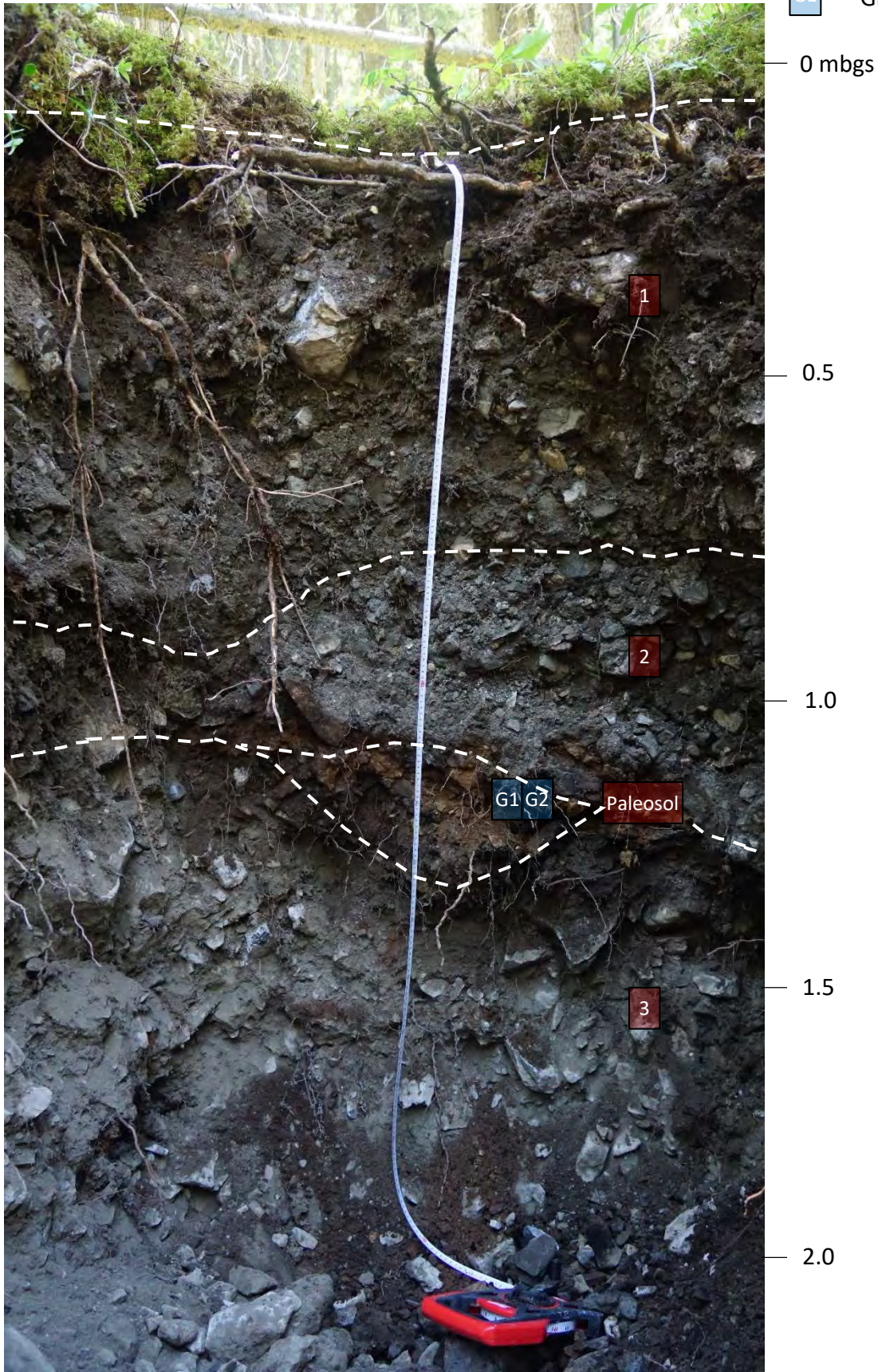
Start Date : 12 Jun 18
Finish Date: 12 Jun 18
Final Depth of Pit (m) : 2.1
Logged by : MJ
Reviewed by : N/A

Depth (m)	Symbol	Sample Material for Dating	Sample Age	Lithologic Description
0				Duff layer removed
0 - 1				UNIT 1: DEBRIS FLOW DEPOSIT Light grey, matrix supported, debris flow diamicton, Dmax = 50 cm, D50 = 5 cm, diffuse lower contact.
1 - 1.2				UNIT 2: DEBRIS FLOW DEPOSIT Upper diffuse contact with less apparent cohesion, lower contact well defined, Dmax = 15 cm, D50 = 2 cm.
1.2 - 1.2		G1 Tephra (1.2 m)	7700 BP	PALEOSOL Ocre coloured lens of possible tephra with organic inclusions.
1.2 - 1.2		G2 Charcoal (1.2 m)	883 BP	UNIT 3: DEBRIS FLOW DEPOSIT Debris flow diamicton, dry, light grey, Dmax = 25 cm, D50 = 5 cm.
2.1				END OF TEST PIT AT 2.1 m
3				
4				
5				

CANMORE (STRAT_CO) CANMORE.GDL BGC.GDT 8/9/18

TP-BGC18-Y-02

- 1 Unit Location Marker
- G1 Grab Sample Marker



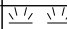


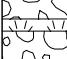


Project: X Y and Z Creeks Steep Creek Hazard and Risk Assessment

Location : Canmore, AB

Project No. : 1261025

Survey Method : GPS
Coordinates : 11U 614032mE 5658582mN
Ground Elevation (m) 1455
Datum : NAD83

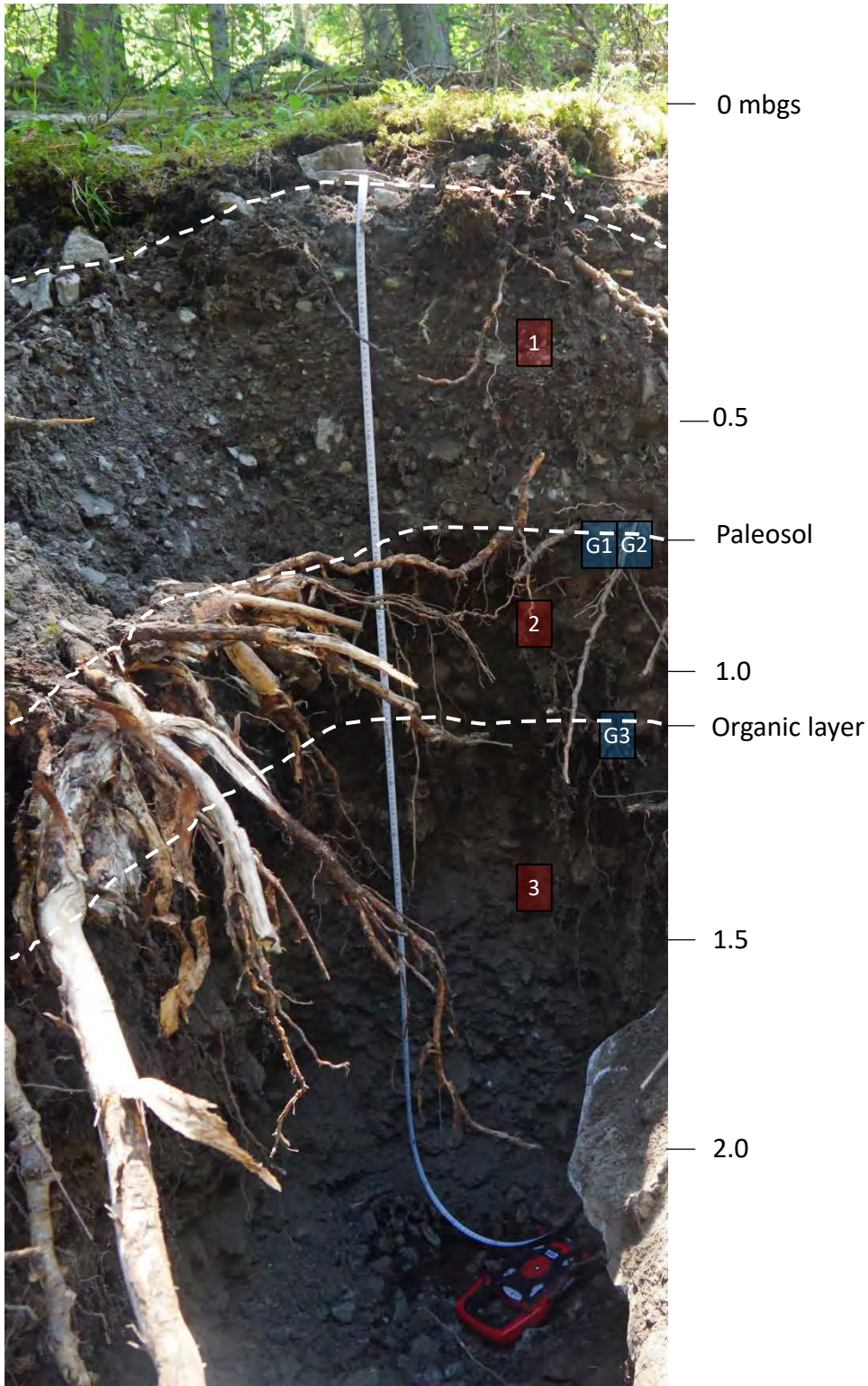
Start Date : 12 Jun 18
Finish Date: 12 Jun 18
Final Depth of Pit (m) : 2.3
Logged by : MJ
Reviewed by : N/A

Depth (m)	Symbol	Sample Material for Dating	Sample Age	Lithologic Description
0				Duff layer removed
				UNIT 1: DEBRIS FLOW DEPOSIT Matrix supported, debris flow diamicton, Dmax = 20 cm, D50 = 1 cm.
1				PALEOSOL Organic inclusions
		G3 Plant Material (1.1 m)	Modern	UNIT 2: DEBRIS FLOW DEPOSIT Dmax = 20 cm, D50 = 2 cm
				ORGANIC HORIZON Black, organic rich, continuous layer
				UNIT 3: DEBRIS FLOW DEPOSIT Undifferentiated debris flow diamicton, grey, dry, non-cohesive, D50 = 5 cm. Very large boulder, 1.0 x 0.5 x ? M at 1.8 m depth.
2				END OF TEST PIT AT 2.3 m
3				
4				
5				

CANMORE (STRAT_CO) CANMORE.GDL BGC.GDT 8/9/18

TP-BGC18-Y-03

- 1 Unit Location Marker
- G1 Grab Sample Marker



Project: X Y and Z Creeks Steep Creek Hazard and Risk Assessment

Location : Canmore, AB

Project No. : 1261025

Survey Method : GPS
Coordinates : 11U 613973mE 5658631mN
Ground Elevation (m) 1446
Datum : NAD83

Start Date : 12 Jun 18
Finish Date: 12 Jun 18
Final Depth of Pit (m) : 2.3
Logged by : MJ
Reviewed by : N/A

Depth (m)	Symbol	Sample Material for Dating	Sample Age	Lithologic Description
0				Duff layer removed
				UNIT 1: DEBRIS FLOW DEPOSIT Debris flow diamicton, matrix supported, apparent cohesion, silty, gravels, Dmax = 30 cm, D50 = 3 cm
1		G1 Wood (0.9 m)	230 BP	PALEOSOL Discontinuous layer of organics, light grey, horizontally bedded sand
				UNIT 2: Light grey, low apparent cohesion, gravel in sandy matrix, Dmax = 10 cm, D50 = 1 cm
				ORGANIC HORIZON Organic rich horizon
				UNIT 3: DEBRIS FLOW DEPOSIT Debris flow diamicton, brown, matrix supported, apparent cohesion, silty gravels, Dmax = 30 cm, D50 = 3 cm
2		G3 Charcoal (1.8 m)	798 BP	ORGANIC HORIZON 1 cm thick black organic horizon
				SAND Stratified light grey sand with interbedded organics
				UNIT 4: Light grey, low apparent cohesion, gravel in sandy matrix, Dmax = 10 cm, D50 = 1 cm
				END OF TEST PIT AT 2.3 m
3				
4				
5				

CANMORE (STRAT_CO) CANMORE.GDL BGC.GDT 8/9/18

TP-BGC18-Y-04

1

Unit Location Marker

G1

Grab Sample Marker

0 mbgs

0.5

1

Paleosol

G1

1.0

2

Organic

1.5

3

Paleosol

G3

2.0

4



Project: X Y and Z Creeks Steep Creek Hazard and Risk Assessment

Location : Canmore, AB

Project No. : 1261025

Survey Method : GPS
Coordinates : 11U 613972mE 5658671mN
Ground Elevation (m) 1449
Datum : NAD83

Start Date : 12 Jun 18
Finish Date: 12 Jun 18
Final Depth of Pit (m) : 2.0
Logged by : MJ
Reviewed by : N/A

Depth (m)	Symbol	Sample Material for Dating	Sample Age	Lithologic Description
0				Duff layer removed
0 - 0.6				UNIT 1: DEBRIS FLOW DEPOSIT Matrix supported, slight cohesion, moist, Dmax = 20 cm, D50 = 1 cm
0.6 - 1.0				UNIT 2: DEBRIS FLOW DEPOSIT Matrix supported, low cohesion, Dmax = 6 cm, D50 = 1 cm
1.0 - 1.1				SAND Fine sand layer, abrupt upper and lower contact
1.1 - 1.2				ORGANIC HORIZON 1 to 2 cm thick organic layer
1.2 - 1.8				UNIT 3: DEBRIS FLOW DEPOSIT Debris flow diamicton, very low cohesion, Dmax = 20 cm, D50 = 2 cm
1.8 - 2.0		G2 Organic Sediment (1.8 m)	1938 BP	ORGANIC HORIZON 1 cm thick organic horizon
2.0 - 2.0				UNIT 4: HYPERCONCENTRATED FLOW DEPOSIT Hyperconcentrated flow, no apparent cohesion, Dmax = 3 cm, D50 = 1 cm END OF TEST PIT AT 2.0 m
3				
4				
5				

CANMORE (STRAT_CO) CANMORE.GDL BGC.GDT 8/9/18

TP-BGC18-Z-01



Unit Location Marker



Grab Sample Marker

0 mbgs

0.5

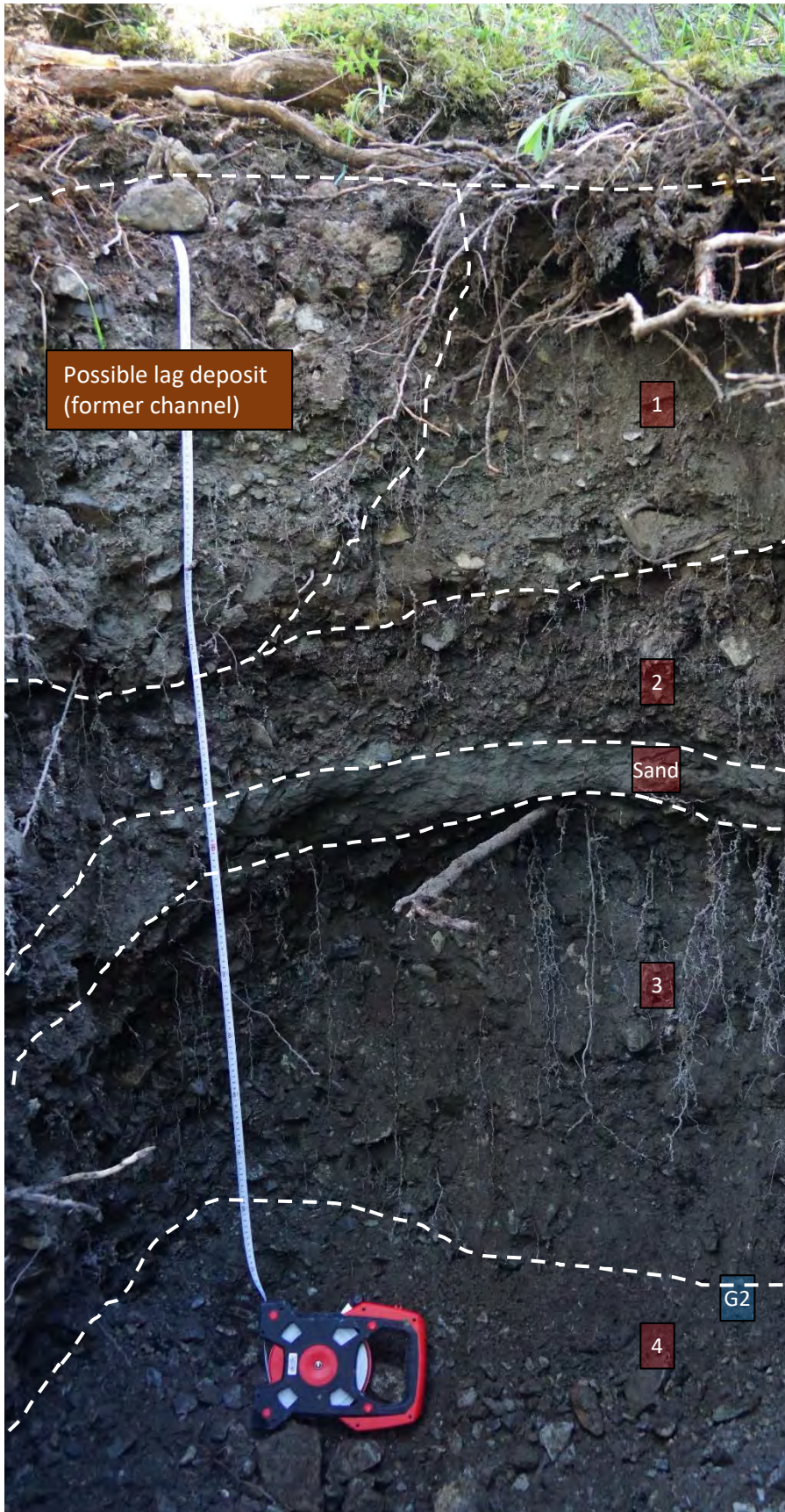
1.0

Paleosol

1.5

Paleosol

2.0



Possible lag deposit
(former channel)

1

2

Sand

3

4

G2



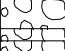

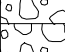

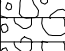


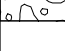

Project: X Y and Z Creeks Steep Creek Hazard and Risk Assessment

Location : Canmore, AB

Project No. : 1261025

Survey Method : GPS
Coordinates : 11U 613932mE 5658715mN
Ground Elevation (m) 1447
Datum : NAD83

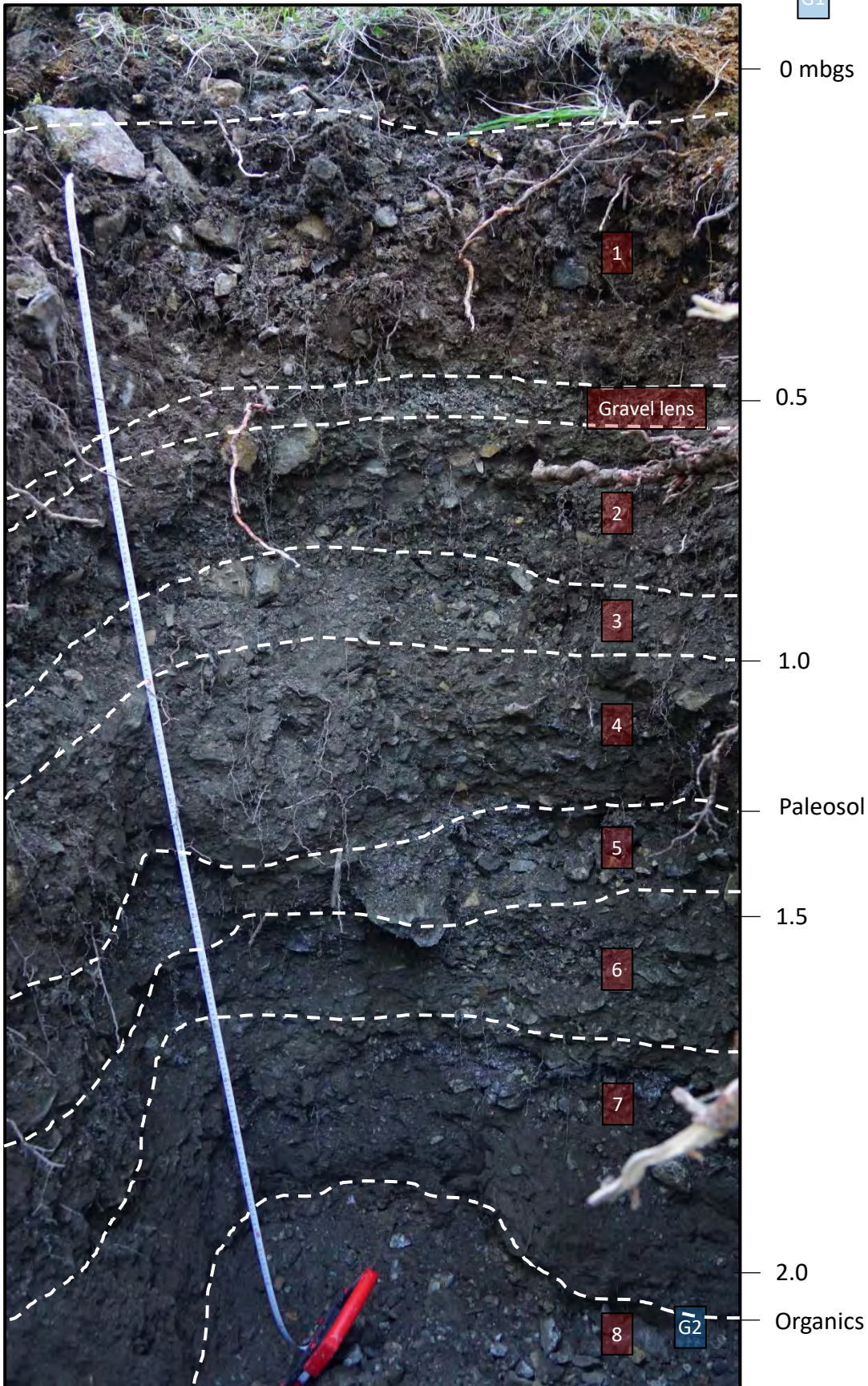
Start Date : 12 Jun 18
Finish Date: 12 Jun 18
Final Depth of Pit (m) : 2.3
Logged by : MJ
Reviewed by : N/A

Depth (m)	Symbol	Sample Material for Dating	Sample Age	Lithologic Description
0				Duff layer removed
				UNIT 1: DEBRIS FLOW DEPOSIT Dmax = 20 cm, D50 = 1 cm
				GRAVEL Cohesionless pea-gravel
				UNIT 2: DEBRIS FLOW DEPOSIT Dmax = 10 cm, D50 = 1 cm
				UNIT 3: GRAVEL Pea-gravel, Dmax = 2 cm, D50 < 1 cm
				UNIT 4: DEBRIS FLOW DEPOSIT Dmax = 10 cm, D50 = 1 cm
				ORGANIC HORIZON 1 to 2 cm thick organic horizon
				UNIT 5: GRAVEL Pea-gravel, Dmax = 2 cm, D50 < 1 cm
				UNIT 6: DEBRIS FLOW DEPOSIT Dmax = 10 cm, D50 = 1 cm
		G2 Charcoal (2.3 m)	3059 BP	UNIT 7/8: GRAVEL Interbedded gravls and pea-gravels
				UNIT 9: GRAVEL Pea-gravel with organic horizon
				END OF TEST PIT 2.3 m
3				
4				
5				

CANMORE (STRAT_CO) CANMORE.GDL BGC.GDT 8/9/18

TP-BGC18-Z-02

- 1 Unit Location Marker
- G1 Grab Sample Marker



Project: X Y and Z Creeks Steep Creek Hazard and Risk Assessment

Location : Canmore, AB

Project No. : 1261025

Survey Method : GPS
Coordinates : 11U 613891mE 5658793mN
Ground Elevation (m) 1436
Datum : NAD83

Start Date : 13 Jun 18
Finish Date: 13 Jun 18
Final Depth of Pit (m) : 2.3
Logged by : MJ
Reviewed by : N/A

Depth (m)	Symbol	Sample Material for Dating	Sample Age	Lithologic Description
0				Duff layer removed
				UNIT 1: DEBRIS FLOW DEPOSIT Debris flow diamicton, matrix supported, dark grey and brown, Dmax = 40 cm, D50 = 1 cm
				UNIT 2: GRAVEL Low cohesion, pea-gravel, light grey, Dmax = 2 cm, D50 = 0.5 cm
				PALEOSOL Well developed paleosol, dark brown with organic inclusions, some cobbles
1				UNIT 3: DEBRIS FLOW DEPOSIT Low cohesion, fines starved, clast supported matrix, Dmax = 25 cm, D50 = 1 cm
				UNIT 4: DEBRIS FLOW DEPOSIT Massive debris flow deposit, light grey, matrix supported, lower boundary diffuse
2				UNIT 5: DEBRIS FLOW DEPOSIT Upper boundary diffuse, lower boundary sharp
		G2 Charcoal (2.3 m)	8680 BP	PALEOSOL Light orange paleosol
				END OF TEST 2.3 m
3				
4				
5				

CANMORE (STRAT_CO) CANMORE.GDL BGC.GDT 8/9/18

TP-BGC18-Z-03

1

Unit Location Marker

G1

Grab Sample Marker

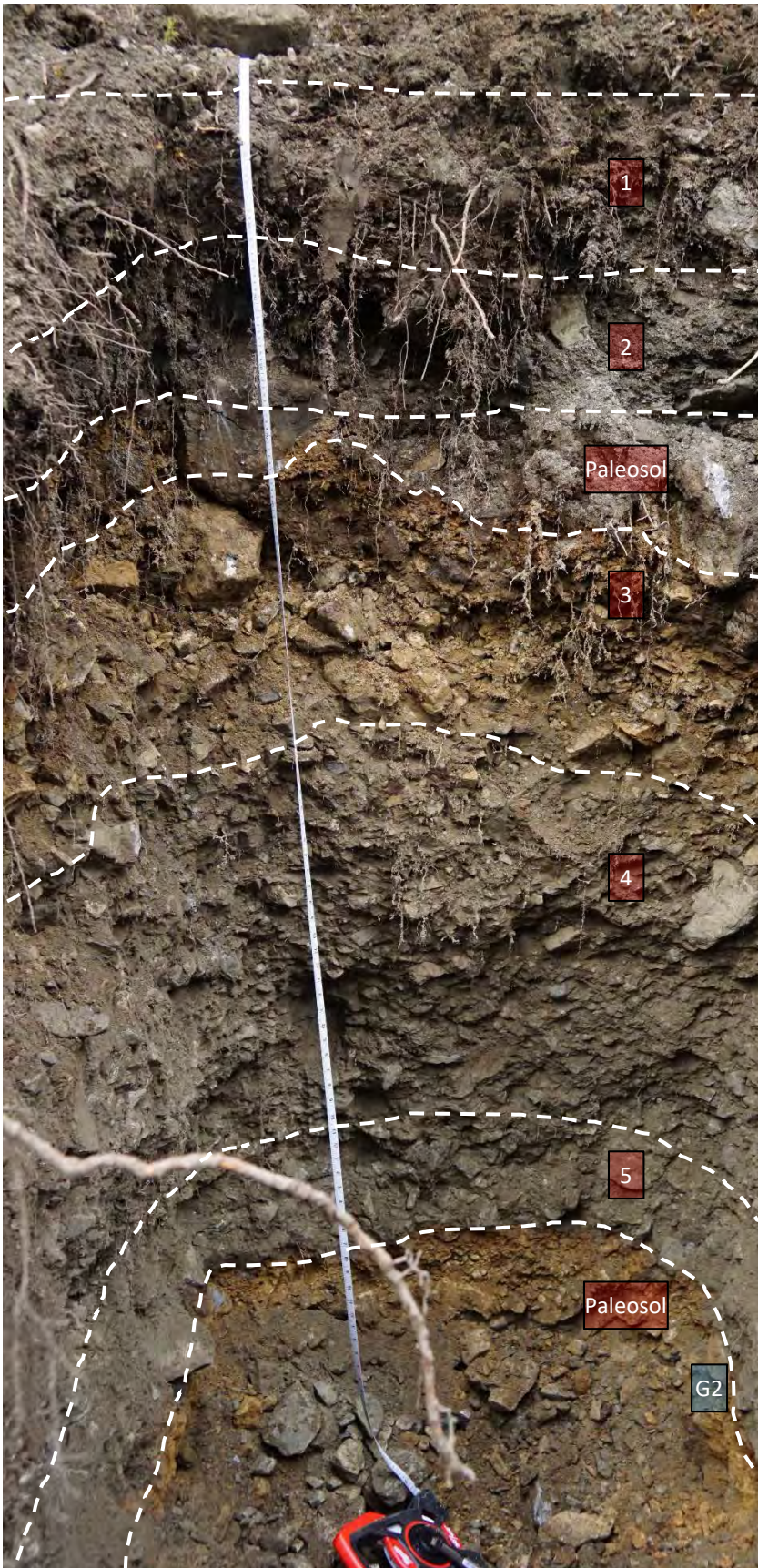
0 mbgs

0.5

1.0

1.5

2.0



1

2

Paleosol

3

4

5

Paleosol

G2

Project: X Y and Z Creeks Steep Creek Hazard and Risk Assessment

Location : Canmore, AB

Project No. : 1261025

Survey Method : GPS
Coordinates : 11U 613831mE 5658859mN
Ground Elevation (m) 1428
Datum : NAD83

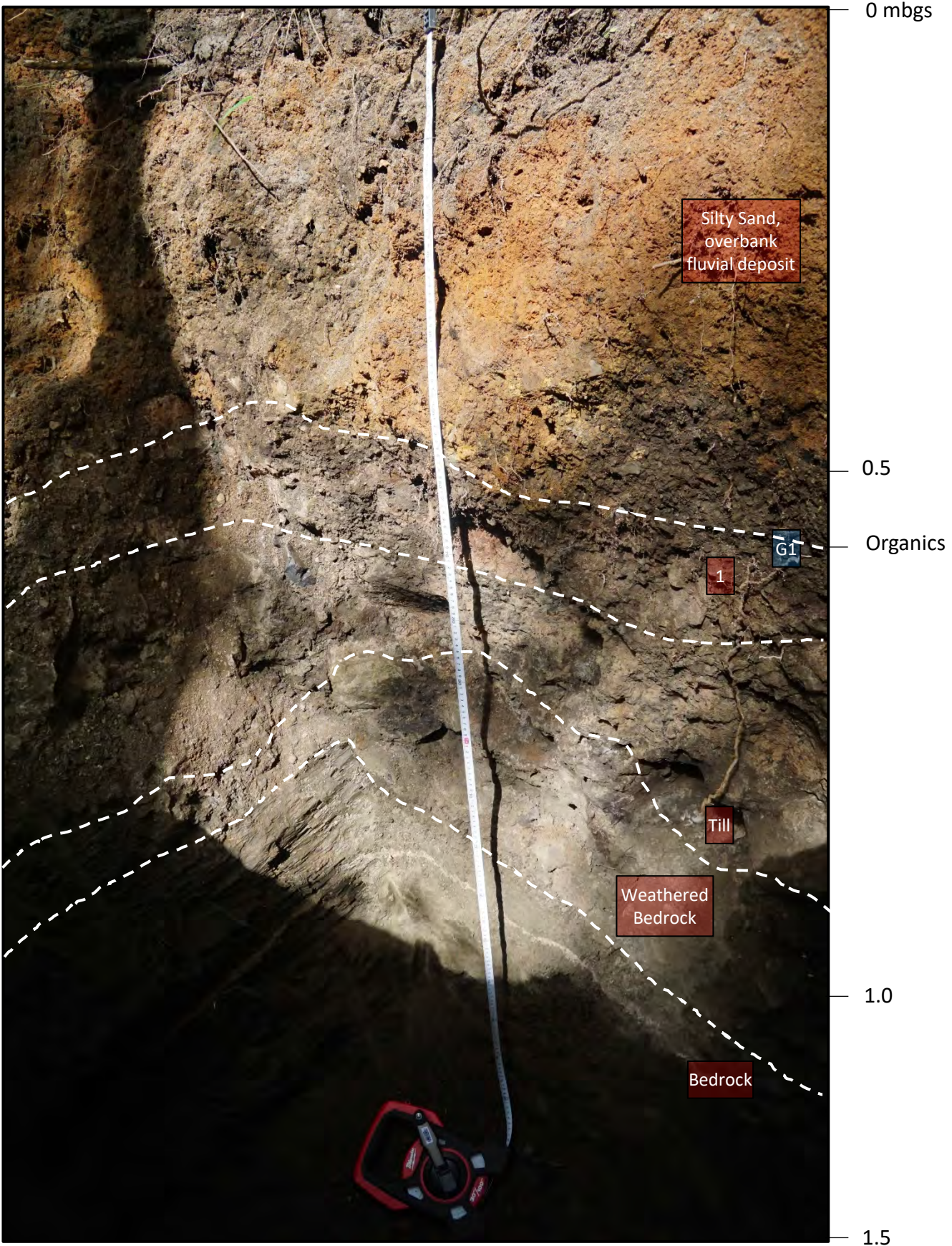
Start Date : 13 Jun 18
Finish Date: 13 Jun 18
Final Depth of Pit (m) : 2.0
Logged by : MJ
Reviewed by : N/A

Depth (m)	Symbol	Sample Material for Dating	Sample Age	Lithologic Description
0				Duff layer removed
				SAND Orange to light brown, mottled B-horizon with charcoal inclusions, moist silty sand
		G1 Organic Sediment (0.55 m)	12113 BP	ORGANIC HORIZON Horizon with some organics
1				UNIT 1: HYPERCONCENTRATED FLOW DEPOSIT Hyperconcentrated flow, dark grey, moist subrounded to subangular, Dmax = 1 cm, D50 = 0.2 cm
				TILL DEPOSIT Till deposit, subrounded to subangular clasts, very dense, matrix supported, sharp lower contact, Dmax = 50 cm, D50 = 5 cm
				BEDROCK Highly friable shale, almost vertical bedding, contact dipping towards NE
				PALEOSOL? 1 cm thick light grey unit, origin unknown
2				BEDROCK Highly friable shale, almost vertical bedding
3				
4				
5				

CANMORE (STRAT_CO) CANMORE.GDL BGC.GDT 8/9/18

TP-BGC18-Z-04

- 1 Unit Location Marker
- G1 Grab Sample Marker



APPENDIX D - RADIOCARBON SAMPLE RESULTS

Table D-1. Summary of samples sent for laboratory testing.

Field Sample ID	Sample Type	Laboratory	Analysis	Beta ID	Unit	Sample Depth (mbgs)	Conventional Age (year)
TP-BGC18-X-1-G3	Organic sediment	Beta Analytics	AMS	497229	4	1.6	38470
TP-BGC18-X-1-G4	Organic sediment	Beta Analytics	AMS	497230	3	1.1	9190
TP-BGC18-X-2-G2	Wood	Beta Analytics	AMS	497231	3	2.0	140
TP-BGC18-X-2-G3	Organic sediment	Beta Analytics	AMS	498936	3	2.0	6440
TP-BGC18-X-3-G2	Charcoal	Beta Analytics	AMS	497232	3	1.9	5130
TP-BGC18-X-4-G1	Organic sediment	Beta Analytics	AMS	497233	1	0.5	430
TP-BGC18-Y-1-G1	Organic sediment	Beta Analytics	AMS	497234	1	0.9	2040
TP-BGC18-Y-1-G2	Charcoal	Beta Analytics	AMS	497235	3	1.8	2810
TP-BGC18-Y-2-G1	Re-worked tephra	University of Alberta	Microprobe	-	2	1.2	re-worked Mazama
TP-BGC18-Y-2-G2	Charcoal	Beta Analytics	AMS	497236	2	1.2	880
TP-BGC18-Y-3-G1	Re-worked tephra	University of Alberta	Microprobe	-	2	0.8	re-worked Mazama
TP-BGC18-Y-3-G2	Organic sediment	Beta Analytics	AMS	498937	2	0.8	660
TP-BGC18-Y-3-G3	Plant material	Beta Analytics	AMS	497237	2	1.1	modern
TP-BGC18-Y-4-G1	Wood	Beta Analytics	AMS	497238	1	0.9	230
TP-BGC18-Y-4-G3	Charcoal	Beta Analytics	AMS	497239	3	1.8	800
TP-BGC18-Z-1-G2	Organic sediment	Beta Analytics	AMS	497240	3	1.8	1940
TP-BGC18-Z-2-G2	Charcoal	Beta Analytics	AMS	497241	8	2.3	3060
TP-BGC18-Z-3-G2	Charcoal	Beta Analytics	AMS	497242	5	2.3	8680
TP-BGC18-Z-4-G1	Organic sediment	Beta Analytics	AMS	497243	1	0.6	12110



Beta Analytic
RADIOCARBON DATING

Beta Analytic Inc
4985 SW 74 Court
Miami, Florida 33155
Tel: 305-667-5167
Fax: 305-663-0964
beta@radiocarbon.com

Mr. Darden Hood
President

Mr. Ronald Hatfield
Mr. Christopher Patrick
Deputy Directors

ISO/IEC 17025:2005 Accredited Test Results: Testing results recognized by all Signatories to the ILAC Mutual Recognition Arrangement

June 29, 2018

Ms. Emily Moase
BGC Engineering
500-980 Howe Street
Vancouver, BC V6Z 0C8
Canada

RE: Radiocarbon Dating Results

Dear Ms. Moase,

Enclosed are the radiocarbon dating results for 15 samples recently sent to us. As usual, the method of analysis is listed on the report with the results and calibration data is provided where applicable. The Conventional Radiocarbon Ages have all been corrected for total fractionation effects and where applicable, calibration was performed using 2013 calibration databases (cited on the graph pages).

The web directory containing the table of results and PDF download also contains pictures, a cvs spreadsheet download option and a quality assurance report containing expected vs. measured values for 3-5 working standards analyzed simultaneously with your samples.

Reported results are accredited to ISO/IEC 17025:2005 Testing Accreditation PJLA #59423 standards and all chemistry was performed here in our laboratory and counted in our own accelerators here. Since Beta is not a teaching laboratory, only graduates trained to strict protocols of the ISO/IEC 17025:2005 Testing Accreditation PJLA #59423 program participated in the analyses.

As always Conventional Radiocarbon Ages and sigmas are rounded to the nearest 10 years per the conventions of the 1977 International Radiocarbon Conference. When counting statistics produce sigmas lower than +/- 30 years, a conservative +/- 30 BP is cited for the result. The reported d13C values were measured separately in an IRMS (isotope ratio mass spectrometer). They are NOT the AMS d13C which would include fractionation effects from natural, chemistry and AMS induced sources.

When interpreting the results, please consider any communications you may have had with us regarding the samples.

Thank you for prepaying the analyses. As always, if you have any questions or would like to discuss the results, don't hesitate to contact us.

Sincerely ,

Darden Hood
Digital signature on file



REPORT OF RADIOCARBON DATING ANALYSES

Emily Moase

Report Date: June 29, 2018

BGC Engineering

Material Received: June 20, 2018

Laboratory Number

Sample Code Number

Conventional Radiocarbon Age (BP) or
Percent Modern Carbon (pMC) & Stable Isotopes

Calendar Calibrated Results: 95.4 % Probability
High Probability Density Range Method (HPD)

Beta - 497229

TP-BGC18-X-1-G3

34010 +/- 240 BP

IRMS $\delta^{13}C$: -23.7 o/oo

(95.4%)

37131 - 35911 cal BC

(39080 - 37860 cal BP)

Submitter Material: Soil

Pretreatment: (organic sediment) acid washes

Analyzed Material: Organic sediment

Analysis Service: AMS-Standard delivery

Percent Modern Carbon: 1.45 +/- 0.04 pMC

Fraction Modern Carbon: 0.0145 +/- 0.0004

D14C: -985.50 +/- 0.43 o/oo

$\Delta^{14}C$: -985.62 +/- 0.43 o/oo(1950:2,018.00)

Measured Radiocarbon Age: (without $\delta^{13}C$ correction): 33990 +/- 240 BP

Calibration: BetaCal3.21: HPD method: INTCAL13

Results are ISO/IEC-17025:2005 accredited. No sub-contracting or student labor was used in the analyses. All work was done at Beta in 4 in-house NEC accelerator mass spectrometers and 4 Thermo IRMSs. The "Conventional Radiocarbon Age" was calculated using the Libby half-life (5568 years), is corrected for total isotopic fraction and was used for calendar calibration where applicable. The Age is rounded to the nearest 10 years and is reported as radiocarbon years before present (BP), "present" = AD 1950. Results greater than the modern reference are reported as percent modern carbon (pMC). The modern reference standard was 95% the ^{14}C signature of NIST SRM-4990C (oxalic acid). Quoted errors are 1 sigma counting statistics. Calculated sigmas less than 30 BP on the Conventional Radiocarbon Age are conservatively rounded up to 30. $\delta^{13}C$ values are on the material itself (not the AMS $\delta^{13}C$). $\delta^{13}C$ and $\delta^{15}N$ values are relative to VPDB-1. References for calendar calibrations are cited at the bottom of calibration graph pages.



REPORT OF RADIOCARBON DATING ANALYSES

Emily Moase

Report Date: June 29, 2018

BGC Engineering

Material Received: June 20, 2018

Laboratory Number

Sample Code Number

Conventional Radiocarbon Age (BP) or
Percent Modern Carbon (pMC) & Stable Isotopes

Calendar Calibrated Results: 95.4 % Probability
High Probability Density Range Method (HPD)

Beta - 497230

TP-BGC18-X-1-G4

8220 +/- 30 BP

IRMS $\delta^{13}C$: -23.1 o/oo

(92.4%)
(3.0%)

7342 - 7133 cal BC
7104 - 7084 cal BC

(9291 - 9082 cal BP)
(9053 - 9033 cal BP)

Submitter Material: Soil

Pretreatment: (organic sediment) acid washes

Analyzed Material: Organic sediment

Analysis Service: AMS-Standard delivery

Percent Modern Carbon: 35.94 +/- 0.13 pMC

Fraction Modern Carbon: 0.3594 +/- 0.0013

D14C: -640.59 +/- 1.34 o/oo

$\Delta^{14}C$: -643.53 +/- 1.34 o/oo(1950:2,018.00)

Measured Radiocarbon Age: (without $\delta^{13}C$ correction): 8190 +/- 30 BP

Calibration: BetaCal3.21: HPD method: INTCAL13

Results are ISO/IEC-17025:2005 accredited. No sub-contracting or student labor was used in the analyses. All work was done at Beta in 4 in-house NEC accelerator mass spectrometers and 4 Thermo IRMSs. The "Conventional Radiocarbon Age" was calculated using the Libby half-life (5568 years), is corrected for total isotopic fraction and was used for calendar calibration where applicable. The Age is rounded to the nearest 10 years and is reported as radiocarbon years before present (BP), "present" = AD 1950. Results greater than the modern reference are reported as percent modern carbon (pMC). The modern reference standard was 95% the ^{14}C signature of NIST SRM-4990C (oxalic acid). Quoted errors are 1 sigma counting statistics. Calculated sigmas less than 30 BP on the Conventional Radiocarbon Age are conservatively rounded up to 30. $\delta^{13}C$ values are on the material itself (not the AMS $\delta^{13}C$). $\delta^{13}C$ and $\delta^{15}N$ values are relative to VPDB-1. References for calendar calibrations are cited at the bottom of calibration graph pages.



REPORT OF RADIOCARBON DATING ANALYSES

Emily Moase

Report Date: June 29, 2018

BGC Engineering

Material Received: June 20, 2018

		Conventional Radiocarbon Age (BP) or Percent Modern Carbon (pMC) & Stable Isotopes
Laboratory Number	Sample Code Number	Calendar Calibrated Results: 95.4 % Probability High Probability Density Range Method (HPD)

Beta - 497231	TP-BGC18-X-2-G2	40 +/- 30 BP	IRMS δ13C: -25.6 o/oo
----------------------	------------------------	---------------------	------------------------------

(56.2%)	1866 - 1919 cal AD	(84 - 31 cal BP)
(20.5%)	1694 - 1728 cal AD	(256 - 222 cal BP)
(18.6%)	1812 - 1854 cal AD	(138 - 96 cal BP)

Submitter Material: Wood
Pretreatment: (wood) acid/alkali/acid
Analyzed Material: Wood
Analysis Service: AMS-Standard delivery
Percent Modern Carbon: 99.50 +/- 0.37 pMC
Fraction Modern Carbon: 0.9950 +/- 0.0037
D14C: -4.97 +/- 3.72 o/oo
Δ14C: -13.12 +/- 3.72 o/oo(1950:2,018.00)
Measured Radiocarbon Age: (without d13C correction): 50 +/- 30 BP
Calibration: BetaCal3.21: HPD method: INTCAL13

Results are ISO/IEC-17025:2005 accredited. No sub-contracting or student labor was used in the analyses. All work was done at Beta in 4 in-house NEC accelerator mass spectrometers and 4 Thermo IRMSs. The "Conventional Radiocarbon Age" was calculated using the Libby half-life (5568 years), is corrected for total isotopic fraction and was used for calendar calibration where applicable. The Age is rounded to the nearest 10 years and is reported as radiocarbon years before present (BP), "present" = AD 1950. Results greater than the modern reference are reported as percent modern carbon (pMC). The modern reference standard was 95% the 14C signature of NIST SRM-4990C (oxalic acid). Quoted errors are 1 sigma counting statistics. Calculated sigmas less than 30 BP on the Conventional Radiocarbon Age are conservatively rounded up to 30. d13C values are on the material itself (not the AMS d13C). d13C and d15N values are relative to VPDB-1. References for calendar calibrations are cited at the bottom of calibration graph pages.



REPORT OF RADIOCARBON DATING ANALYSES

Emily Moase

Report Date: June 29, 2018

BGC Engineering

Material Received: June 20, 2018

		Conventional Radiocarbon Age (BP) or Percent Modern Carbon (pMC) & Stable Isotopes
Laboratory Number	Sample Code Number	Calendar Calibrated Results: 95.4 % Probability High Probability Density Range Method (HPD)

Beta - 497232

TP-BGC18-X-3-G2

4470 +/- 30 BP

IRMS δ13C: -25.5 o/oo

(52.4%)	3339 - 3206 cal BC	(5288 - 5155 cal BP)
(33.3%)	3196 - 3081 cal BC	(5145 - 5030 cal BP)
(9.7%)	3069 - 3026 cal BC	(5018 - 4975 cal BP)

Submitter Material: Paleosol
 Pretreatment: (charred material) acid/alkali/acid
 Analyzed Material: Charred material
 Analysis Service: AMS-Standard delivery
 Percent Modern Carbon: 57.32 +/- 0.21 pMC
 Fraction Modern Carbon: 0.5732 +/- 0.0021
 D14C: -426.77 +/- 2.14 o/oo
 Δ14C: -431.46 +/- 2.14 o/oo(1950:2,018.00)
 Measured Radiocarbon Age: (without d13C correction): 4480 +/- 30 BP
 Calibration: BetaCal3.21: HPD method: INTCAL13

Results are ISO/IEC-17025:2005 accredited. No sub-contracting or student labor was used in the analyses. All work was done at Beta in 4 in-house NEC accelerator mass spectrometers and 4 Thermo IRMSs. The "Conventional Radiocarbon Age" was calculated using the Libby half-life (5568 years), is corrected for total isotopic fraction and was used for calendar calibration where applicable. The Age is rounded to the nearest 10 years and is reported as radiocarbon years before present (BP), "present" = AD 1950. Results greater than the modern reference are reported as percent modern carbon (pMC). The modern reference standard was 95% the 14C signature of NIST SRM-4990C (oxalic acid). Quoted errors are 1 sigma counting statistics. Calculated sigmas less than 30 BP on the Conventional Radiocarbon Age are conservatively rounded up to 30. d13C values are on the material itself (not the AMS d13C). d13C and d15N values are relative to VPDB-1. References for calendar calibrations are cited at the bottom of calibration graph pages.



REPORT OF RADIOCARBON DATING ANALYSES

Emily Moase

Report Date: June 29, 2018

BGC Engineering

Material Received: June 20, 2018

Laboratory Number

Sample Code Number

Conventional Radiocarbon Age (BP) or
Percent Modern Carbon (pMC) & Stable Isotopes

Calendar Calibrated Results: 95.4 % Probability
High Probability Density Range Method (HPD)

Beta - 497233

TP-BGC18-X-4-G1

420 +/- 30 BP

IRMS $\delta^{13}C$: -24.2 o/oo

(87.9%)
(7.5%)

1426 - 1515 cal AD
1598 - 1618 cal AD

(524 - 435 cal BP)
(352 - 332 cal BP)

Submitter Material: Soil with organics

Pretreatment: (organic sediment) acid washes

Analyzed Material: Organic sediment

Analysis Service: AMS-Standard delivery

Percent Modern Carbon: 94.91 +/- 0.35 pMC

Fraction Modern Carbon: 0.9491 +/- 0.0035

D14C: -50.94 +/- 3.54 o/oo

$\Delta^{14}C$: -58.72 +/- 3.54 o/oo(1950:2,018.00)

Measured Radiocarbon Age: (without $\delta^{13}C$ correction): 410 +/- 30 BP

Calibration: BetaCal3.21: HPD method: INTCAL13

Results are ISO/IEC-17025:2005 accredited. No sub-contracting or student labor was used in the analyses. All work was done at Beta in 4 in-house NEC accelerator mass spectrometers and 4 Thermo IRMSs. The "Conventional Radiocarbon Age" was calculated using the Libby half-life (5568 years), is corrected for total isotopic fraction and was used for calendar calibration where applicable. The Age is rounded to the nearest 10 years and is reported as radiocarbon years before present (BP), "present" = AD 1950. Results greater than the modern reference are reported as percent modern carbon (pMC). The modern reference standard was 95% the ^{14}C signature of NIST SRM-4990C (oxalic acid). Quoted errors are 1 sigma counting statistics. Calculated sigmas less than 30 BP on the Conventional Radiocarbon Age are conservatively rounded up to 30. $\delta^{13}C$ values are on the material itself (not the AMS $\delta^{13}C$). $\delta^{13}C$ and $\delta^{15}N$ values are relative to VPDB-1. References for calendar calibrations are cited at the bottom of calibration graph pages.



REPORT OF RADIOCARBON DATING ANALYSES

Emily Moase

Report Date: June 29, 2018

BGC Engineering

Material Received: June 20, 2018

Laboratory Number

Sample Code Number

Conventional Radiocarbon Age (BP) or
Percent Modern Carbon (pMC) & Stable Isotopes

Calendar Calibrated Results: 95.4 % Probability
High Probability Density Range Method (HPD)

Beta - 497234

TP-BGC18-Y-1-G1

2070 +/- 30 BP

IRMS $\delta^{13}C$: -24.3 o/oo

(92.6%)
(2.8%)

174 - 19 cal BC
13 - 0 cal BC

(2123 - 1968 cal BP)
(1962 - 1950 cal BP)

Submitter Material: Soil

Pretreatment: (organic sediment) acid washes

Analyzed Material: Organic sediment

Analysis Service: AMS-Standard delivery

Percent Modern Carbon: 77.28 +/- 0.29 pMC

Fraction Modern Carbon: 0.7728 +/- 0.0029

D14C: -227.16 +/- 2.89 o/oo

$\Delta^{14}C$: -233.50 +/- 2.89 o/oo(1950:2,018.00)

Measured Radiocarbon Age: (without $\delta^{13}C$ correction): 2060 +/- 30 BP

Calibration: BetaCal3.21: HPD method: INTCAL13

Results are ISO/IEC-17025:2005 accredited. No sub-contracting or student labor was used in the analyses. All work was done at Beta in 4 in-house NEC accelerator mass spectrometers and 4 Thermo IRMSs. The "Conventional Radiocarbon Age" was calculated using the Libby half-life (5568 years), is corrected for total isotopic fraction and was used for calendar calibration where applicable. The Age is rounded to the nearest 10 years and is reported as radiocarbon years before present (BP), "present" = AD 1950. Results greater than the modern reference are reported as percent modern carbon (pMC). The modern reference standard was 95% the ^{14}C signature of NIST SRM-4990C (oxalic acid). Quoted errors are 1 sigma counting statistics. Calculated sigmas less than 30 BP on the Conventional Radiocarbon Age are conservatively rounded up to 30. $\delta^{13}C$ values are on the material itself (not the AMS $\delta^{13}C$). $\delta^{13}C$ and $\delta^{15}N$ values are relative to VPDB-1. References for calendar calibrations are cited at the bottom of calibration graph pages.



REPORT OF RADIOCARBON DATING ANALYSES

Emily Moase

Report Date: June 29, 2018

BGC Engineering

Material Received: June 20, 2018

Laboratory Number

Sample Code Number

Conventional Radiocarbon Age (BP) or
Percent Modern Carbon (pMC) & Stable Isotopes

Calendar Calibrated Results: 95.4 % Probability
High Probability Density Range Method (HPD)

Beta - 497235

TP-BGC18-Y-1-G2

2700 +/- 30 BP

IRMS $\delta^{13}C$: -24.1 o/oo

(95.4%)

905 - 806 cal BC

(2854 - 2755 cal BP)

Submitter Material: Paleosol

Pretreatment: (charred material) acid/alkali/acid

Analyzed Material: Charred material

Analysis Service: AMS-Standard delivery

Percent Modern Carbon: 71.45 +/- 0.27 pMC

Fraction Modern Carbon: 0.7145 +/- 0.0027

D14C: -285.46 +/- 2.67 o/oo

$\Delta^{14}C$: -291.31 +/- 2.67 o/oo(1950:2,018.00)

Measured Radiocarbon Age: (without $\delta^{13}C$ correction): 2680 +/- 30 BP

Calibration: BetaCal3.21: HPD method: INTCAL13

Results are ISO/IEC-17025:2005 accredited. No sub-contracting or student labor was used in the analyses. All work was done at Beta in 4 in-house NEC accelerator mass spectrometers and 4 Thermo IRMSs. The "Conventional Radiocarbon Age" was calculated using the Libby half-life (5568 years), is corrected for total isotopic fraction and was used for calendar calibration where applicable. The Age is rounded to the nearest 10 years and is reported as radiocarbon years before present (BP), "present" = AD 1950. Results greater than the modern reference are reported as percent modern carbon (pMC). The modern reference standard was 95% the ^{14}C signature of NIST SRM-4990C (oxalic acid). Quoted errors are 1 sigma counting statistics. Calculated sigmas less than 30 BP on the Conventional Radiocarbon Age are conservatively rounded up to 30. $\delta^{13}C$ values are on the material itself (not the AMS $\delta^{13}C$). $\delta^{13}C$ and $\delta^{15}N$ values are relative to VPDB-1. References for calendar calibrations are cited at the bottom of calibration graph pages.



REPORT OF RADIOCARBON DATING ANALYSES

Emily Moase

Report Date: June 29, 2018

BGC Engineering

Material Received: June 20, 2018

		Conventional Radiocarbon Age (BP) or Percent Modern Carbon (pMC) & Stable Isotopes
Laboratory Number	Sample Code Number	Calendar Calibrated Results: 95.4 % Probability High Probability Density Range Method (HPD)

Beta - 497236

TP-BGC18-Y-2-G2

1000 +/- 30 BP

IRMS δ13C: -22.9 o/oo

(71.0%)	983 - 1051 cal AD	(967 - 899 cal BP)
(19.2%)	1082 - 1128 cal AD	(868 - 822 cal BP)
(5.2%)	1135 - 1152 cal AD	(815 - 798 cal BP)

Submitter Material: Organics
 Pretreatment: (charred material) acid/alkali/acid
 Analyzed Material: Charred material
 Analysis Service: AMS-Standard delivery
 Percent Modern Carbon: 88.29 +/- 0.33 pMC
 Fraction Modern Carbon: 0.8829 +/- 0.0033
 D14C: -117.05 +/- 3.30 o/oo
 Δ14C: -124.28 +/- 3.30 o/oo(1950:2,018.00)
 Measured Radiocarbon Age: (without d13C correction): 960 +/- 30 BP
 Calibration: BetaCal3.21: HPD method: INTCAL13

Results are ISO/IEC-17025:2005 accredited. No sub-contracting or student labor was used in the analyses. All work was done at Beta in 4 in-house NEC accelerator mass spectrometers and 4 Thermo IRMSs. The "Conventional Radiocarbon Age" was calculated using the Libby half-life (5568 years), is corrected for total isotopic fraction and was used for calendar calibration where applicable. The Age is rounded to the nearest 10 years and is reported as radiocarbon years before present (BP), "present" = AD 1950. Results greater than the modern reference are reported as percent modern carbon (pMC). The modern reference standard was 95% the 14C signature of NIST SRM-4990C (oxalic acid). Quoted errors are 1 sigma counting statistics. Calculated sigmas less than 30 BP on the Conventional Radiocarbon Age are conservatively rounded up to 30. d13C values are on the material itself (not the AMS d13C). d13C and d15N values are relative to VPDB-1. References for calendar calibrations are cited at the bottom of calibration graph pages.



REPORT OF RADIOCARBON DATING ANALYSES

Emily Moase

Report Date: June 29, 2018

BGC Engineering

Material Received: June 20, 2018

Laboratory Number

Sample Code Number

Conventional Radiocarbon Age (BP) or
Percent Modern Carbon (pMC) & Stable Isotopes

Calendar Calibrated Results: 95.4 % Probability
High Probability Density Range Method (HPD)

Beta - 497237

TP-BGC18-Y-3-G3

100.88 +/- 0.38 pMC

IRMS $\delta^{13}C$: -26.5 o/oo

(95.4%)

1954 - 1956 cal AD

(-5 - -7 cal BP)

Submitter Material: Organics

Pretreatment: (plant material) acid/alkali/acid

Analyzed Material: Plant material

Analysis Service: AMS-Standard delivery

Conventional Radiocarbon Age: -70 +/- 30 BP

Fraction Modern Carbon: 1.0088 +/- 0.0038

D14C: 8.75 +/- 3.77 o/oo

$\Delta^{14}C$: 0.49 +/- 3.77 o/oo(1950:2,018.00)

Raw pMC: (without $\delta^{13}C$ correction): 100.57 +/- 0.38 pMC

Calibration: BetaCal3.21: HPD method: INTCAL13 + NHZ1

Results are ISO/IEC-17025:2005 accredited. No sub-contracting or student labor was used in the analyses. All work was done at Beta in 4 in-house NEC accelerator mass spectrometers and 4 Thermo IRMSs. The "Conventional Radiocarbon Age" was calculated using the Libby half-life (5568 years), is corrected for total isotopic fraction and was used for calendar calibration where applicable. The Age is rounded to the nearest 10 years and is reported as radiocarbon years before present (BP), "present" = AD 1950. Results greater than the modern reference are reported as percent modern carbon (pMC). The modern reference standard was 95% the ^{14}C signature of NIST SRM-4990C (oxalic acid). Quoted errors are 1 sigma counting statistics. Calculated sigmas less than 30 BP on the Conventional Radiocarbon Age are conservatively rounded up to 30. $\delta^{13}C$ values are on the material itself (not the AMS $\delta^{13}C$). $\delta^{13}C$ and $\delta^{15}N$ values are relative to VPDB-1. References for calendar calibrations are cited at the bottom of calibration graph pages.



REPORT OF RADIOCARBON DATING ANALYSES

Emily Moase

Report Date: June 29, 2018

BGC Engineering

Material Received: June 20, 2018

Laboratory Number

Sample Code Number

Conventional Radiocarbon Age (BP) or
Percent Modern Carbon (pMC) & Stable Isotopes

Calendar Calibrated Results: 95.4 % Probability
High Probability Density Range Method (HPD)

Beta - 497238

TP-BGC18-Y-4-G1

230 +/- 30 BP

IRMS δ13C: -25.9 o/oo

(45.8%)	1635 - 1684 cal AD	(315 - 266 cal BP)
(40.1%)	1736 - 1805 cal AD	(214 - 145 cal BP)
(8.6%)	1935 - Post AD 1950	(15 - Post BP 0)
(0.9%)	1530 - 1538 cal AD	(420 - 412 cal BP)

Submitter Material: Soil

Pretreatment: (wood) acid/alkali/acid

Analyzed Material: Wood

Analysis Service: AMS-Standard delivery

Percent Modern Carbon: 97.18 +/- 0.36 pMC

Fraction Modern Carbon: 0.9718 +/- 0.0036

D14C: -28.23 +/- 3.63 o/oo

Δ14C: -36.19 +/- 3.63 o/oo(1950:2,018.00)

Measured Radiocarbon Age: (without d13C correction): 240 +/- 30 BP

Calibration: BetaCal3.21: HPD method: INTCAL13

Results are ISO/IEC-17025:2005 accredited. No sub-contracting or student labor was used in the analyses. All work was done at Beta in 4 in-house NEC accelerator mass spectrometers and 4 Thermo IRMSs. The "Conventional Radiocarbon Age" was calculated using the Libby half-life (5568 years), is corrected for total isotopic fraction and was used for calendar calibration where applicable. The Age is rounded to the nearest 10 years and is reported as radiocarbon years before present (BP), "present" = AD 1950. Results greater than the modern reference are reported as percent modern carbon (pMC). The modern reference standard was 95% the 14C signature of NIST SRM-4990C (oxalic acid). Quoted errors are 1 sigma counting statistics. Calculated sigmas less than 30 BP on the Conventional Radiocarbon Age are conservatively rounded up to 30. d13C values are on the material itself (not the AMS d13C). d13C and d15N values are relative to VPDB-1. References for calendar calibrations are cited at the bottom of calibration graph pages.



REPORT OF RADIOCARBON DATING ANALYSES

Emily Moase

Report Date: June 29, 2018

BGC Engineering

Material Received: June 20, 2018

Laboratory Number

Sample Code Number

Conventional Radiocarbon Age (BP) or
Percent Modern Carbon (pMC) & Stable Isotopes

Calendar Calibrated Results: 95.4 % Probability
High Probability Density Range Method (HPD)

Beta - 497239

TP-BGC18-Y-4-G3

860 +/- 30 BP

IRMS δ13C: -22.2 o/oo

(83.5%)	1150 - 1256 cal AD	(800 - 694 cal BP)
(9.9%)	1049 - 1084 cal AD	(901 - 866 cal BP)
(2.0%)	1124 - 1136 cal AD	(826 - 814 cal BP)

Submitter Material: Soil

Pretreatment: (charred material) acid/alkali/acid

Analyzed Material: Charred material

Analysis Service: AMS-Standard delivery

Percent Modern Carbon: 89.85 +/- 0.34 pMC

Fraction Modern Carbon: 0.8985 +/- 0.0034

D14C: -101.53 +/- 3.36 o/oo

Δ14C: -108.89 +/- 3.36 o/oo(1950:2,018.00)

Measured Radiocarbon Age: (without d13C correction): 810 +/- 30 BP

Calibration: BetaCal3.21: HPD method: INTCAL13

Results are ISO/IEC-17025:2005 accredited. No sub-contracting or student labor was used in the analyses. All work was done at Beta in 4 in-house NEC accelerator mass spectrometers and 4 Thermo IRMSs. The "Conventional Radiocarbon Age" was calculated using the Libby half-life (5568 years), is corrected for total isotopic fraction and was used for calendar calibration where applicable. The Age is rounded to the nearest 10 years and is reported as radiocarbon years before present (BP), "present" = AD 1950. Results greater than the modern reference are reported as percent modern carbon (pMC). The modern reference standard was 95% the 14C signature of NIST SRM-4990C (oxalic acid). Quoted errors are 1 sigma counting statistics. Calculated sigmas less than 30 BP on the Conventional Radiocarbon Age are conservatively rounded up to 30. d13C values are on the material itself (not the AMS d13C). d13C and d15N values are relative to VPDB-1. References for calendar calibrations are cited at the bottom of calibration graph pages.



REPORT OF RADIOCARBON DATING ANALYSES

Emily Moase

Report Date: June 29, 2018

BGC Engineering

Material Received: June 20, 2018

Laboratory Number

Sample Code Number

Conventional Radiocarbon Age (BP) or
Percent Modern Carbon (pMC) & Stable Isotopes

Calendar Calibrated Results: 95.4 % Probability
High Probability Density Range Method (HPD)

Beta - 497240

TP-BGC18-Z-1-G2

1990 +/- 30 BP

IRMS $\delta^{13}C$: -25.0 o/oo

(95.4%)

49 cal BC - 72 cal AD

(1998 - 1878 cal BP)

Submitter Material: Soil

Pretreatment: (organic sediment) acid washes

Analyzed Material: Organic sediment

Analysis Service: AMS-Standard delivery

Percent Modern Carbon: 78.06 +/- 0.29 pMC

Fraction Modern Carbon: 0.7806 +/- 0.0029

D14C: -219.43 +/- 2.92 o/oo

$\Delta^{14}C$: -225.82 +/- 2.92 o/oo(1950:2,018.00)

Measured Radiocarbon Age: (without $\delta^{13}C$ correction): 1990 +/- 30 BP

Calibration: BetaCal3.21: HPD method: INTCAL13

Results are ISO/IEC-17025:2005 accredited. No sub-contracting or student labor was used in the analyses. All work was done at Beta in 4 in-house NEC accelerator mass spectrometers and 4 Thermo IRMSs. The "Conventional Radiocarbon Age" was calculated using the Libby half-life (5568 years), is corrected for total isotopic fraction and was used for calendar calibration where applicable. The Age is rounded to the nearest 10 years and is reported as radiocarbon years before present (BP), "present" = AD 1950. Results greater than the modern reference are reported as percent modern carbon (pMC). The modern reference standard was 95% the ^{14}C signature of NIST SRM-4990C (oxalic acid). Quoted errors are 1 sigma counting statistics. Calculated sigmas less than 30 BP on the Conventional Radiocarbon Age are conservatively rounded up to 30. $\delta^{13}C$ values are on the material itself (not the AMS $\delta^{13}C$). $\delta^{13}C$ and $\delta^{15}N$ values are relative to VPDB-1. References for calendar calibrations are cited at the bottom of calibration graph pages.



REPORT OF RADIOCARBON DATING ANALYSES

Emily Moase

Report Date: June 29, 2018

BGC Engineering

Material Received: June 20, 2018

Laboratory Number

Sample Code Number

Conventional Radiocarbon Age (BP) or
Percent Modern Carbon (pMC) & Stable Isotopes

Calendar Calibrated Results: 95.4 % Probability
High Probability Density Range Method (HPD)

Beta - 497241

TP-BGC18-Z-2-G2

2910 +/- 30 BP

IRMS $\delta^{13}C$: -22.5 o/oo

(95.4%)

1209 - 1011 cal BC

(3158 - 2960 cal BP)

Submitter Material: Soil

Pretreatment: (charred material) acid/alkali/acid

Analyzed Material: Charred material

Analysis Service: AMS-Standard delivery

Percent Modern Carbon: 69.61 +/- 0.26 pMC

Fraction Modern Carbon: 0.6961 +/- 0.0026

D14C: -303.90 +/- 2.60 o/oo

$\Delta^{14}C$: -309.60 +/- 2.60 o/oo(1950:2,018.00)

Measured Radiocarbon Age: (without $\delta^{13}C$ correction): 2870 +/- 30 BP

Calibration: BetaCal3.21: HPD method: INTCAL13

Results are ISO/IEC-17025:2005 accredited. No sub-contracting or student labor was used in the analyses. All work was done at Beta in 4 in-house NEC accelerator mass spectrometers and 4 Thermo IRMSs. The "Conventional Radiocarbon Age" was calculated using the Libby half-life (5568 years), is corrected for total isotopic fraction and was used for calendar calibration where applicable. The Age is rounded to the nearest 10 years and is reported as radiocarbon years before present (BP), "present" = AD 1950. Results greater than the modern reference are reported as percent modern carbon (pMC). The modern reference standard was 95% the ^{14}C signature of NIST SRM-4990C (oxalic acid). Quoted errors are 1 sigma counting statistics. Calculated sigmas less than 30 BP on the Conventional Radiocarbon Age are conservatively rounded up to 30. $\delta^{13}C$ values are on the material itself (not the AMS $\delta^{13}C$). $\delta^{13}C$ and $\delta^{15}N$ values are relative to VPDB-1. References for calendar calibrations are cited at the bottom of calibration graph pages.



REPORT OF RADIOCARBON DATING ANALYSES

Emily Moase

Report Date: June 29, 2018

BGC Engineering

Material Received: June 20, 2018

Laboratory Number

Sample Code Number

Conventional Radiocarbon Age (BP) or
Percent Modern Carbon (pMC) & Stable Isotopes

Calendar Calibrated Results: 95.4 % Probability
High Probability Density Range Method (HPD)

Beta - 497242

TP-BGC18-Z-3-G2

7870 +/- 30 BP

IRMS $\delta^{13}C$: -24.0 o/oo

(95.4%)

6821 - 6640 cal BC

(8770 - 8589 cal BP)

Submitter Material: Paleosol

Pretreatment: (charred material) acid/alkali/acid

Analyzed Material: Charred material

Analysis Service: AMS-Standard delivery

Percent Modern Carbon: 37.54 +/- 0.14 pMC

Fraction Modern Carbon: 0.3754 +/- 0.0014

D14C: -624.58 +/- 1.40 o/oo

$\Delta^{14}C$: -627.66 +/- 1.40 o/oo(1950:2,018.00)

Measured Radiocarbon Age: (without $\delta^{13}C$ correction): 7850 +/- 30 BP

Calibration: BetaCal3.21: HPD method: INTCAL13

Results are ISO/IEC-17025:2005 accredited. No sub-contracting or student labor was used in the analyses. All work was done at Beta in 4 in-house NEC accelerator mass spectrometers and 4 Thermo IRMSs. The "Conventional Radiocarbon Age" was calculated using the Libby half-life (5568 years), is corrected for total isotopic fraction and was used for calendar calibration where applicable. The Age is rounded to the nearest 10 years and is reported as radiocarbon years before present (BP), "present" = AD 1950. Results greater than the modern reference are reported as percent modern carbon (pMC). The modern reference standard was 95% the ^{14}C signature of NIST SRM-4990C (oxalic acid). Quoted errors are 1 sigma counting statistics. Calculated sigmas less than 30 BP on the Conventional Radiocarbon Age are conservatively rounded up to 30. $\delta^{13}C$ values are on the material itself (not the AMS $\delta^{13}C$). $\delta^{13}C$ and $\delta^{15}N$ values are relative to VPDB-1. References for calendar calibrations are cited at the bottom of calibration graph pages.



REPORT OF RADIOCARBON DATING ANALYSES

Emily Moase

Report Date: June 29, 2018

BGC Engineering

Material Received: June 20, 2018

Laboratory Number

Sample Code Number

Conventional Radiocarbon Age (BP) or
Percent Modern Carbon (pMC) & Stable Isotopes

Calendar Calibrated Results: 95.4 % Probability
High Probability Density Range Method (HPD)

Beta - 497243

TP-BGC18-Z-4-G1

10300 +/- 40 BP

IRMS δ13C: -26.3 o/oo

(83.8%)	10293 - 9998 cal BC	(12242 - 11947 cal BP)
(6.3%)	10431 - 10376 cal BC	(12380 - 12325 cal BP)
(3.6%)	10363 - 10321 cal BC	(12312 - 12270 cal BP)
(1.6%)	9920 - 9896 cal BC	(11869 - 11845 cal BP)

Submitter Material: Soil

Pretreatment: (organic sediment) acid washes

Analyzed Material: Organic sediment

Analysis Service: AMS-Standard delivery

Percent Modern Carbon: 27.74 +/- 0.14 pMC

Fraction Modern Carbon: 0.2774 +/- 0.0014

D14C: -722.58 +/- 1.38 o/oo

Δ14C: -724.85 +/- 1.38 o/oo(1950:2,018.00)

Measured Radiocarbon Age: (without d13C correction): 10320 +/- 40 BP

Calibration: BetaCal3.21: HPD method: INTCAL13

Results are ISO/IEC-17025:2005 accredited. No sub-contracting or student labor was used in the analyses. All work was done at Beta in 4 in-house NEC accelerator mass spectrometers and 4 Thermo IRMSs. The "Conventional Radiocarbon Age" was calculated using the Libby half-life (5568 years), is corrected for total isotopic fraction and was used for calendar calibration where applicable. The Age is rounded to the nearest 10 years and is reported as radiocarbon years before present (BP), "present" = AD 1950. Results greater than the modern reference are reported as percent modern carbon (pMC). The modern reference standard was 95% the 14C signature of NIST SRM-4990C (oxalic acid). Quoted errors are 1 sigma counting statistics. Calculated sigmas less than 30 BP on the Conventional Radiocarbon Age are conservatively rounded up to 30. d13C values are on the material itself (not the AMS d13C). d13C and d15N values are relative to VPDB-1. References for calendar calibrations are cited at the bottom of calibration graph pages.

Calibration of Radiocarbon Age to Calendar Years

(High Probability Density Range Method (HPD): INTCAL13)

(Variables: $\delta^{13}\text{C} = -23.7$ o/oo)

Laboratory number **Beta-497229**

Conventional radiocarbon age **34010 \pm 240 BP**

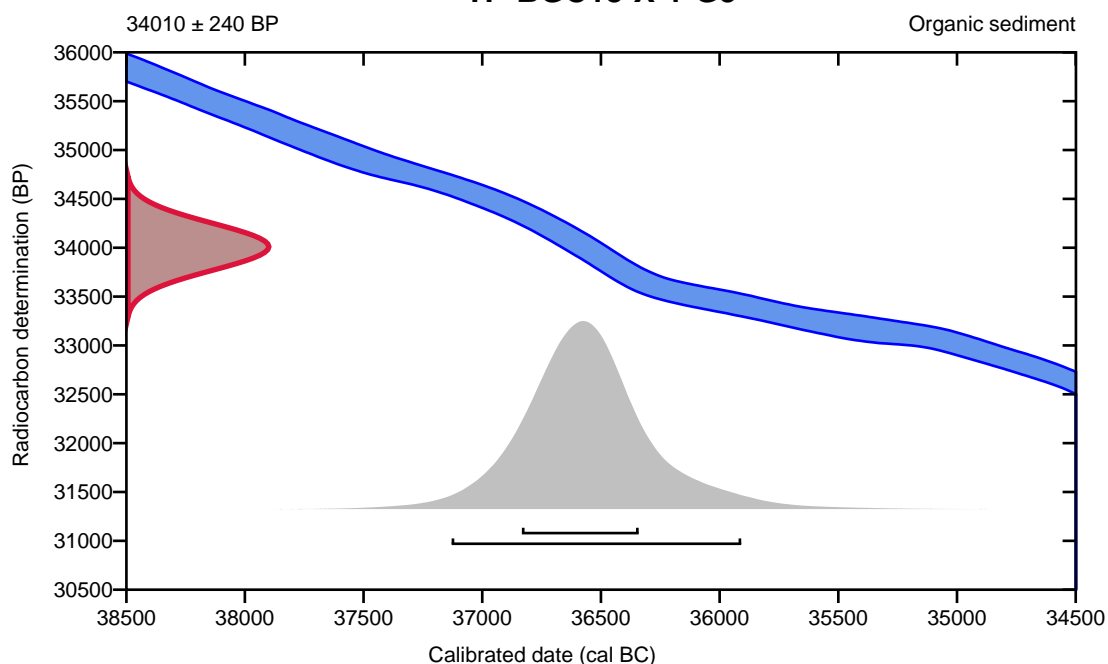
95.4% probability

(95.4%) 37131 - 35911 cal BC (39080 - 37860 cal BP)

68.2% probability

(68.2%) 36835 - 36343 cal BC (38784 - 38292 cal BP)

TP-BGC18-X-1-G3



Database used
INTCAL13

References

References to Probability Method

Bronk Ramsey, C. (2009). Bayesian analysis of radiocarbon dates. *Radiocarbon*, 51(1), 337-360.

References to Database INTCAL13

Reimer, et.al., 2013, *Radiocarbon*55(4).

Calibration of Radiocarbon Age to Calendar Years

(High Probability Density Range Method (HPD): INTCAL13)

(Variables: $\delta^{13}\text{C} = -23.1$ o/oo)

Laboratory number **Beta-497230**

Conventional radiocarbon age **8220 \pm 30 BP**

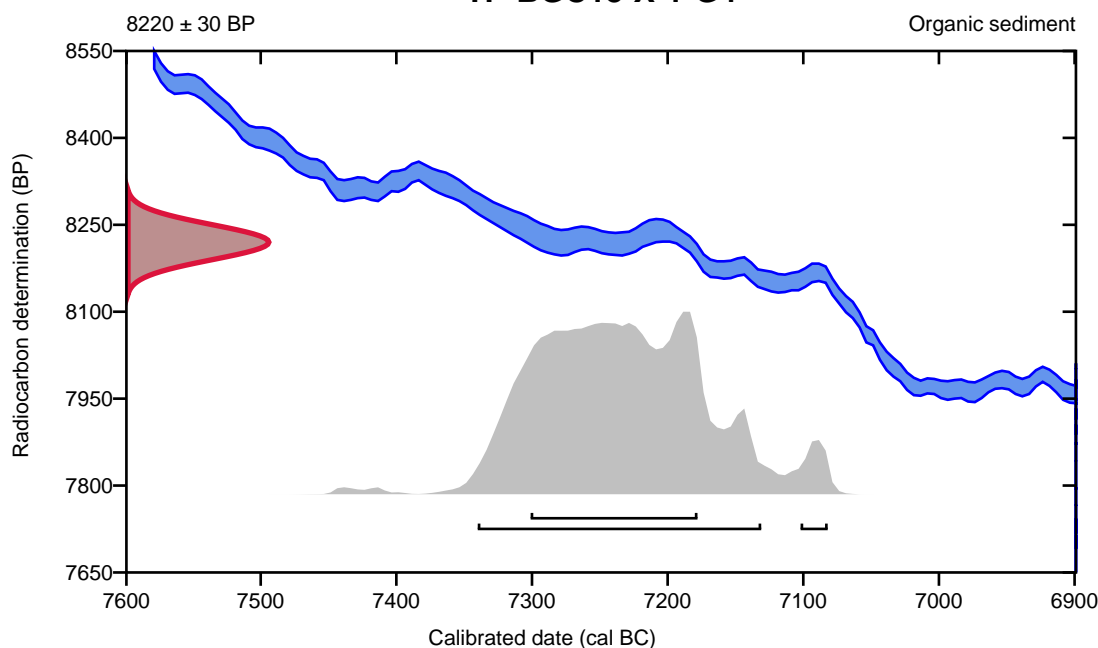
95.4% probability

(92.4%)	7342 - 7133 cal BC	(9291 - 9082 cal BP)
(3%)	7104 - 7084 cal BC	(9053 - 9033 cal BP)

68.2% probability

(68.2%)	7303 - 7180 cal BC	(9252 - 9129 cal BP)
---------	--------------------	----------------------

TP-BGC18-X-1-G4



Database used
INTCAL13

References

References to Probability Method

Bronk Ramsey, C. (2009). Bayesian analysis of radiocarbon dates. *Radiocarbon*, 51(1), 337-360.

References to Database INTCAL13

Reimer, et.al., 2013, *Radiocarbon*55(4).

Calibration of Radiocarbon Age to Calendar Years

(High Probability Density Range Method (HPD): INTCAL13)

(Variables: $\delta^{13}\text{C} = -25.6$ o/oo)

Laboratory number **Beta-497231**

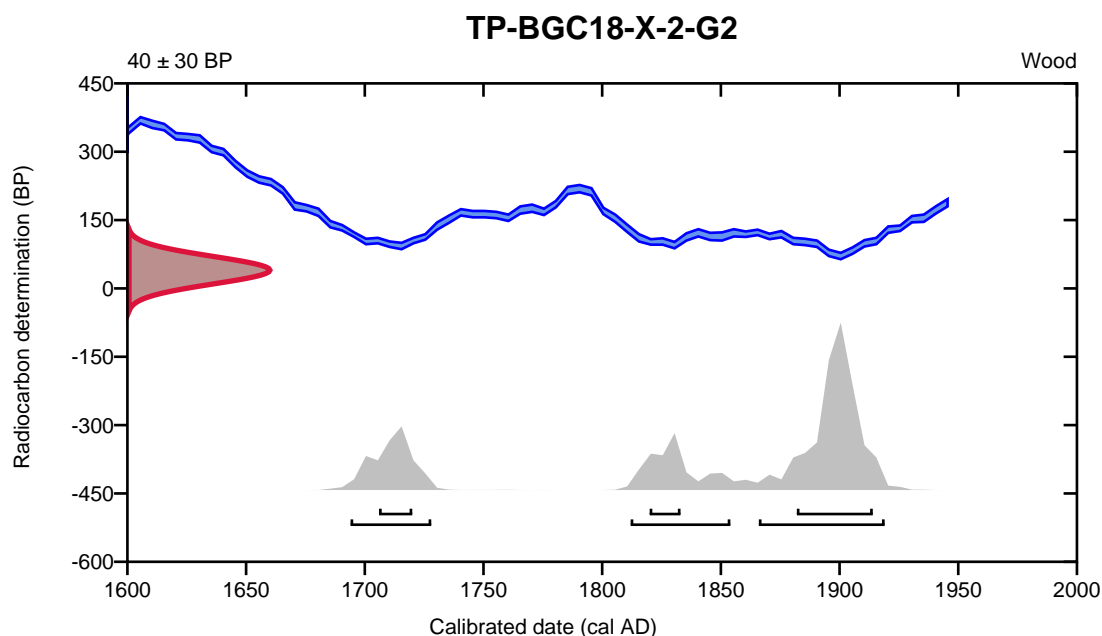
Conventional radiocarbon age **40 ± 30 BP**

95.4% probability

(56.2%)	1866 - 1919 cal AD	(84 - 31 cal BP)
(20.5%)	1694 - 1728 cal AD	(256 - 222 cal BP)
(18.6%)	1812 - 1854 cal AD	(138 - 96 cal BP)

68.2% probability

(47.1%)	1882 - 1914 cal AD	(68 - 36 cal BP)
(11.5%)	1706 - 1720 cal AD	(244 - 230 cal BP)
(9.6%)	1820 - 1833 cal AD	(130 - 117 cal BP)



Database used
INTCAL13

References

References to Probability Method

Bronk Ramsey, C. (2009). Bayesian analysis of radiocarbon dates. *Radiocarbon*, 51(1), 337-360.

References to Database INTCAL13

Reimer, et.al., 2013, *Radiocarbon*55(4).

Calibration of Radiocarbon Age to Calendar Years

(High Probability Density Range Method (HPD): INTCAL13)

(Variables: $\delta^{13}\text{C} = -25.5$ o/oo)

Laboratory number **Beta-497232**

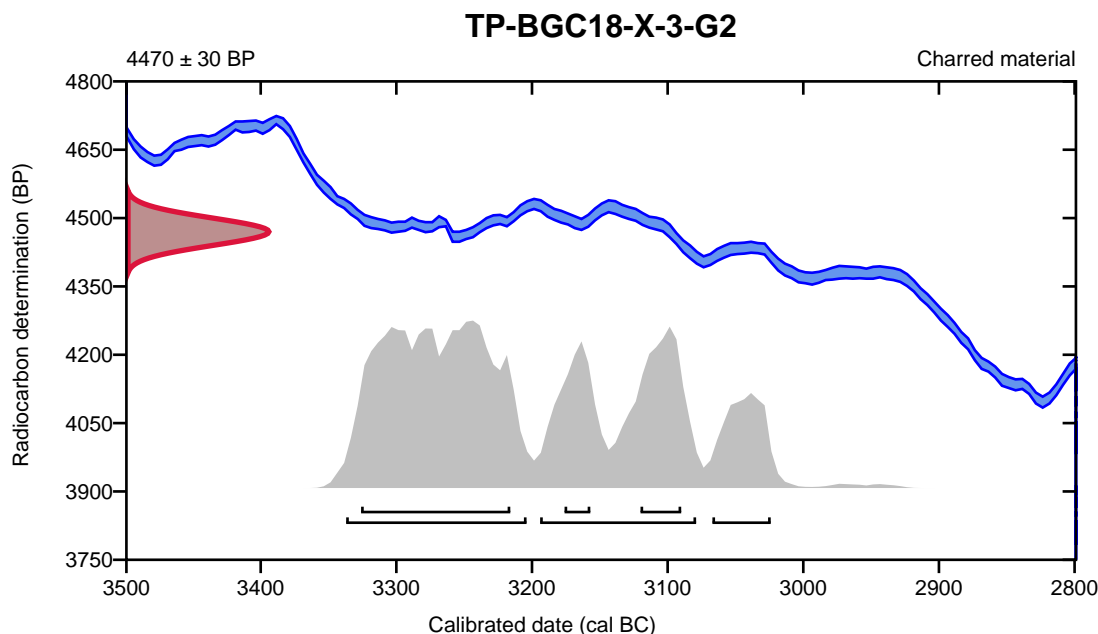
Conventional radiocarbon age **4470 \pm 30 BP**

95.4% probability

(52.4%)	3339 - 3206 cal BC	(5288 - 5155 cal BP)
(33.3%)	3196 - 3081 cal BC	(5145 - 5030 cal BP)
(9.7%)	3069 - 3026 cal BC	(5018 - 4975 cal BP)

68.2% probability

(48.2%)	3328 - 3218 cal BC	(5277 - 5167 cal BP)
(12.7%)	3122 - 3092 cal BC	(5071 - 5041 cal BP)
(7.3%)	3178 - 3159 cal BC	(5127 - 5108 cal BP)



Database used
INTCAL13

References

References to Probability Method

Bronk Ramsey, C. (2009). Bayesian analysis of radiocarbon dates. *Radiocarbon*, 51(1), 337-360.

References to Database INTCAL13

Reimer, et.al., 2013, *Radiocarbon*55(4).

Calibration of Radiocarbon Age to Calendar Years

(High Probability Density Range Method (HPD): INTCAL13)

(Variables: $\delta^{13}C = -24.2$ o/oo)

Laboratory number **Beta-497233**

Conventional radiocarbon age **420 ± 30 BP**

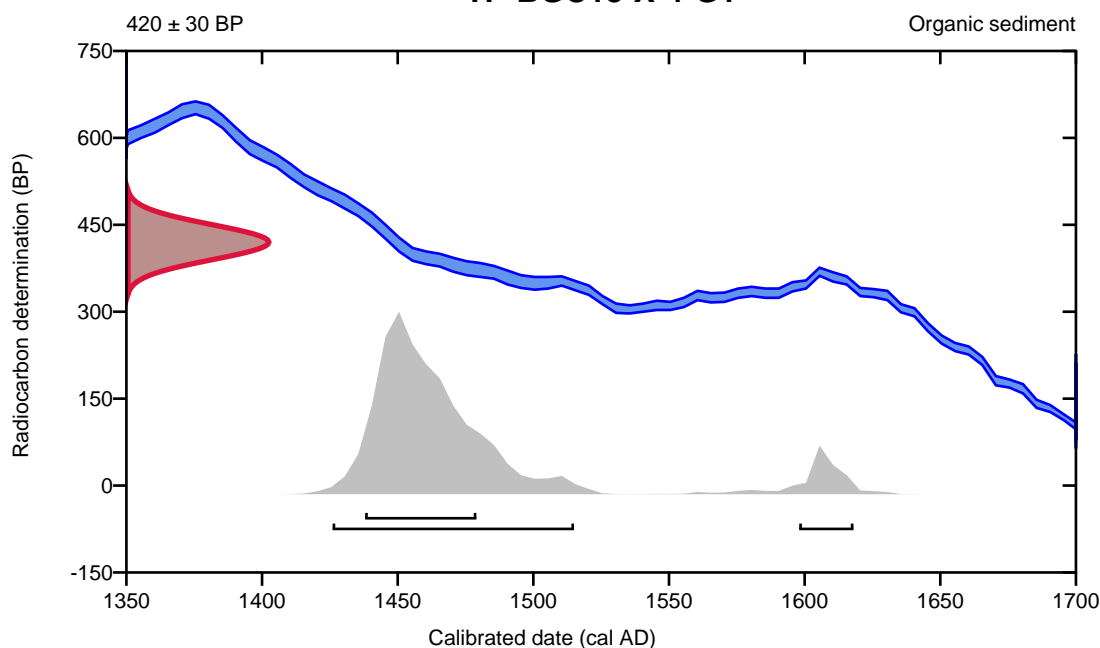
95.4% probability

(87.9%)	1426 - 1515 cal AD	(524 - 435 cal BP)
(7.5%)	1598 - 1618 cal AD	(352 - 332 cal BP)

68.2% probability

(68.2%)	1438 - 1479 cal AD	(512 - 471 cal BP)
---------	--------------------	--------------------

TP-BGC18-X-4-G1



Database used
INTCAL13

References

References to Probability Method

Bronk Ramsey, C. (2009). Bayesian analysis of radiocarbon dates. *Radiocarbon*, 51(1), 337-360.

References to Database INTCAL13

Reimer, et.al., 2013, *Radiocarbon*55(4).

Calibration of Radiocarbon Age to Calendar Years

(High Probability Density Range Method (HPD): INTCAL13)

(Variables: $\delta^{13}\text{C} = -24.3$ o/oo)

Laboratory number **Beta-497234**

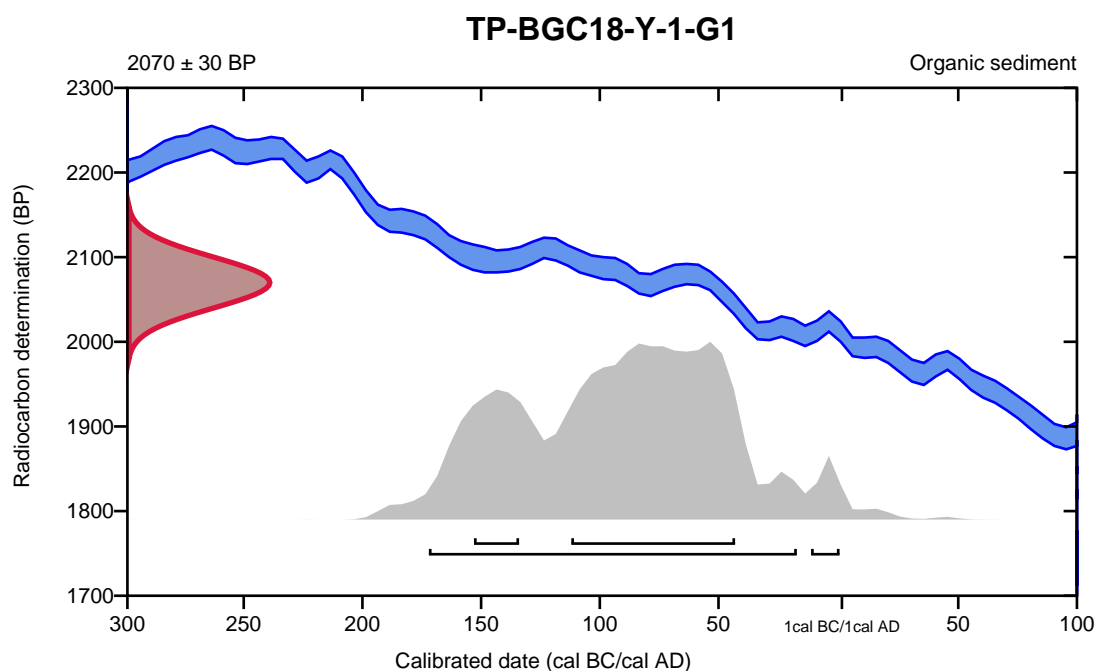
Conventional radiocarbon age **2070 \pm 30 BP**

95.4% probability

(92.6%)	174 - 19 cal BC	(2123 - 1968 cal BP)
(2.8%)	13 - 0 cal BC	(1962 - 1950 cal BP)

68.2% probability

(56%)	114 - 45 cal BC	(2063 - 1994 cal BP)
(12.2%)	155 - 136 cal BC	(2104 - 2085 cal BP)



Database used
INTCAL13

References

References to Probability Method

Bronk Ramsey, C. (2009). Bayesian analysis of radiocarbon dates. *Radiocarbon*, 51(1), 337-360.

References to Database INTCAL13

Reimer, et.al., 2013, *Radiocarbon*55(4).

Calibration of Radiocarbon Age to Calendar Years

(High Probability Density Range Method (HPD): INTCAL13)

(Variables: $\delta^{13}\text{C} = -24.1$ o/oo)

Laboratory number **Beta-497235**

Conventional radiocarbon age **2700 ± 30 BP**

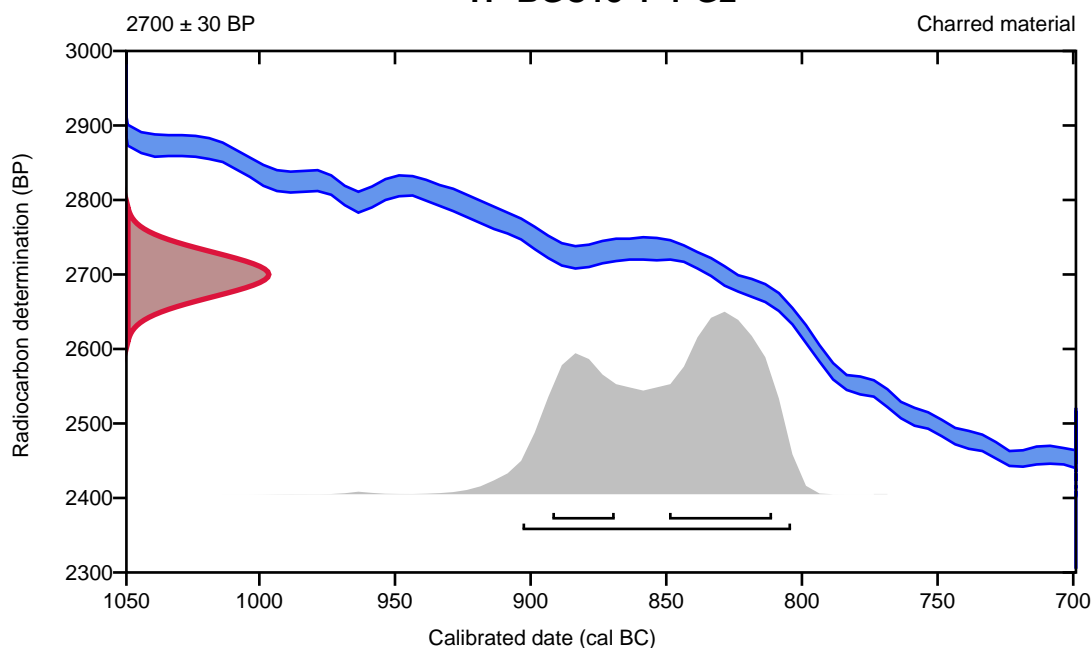
95.4% probability

(95.4%) 905 - 806 cal BC (2854 - 2755 cal BP)

68.2% probability

(45.6%) 851 - 813 cal BC (2800 - 2762 cal BP)
(22.6%) 894 - 871 cal BC (2843 - 2820 cal BP)

TP-BGC18-Y-1-G2



Database used
INTCAL13

References

References to Probability Method

Bronk Ramsey, C. (2009). Bayesian analysis of radiocarbon dates. *Radiocarbon*, 51(1), 337-360.

References to Database INTCAL13

Reimer, et.al., 2013, *Radiocarbon*55(4).

Calibration of Radiocarbon Age to Calendar Years

(High Probability Density Range Method (HPD): INTCAL13)

(Variables: $\delta^{13}\text{C} = -22.9$ o/oo)

Laboratory number **Beta-497236**

Conventional radiocarbon age **1000 \pm 30 BP**

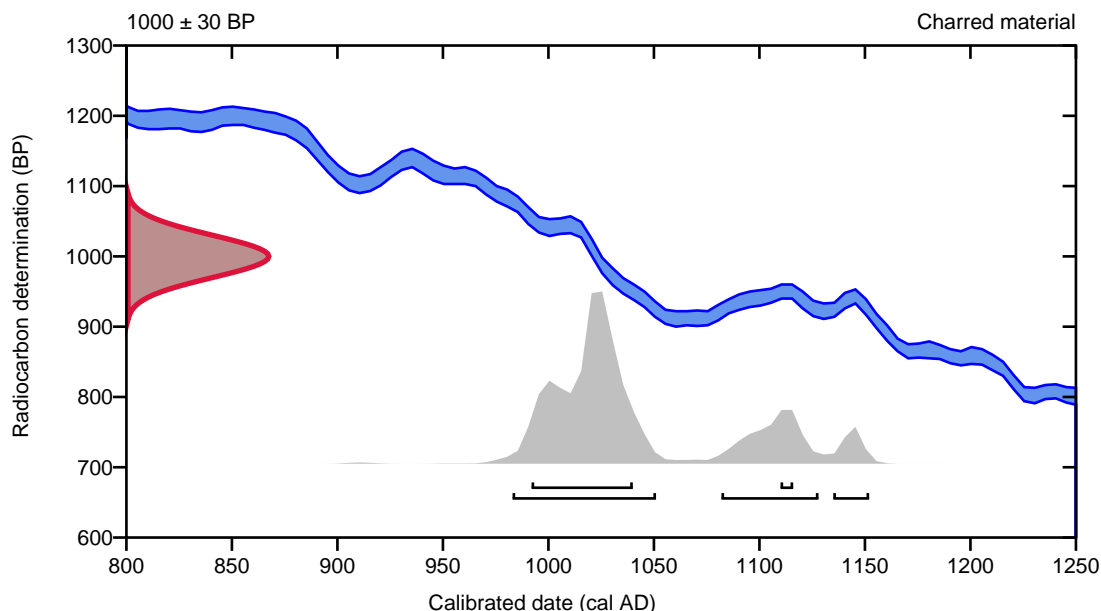
95.4% probability

(71%)	983 - 1051 cal AD	(967 - 899 cal BP)
(19.2%)	1082 - 1128 cal AD	(868 - 822 cal BP)
(5.2%)	1135 - 1152 cal AD	(815 - 798 cal BP)

68.2% probability

(63.9%)	992 - 1040 cal AD	(958 - 910 cal BP)
(4.3%)	1110 - 1116 cal AD	(840 - 834 cal BP)

TP-BGC18-Y-2-G2



Database used
INTCAL13

References

References to Probability Method

Bronk Ramsey, C. (2009). Bayesian analysis of radiocarbon dates. *Radiocarbon*, 51(1), 337-360.

References to Database INTCAL13

Reimer, et.al., 2013, *Radiocarbon*55(4).

Calibration of Radiocarbon Age to Calendar Years

(High Probability Density Range Method (HPD): INTCAL13 + NHZ1)

(Variables: $\delta^{13}\text{C} = -26.5$ o/oo)

Laboratory number **Beta-497237**

Percent modern carbon **100.88 +/- 0.38 pMC**

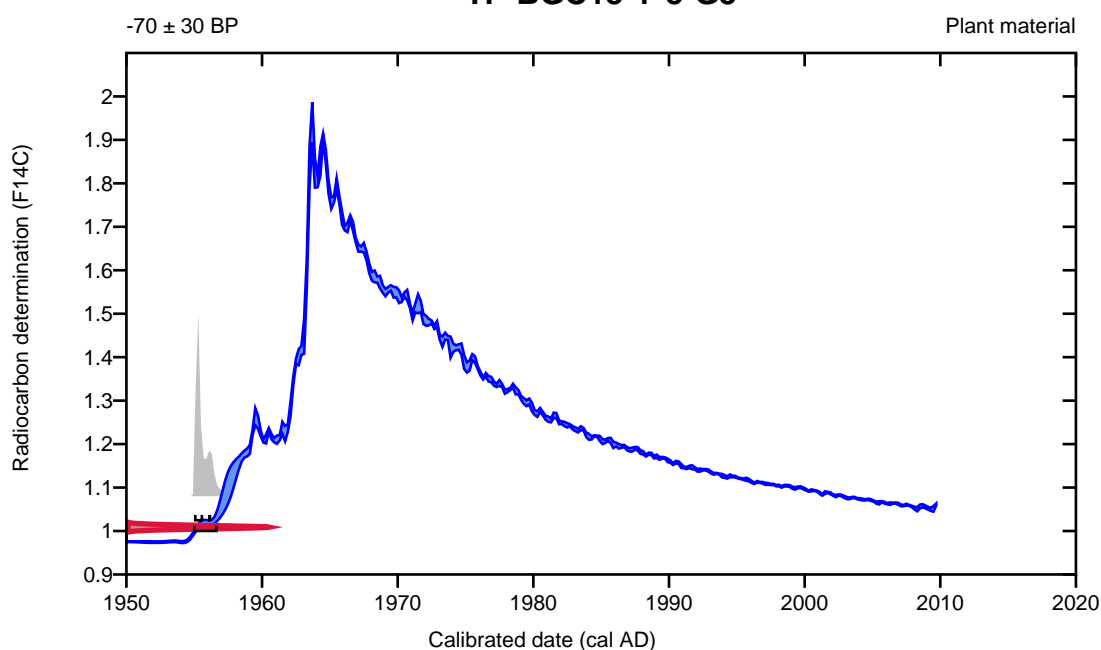
95.4% probability

(95.4%) 1954 - 1956 cal AD (-5 - -7 cal BP)

68.2% probability

(59.4%) 1954 - 1955 cal AD (-5 - -6 cal BP)
(8.8%) 1956 cal AD (-7 cal BP)

TP-BGC18-Y-3-G3



Database used

INTCAL13 + NHZ1

References

References to Probability Method

Bronk Ramsey, C. (2009). Bayesian analysis of radiocarbon dates. *Radiocarbon*, 51(1), 337-360.

References to Database INTCAL13 + NHZ1

Hua, et.al., 2013, *Radiocarbon*, 55(4). Reimer, et.al., 2013, *Radiocarbon* 55(4).

Calibration of Radiocarbon Age to Calendar Years

(High Probability Density Range Method (HPD): INTCAL13)

(Variables: $\delta^{13}\text{C} = -25.9$ o/oo)

Laboratory number **Beta-497238**

Conventional radiocarbon age **230 ± 30 BP**

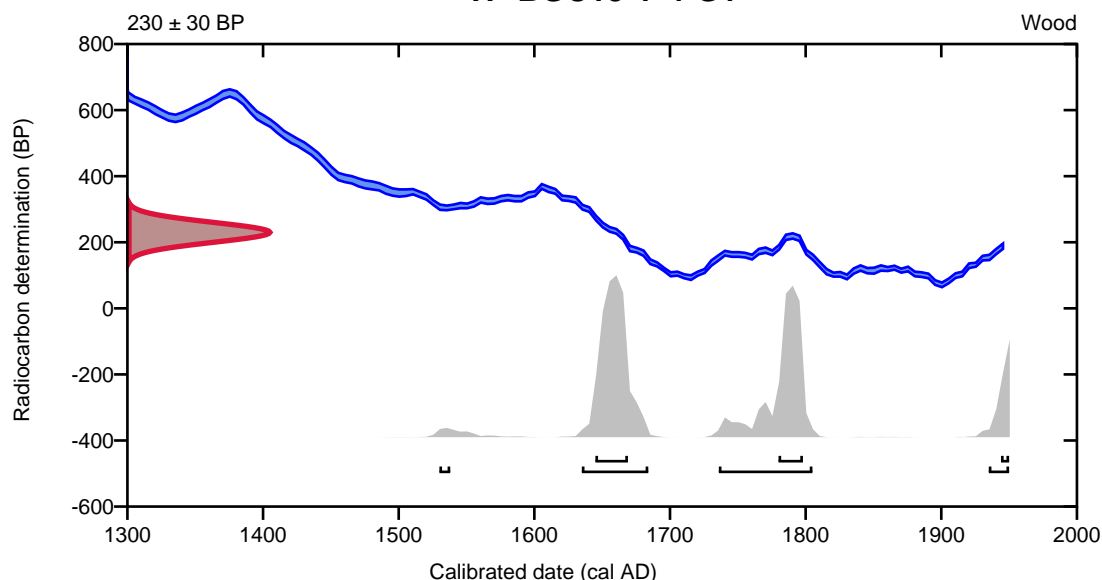
95.4% probability

(45.8%)	1635 - 1684 cal AD	(315 - 266 cal BP)
(40.1%)	1736 - 1805 cal AD	(214 - 145 cal BP)
(8.6%)	1935 - Post cal AD 1950	(15 - Post cal BP 0)
(0.9%)	1530 - 1538 cal AD	(420 - 412 cal BP)

68.2% probability

(36.7%)	1645 - 1669 cal AD	(305 - 281 cal BP)
(26.4%)	1780 - 1798 cal AD	(170 - 152 cal BP)
(5.1%)	1944 - Post cal AD 1950	(6 - Post cal BP 0)

TP-BGC18-Y-4-G1



Database used
INTCAL13

References

References to Probability Method

Bronk Ramsey, C. (2009). Bayesian analysis of radiocarbon dates. *Radiocarbon*, 51(1), 337-360.

References to Database INTCAL13

Reimer, et.al., 2013, *Radiocarbon*55(4).

Calibration of Radiocarbon Age to Calendar Years

(High Probability Density Range Method (HPD): INTCAL13)

(Variables: $\delta^{13}\text{C} = -22.2$ o/oo)

Laboratory number **Beta-497239**

Conventional radiocarbon age **860 ± 30 BP**

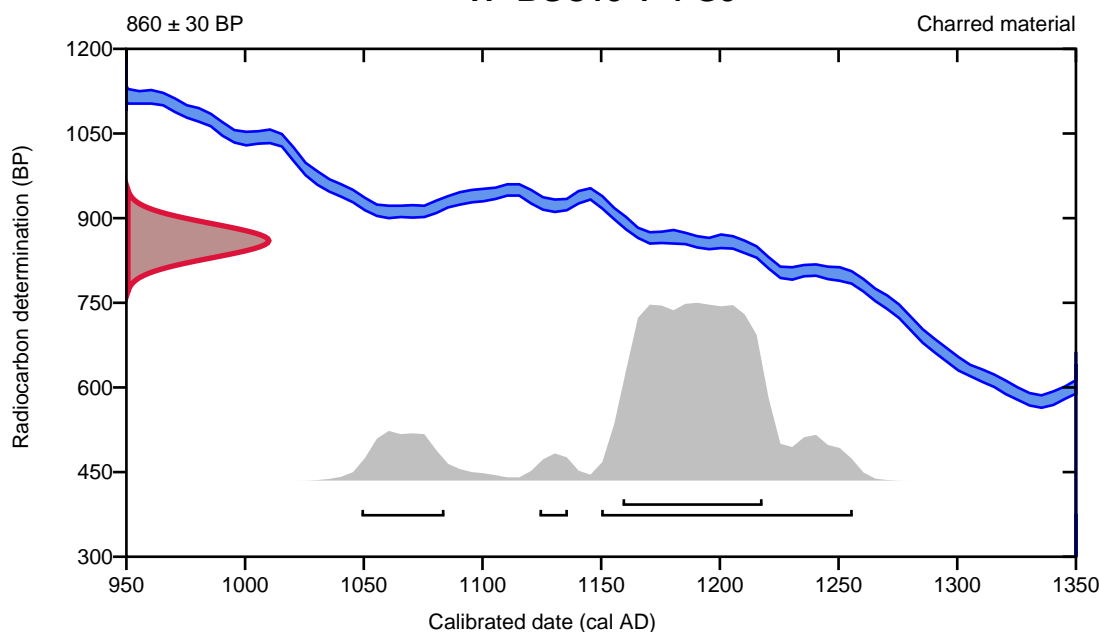
95.4% probability

(83.5%)	1150 - 1256 cal AD	(800 - 694 cal BP)
(9.9%)	1049 - 1084 cal AD	(901 - 866 cal BP)
(2%)	1124 - 1136 cal AD	(826 - 814 cal BP)

68.2% probability

(68.2%)	1159 - 1218 cal AD	(791 - 732 cal BP)
---------	--------------------	--------------------

TP-BGC18-Y-4-G3



Database used
INTCAL13

References

References to Probability Method

Bronk Ramsey, C. (2009). Bayesian analysis of radiocarbon dates. *Radiocarbon*, 51(1), 337-360.

References to Database INTCAL13

Reimer, et.al., 2013, *Radiocarbon*55(4).

Calibration of Radiocarbon Age to Calendar Years

(High Probability Density Range Method (HPD): INTCAL13)

(Variables: $\delta^{13}\text{C} = -25.0$ o/oo)

Laboratory number **Beta-497240**

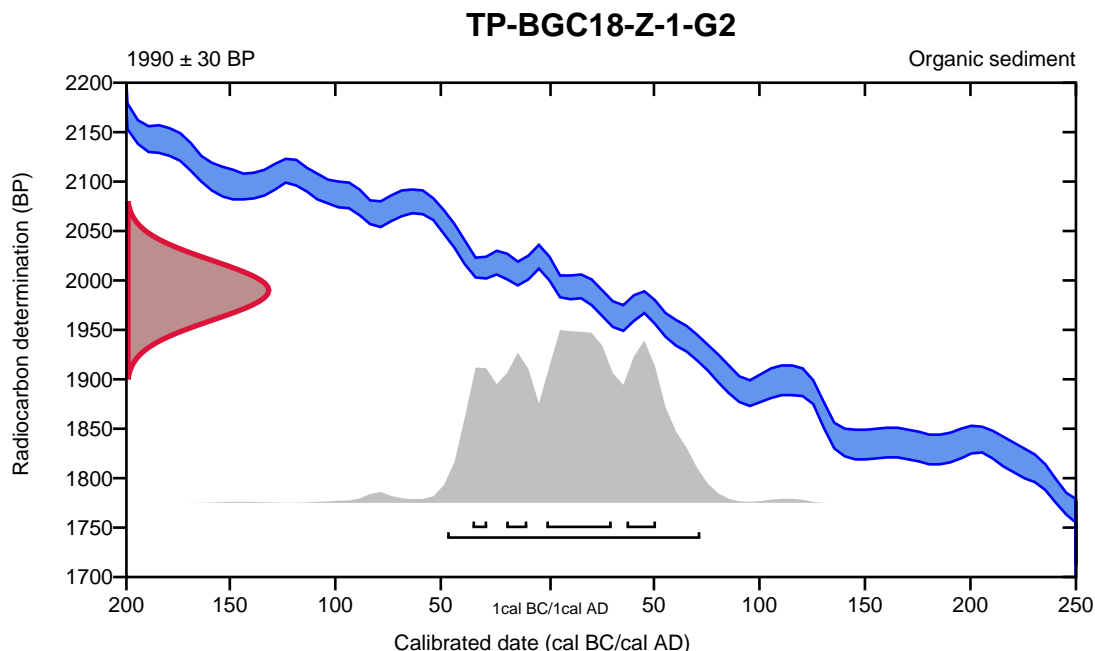
Conventional radiocarbon age **1990 \pm 30 BP**

95.4% probability

(95.4%) 49 cal BC - 72 cal AD (1998 - 1878 cal BP)

68.2% probability

(36%)	2 cal BC - 30 cal AD	(1951 - 1920 cal BP)
(14.8%)	37 - 51 cal AD	(1913 - 1899 cal BP)
(10.6%)	21 - 11 cal BC	(1970 - 1960 cal BP)
(6.7%)	37 - 30 cal BC	(1986 - 1979 cal BP)



Database used
INTCAL13

References

References to Probability Method

Bronk Ramsey, C. (2009). Bayesian analysis of radiocarbon dates. *Radiocarbon*, 51(1), 337-360.

References to Database INTCAL13

Reimer, et.al., 2013, *Radiocarbon*55(4).

Calibration of Radiocarbon Age to Calendar Years

(High Probability Density Range Method (HPD): INTCAL13)

(Variables: $\delta^{13}C = -22.5$ o/oo)

Laboratory number **Beta-497241**

Conventional radiocarbon age **2910 \pm 30 BP**

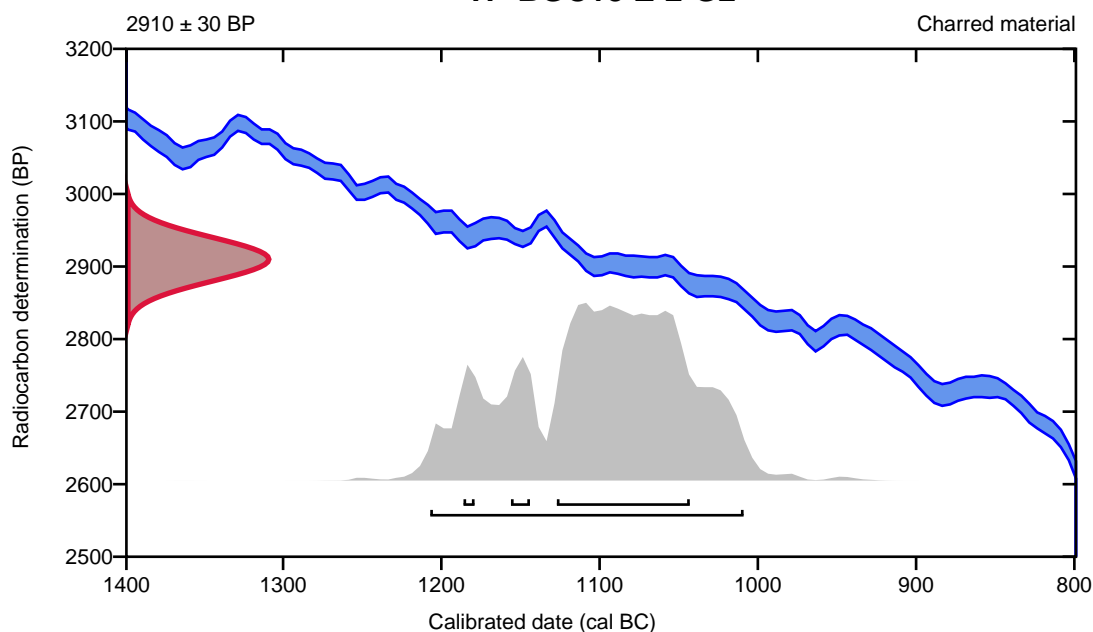
95.4% probability

(95.4%) 1209 - 1011 cal BC (3158 - 2960 cal BP)

68.2% probability

(58.9%) 1129 - 1045 cal BC (3078 - 2994 cal BP)
(6%) 1158 - 1146 cal BC (3107 - 3095 cal BP)
(3.3%) 1188 - 1181 cal BC (3137 - 3130 cal BP)

TP-BGC18-Z-2-G2



Database used
INTCAL13

References

References to Probability Method

Bronk Ramsey, C. (2009). Bayesian analysis of radiocarbon dates. *Radiocarbon*, 51(1), 337-360.

References to Database INTCAL13

Reimer, et.al., 2013, *Radiocarbon*55(4).

Calibration of Radiocarbon Age to Calendar Years

(High Probability Density Range Method (HPD): INTCAL13)

(Variables: $\delta^{13}\text{C} = -24.0$ o/oo)

Laboratory number **Beta-497242**

Conventional radiocarbon age **7870 \pm 30 BP**

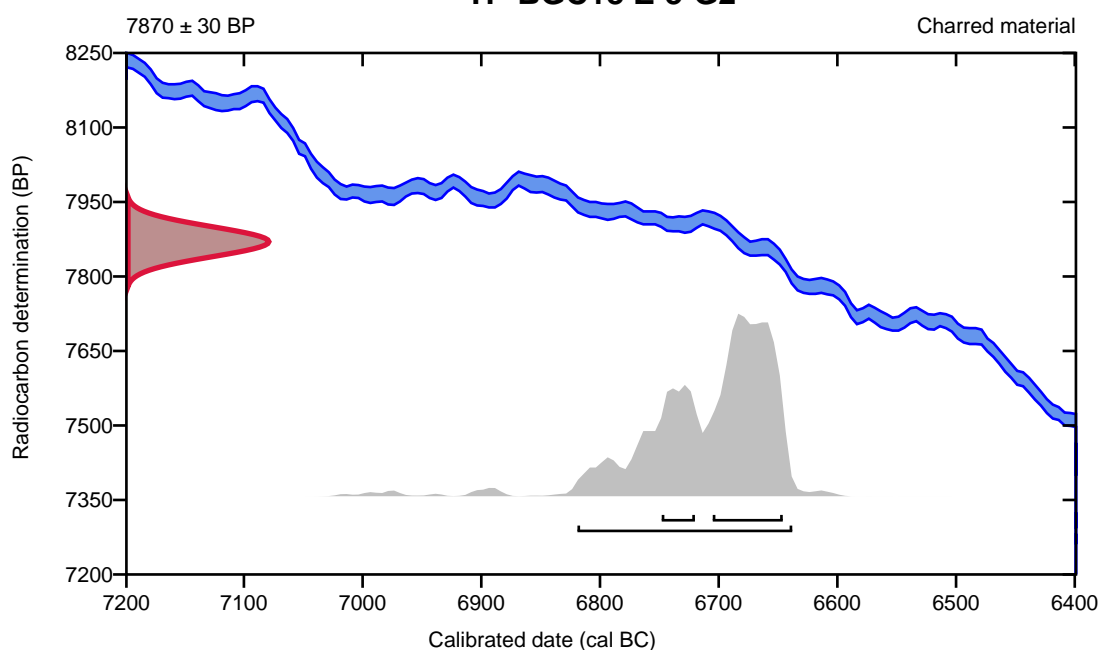
95.4% probability

(95.4%) 6821 - 6640 cal BC (8770 - 8589 cal BP)

68.2% probability

(51.4%) 6707 - 6648 cal BC (8656 - 8597 cal BP)
(16.8%) 6750 - 6722 cal BC (8699 - 8671 cal BP)

TP-BGC18-Z-3-G2



Database used
INTCAL13

References

References to Probability Method

Bronk Ramsey, C. (2009). Bayesian analysis of radiocarbon dates. *Radiocarbon*, 51(1), 337-360.

References to Database INTCAL13

Reimer, et.al., 2013, *Radiocarbon*55(4).

Calibration of Radiocarbon Age to Calendar Years

(High Probability Density Range Method (HPD): INTCAL13)

(Variables: $\delta^{13}\text{C} = -26.3$ o/oo)

Laboratory number **Beta-497243**

Conventional radiocarbon age **10300 \pm 40 BP**

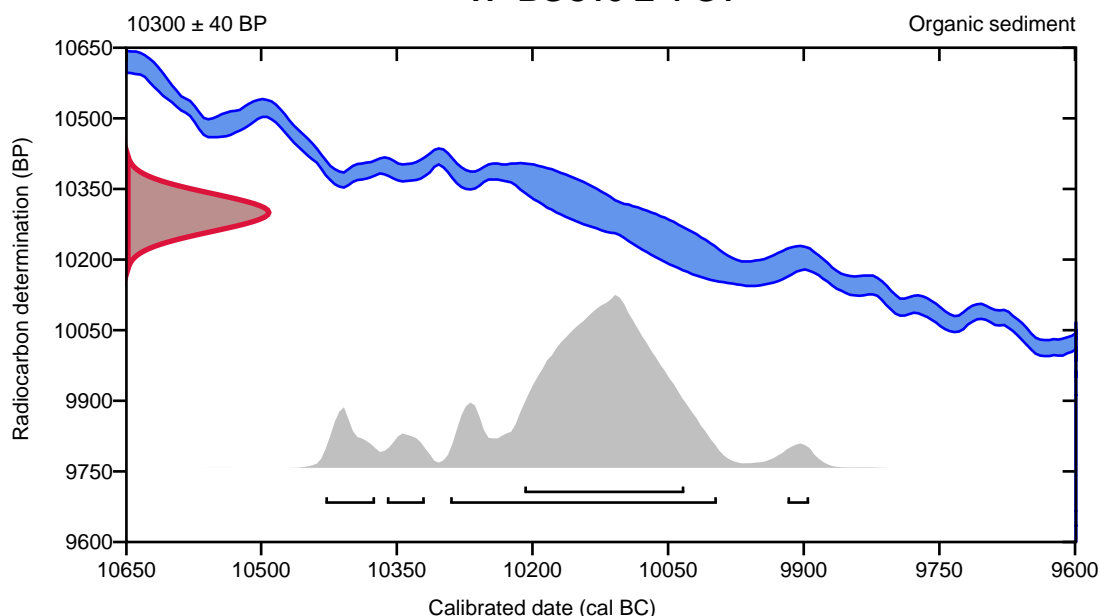
95.4% probability

(83.8%)	10293 - 9998 cal BC	(12242 - 11947 cal BP)
(6.3%)	10431 - 10376 cal BC	(12380 - 12325 cal BP)
(3.6%)	10363 - 10321 cal BC	(12312 - 12270 cal BP)
(1.6%)	9920 - 9896 cal BC	(11869 - 11845 cal BP)

68.2% probability

(68.2%)	10211 - 10034 cal BC	(12160 - 11983 cal BP)
---------	----------------------	------------------------

TP-BGC18-Z-4-G1



Database used
INTCAL13

References

References to Probability Method

Bronk Ramsey, C. (2009). Bayesian analysis of radiocarbon dates. *Radiocarbon*, 51(1), 337-360.

References to Database INTCAL13

Reimer, et.al., 2013, *Radiocarbon*55(4).



Quality Assurance Report

This report provides the results of reference materials used to validate radiocarbon analyses prior to reporting. Known-value reference materials were analyzed quasi-simultaneously with the unknowns. Results are reported as expected values vs measured values. Reported values are calculated relative to NIST SRM-4990B and corrected for isotopic fractionation. Results are reported using the direct analytical measure percent modern carbon (pMC) with one relative standard deviation. Agreement between expected and measured values is taken as being within 2 sigma agreement (error x 2) to account for total laboratory error.

Report Date: July 02, 2018
Submitter: Ms. Emily Moase

QA MEASUREMENTS

Reference 1

Expected Value: 129.41 +/- 0.06 pMC

Measured Value: 129.43 +/- 0.35 pMC

Agreement: Accepted

Reference 2

Expected Value: 0.49 +/- 0.10 pMC

Measured Value: 0.50 +/- 0.04 pMC

Agreement: Accepted

Reference 3

Expected Value: 96.69 +/- 0.50 pMC

Measured Value: 97.20 +/- 0.29 pMC

Agreement: Accepted

COMMENT: All measurements passed acceptance tests.

Validation:

Date: July 02, 2018



Beta Analytic
RADIOCARBON DATING

Beta Analytic Inc
4985 SW 74 Court
Miami, Florida 33155
Tel: 305-667-5167
Fax: 305-663-0964
beta@radiocarbon.com

Mr. Darden Hood
President

Mr. Ronald Hatfield
Mr. Christopher Patrick
Deputy Directors

ISO/IEC 17025:2005 Accredited Test Results: Testing results recognized by all Signatories to the ILAC Mutual Recognition Arrangement

July 19, 2018

Ms. Emily Moase
BGC Engineering
500-980 Howe Street
Vancouver, BC V6Z 0C8
Canada

RE: Radiocarbon Dating Results

Dear Ms. Moase,

Enclosed are the radiocarbon dating results for two samples recently sent to us. As usual, the method of analysis is listed on the report with the results and calibration data is provided where applicable. The Conventional Radiocarbon Ages have all been corrected for total fractionation effects and where applicable, calibration was performed using 2013 calibration databases (cited on the graph pages).

The web directory containing the table of results and PDF download also contains pictures, a cvs spreadsheet download option and a quality assurance report containing expected vs. measured values for 3-5 working standards analyzed simultaneously with your samples.

Reported results are accredited to ISO/IEC 17025:2005 Testing Accreditation PJLA #59423 standards and all chemistry was performed here in our laboratory and counted in our own accelerators here. Since Beta is not a teaching laboratory, only graduates trained to strict protocols of the ISO/IEC 17025:2005 Testing Accreditation PJLA #59423 program participated in the analyses.

As always Conventional Radiocarbon Ages and sigmas are rounded to the nearest 10 years per the conventions of the 1977 International Radiocarbon Conference. When counting statistics produce sigmas lower than +/- 30 years, a conservative +/- 30 BP is cited for the result. The reported $\delta^{13}C$ values were measured separately in an IRMS (isotope ratio mass spectrometer). They are NOT the AMS $\delta^{13}C$ which would include fractionation effects from natural, chemistry and AMS induced sources.

When interpreting the results, please consider any communications you may have had with us regarding the samples.

Thank you for prepaying the analyses. As always, if you have any questions or would like to discuss the results, don't hesitate to contact us.

Sincerely ,



Digital signature on file



REPORT OF RADIOCARBON DATING ANALYSES

Emily Moase

Report Date: July 19, 2018

BGC Engineering

Material Received: July 06, 2018

Laboratory Number

Sample Code Number

Conventional Radiocarbon Age (BP) or
Percent Modern Carbon (pMC) & Stable Isotopes

Calendar Calibrated Results: 95.4 % Probability
High Probability Density Range Method (HPD)

Beta - 498936

TP-BGC18-X02-G3

5640 +/- 30 BP

IRMS $\delta^{13}C$: -23.7 o/oo

(79.1%)
(16.3%)

4542 - 4441 cal BC
4425 - 4371 cal BC

(6491 - 6390 cal BP)
(6374 - 6320 cal BP)

Submitter Material: Organics

Pretreatment: (organic sediment) acid washes

Analyzed Material: Organic sediment

Analysis Service: AMS-Standard delivery

Percent Modern Carbon: 49.55 +/- 0.19 pMC

Fraction Modern Carbon: 0.4955 +/- 0.0019

D14C: -504.46 +/- 1.85 o/oo

$\Delta^{14}C$: -508.52 +/- 1.85 o/oo(1950:2,018.00)

Measured Radiocarbon Age: (without $\delta^{13}C$ correction): 5620 +/- 30 BP

Calibration: BetaCal3.21: HPD method: INTCAL13

Results are ISO/IEC-17025:2005 accredited. No sub-contracting or student labor was used in the analyses. All work was done at Beta in 4 in-house NEC accelerator mass spectrometers and 4 Thermo IRMSs. The "Conventional Radiocarbon Age" was calculated using the Libby half-life (5568 years), is corrected for total isotopic fraction and was used for calendar calibration where applicable. The Age is rounded to the nearest 10 years and is reported as radiocarbon years before present (BP), "present" = AD 1950. Results greater than the modern reference are reported as percent modern carbon (pMC). The modern reference standard was 95% the ^{14}C signature of NIST SRM-4990C (oxalic acid). Quoted errors are 1 sigma counting statistics. Calculated sigmas less than 30 BP on the Conventional Radiocarbon Age are conservatively rounded up to 30. $\delta^{13}C$ values are on the material itself (not the AMS $\delta^{13}C$). $\delta^{13}C$ and $\delta^{15}N$ values are relative to VPDB-1. References for calendar calibrations are cited at the bottom of calibration graph pages.



REPORT OF RADIOCARBON DATING ANALYSES

Emily Moase

Report Date: July 19, 2018

BGC Engineering

Material Received: July 06, 2018

Laboratory Number

Sample Code Number

Conventional Radiocarbon Age (BP) or
Percent Modern Carbon (pMC) & Stable Isotopes

Calendar Calibrated Results: 95.4 % Probability
High Probability Density Range Method (HPD)

Beta - 498937

TP-BGC18-Y-03-G2

690 +/- 30 BP

IRMS $\delta^{13}C$: -25.6 o/oo

(68.9%)

1265 - 1312 cal AD

(685 - 638 cal BP)

(26.5%)

1358 - 1388 cal AD

(592 - 562 cal BP)

Submitter Material: Organics

Pretreatment: (organic sediment) acid washes

Analyzed Material: Organic sediment

Analysis Service: AMS-Standard delivery

Percent Modern Carbon: 91.77 +/- 0.34 pMC

Fraction Modern Carbon: 0.9177 +/- 0.0034

D14C: -82.31 +/- 3.43 o/oo

$\Delta^{14}C$: -89.83 +/- 3.43 o/oo(1950:2,018.00)

Measured Radiocarbon Age: (without $\delta^{13}C$ correction): 700 +/- 30 BP

Calibration: BetaCal3.21: HPD method: INTCAL13

Results are ISO/IEC-17025:2005 accredited. No sub-contracting or student labor was used in the analyses. All work was done at Beta in 4 in-house NEC accelerator mass spectrometers and 4 Thermo IRMSs. The "Conventional Radiocarbon Age" was calculated using the Libby half-life (5568 years), is corrected for total isotopic fraction and was used for calendar calibration where applicable. The Age is rounded to the nearest 10 years and is reported as radiocarbon years before present (BP), "present" = AD 1950. Results greater than the modern reference are reported as percent modern carbon (pMC). The modern reference standard was 95% the ^{14}C signature of NIST SRM-4990C (oxalic acid). Quoted errors are 1 sigma counting statistics. Calculated sigmas less than 30 BP on the Conventional Radiocarbon Age are conservatively rounded up to 30. $\delta^{13}C$ values are on the material itself (not the AMS $\delta^{13}C$). $\delta^{13}C$ and $\delta^{15}N$ values are relative to VPDB-1. References for calendar calibrations are cited at the bottom of calibration graph pages.

Calibration of Radiocarbon Age to Calendar Years

(High Probability Density Range Method (HPD): INTCAL13)

(Variables: $\delta^{13}C = -23.7$ o/oo)

Laboratory number **Beta-498936**

Conventional radiocarbon age **5640 \pm 30 BP**

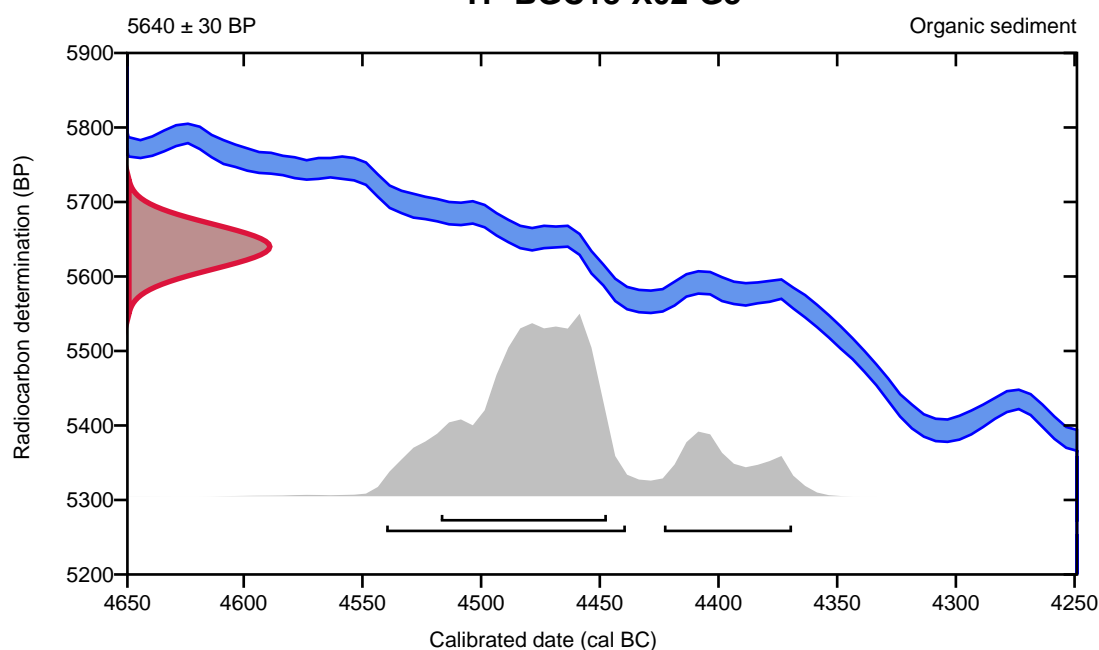
95.4% probability

(79.1%)	4542 - 4441 cal BC	(6491 - 6390 cal BP)
(16.3%)	4425 - 4371 cal BC	(6374 - 6320 cal BP)

68.2% probability

(68.2%)	4519 - 4449 cal BC	(6468 - 6398 cal BP)
---------	--------------------	----------------------

TP-BGC18-X02-G3



Database used
INTCAL13

References

References to Probability Method

Bronk Ramsey, C. (2009). Bayesian analysis of radiocarbon dates. *Radiocarbon*, 51(1), 337-360.

References to Database INTCAL13

Reimer, et.al., 2013, *Radiocarbon*55(4).

Calibration of Radiocarbon Age to Calendar Years

(High Probability Density Range Method (HPD): INTCAL13)

(Variables: $\delta^{13}C = -25.6$ o/oo)

Laboratory number **Beta-498937**

Conventional radiocarbon age **690 ± 30 BP**

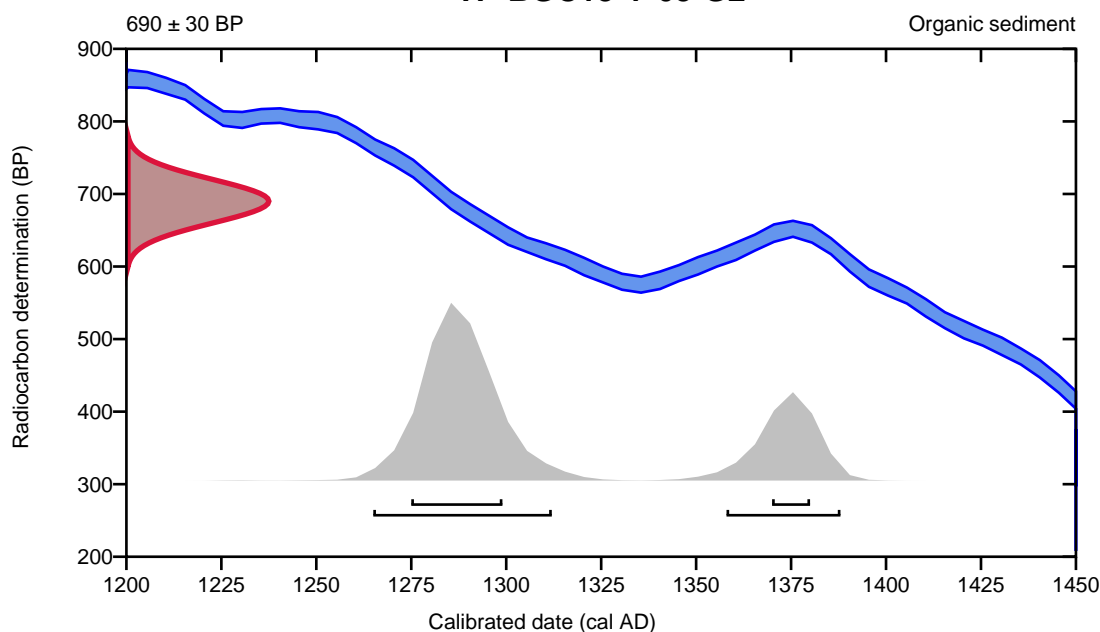
95.4% probability

(68.9%)	1265 - 1312 cal AD	(685 - 638 cal BP)
(26.5%)	1358 - 1388 cal AD	(592 - 562 cal BP)

68.2% probability

(54.2%)	1275 - 1299 cal AD	(675 - 651 cal BP)
(14%)	1370 - 1380 cal AD	(580 - 570 cal BP)

TP-BGC18-Y-03-G2



Database used
INTCAL13

References

References to Probability Method

Bronk Ramsey, C. (2009). Bayesian analysis of radiocarbon dates. *Radiocarbon*, 51(1), 337-360.

References to Database INTCAL13

Reimer, et.al., 2013, *Radiocarbon*55(4).



Quality Assurance Report

This report provides the results of reference materials used to validate radiocarbon analyses prior to reporting. Known-value reference materials were analyzed quasi-simultaneously with the unknowns. Results are reported as expected values vs measured values. Reported values are calculated relative to NIST SRM-4990B and corrected for isotopic fractionation. Results are reported using the direct analytical measure percent modern carbon (pMC) with one relative standard deviation. Agreement between expected and measured values is taken as being within 2 sigma agreement (error x 2) to account for total laboratory error.

Report Date: July 19, 2018
Submitter: Ms. Emily Moase

QA MEASUREMENTS

Reference 1

Expected Value: 134.07 +/- 0.20 pMC

Measured Value: 133.97 +/- 0.18 pMC

Agreement: Accepted

Reference 2

Expected Value: 0.49 +/- 0.10 pMC

Measured Value: 0.49 +/- 0.03 pMC

Agreement: Accepted

Reference 3

Expected Value: 129.41 +/- 0.06 pMC

Measured Value: 129.65 +/- 0.39 pMC

Agreement: Accepted

COMMENT: All measurements passed acceptance tests.

Validation:

Date: July 19, 2018

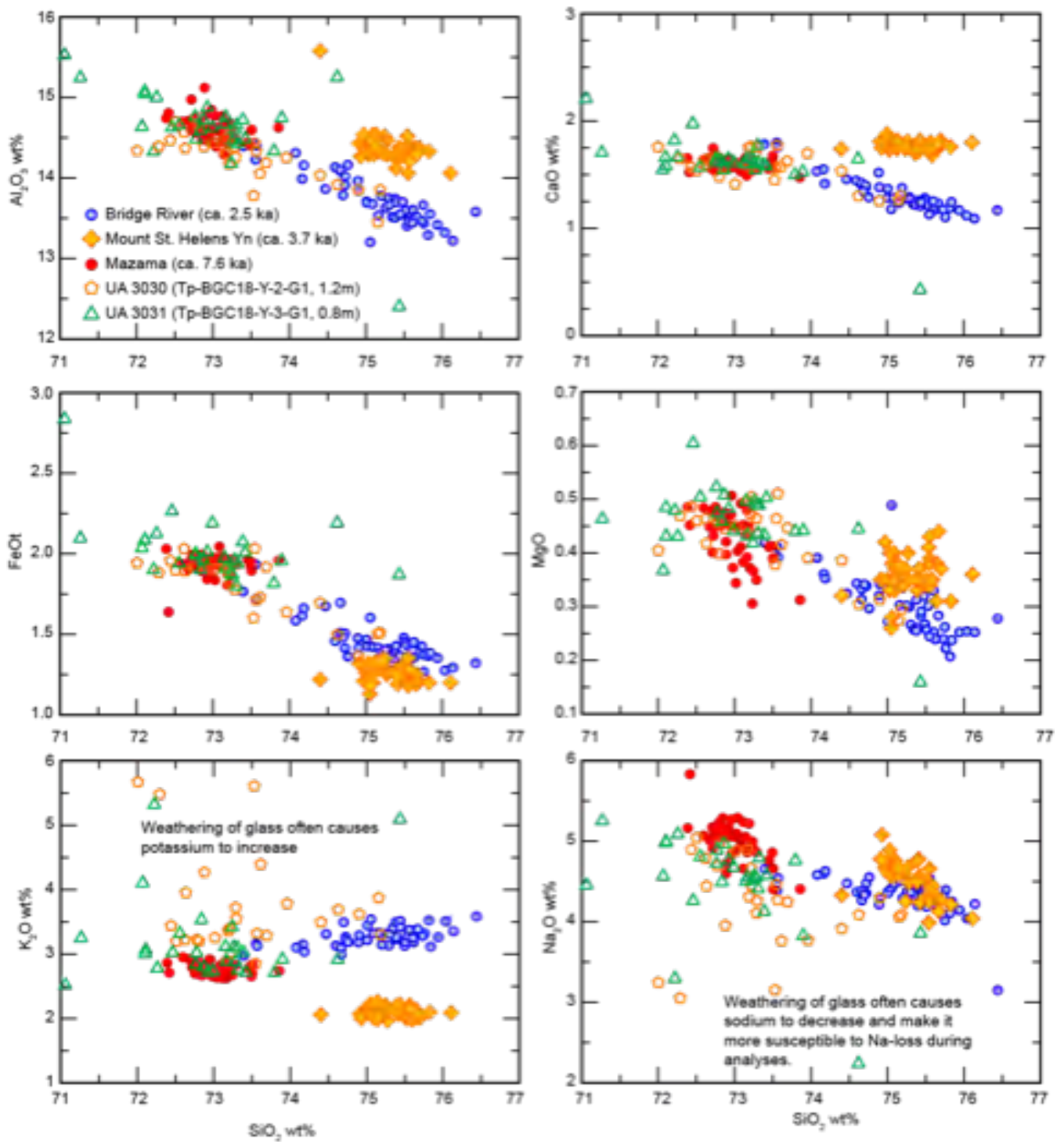


Figure X-1. Results of tephrochronology testing at University of Alberta. Sodium and potassium plots show increased weathering profile that is most likely from tephra material being re-worked by later events.

APPENDIX E - RISK ASSESSMENT METHODS

APPENDIX E – RISK ASSESSMENT

E.1. GENERAL

Risk assessment involves estimation of the likelihood that a steep creek hazard scenario will occur, impact elements at risk, and cause particular types and severities of consequences. In this study, the assessment involves estimating the risk that debris flows occurring on X, Y, and Z Creeks will impact residential buildings and cause loss of life.

The primary objective of the risk assessment is to support risk management decision making. Importantly, the assessment does not consider all possible risks that could be associated with a debris flow. Rather, the risk assessment considers key risks that can be systematically estimated, compared to risk tolerance standards, and then used to optimize mitigation strategies. These mitigation strategies, once implemented, would also reduce relative levels risk for a broader spectrum of elements than those explicitly considered in this report. Debris-flow impact and resulting consequences are determined by relating the characteristics of debris-flow scenarios (flow velocity and depth) to impacted elements at risk at a given location.

This assessment uses two different metrics to estimate safety risk: individual risk and group risk. Individual risk evaluates the chance that a specific individual (the person judged to be most at risk) will be affected by the hazard. For example, an assessment of individual risk evaluates the chance that a specific person living in a dwelling would be affected by the hazard. Individual risk is independent of the number of people exposed to the hazard, as it focusses on a single individual.

Group risk, also known as societal risk, evaluates the chance that any people present in the area will be affected by the hazard. A low-frequency, high magnitude event might result in a very small, tolerable risk to an individual, but the same event may be considered intolerable if a large number of people are affected. Group risk assessments are completed in addition to individual risk assessments because society is less tolerant of events that affect multiple people. In a given home, the probability of any individual being affected (group risk) will be at least as high as the probability of a specific individual being affected (individual risk).

This risk assessment considers the existing channel configuration and does not consider any additional debris-flow mitigation. This approach provides a baseline estimation of risk to facilitate comparison of different debris-flow risk reduction options. BGC conservatively assumes that no evacuation of persons is possible during the event.

Lastly, this assessment was done at a building lot level of detail, where the likelihood of debris-flow impact is based on the location of a given building in relation to hazard areas. For the purposes of land use planning, lots containing buildings that exceeding risk tolerance criteria were identified at a lot level of detail on risk maps (Drawing 10).

E.2. GEOHAZARD SCENARIOS

This risk analysis is based on debris-flow scenarios, which are defined as hydrogeomorphic events with particular volumes and likelihoods of occurrence.

Geohazard scenarios were chosen to represent the spectrum of possible debris-flow event magnitudes on each creek, from the smallest and most frequent to the largest credible. Along with their probability of occurrence, these scenarios are the primary outcome of the hazard assessment that is carried forward into the risk analysis.

Drawings 06, 07 and 08 show the geohazard scenarios considered for X, Y, and Z Creeks, respectively. Methods to develop these maps are described in Section 3.6 of the main report. The results were evaluated against risk tolerance criteria defined in Section 3.7 of the main report.

E.3. ELEMENTS AT RISK

This section describes “elements at risk” potentially exposed to (at risk from) the geohazard scenarios considered in the risk analysis.

E.3.1. Background

The study area intersects the Peaks of Grassi neighbourhood and resort accommodations. Further description of the community is provided in the main report, and Table E-1 lists the elements at risk considered in this assessment. Table E-1 does not include all elements that could suffer direct or indirect consequences due to a geohazard event, but focuses on those that can be reasonably assessed, based on the information available. The sections following describe methods used to identify and characterize elements at risk, and lists data gaps and uncertainties.

Table E-1. List of elements at risk considered in the risk assessment.

Element at Risk	Description
Building Structures	Commercial, residential, transportation.
Persons	Persons located within buildings.
Lifelines	Sewerage, stormwater management, gas distribution, electrical power and telephone line distribution, roads ¹ .
Critical facilities	None.
Business activity	Businesses located on the fan that have the potential to be directly impacted by geohazards, either due to building damage or interruption of business activity due to loss of access.
Cultural/ecological significance	Peaks of Grassi Park, Highline Trail, Powerline Trail.

Note:

1. Local roads include: Kamenka Green, Lawrence Grassi Ridge, Peaks Drive, Shellian Lane, Three Sisters Drive, and Wilson Way.

E.3.2. Buildings

Information on building types and locations of buildings (building footprints) was obtained from the Town of Canmore. These data were used in the risk analysis to identify location(s) of buildings within parcels that could be impacted by geohazard scenarios.

The study areas of X, Y, and Z Creeks contain approximately 98, 144, and 90 residential dwellings respectively (a mixture of single detached houses and townhouses). Additionally, the X Creek study area contains 1 resort building. These are estimated from the data provided by the Town of Canmore. Each land parcel contains a unique identification number (“PID”) and unique lookup code identifying the primary use and type of building within the parcel. In the case of single buildings (e.g., residential houses), each parcel typically contains only one assessed land and building value. Data on building structure type or contents were not available.

The total estimated value of buildings development within the study areas is \$51M, \$56M, and \$44M for X, Y, and Z Creeks respectively. Assessed building values do not necessarily correspond to replacement value, which may be higher.

Table E-2 summarizes the main uncertainties associated with the buildings attributes data provided.

Table E-2. Building data uncertainties.

Type	Description
Building Value	Building value was assigned as the total improvement value within a given parcel, based on tax assessment data provided by the Town of Canmore. This data is assumed to be correct as provided.
Building Structure	No information describing building structure was available, such as construction type, foundation type, number of stories, presence of sub-grade basement, Flood Construction Level (FCL), first-floor elevation, or floor area. This data gap will decrease confidence in damage and risk estimation. BGC applied assumed values based on the associated land use code for each parcel.
Building Type	Information on building type was provided by the Town of Canmore in the form of land use codes.

E.3.3. Lifelines

Lifelines considered in this assessment include local roads. Lifelines within the study area are shown on Drawings 06 through 10. Local roads include the following:

- Kamenka Green
- Lawrence Grassi Ridge
- Peaks Drive
- Shellian Lane
- Three Sisters Drive
- Wilson Way.

E.3.4. Critical Facilities

Critical facilities were defined according to Alberta Infrastructure (2013) as those that:

- Provide vital services in saving and avoiding loss of human life
- Accommodate and support activities important to rescue and treatment operations
- Are required for the maintenance of public order
- House substantial populations
- Confine activities that, if disturbed or damaged, could be hazardous to the region
- Contain hazardous products or irreplaceable artifacts and historical documents.

No critical facilities were identified within the study areas.

E.3.5. Persons

Population estimates used in this assessment are based on 2014 Census summaries (Canmore, 2015), dwelling counts from tax roll classification data (Canmore, 2013), and business data (Hoovers, 2013).

The X, Y, and Z Creeks study area intersects a portion of Municipal Census District nos. 18B, 18C, 18D, and 23. Census data for municipal districts within the X, Y, and Z Creeks study area is summarized in Table E-3.

Table E-3. 2014 census data for municipal districts within the X, Y, and Z Creeks study area.

Municipal District	Permanent population	Non-permanent population ¹	Approximate proportion in study area (%)	Permanent Population in Study Area	Non-permanent population in Study Area
18B	13	4	1	0	0
18C	7	5	23	2	1
18D	0	0	5	0	0
23	750	256	92	689	235

Note:

1. Non-Permanent Residents are defined as “persons with permanent address elsewhere and usually occupy the household on a non-permanent basis” (Canmore 2011). It does not include persons staying in hotels.

Based on 2014 Census data, the X, Y, and Z Creeks study area is home to a permanent population of approximately 691 permanent residents and 236 non-permanent residents, which corresponds to a total estimated population of 927.

Assessment of risk at a parcel level of detail requires estimation of the number of persons in each parcel on the fan. However, Census data does not provide estimates at this resolution. As such, individual parcel populations were estimated based on the number of building units of a given type, in each parcel, and the estimated number of persons in a given unit type. An average occupancy rate of 2.4 persons per building was used.

Population estimates for non-residential parcels are based on the number of employees listed in business data obtained from Dun & Bradstreet (Hoovers, 2013).

Table E-4 summarizes calculated populations used in the risk analysis. Table E-5 lists factors affecting confidence in these estimates, with implications for possible over- or underestimation of group safety risk depending on whether the number of persons was over- or underestimated, respectively. BGC believes that the accuracy of population estimates is sufficient to allow risk management decisions. However, the estimates should not be used for detailed assessment of individual parcels (e.g., for building permit applications) without being manually checked.

Table E-4. Summary of calculated population estimates used in risk analysis.

Building Type	Population Total		
	X Creek	Y Creek	Z Creek
Residential	246	144	235
Hotel	187	0	0
Total	433	144	235

Table E-5. Uncertainties associated with estimating the number of occupants of a building.

Uncertainty	Implication
Average occupancy rates may not correspond to actual occupancy rates for a given dwelling unit.	Over- or underestimation of occupant numbers
Seasonal population fluctuations (including tourists) exist that were not accounted for.	
No employee data available (either not listed in Dun and Bradstreet (D&B) (Hoovers, 2017)) or could not be assigned to specific parcels.	
Errors in employee data sourced from Dun and Bradstreet (D&B) (Hoovers, 2017) may exist. These data were not verified by BGC.	
Errors in assignment of D&B employee data to specific parcels may exist, due to inconsistencies in building address data.	
Overlap between some population types (e.g., employees might also live in the consultation zone).	
Occupancy rates for the hotel are higher or lower than BGC's estimate.	
Distribution of persons within a building are unknown. As such, the number of persons most vulnerable to geohazard impact on the first floor or basement is unknown.	Uncertainty in estimation of human vulnerability to geohazard impact
Seasonal visitors may occupy private residences, and additional visitors temporarily occupy service businesses.	

E.3.6. Business Activity

Approximately 12 businesses, located on 11 parcels and employing 122 people are located within the study area. Annual business revenues data were available for all identified businesses and totals approximately \$11.4 million (Hoovers, 2013). A breakdown of businesses per creek is included in Table E-6.

Table E-6. Business data by creek.

Creek	No. of Businesses	No. of Parcels	No. of Employees	Annual Business Revenue (\$M)
X Creek	5	4	94	4.7
Y Creek	2	2	14	3.2
Z Creek	5	5	14	3.5

Business activity impacts listed in this report are likely underestimated due to uncertainties in the business data. Table E-7 summarizes sources of uncertainty. In addition to these uncertainties, business activity estimates do not include individuals working at home for businesses located elsewhere. Inclusion of these figures would increase the level of business activity that could be affected by a geohazard event. Such estimates are outside the scope of this assessment.

Table E-7. Business data uncertainties.

Type	Description
D&B data quality	BGC has not reviewed the accuracy of business data obtained for this assessment.
Worker location	Whether the employee primarily works at the office or some other location is not known. The estimates also do not include individuals working at home for businesses located elsewhere.
Source of revenue	Whether a business' source of revenue is geographically tied to its physical location (e.g., a retail store with inventory, versus an office space with revenue generated elsewhere) is not known and is outside the scope of this assessment.

E.4. QUANTITATIVE RISK ASSESSMENT (QRA)

E.4.1. Risk Equation

Risk (P_E) was estimated using the following equation:

$$P_E = \sum_{i=1}^n P(H)_i P(S:H)_i P(T:S)_i N \quad [\text{Eq. E-1}]$$

where:

$P(H)_i$ is the annual hazard probability of geohazard scenario i of n , defined as an annual frequency ranges.

$P(S:H)_i$ is the probability that the scenario would reach the element at risk, given that it occurs.

$P(T:S)_i$ is the probability that the element at risk (e.g., persons within buildings) is in the impact zone, given that the scenario reaches the location of the element at risk. This parameter is considered certain (equal to 1) for buildings and infrastructure.

$N = V_i E_i$ describes the consequences [Eq. E-2]

where:

V_i is the vulnerability, which is the probability elements at risk will suffer consequences given hazard impact with a certain severity. For persons, vulnerability is defined as the likelihood of fatality given impact. For buildings, it is defined as the level of damage, measured as a proportion of the building replacement cost or as an absolute cost.

E_i is a measure of the elements at risk, quantifying the value of the elements that could potentially suffer damage or loss. For persons, it is the number of persons exposed to hazard, equal to 1 in the case of individual risk assessment. For buildings, it is defined as the assessed value of buildings potentially subject to damage.

Risk is estimated separately for individuals and groups (societal) risk. Estimated risk for combined debris-flow scenarios is calculated by summing the risk quantified for each individual debris-flow scenario.

Individual risk is reported as the annual Probability of Death of an Individual (PDI). Individual risk levels are independent of the number of persons exposed to risk.

Group risk was estimated as the probability of a certain number of fatalities, represented graphically on an F-N curve as shown in Section 3-7 of the main report. The Y-axis shows the annual cumulative frequency, f_i , of each hazard scenario, and the X-axis shows the estimated number of fatalities, N_i , where:

$$f_i = \sum_{i=1}^n P(H)_i P(S:H)_i P(T:S)_i \quad [\text{Eq. E-3}]$$

and N_i is represented by equation [H-2].

E.4.2. Hazard Probability

Hazard probability, $P(H)_i$, corresponds to the annual probability of occurrence of each hazard scenario, which are defined as annual frequency ranges. The bounds of a given range are exceedance probabilities. For example, the 10 to 100-year scenario represents the probability that the event will be larger than the 10-year event but not larger than the 100-year event.

Given a scenario with the annual exceedance probability range P_{min} to P_{max} , the probability of events within this range corresponds to:

$$P(H)_i = P_{min} - P_{max} \quad [\text{Eq. E-4}]$$

For example, for the 1:10 to 1:100 -year range, this would correspond to:

$$P(H)_i = \frac{1}{10} - \frac{1}{100} = \frac{1}{11} \quad [\text{Eq. E-5}]$$

The upper and lower bounds of each range were used in the risk analysis as approximate upper and lower uncertainty bounds for each frequency range.

E.4.3. Spatial Probability

A wide range of flow characteristics is possible for a given debris-flow or debris-flood magnitude. Specifically, more watery flows are expected to run out further than those with higher sediment concentration. Moreover, flow avulsions near the fan apex can result in flow trajectories primarily towards a certain sector of the fan. For a given hazard scenario, these factors influence the spatial probability of debris-flow impact.

As such, spatial probability estimates were developed for different zones in the study area and are shown on Drawing 06 through 08. These were assigned based on judgement, field observation and reference to model scenarios, and reflect differences in the likelihood flows will propagate to different areas of the fan given scenario occurrence.

E.4.4. Temporal Probability

Temporal probability considers the proportion of time residents spend within their dwelling. All else being equal, safety risk is directly proportional to the time residents spend at home (e.g., a resident who is rarely home has less chance of being struck by a debris flow).

There is strong variation in the proportion of time residents spend in dwellings within the study area, from occasional to full time occupants. There is also seasonal variation and likely variations from year to year.

BGC assumed full-time occupancy to assess baseline risk for land use planning and permitting. “Full-time” is defined in this report as occupancy about 50% of the time on average, 365 days/year. A more conservative value of 0.9 was used for estimation of individual risk, corresponding to a person spending the greatest proportion of time at home, such as a young child, stay-at-home person, or an elderly person. For non-residential buildings (e.g., hotel, businesses), BGC assumed building were occupied approximately 25% of the time on average, 365 days/year.

E.4.5. Vulnerability

Table E-7 lists vulnerability criteria for buildings, which were developed from judgement with reference to Jakob et al. (2012). The values used are also consistent with those used by BGC to assess debris-flood and debris-flow risk for alluvial fans in the Town of Canmore and Municipal District of Bighorn (e.g., BGC, 2014; 2015a-e, 2016). The vulnerability estimates contain uncertainty due to factors that cannot be captured at the scale of assessment, such as variations in the structure and contents of a given building and the location of persons within the building at the time of impact.

Table E-8. Vulnerability criteria for buildings.

Hazard Intensity Index (Range)	Building Damage Description		Building Vulnerability ¹
	Category	Description	Best Estimate
<1	Minor	Low likelihood of building structure damage due to impact pressure. High likelihood of major sediment and/or water damage. Damage level and cost primarily a function of flood-related damages.	0.1
1-10	Moderate	High likelihood of moderate to major building structure damage due to impact pressure. Certain severe sediment and water damage. Building repairs required, possibly including some structural elements.	0.5
10-100	Major	High likelihood of major to severe building structure damage due to impact pressure. Certain severe sediment and water damage. Major building repairs required including to structural elements.	0.825
>100	Complete	Very high likelihood of severe building structure damage or collapse. Near complete building replacement required.	0.95

Note:

1. Value indicate estimated proportion of building replacement value.

Table E-8 shows the criteria used to estimate the vulnerability of persons within buildings to debris-flow or debris-flood impact, where vulnerability is primarily an indirect outcome of building damage or collapse. Estimates for individual risk correspond to an individual most at risk, who may be located on the building ground floor. Estimates used for group risk are 50% lower, with the exception of the highest damage category. This reflects an average estimate for the parcel, recognizing that persons on upper floors will have a relatively lower vulnerability to debris-flood impact except in the case of building destruction.

As indicated in Section E.4.3, lower fan areas are subject to low intensity flows that are unlikely to impact all buildings during a single event. These flows are also likely be shallow (<0.3 m). In these areas, BGC assigned a lower building vulnerability estimate of 0.01 to account for nuisance damage that may occur at some buildings.

Table E-9. Vulnerability criteria for persons within buildings.

Hazard Intensity Index (Range)	Individual Risk	Group Risk
<1	~0	~0
1-10	0.02	0.01
10-100	0.1	0.05
>100	0.5	0.5

Note: Values indicate estimated probability of loss of life given impact

REFERENCES

- Alberta Infrastructure, 2013. Flood Risk Management Guidelines For Location of New Facilities Funded by Alberta Infrastructure. December 2013.
- BGC Engineering Inc. (BGC). 2014. Cougar Creek Debris Flood Risk Assessment. Report prepared for the Town of Canmore dated June 11, 2014.
- BGC Engineering Inc., 2015a. Catiline Creek Debris-Flow Hazard and Risk Assessment. Report prepared for the Squamish-Lillooet Regional District dated January 22, 2015.
- BGC Engineering Inc. (BGC). 2015b. Harvie Heights Creek Debris-Flood Risk Assessment. Report prepared for the Town of Canmore dated May 27, 2015.
- BGC Engineering Inc. (BGC). 2015c. Heart Creek Debris-Flood Risk Assessment. Report prepared for the Town of Canmore dated April 27, 2015. Report prepared for the Town of Canmore dated January 16, 2015.
- BGC Engineering Inc. (BGC). 2015d. Stone Creek Debris-Flow Risk Assessment. Report prepared for the Town of Canmore dated January 13, 2015.
- BGC Engineering Inc. (BGC). 2015e. Three Sisters Creek Debris Flood Risk Assessment. Report prepared for the Town of Canmore dated January 20, 2015.
- BGC Engineering Inc. (BGC). 2015f. Exshaw Creek and Jura Creek Debris Flood Risk Assessment. Report prepared for the Municipal District of Bighorn dated March 1, 2015.
- BGC Engineering Inc. (BGC). 2016. Stoneworks Creek Debris Flood Risk Assessment. Draft Report Prepared for the Town of Canmore dated May 17, 2016.
- Canmore, 2013. List of registered Canmore Businesses. Data provided in spreadsheet format dated November 8, 2013.
- Canmore, 2015. 2014 Municipal Census Summary, dated February 24, 2015.
- Hoovers, 2013. Company Lead List: Complete Gold. Obtained from Hoovers, a Dunn and Bradstreet (D&B) Company, on October 9, 2013.
- Jakob M, Stein D, and Ulmi M. 2012. Vulnerability of buildings to debris flow impact. Natural Hazards 60(2): 241-261.